Redox Signalling in Myeloid Leukaemia

A thesis submitted to the National University of Ireland, Cork,
in fulfilment of the requirements for the degree of

Doctor of Philosophy

by

Jennifer Noreen Moloney BSc.

School of Biochemistry and Cell Biology,

University College Cork, Ireland

March 2018

Supervisor: **Professor Thomas G. Cotter**

Head of Department: **Professor Rosemary O'Connor**

Table of Contents

Author's Declaration

This thesis has not been submitted in whole or part to University College Cork or any other university for any degree. This thesis is, unless stated, the original work of the author.

Signed: _____

Jennifer Noreen Moloney

Acknowledgements

First and foremost, I would like to thank my lecturer and supervisor Prof. Tom Cotter for seeding research enthusiasm during my Bachelors degree and for giving me the opportunity to undertake a PhD in the Tumour Biology laboratory in UCC. I have been very lucky to have worked in your laboratory over the past three years and I am very grateful for the constant guidance, support and motivation that has allowed me to complete the work presented in this thesis. I honestly couldn't have asked for a better supervisor.

I am so thankful to the members of the TC laboratory, past and present, with whom I had the pleasure of working with. Kate, Will, Joanna, Eileen, Alice, Sarah, Ash and Ani- thank you so much for your help, support and encouragement. Here I would especially like to thank Joanna and Eileen for teaching me various techniques in the laboratory and for answering all of my questions. Joanna: a big thank you for all your support and guidance over the past three years, for teaching me how to think like a scientist and how to critically analyse data. This PhD would not have been possible without you. Alice: thank you for the constant interest in my research, for all your support throughout my PhD and for the welcome distractions when they were needed the most. Sarah: especial thanks to you for your support, guidance and reassurance especially over the past year. As a result you probably know more than you ever wanted to know about AML, FLT3-ITD and NOX4/NOX4D! You are without doubt one of the most passionate researchers I have met and will make an excellent supervisor/PI in the near future given your guidance, professionalism and wealth of knowledge. Ash: thank you for the many ROS and antioxidant conversations and for

your guidance and support. Ani: thank you for all the chats, support, adventures and friendship over the past three years. You have been by my side for all of the PhD experience and I wish you every success in the completion of your PhD. Gracias amiga mía.

I was extremely lucky during my PhD as not only did I get to work with members of the TC lab but I also had excellent collaborators. Prof. Frank D. Böhmer and Dr. Ashok Kumar Jayavelu from the Universitatsklinkium Jena and Dr. Sebastian Scholl from Jena University Hospital in Germany are all due a great deal of credit for facilitating in my NOX4D research.

To all my friends I have made in UCC (you know who you are!) and beyond 'the girls' (in no particular order!): Mary, Jess, Liz, Saoirse, Diana, Catarina and Joana. Thank you for all the chats, support and adventures.

Last but not least, I would like to thank my family: Mom, Dad and Paddy for all their love, support and encouragement over the past three years and over my entire life. I could not have achieved this without you.

Abstract

FMS-like tyrosine kinase 3 (FLT3) is a type III receptor tyrosine kinase (RTK) expressed in approximately 90% of acute myeloid leukaemia (AML) patients. Internal tandem duplication of sequences in the juxtamembrane domain of the FLT3 receptor (FLT3-ITD) is the most prevalent FLT3 mutation accounting for 15-35% of AML cases. FLT3-ITD expressing cells produce elevated levels of reactive oxygen species (ROS), particularly NADPH oxidase 4 (NOX4) - and $p22^{phox}$-generated ROS which act as pro-survival signals. Increased ROS production in AML is linked to enhanced cell survival and proliferation as well as a differentiation block. Little was known of the mechanism in which the FLT3-ITD oncoprotein activates NOX4-generated hydrogen peroxide (H_2O_2) and thus this PhD project was designed to elucidate the mechanism.

The FLT3-ITD mutation results in ligand-independent constitutive activation of the FLT3 receptor at the plasma membrane and impaired trafficking of the FLT3 receptor in compartments of the endomembrane system, such as the endoplasmic reticulum (ER). Firstly, we investigated FLT3-ITD-induced activation of aberrant pro-survival signalling cascades resulting in the activation and generation of NOX4- and $p22^{phox}$-generated H_2O_2 at the plasma membrane and ER. To this end, receptor trafficking inhibitors, tunicamycin and brefeldin A were employed and resulted in ER retention of FLT3-ITD in the FLT3-ITD expressing AML MV4-11 cell line. Inhibition of FLT3-ITD cell surface expression resulted in decreased NOX4 and $p22^{phox}$ protein levels, suggesting an important role for FLT3-ITD subcellular localisation in the generation of pro-survival ROS. We found that PI3K/AKT signalling only occurs downstream of FLT3-ITD at the plasma membrane and is required for the generation

of NOX4- and $p22^{phox}$-generated pro-survival H_2O_2 in AML. Taken together, these findings identify that FLT3-ITD at the plasma membrane is responsible for the production of NOX4- and $p22^{phox}$-generated H_2O_2.

Next, we investigated and identified the pro-survival signalling pathways downstream of FLT3-ITD at the plasma membrane and the ER. The PI3K/AKT and ERK1/2 signalling pathways are activated and GSK3β signalling is inhibited downstream of FLT3-ITD at the plasma membrane. STAT5 signalling is activated downstream of FLT3-ITD at the ER. Activation of the ERK1/2 pathway results in the inhibition of GSK3β signalling through phosphorylation of serine at position 9.

NOX4 is a major source of ROS in AML. Given its constitutive activity we investigated its subcellular localisation. We show for the first time that FLT3-ITD expressing patient samples and cells express the NOX4 splice variant D (NOX4D 28 kDa). FLT3-ITD expressing AML cells express NOX4D in the nuclear membrane where it is contributing to endogenous H_2O_2 and may be involved in genetic instability. We have also identified that prototype NOX4 and $p22^{phox}$ colocalise to the nuclear membrane of MV4-11 and 32D/FLT3-ITD cells. Glycosylation of NOX4 and NOX4D is critical for their oncogenic effects. We have shown that the PI3K/AKT and STAT5 pathways are responsible for the production of NOX4D-generated pro-survival H_2O_2 in FLT3-ITD expressing AML.

In summary, this thesis elucidates the mechanism in which activation and localisation of FLT3-ITD stimulates the PI3K/AKT and STAT5 pro-survival signalling pathways. This in turn leads to elevated production of NOX4-, NOX4D- and $p22^{phox}$-generated H_2O_2 in AML which may contribute to DNA damage and

genetic instability. My work therefore presents FLT3-ITD at the plasma membrane and NOXs as attractive therapeutic targets in the treatment of AML.

Abbreviations

AC220	Quizartinib
AEBSF	4-(2-Aminoethyl) benzenesulfonyl fluoride hydrochloride
AEJ	Alternative end joining
AG1295	Tyrphostin
AKT	Protein kinase B
ALL	Acute lymphoblastic leukaemia
AML	Acute myeloid leukaemia
ANOVA	Analysis of variance
Apaf-1	Apoptotic protease activating factor 1
APL	Acute promyelocytic leukaemia
ARF	Adenosine diphosphate-ribosylation factor
ASK1	Apoptosis signal-regulating kinase 1
ASXL-1	Additional sex combs-like-1
ATP	Adenosine triphosphate
Bad	Bcl-2-associated death promoter
Bak	Bcl-2-antagonist/killer
Bax	Bcl-2-like protein 4
Bcl-2	B-cell lymphoma 2
Bcl-xL	Bcl-2-extra large
Bcl-w	Bcl-2-like protein 2
BCR-ABL	Breakpoint cluster-Abelson murine leukaemia viral oncogene
Bid	A BH3 domain-only death agonist protein
Bim	Bcl-2-like 11
BMP-2	Bone morphogenetic protein-2
B2M	Beta-2-microglobulin
BSA	Bovine serum albumin
CAT	Catalase
Ca^{2+}	Calcium
$CaCl_2$	Calcium chloride
CBF-AML	Core-binding factor-acute myeloid leukaemia
cDNA	Complementary DNA

CEBPA	CCAAT/enhancer binding protein α
CEP-701	Lestaurtinib
ChIP	Chromatin immunoprecipitation
chr.b.nuclear	Chromatin bound nuclear
CLL	Chronic lymphocytic leukaemia
CML	Chronic myeloid leukaemia
COX	Cyclooxygenase
CO_2	Carbon dioxide
CpG	Cytosine-phosphate-guanine
Cq	Quantification cycle
Cu^{2+}	Copper
Cu/ZnSOD	Copper/zinc superoxide dismutase
Cys-SH	Cysteine
Cys-SOH	Cysteine sulphenic acid
Cys-S-S-Cys	Cysteine disulphide
DEP-1	Density-enhanced phosphatase-1
2DG	2 Deoxy-glucose
DMEM	Dulbecco's Modified Eagle's Medium
DMSO	Dimethyl sulfoxide
DNA	Deoxyribonucleic acid
DNMT3A	DNA methyltransferase 3A
DPI	Diphenyleneiodonium
DPX	Distyrene plasticizer xylene
Dsbs	Double strand breaks
DUOX	Dual oxidase
DUSP6	Dual-specificity phosphatase 6
D835Y	Aspartic acid substituted with a tyrosine at amino acid 835
EGF	Epidermal growth factor
EGTA	Ethylene glycol tetraacetic acid
ER	Endoplasmic reticulum
ERK1/2	Extracellular signal-regulated kinase 1/2
ETC	Electron transport chain
EV	Empty vector
EZH2	Enhancer of zeste homologue 2

E76K	Glutamic acid substituted with a lysine at amino acid 76
FAB	French-American-British
FACS	Fluorescence Activated Cell Sorting
FAD	Flavin adenine dinucleotide
FADD	Fas-associated protein with death domain
FBS	Foetal bovine serum
FDA	Food and Drug Administration
Fe^{2+}	Iron
FSC-H	Forward scatter-height
FMS	Macrophage colony-stimulating factor receptor
FL	FMS-like tyrosine kinase 3 ligand
FLK-2	Foetal liver kinase 2
FLT3	FMS-like tyrosine kinase 3
FLT3-ITD	FLT3-internal tandem duplication
FLT3-TKD	FLT3-tyrosine kinase domain
FLT3-WT	FLT3-wild type
FOXO	Forkhead transcription factor
GAPDH	Glyceraldehyde 3-phosphate dehydrogenase
GF	Growth factor
GSH	Glutathione
GSK3β	Glycogen synthase kinase-3 β
GPX	Glutathione peroxidase
HA	Human influenza hemagglutinin
HBSS	Hanks' balanced salt solution
HCl	Hydrochloric acid
HDAC	Histone deacetylase
HDAC1	Histone deacetylase 1
HEK	Human embryonic kidney
HIF-1	Hypoxia-inducible factor 1
HOCl	Hypochloric acid
HSC	Haematopoietic stem cells
H_2O_2	Hydrogen peroxide
H_2O	Water
HUVEC	Human umbilical vein endothelium cells

γH2AX	Gamma histone H2A, member X (phosphorylated H2AX)
IDH	Isocitrate dehydrogenase
IGF-1	Insulin like growth factor-1
IL-3	Interleukin-3
JAK2 V617F	Janus Kinase 2 substitution of valine for phenylalanine at amino acid 617
JM	Juxtamembrane
JNK	c-Jun N-terminal protein kinase
kDa	Kilodalton
KDEL	K-lysine D-aspartic acid E-glutamic acid L-leucine
Keap1	Kelch-like ECH-associated protein 1
KIT	Stem cell/steel factor receptor
LiCl	Lithium chloride
LPS	Lipopolysaccharide
LSC	Leukaemic stem cell
MAPK	Mitogen activated-protein kinase
MDS	Myelodysplastic syndromes
MLL	Mixed lineage leukaemia
Mn^{2+}	Manganese
MnSOD	Manganese superoxide dismutase
MPNs	Myeloproliferative neoplasms
mRNA	Messenger RNA
NaCl	Sodium chloride
NAD/NADH	Nicotinamide adenine dinucleotide
NADP	Nicotinamide adenine dinucleotide phosphate
NADPH	Reduced nicotinamide adenine dinucleotide phosphate
NF-κB	Nuclear factor-κB
NHEJ	Non-homologous end joining
NOX	NADPH oxidase
NOXA1	NOX activator 1
NOXO1	NOX organiser 1
NOX4D	NOX4 splice variant D (28 kDa)
NO_3^-	Peroxynitrite
NPM1	Nucleophosmin 1

NP-40	Nonyl Phenoxypolyethoxylethanol-40
NRAS	Neuroblastoma RAS Viral Oncogene Homologue
Nrf2	Nuclear factor (erythroid-derived 2)-like 2
NSAID	Nonsteroidal anti-inflammatory drug
NucPE1	Nuclear Peroxy Emerald 1
NUP98	Nucleoporin 98 kDa
O_2	Oxygen
$O_2^{\bullet-}$	Superoxide
$OH^{\bullet}$	Hydroxyl
8-OHdG	8-hydroxy-2'-deoxyguanosine
$p22^{phox}$	p22 phagocyte oxidase
PARP	Poly ADP ribose polymerase
PBS	Phosphate-buffered saline
PCR	Polymerase chain reaction
PDGF	Platelet-derived growth factor
p-FLT3	Phospho-FLT3
PFA	Paraformaldehyde
PI3K	Phosphoinositide-3-kinase
PKC412	Midostaurin/Rydapt
PKD	Protein kinase D
PM	Plasma membrane
PMSF	Phenylmethylsulfonyl fluoride
PO1	Peroxy Orange 1
PRL2	Phosphatase of regenerating liver 2
PRL3	Phosphatase of regenerating liver 3
PSMB2	Proteasome (prosoma/macropain) subunit, beta type, 2
PTEN	Phosphatase and tensin homolog
PTK	Protein-tyrosine kinase
PTP	Protein tyrosine phosphatase
PTP1B	Protein tyrosine phosphatase 1B
PTPN11	Protein tyrosine phosphatase non-receptor type 11
PTPRD	Protein tyrosine phosphatase receptor type D
PTPRJ	Protein tyrosine phosphatase receptor type J
PRX	Peroxiredoxin

RAC1/2	RAS-related C3 Botulinum Toxin Substrate 1/2
RAS	Rat Sarcoma viral oncogene
Redox	Reduction-oxidation
RIPA	Radio-immunoprecipitation assay
RNA	Ribonucleic acid
RNAi	RNA interference
ROS	Reactive oxygen species
[ROS]	Concentration of ROS
Rpm	Rotations per minute
RPMI	Roswell Park Memorial Institute
rRNA	Ribosomal RNA
RT	Room temperature
RT-qPCR	Reverse transcription quantitative real time polymerase chain reaction
RTK	Receptor tyrosine kinase
RUNX1	Runt-related transcription factor 1
RUNX1T1	RUNX1 translocation partner 1
SD	Standard Deviation
SDS	Sodium Dodecyl Sulphate
SDS-PAGE	SDS-Polyacrylamide Gel Electrophoresis
Ser	Serine
SHP-2	Src homology region 2-containing protein tyrosine phosphatase 2
shRNA	Small hairpin RNA
siRNA	Small interfering RNA
SOD	Superoxide dismutase
Src	Rous sarcoma oncogene cellular homolog
SSC-H	Side scatter-height
STAT5	Signal transducer and activator of transcription 5
STS1	Suppressor of T cell signalling protein 1
STS2	Suppressor of T cell signalling protein 2
TBS	Tris-Buffered Saline
TBST	Tris-Buffered Saline/0.1% Tween-20
TCA	Tricarboxylic acid cycle
TET2	Tet methylcytosine dioxygenase 2
TGFβ	Transforming growth factor β

Thr	Threonine
TKI	Tyrosine kinase inhibitor
TLR4	Toll like receptor 4
TNFα	Tumour necrosis factor α
TNFR1	TNF receptor 1
TRX	Thioredoxin
Tyr	Tyrosine
UBASH3A	Ubiquitin-associated and SH3 domain containing protein 3A
UBASH3B	Ubiquitin-associated and SH3 domain containing protein 3B
UT	Untreated
U0126	Monoethanolate
VSMC	Vascular smooth muscle cells
WEHI-CM	WEHI-conditioned medium
WHO	World Health Organization
w/v	Weight per volume
Zn^{2+}	Zinc
µg/ml	Microgram per millitre
°C	Degrees Celsius

Publications and Presentations

Publications

Moloney JN, Jayavelu AK, Stanicka J, Roche SL, O'Brien RL, Scholl S, Böhmer F-D, Cotter TG. Nuclear membrane-localised NOX4D generates pro-survival ROS in FLT3-ITD-expressing AML. Oncotarget. 2017; 8: 105440-57.

Moloney JN, Cotter TG. ROS signalling in the biology of cancer. Seminars in Cell & Developmental Biology. 2017, http://dx.doi.org/10.1016/j.semcdb.2017.05.023 (In Press)

Moloney JN, Stanicka J, Cotter TG. Subcellular localization of the FLT3-ITD oncogene plays a significant role in the production of NOX- and $p22^{phox}$-derived reactive oxygen species in acute myeloid leukemia. Leukemia Research. 2017; 52: 34-42.

Moloney JN, Cotter TG. Subcellular Localization of the FLT3-ITD Oncogene Is Critical for the Production of NOX4- Generated Hydrogen Peroxide in Leukemia. Free Radical Biology and Medicine. 2016; 100: S127. *(SFRBM Conference Abstract)*

Moloney JN*, Jayavelu AK*, Böhmer F-D, Cotter TG. NOX-driven ROS formation in cell transformation of FLT3-ITD-positive AML. Experimental Hematology. 2016; 44(12): 1113-22.

Presentations

February 2016:	Irish Association for Cancer Research Conference, Cork, Ireland. *Poster Presentation.*
June 2016:	International Cell Death Society Conference, Cork, Ireland. *Poster Presentation.*
November 2016:	Society for Redox Biology and Medicine Conference, San Francisco, CA, USA. *Poster Presentation.*

Listed as a co-author in the following publications:

Roche SL, Ruiz-Lopez AM, **Moloney JN**, Byrne AM, Cotter TG. Microglial-induced Müller cell gliosis is attenuated by progesterone in a mouse model of retinitis pigmentosa. Glia. 2018; 66: 295-310.

Ruiz Lopez AM, Roche SL, Wyse Jackson AC, **Moloney JN**, Byrne AM, Cotter TG. Pro-survival redox signalling in progesterone-mediated retinal neuroprotection. European Journal of Neuroscience. 2017; 46: 1663-72.

Wyse-Jackson AC, Roche SL, Ruiz-Lopez AM, **Moloney JN**, Byrne AM, Cotter TG. Progesterone analogue protects stressed photoreceptors via bFGF-mediated calcium influx. European Journal of Neuroscience. 2016; 44: 3067-79.

Byrne AM, Ruiz-Lopez AM, Roche SL, **Moloney JN**, Wyse -Jackson AC, Cotter TG. The synthetic progestin norgestrel modulates Nrf2 signaling and acts as an antioxidant in a model of retinal degeneration. Redox Biology. 2016; 10: 128-39.

Chapter 1. Introduction

1.1. Leukaemia

The term leukaemia refers to cancer of the blood and bone marrow and is characterised by the abnormal growth and proliferation of white blood cells or leukocytes. The word leukaemia is derived from the Greek words *leukos* 'white' and *haima* 'blood'. In 2012, 352,000 new leukaemia cases were diagnosed worldwide, which accounts for 2.5% of all cancers (Ferlay et al., 2015). Leukaemia is classified according to the lineage of the white blood cells affected, myeloid or lymphoid, and acute or chronic depending on the aggressiveness of the disease. Chronic forms of leukaemia are characterised by the excessive accumulation of mature, abnormal blood cells, and acute forms of leukaemia are characterised by the rapid increase in immature blood cells or 'blasts'. There are four major subtypes of leukaemia: Chronic Myeloid Leukaemia (CML), Chronic Lymphocytic Leukaemia (CLL), Acute Myeloid Leukaemia (AML) and Acute Lymphocytic Leukaemia (ALL) (LLS, 2011).

1.1.1. Acute Myeloid Leukaemia (AML)

1.1.1.1. Epidemiology and current treatment of AML

AML accounts for approximately 25% of all leukaemia cases (Kumar, 2011) and is the second most frequent form of leukaemia after CLL (Bhayat et al., 2009, Yamamoto and Goodman, 2008). AML is the most common malignant myeloid disorder in adults and has an incidence of 3.8 cases per 100,000 rising to 17.9 per 100,000 in adults aged 65 years and over (Estey and Döhner, 2006). It is responsible for approximately 50% of leukaemic deaths in children (Meshinchi and Arceci, 2007). Acute myeloid leukaemia is a heterogeneous clonal disorder of haematopoietic progenitor cells 'blasts' which are unable to differentiate into mature and functional

monocytes or granulocytes, but accumulate in bone marrow, peripheral blood and spleen and interfere with normal haematopoiesis (Bonnet and Dick, 1997, Estey and Döhner, 2006, Preisler and Lyman, 1977). Several factors that influence the risk of acquiring AML include epigenetics, chromosomal aberrations, genetic mutations, gender, environmental conditions and haematological disorders (Levine and Bloomfield, 1992).

The strategy of AML treatment has not changed substantially in over 30 years. The worldwide standard of care for AML patients who are not participating in clinical trials, receive an induction of chemotherapy with a cytarabine and an anthracycline (idarubicin and daunorubicin), followed by either one to four cycles of consolidation chemotherapy, autologous stem cell transplantation or allogeneic stem cell transplantation (Roboz, 2012). This standard treatment with chemotherapy maximally results in 70-80% of patients less than 65 years achieving complete remission, most will eventually relapse and an overall survival rate of only 40-50% at 5 years (Emadi and Karp, 2014). Several factors have been associated with more severe outcomes at relapse including unfavourable cytogenetics at diagnosis, old age and also prior history of haematopoietic stem cell transplantation (Breems et al., 2005). More novel treatments have not been approved in recent times due to high levels of toxicity or little level of effectiveness. This demonstrates the importance and need for development of new drugs.

1.1.1.2. Haematopoiesis

Haematopoiesis is the process of creating new blood cells in the body and is derived from the Greek words *haima* ‘blood’ and *poiesis* ‘to make’ (Figure 1.1.).

Normal haematopoiesis is dependent upon tightly controlled and inter-related mechanisms regulating cell survival, proliferation and differentiation. It is initiated in the bone by haematopoietic stem cells (HSC). The HSC population is relatively quiescent (Bradford et al., 1997), however, upon entry to the cell cycle it gives rise to differentiating progenitor cells that undergo extensive proliferative expansion in order to replenish the blood system and also in response to stresses including infection and injury (Pietras, 2017). In haematological malignancies normal haematopoiesis is interrupted due to the uncontrolled growth of genetically altered stem cells that retain the ability of self-renewal (Aleem and Arceci, 2015).

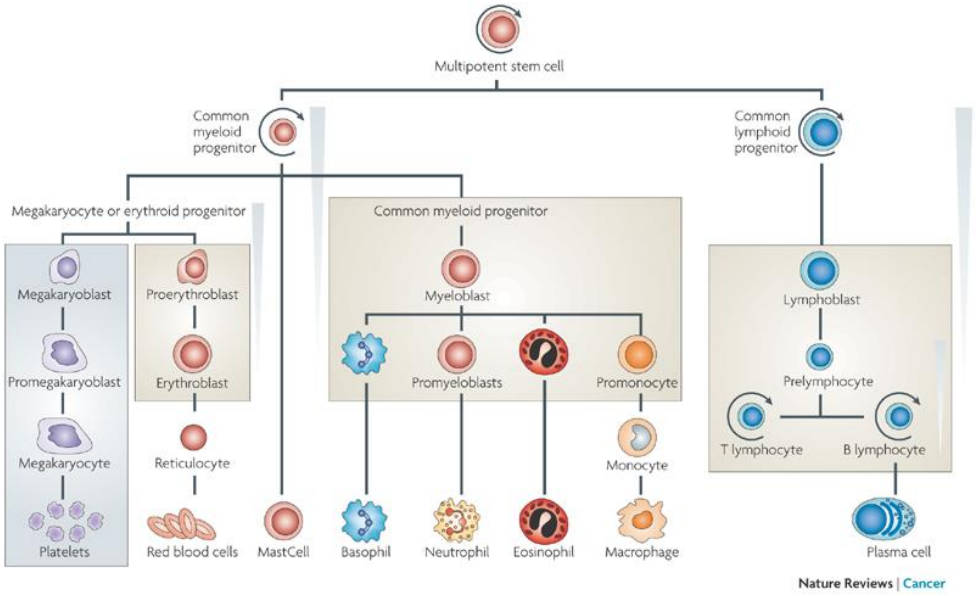

Figure 1.1. Schematic of haematopoiesis. AML is an aggressive malignancy characterised by a block in myeloid differentiation. HSCs are responsible for the generation of mature blood cells. Normal haematopoiesis is interrupted in AML due to the uncontrolled growth of genetically altered leukaemic stem cells resulting in the uncontrolled accumulation and proliferation of abnormal myeloid progenitors that accumulate in the peripheral blood, bone marrow and spleen. (Taken from (Ramsay and Gonda, 2008))

In AML, the haematopoietic progenitor acquires abnormalities including the imbalance of the three key processes: cell survival, proliferation and differentiation

resulting in the expansion of the leukaemic stem cell (LSC) (Bonnet and Dick, 1997). In order to develop into a fully malignant disease, these abnormalities require multiple independent genetic and epigenetic alterations in oncogenes and/or tumour suppressor genes. LSCs are characterised by unlimited self-renewal, cytoprotection and attenuated telomerase activity (Lane and Gilliland, 2010). LSCs are not found circulating in the blood, they primarily reside in the bone marrow microenvironment. This is of great importance from a clinical perspective as it enables them to avoid the cytotoxic effects of chemotherapy and to re-emerge, resulting in relapse of the disease (Lane et al., 2009).

1.1.1.3. Pathogenesis in AML

AML refers to a heterogeneous group of diseases, the molecular basis of which can be multi-factorial or complex. A range of genetic, as well as cytogenetic abnormalities, have been identified that lead to the molecular alterations giving rise to the AML phenotype. The European Leukaemia Net Prognostic system categorises AML patients into four risk groups: favourable, intermediate-I, intermediate-II and adverse (Mrózek et al., 2012). The groups are classified depending on the subsets of cytogenetic and molecular markers. This classification allows prediction of response to chemotherapy or stem cell transplantation. For example, internal tandem duplications of sequences in the juxtamembrane domain of macrophage colony-stimulating factor receptor (FMS)-like tyrosine kinase 3 (FLT3-ITD) are associated with a poor prognosis due to an aggressive disease phenotype. The primary diagnosis of AML is based on the presence of leukaemic myeloblasts in preparations of peripheral blood and bone marrow stained with Wright-Giemsa. Once AML diagnosis is confirmed, the genetic and morphological subtype must be identified. The most

commonly used method of classification was developed by the French-American-British (FAB) group which categorises AML into nine distinct subgroups that differ in respect to the myeloid lineage involved and the rate of leukaemia-cell differentiation (Table 1.1.) (Lowenberg et al., 1999). The World Health Organization (WHO) has a newer system of classifying AML *'World Health Organization (WHO) Classification of Tumours of Haematopoietic and Lymphoid Tissues'* into several groups based on genetic abnormalities such as translocation or inversion of chromosomes, revised in 2016 (Cazzola, 2016).

FAB subtype	**Name**	**% of cases**
M0	Undifferentiated acute myeloblastic leukaemia	3%
M1	Acute myeloblastic leukaemia with minimal maturation	15-20%
M2	Acute myeloblastic leukaemia with maturation	25-30%
M3	Acute promyelocytic leukaemia (APL)	5-10%
M4	Acute myelomonocytic leukaemia	20%
M4Eo	Acute myelomonocytic leukaemia with eosinophilia	5-10%
M5	Acute monocytic leukaemia	2-9%
M6	Acute erythroid leukaemia	3-5%
M7	Acute megakaryocytic leukaemia	3-12%

Table 1.1. **The French-American-British (FAB) classification of AML.**

1.1.1.4. Chromosomal aberrations in AML

AML is polyclonal, particularly at initial diagnosis (Levis, 2013). The clonal origin of AML was initially described by the presence of acquired non-random chromosomal aberrations present in haematopoietic progenitor cells (Guan et al., 2002, Döhner and Döhner, 2008). 749 chromosomal abnormalities have been recorded in AML (Kumar, 2011). Non-random chromosomal aberrations including deletions, translocations, inversions and monosomies have been detected in 55% of AML patients and are very important prognostic factors in terms of remission, relapse and survival (Döhner and Döhner, 2008). This evidence suggests that leukaemogenesis is a multi-step process. The most prevalent targets of chromosomal-associated translocations in AML are genes that encode DNA-binding transcription factors or the regulatory components of transcriptional complexes (Lowenberg et al., 1999).

Patients with myelodysplastic syndromes (MDS) have an increased risk of disease evolution to leukaemia and this is associated with chromosomal alterations. Approximately 30% of MDS cases progress to AML (Nolte and Hofmann, 2010). The most common chromosomal aberrations in AML include 1% inversion (3)/translocation (3;3), 1% translocation (6;9), 2% translocation (11q23), 6% inversion (16)/translocation (16;16), 5% translocation (8;21), 23% are described as having various karyotypes including trisomy 8, 11, 13, 21 and 22, loss of 5q and chromosome X, Y or 7 (CCAAT/enhancer binding protein α (CEBPA), mixed lineage leukaemia gene (MLL) and Nucleophosmin 1 (NPM1) and Runt-related transcription factor 1 (RUNX1) mutations), and 11% defined as having a complex karyotype of multiple gains, losses and rearrangements (*TP53* mutations) (Nolte and Hofmann, 2010, Döhner and Döhner, 2008, Lal et al., 2017).

Oncogenic fusion proteins are generated as a consequence of specific chromosomal translocations and at sites of chromosomal breaks. For example, chromosomal translocations, such as translocation (8;21) in core-binding factor AML (CBF-AML) result in the formation of chimeric fusion protein Runt-related transcription factor 1 (RUNX1)-RUNX1 translocation partner 1 (RUNX1T1) (Döhner and Döhner, 2008). The RUNX1-RUNX1T1 fusion protein results in impaired myeloid differentiation (De Kouchkovsky and Abdul-Hay, 2016), however the fusion protein does not result in a fully leukaemic phenotype in a murine model (Döhner and Döhner, 2008). The initiating fusion oncogenes have to be followed by a complementing mutation that activates signal transduction pathways, resulting in increased cell survival and proliferation, and a block in differentiation and apoptosis. Often these mutations result in the activation of receptor tyrosine kinase signalling pathways, for example, FLT3, stem cell/steel factor receptor (KIT) and Neuroblastoma RAS Viral Oncogene Homologues (NRAS) (Döhner and Döhner, 2008).

1.1.1.5. Genetic alterations in AML

AML mutations have been classified into two classes collectively known as the 'two-hit' model. Class I mutations are mutations that result in the activation of signal transduction pathways leading to increased cell survival and proliferation, for example, FLT3, Breakpoint cluster-Abelson murine leukaemia viral oncogene (BCR-ABL), Rat sarcoma viral oncogene (RAS) or Janus kinase 2 (JAK2) (Conway O'Brien et al., 2014). Class II mutations are mutations that affect differentiation preventing the maturation of cells and also affect self-renewal, for instance, CCAAT/enhancer binding protein α (CEBPA), mixed lineage leukaemia gene (MLL) and

Nucleophosmin 1 (NPM1). In order for the disease to develop, a class I AML mutation must be accompanied by a class II mutation (Shih et al., 2012, Naoe and Kiyoi, 2013).

1.1.1.6. Epigenetic abnormalities in AML

For many years, AML mutations also known as the 'two-hit' model were the accepted model of leukaemogenesis in AML (Conway O'Brien et al., 2014, Shih et al., 2012). However, class I and class II AML mutations are only one part of a more complex picture. Epigenetic alterations are now recognised as playing an equally important role in the pathogenesis of AML (Plass et al., 2008). The term epigenetics is the study of inheritable changes in gene expression that do not involve changes in the DNA sequence itself (Shih et al., 2012). Epigenetics involves the interplay between three main components: DNA methylation, chromatin and non-coding RNA (Plass et al., 2008). DNA methyltransferases and histone methyltransferases are well known epigenetic modifiers (Islam et al., 2017). Mutations in genes regulating histone modification, DNA methylation and DNA hydroxymethylation states in haematopoietic progenitors are emerging as critical events in AML (Shih et al., 2012).

Studies have identified more than 1,300 highly methylated gene promoters in AML. Approximately 1,100 of these genes are hypermethylated in 5% of AML patients while 200 gene promoters are hypermethylated in 90% of AML patients (Islam et al., 2017). DNA methyltransferases are responsible for *de novo* methylation and are frequently mutated in AML, for example, DNA methyltransferase 3A (DNMT3A) (Islam et al., 2017, Conway O'Brien et al., 2014). DNA methyltransferases catalyse the addition of a methyl group to the 5' position of the cytosine ring specifically in 5'-cytosine-phosphate-guanine-3' (CpG) dinucleotide

sequences (Plass et al., 2008, Conway O'Brien et al., 2014). DNMT3A is mutated in 15-25% of AML (Shih et al., 2012, Ley et al., 2010, Patel et al., 2012, Conway O'Brien et al., 2014, Ferreira et al., 2015), resulting in impaired catalytic activity (Holz-Schietinger et al., 2012). DNMT3A is necessary for normal haematopoietic cell differentiation (Mehdipour et al., 2015, Challen et al., 2011). Mutations in DNMT3A have been linked to decreased methylation of some genes in AML (Hájková et al., 2012). Other genes involved in the regulation of DNA hydroxymethylation include Tet methylcytosine dioxygenase 2 (TET2) and isocitrate dehydrogenase 1 and 2 (IDH1 and IDH2) (Mehdipour et al., 2015, Conway O'Brien et al., 2014). TET2 is mutated in 7-23% of AML (Metzeler et al., 2011, Ahn et al., 2015, Shih et al., 2012) and IDH1 and IDH2 are mutated in 15-30% of AML (Figueroa et al., 2010, Rakheja et al., 2012, Paschka et al., 2010). Cancers have altered patterns of DNA methylation and the global level of DNA methylation is often lower in malignant cells (Wajed et al., 2001, Ehrlich, 2009). Hypermethylation of cytosines in CpG islands is associated with silencing of tumour suppressor genes contributing to carcinogenesis (Plass et al., 2008, Conway O'Brien et al., 2014, Mehdipour et al., 2015, Baylin, 2005, Ehrlich, 2009). Some of the genes implicated in the regulation of histones are also mutated in AML, for example, enhancer of zeste homologue 2 (EZH2) and additional sex combs-like 1 (ASXL-1) (Conway O'Brien et al., 2014, Shih et al., 2012).

Alterations in genome wide methylation patterns and mutations in epigenetic modifiers presents deregulation of epigenetics as one of the fundamental causal agents in the development of AML (Islam et al., 2017). Pharmacological reversal of aberrant epigenetic changes that result in silencing of genes in haematopoiesis can restore the normal function of the bone marrow as well as showing a clinical response in AML (Plass et al., 2008). Some of the epigenetic compounds currently approved for clinical

use in myeloid malignancies include inhibitors of DNA methyltransferases, 5-azacytidine (azacitidine) and 5-aza-2' deoxycytidine (decitabine) and histone deacetylase (HDAC) inhibitors that have been tested in clinical trials for the treatment of malignancies including AML (Wouters and Delwel, 2016).

1.1.2. FLT3 signalling in AML

1.1.2.1. FLT3

FMS-like tyrosine kinase 3 (FLT3) also known as foetal liver kinase-2 (FLK-2), is a type III receptor tyrosine kinase (RTK) expressed in approximately 90% of acute myeloid leukaemia cases. FLT3 is involved in the early stages of haematopoiesis and is important for normal development of stem cells and the immune system (Stirewalt and Radich, 2003, Gilliland and Griffin, 2002). Mutations in FLT3 are present in 25-45% of AML patients, making it the most prevalent genetic aberration in AML (Stirewalt and Radich, 2003). FLT3 has structural similarities to other class III RTKs including macrophage colony-stimulating factor receptor (FMS) and platelet-derived growth factor receptor (PDGF). Class III RTKs play an important role in cell growth and differentiation of leukaemic cells (Berenstein, 2015).

1.1.2.2. FLT3 structure

The FLT3 gene encodes a 993-amino acid protein in humans and is expressed in early lymphoid and myeloid haematopoietic cells (Rosnet et al., 1996). The RTK FLT3 is composed of five extracellular immunoglobulin-like domains, a transmembrane domain, a juxtamembrane dimerization domain and two cytoplasmic domains or an interrupted kinase domain (Levis and Small, 2003) (Figure 1.2.). Two

forms of FLT3 exist, a mature glycosylated 160 kDa protein and an immature unglycosylated 130 kDa protein (Stirewalt and Radich, 2003).

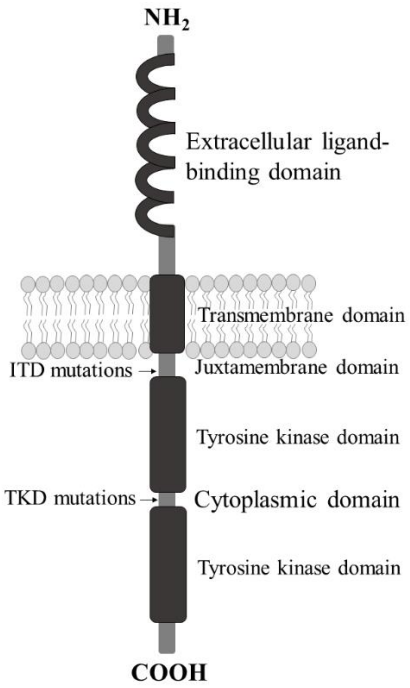

Figure 1.2. FLT3 structure. The FLT3 protein is composed of an extracellular ligand-binding domain, a transmembrane domain, a juxtamembrane domain, and two cytoplasmic domains with tyrosine kinase motifs.

The unstimulated form of the FLT3 receptor resides as a monomer in the plasma membrane, unphosphorylated with an inactive kinase domain (Köthe et al., 2013, Grafone et al., 2012). Upon interaction with the FLT3 ligand (FL), the receptor autophosphorylates and undergoes a conformational change resulting in unfolding of the protein, leading to the exposure of the dimerization domain, thus allowing receptor-receptor dimerization and activation of the kinase domain to occur (Levis and Small, 2003). FLT3 signalling is tightly controlled by the internalisation of FLT3-FL complex and is partly involved in the negative regulation of FLT3 signalling

monitoring survival and proliferation in these cells (Turner et al., 1996). Activation of the FLT3 receptor results in the activation of pro-survival cell signalling pathways including Raf/MEK/ERK, PI3K/AKT and JAK/STAT (Masson and Rönnstrand, 2009).

1.1.2.3. FLT3 mutations in haematological malignancies

There are two types of FLT3 mutations implicated in AML- the FLT3 internal tandem duplication (FLT3-ITD) mutation and mutations within the activation loop of the tyrosine kinase domain of FLT3 (FLT3-TKD). Internal tandem duplications in exons 14 and 15 of FLT3 (FLT3-ITD) are the most common mutation expressed in 15-35% of AML cases, 1-3% of ALL cases and 5-10% of patients with myelodysplastic syndromes (MDS) (Stirewalt and Radich, 2003). FLT3-ITD results in structural and conformational changes to the juxtamembrane domain, disrupting auto-inhibitory functions of the receptor resulting in constitutive activation of the receptor at the plasma membrane, and impaired trafficking of the receptor in compartments of its biosynthetic route, such as the endoplasmic reticulum (ER) (Choudhary et al., 2009, Moloney et al., 2017b), as well as activation of downstream effectors. AML patients with the FLT3-ITD mutation have a poor prognosis (Thiede et al., 2002, Small, 2008), with an increased risk of relapse following treatment with chemotherapy and a lower rate of overall survival (Grafone et al., 2012, Stirewalt and Radich, 2003). FLT3-ITD harbouring cases relapse more often and quicker than people without the mutation (Grafone et al., 2012) and patients with other AML subtypes (Levis and Small, 2003). The FLT3-TKD mutation is less common with an incidence of approximately 7% in AML (Thiede et al., 2002). In its inactive state, the conformation of the activation loop prevents access for adenosine triphosphate (ATP)

and substrate, resulting in an inactive kinase. Following interaction with FL, phosphorylation of the activation loop results in a folded out conformation providing access for ATP and substrate (Weiss and Schlessinger, 1998). One of the most common FLT3-TKD mutations is a missense mutation where aspartic acid is substituted with a tyrosine in exon 20 (D835Y) causing the activation loop to remain in the folded out conformation, resulting in tyrosine kinase activity. This mutation occurs in 5-10% of AML cases, 1-3% of ALL cases and 2-5% of patients with MDS (Yamamoto et al., 2001).

1.1.2.4. Current treatment of AML patients with FLT3 mutations

Newly diagnosed FLT3-ITD patients receive standard induction chemotherapy with similar results to other AML patients. However, patients that are hemizygous for FLT3-ITD mutations have a shorter remission and relapse at much higher rate compared to patients without the mutation (Grafone et al., 2012, Levis and Small, 2003). The median rate of survival in FLT3-ITD AML cases after first remission is less than five months (Ravandi et al., 2010, Levis et al., 2011, Levis, 2011). The survival rate is also the poorest in patients with the FLT3-ITD mutation (Grafone et al., 2012). Allogeneic stem cell transplantation in patients with the FLT3-ITD mutation at first remission have a better outcome than the conventional consolidation chemotherapy (Levis, 2013). Yet there are some patients that cannot undergo intensive induction chemotherapy or allogeneic stem cell transplantation, for example, the elderly, hence treatment options for these patients are limited.

The current rationale in terms of treatment of FLT3 mutations in AML is to target deregulated pathways that drive blast proliferation. Inhibition of tyrosine

kinases using tyrosine kinase inhibitors (TKIs) has been identified as a popular strategy. However, TKIs have been shown to have inhibitory effects against other RTKs due to the structural homology of the receptor, causing off-target effects. Some of the tyrosine kinase inhibitors currently undergoing clinical trials include lestaurtinib (CEP-701) and quizartinib (AC220). Lestaurtinib and midostaurin are two of the most extensively studied TKIs in FLT3-expressing AML (Grafone et al., 2012). However, treatment with lestaurtinib following chemotherapy has been shown to have no effect on response rate and survival (Levis et al., 2011). Quizartinib is the most recent FLT3 tyrosine kinase inhibitor under clinical investigation (Fathi and Levis, 2011) and has been shown to increase survival rate *in vivo* in a mouse model of FLT3-ITD AML. It has also been found to inhibit FLT3 activity in primary AML cells (Zarrinkar et al., 2009). Rydapt (midostaurin, formerly known as PKC412), a protein tyrosine kinase inhibitor targeted towards FLT3-ITD positive AML is the first new treatment in over 25 years (Schiller, 2013, Lin and Levy, 2012, Rydapt, 2017) following Food and Drug Administration (FDA) approval in 2017. Rydapt treatment regime in FLT3-ITD expressing AML demonstrated a significant improvement in overall survival with a 23% reduction in the risk of death (Rydapt, 2017). Rydapt will be used in combination with certain chemotherapy drugs to effectively target FLT3-ITD in AML.

1.1.2.5. FLT3 glycosylation

Glycosylation is the most common post-translational modification (Zhang and Wang, 2016, Stanley, 2011, Ungar, 2009) occurring in approximately 50% of proteins in cells (Jefferis, 2007, An et al., 2009, Christiansen et al., 2014) providing greater proteomic diversity than any other post-translational modification (Lis and Sharon, 1993). Some of the proteins known to be glycosylated within a cell include secreted

proteins (Lis and Sharon, 1993), cell surface receptors and ligands and organelle-resident proteins (Bieberich, 2014). The glycosylation reaction involves the covalent attachment of a carbohydrate or sugar moiety to functional groups of amino acids in proteins and lipids (Spiro, 2002). Accurate glycosylation must occur in the ER to ensure that only correctly folded proteins are trafficked to the Golgi apparatus, the centre of the secretory pathway (Zhang and Wang, 2016, Lis and Sharon, 1993). Glycosylation is the most complex post-translational modification as there is no template involved compared to other cell processes including transcription and translation (An et al., 2009). Cells rely on highly ordered stepwise reactions and a host of enzymes including glycotransferases, glycosidases and nucleic sugar transporters (Zhang and Wang, 2016). There are several types of glycosylation classified according to the identity of the atom of the amino acid that binds to the carbohydrate chain. These include C-linked glycosylation, N-linked glycosylation, O-linked glycosylation, phosphoglycosylation and glypiated linkage (Spiro, 2002, Zhang and Wang, 2016). C-linked glycosylation involves the covalent attachment of mannose to the indole ring of the amino acid tryptophan within extracellular proteins in the ER (Zhang and Wang, 2016, Gonzalez de Peredo et al., 2002, Spiro, 2002). N-linked glycosylation is the most complex form of glycosylation in which oligosaccharides bind to the amino group of asparagine in the ER (Zhang and Wang, 2016, An et al., 2009, Helenius and Aebi, 2004, Bieberich, 2014). O-linked glycosylation occurs when monosaccharides bind to the hydroxyl group of serine or threonine in the ER, Golgi, cytosol and nucleus (Zhang and Wang, 2016, An et al., 2009, Gonzalez de Peredo et al., 2002, Hounsell et al., 1996). Phosphoglycosylation reaction involves the binding of a glycan to serine via a phosphodiester bond (Haynes, 1998). Glypiation linkage occurs when the glycan core links a phospholipid and a protein (Zhang and Wang, 2016, Pierleoni et al., 2008).

Protein glycosylation has been shown to play a role in protein folding and trafficking, stability and sorting of proteins, protein-protein interactions, cell attachment, stimulation of signal transduction, cell-cell interactions and immunity (Stanley, 2011, Freeze and Ng, 2011, Moremen et al., 2012, Ungar, 2009).

Two forms of FLT3 exist, a mature glycosylated 160 kDa protein and an immature unglycosylated 130 kDa protein (Stirewalt and Radich, 2003). The 130 kDa protein is predominantly present in FLT3-ITD expressing cells and there is proportionally more 160 kDa protein in FLT3-WT expressing cells (Schmidt-Arras et al., 2005, Koch et al., 2008). Previous studies have proven that the two forms of FLT3 differ in size due to differences in glycosylation. In this study they showed that the mannose rich 130 kDa glycoprotein is exclusively present in the ER and also showed evidence of the 160 kDa FLT3 glycosylation to be complex (Schmidt-Arras et al., 2005). Initially the nascent 110 kDa FLT3 polypeptide chains become glycosylated with mannose rich oligosaccharides in the ER to produce the 130 kDa protein. This protein is then subjected to partial deglycosylation by glycosidases prior to transport to the Golgi apparatus where further processing leads to the production of the mature 160 kDa protein which translocates to the cell surface (Schmidt-Arras et al., 2005). Tunicamycin inhibits N-linked glycosylation and has been show to inhibit FLT3 glycosylation (Choudhary et al., 2009, Williams et al., 2012) as well as prevent the binding of the FLT3 ligand to the receptor and consequently inhibit FLT3 activity (Williams et al., 2012). This data presents FLT3 glycosylation as having an important role in signal transduction in FLT3-ITD expressing AML.

1.2. Reactive oxygen species (ROS)

Reactive oxygen species (ROS), are generally considered by-products of oxygen consumption and cellular metabolism (Giorgio et al., 2007, Zorov et al., 2014). ROS are short-lived molecules containing unpaired electrons, formed by the partial reduction of molecular oxygen. They are oxygen containing derivatives comprised of highly unstable oxygen free radicals, for example, superoxide ($O_2^{\bullet-}$) and hydroxyl ($OH^{\bullet}$), which can be quickly converted into more stable, freely diffusible non-radicals including hydrogen peroxide (H_2O_2) and hypochlorous acid (Dickinson and Chang, 2011, Jayavelu et al., 2016b, Winterbourn and Hampton, 2008).

$O_2^{\bullet-}$ and H_2O_2 are the most well studied ROS in cancer, and H_2O_2 is the best described ROS signalling molecule (Finkel, 2011, Reczek and Chandel, 2015). It is important to note that although the sources of H_2O_2 (discussed in section 1.2.1.1) are important when considering its role in pro-survival in cancer, it is also important to understand H_2O_2 signalling and its interactions with downstream target molecules. H_2O_2 is distinct in its signalling activity; it oxidises nucleic acids and critical residues in proteins. Due to their abundance, proteins are the biomolecules most frequently affected by oxidation and are believed to be the main target of ROS (Davies, 2005). Elevated ROS levels can cause reversible post-translational modification of cysteine (Miki and Funato, 2012), selenocysteine (Hawkes and Alkan, 2010), methionine (Hoshi and Heinemann, 2001) and histidine (Lee and Helmann, 2006). For example, cysteines (Cys-SH) are readily oxidised by H_2O_2 to cysteine sulphenic acid (Cys-SOH) or cysteine disulphide (Cys-S-S-Cys). Exposure to ROS leads to oxidation of thiol groups of key cysteine residues in many proteins including kinases, phosphatases and transcription factors (Groeger et al., 2009, Veal et al., 2007).

ROS have long been associated with cancer where different types of tumour cells have been shown to produce elevated levels of ROS compared to their normal counterpart (Panieri and Santoro, 2016). Increased levels of ROS are thought to be oncogenic, causing damage to DNA, proteins and lipids, promoting genetic instability and leading to tumourigenesis (Figure 1.3.) (Liou and Storz, 2010, Roy et al., 2015, Stanicka et al., 2015, Ames et al., 1993, Szatrowski and Nathan, 1991).

1.2.1. Cellular sources and regulation of ROS

1.2.1.1. Cellular sources of ROS

Elevated levels of ROS and $O_2^{\bullet-}$ in cancer may be as a result of reduced free radical scavenging enzymes, increased glucose metabolism (Warburg effect), increased receptor activity in the cell, oncogenic activity, increased presence of growth factors and cytokines. Increased intracellular oxidant production from mitochondria, NADPH oxidases (NOX), cyclooxygenases, lipoxygenases, xanthine oxidases and cytochrome P450 enzymes (Panieri and Santoro, 2016, Vander Heiden et al., 2009, Finkel, 2011, Holmstrom and Finkel, 2014, Sundaresan et al., 1995) results in elevated levels of ROS and $O_2^{\bullet-}$. Mitochondria and NADPH oxidases are two major contributors of endogenous ROS in cancer. Recent studies have shown that crosstalk exists between these two producers (Kröller-Schön et al., 2014).

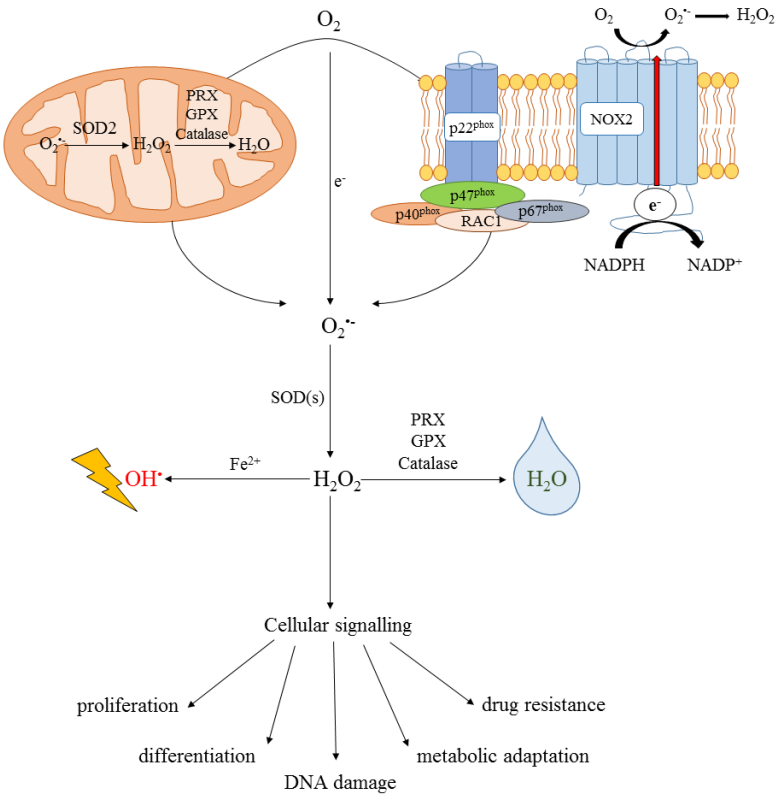

Figure 1.3. Production and regulation of reactive oxygen species (ROS). Mitochondria and membrane bound NADPH oxidases (NOXs) are the two main contributors of endogenous ROS. $O_2^{\bullet-}$ is formed from molecular oxygen (O_2) by accepting a single electron from the electron transport chain (ETC) in the mitochondria or from NOXs. The superoxide dismutase (SOD) enzymes convert $O_2^{\bullet-}$ into H_2O_2. H_2O_2 can then undergo Fenton chemistry with Fe^{2+} to form $OH^{\bullet}$, which is extremely reactive causing damage to DNA, proteins and lipids. H_2O_2 can be reduced and converted to H_2O by peroxiredoxins (PRX), glutathione peroxidases (GPX) and catalase. H_2O_2 is a major signalling molecule involved in cancer resulting in the development and progression of the disease.

1.2.1.1.1 Mitochondria

Mitochondria are one of the largest contributors to the endogenous ROS pool, and it has been estimated that approximately 1% of oxygen (O_2) consumed by mitochondria is used to produce $O_2^{\bullet-}$ (Handy and Loscalzo, 2012). This organelle also generates ATP through the oxidation of amino acids, glucose and lipids. The tricarboxylic acid (TCA) cycle is involved in the removal of one electron from these metabolites and transfer to the electron transport chain (ETC) resulting in a reduction of O_2 to $O_2^{\bullet-}$ (Sabharwal and Schumacker, 2014). Mitochondria have up to ten known sites capable of generating $O_2^{\bullet-}$ (Goncalves et al., 2015). ROS generated from complex I and III of the ETC have been documented to have a role in cellular signalling (Murphy, 2009) (Figure 1.4.). Complex III has been shown to release $O_2^{\bullet-}$ and H_2O_2 into both the intermembrane space and the mitochondrial matrix, and these ROS are required for many biological processes including cell differentiation, oxygen cell sensing and adaptive immunity (Muller et al., 2004, Sena and Chandel, 2012). Most of the $O_2^{\bullet-}$ generated in mitochondria are dismutated to H_2O_2 by manganese superoxide dismutase (MnSOD) in the mitochondrial matrix (Murphy, 2009, Buettner et al., 2006). H_2O_2 is a second messenger that is highly diffusible and has been shown to cross the mitochondrial membrane through specific members of the aquaporin family (Bienert et al., 2007).

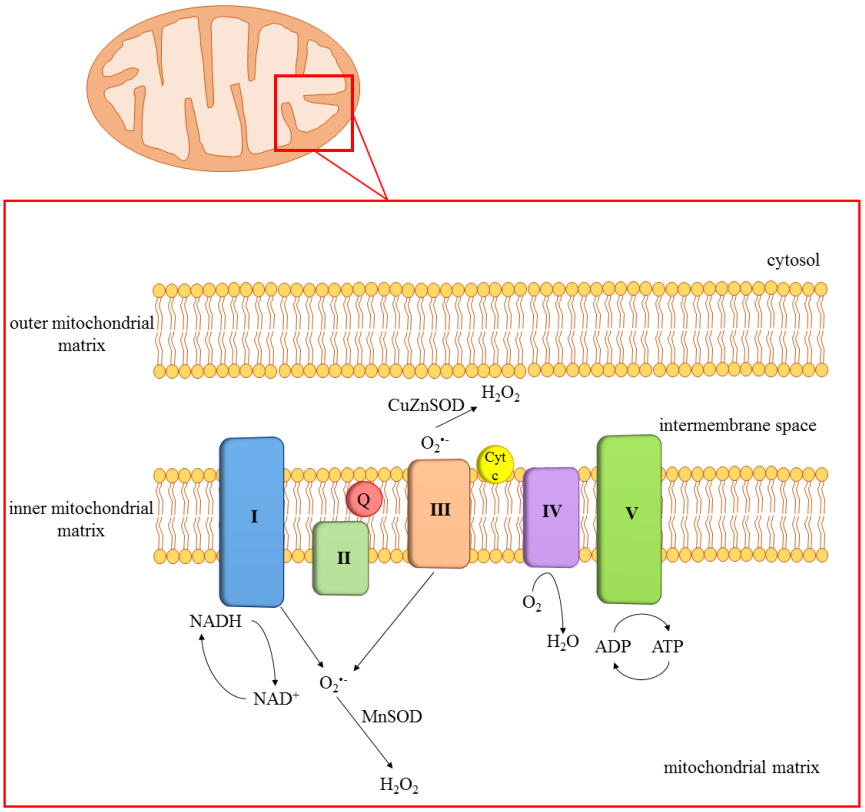

Figure 1.4. ROS production by the mitochondrial respiratory chain. The inner mitochondrial membrane-bound respiratory chain consists of complex I-V. Complex I- NADH dehydrogenase complex, II- succinate dehydrogenase coenzyme Q reductase, III- cytochrome b-c1 complex, IV- cytochrome oxidase complex and V- ATP synthase. $O_2^{\bullet-}$ is produced in the mitochondria at complex I and III of the respiratory chain during the transfer of electrons from NADPH to O_2 and through the generation of ATP. Mitochondrial antioxidants manganese SOD (MnSOD) in the mitochondrial matrix and copper/zinc SOD (Cu/ZnSOD), localised to the intermembrane space, converts $O_2^{\bullet-}$ into membrane permeable H_2O_2.

Mitochondrial ROS can have a damaging role, in addition to their cellular signalling properties. Deregulation of mitochondrial ROS can result in the initiation and progression of various cancers. Some of the cancer cases associated with elevated mitochondrial ROS levels include chronic lymphocytic leukaemia (CLL) (Jitschin et al., 2014), AML (Moloney et al., 2017b) and breast cancer (Hart et al., 2015).

1.2.1.1.2. NADPH oxidase (NOX)

NADPH oxidases (NOXs) are thought to be the first family of enzymes that generate ROS not as a by-product, but as their primary function (Bedard and Krause, 2007, Brewer et al., 2015). The NOX family were first described in the context of leukocytes where they produce ROS in response to inflammatory mediators (Holmstrom and Finkel, 2014). The NOX family consists of seven NOX isoforms NOX1-5 and dual oxidase (DUOX) 1-2, which possess similarities in terms of structure and enzyme function (Figure 1.5.). The seven isoforms are all transmembrane proteins with a NADPH-binding site, a flavin adenine dinucleotide (FAD)-binding site, six transmembrane domains and four heme-binding histidines. NOXs transfer electrons across biological membranes to produce $O_2^{\bullet-}$ (Bedard and Krause, 2007) that is rapidly converted into H_2O_2. H_2O_2 can diffuse across the membrane through aquaporin channel proteins with the potential to affect multiple cellular signalling events (Bienert and Chaumont, 2014). Although the NOX proteins are structurally similar, each is activated by specific mechanisms and regulatory subunits. Furthermore, activation of each system is initiated in response to a variety of stimuli, ranging from B and T cell receptor stimulation (Jackson et al., 2004, Richards and Clark, 2009), inflammatory mediators including lipopolysaccharide (LPS), the activity of oncoproteins including FLT3-ITD in AML and BCR-ABL in chronic myeloid leukaemia (CML) (Naughton et al., 2009, Woolley et al., 2012), as well as stimulation from growth factors, including platelet-derived growth factor (PDGF) and tumour necrosis factor-α (TNF-α) (Brown and Griendling, 2009).

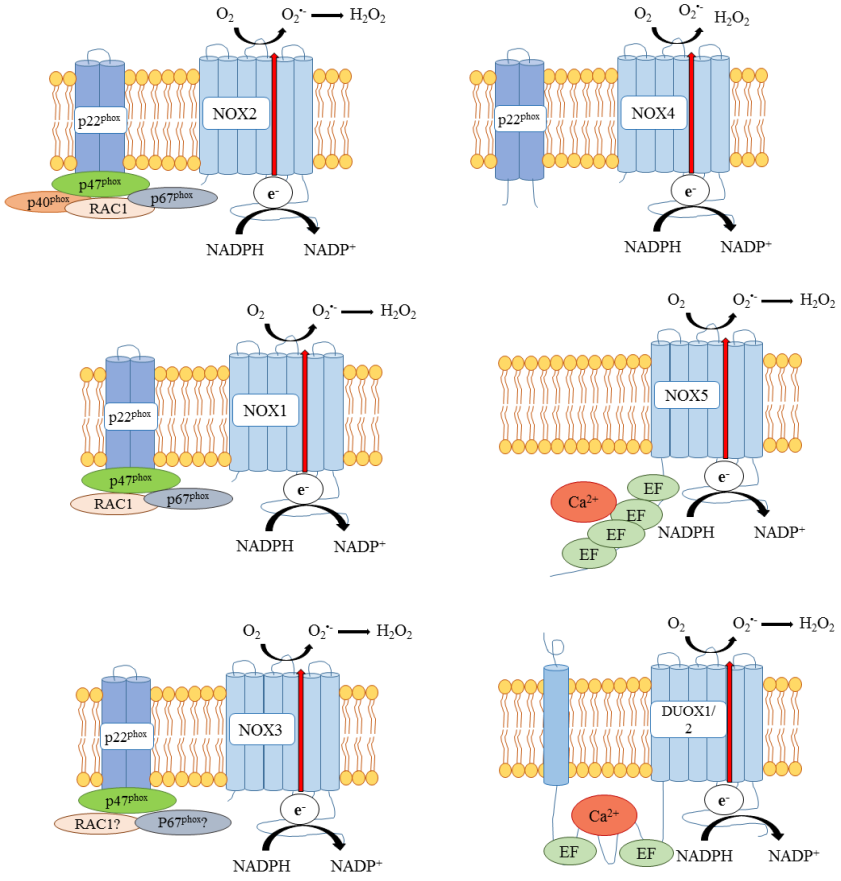

Figure 1.5. Activation of NOX isoforms and the production of ROS. The NOX family consists of seven family members NOX1-5 and DUOX1 and 2. Upon activation, the catalytic subunit removes an electron from cytosolic NADPH and transfers this electron to O_2, to produce $O_2^{\bullet-}$. $p22^{phox}$ is required for activation of NOX1-4. NOX1-3 activation also requires the recruitment of cytosolic subunits and RAC1. NOX5 as well as DUOX1 and 2 appear to only require Ca^{2+} for activation, and they contain a Ca^{2+} binding site in the EF hand region. DUOX1 and 2 also require a peroxidase-like transmembrane domain; however, the function of this is not known.

NOX2, also known as $gp91^{phox}$, is the prototype of the NOX family and was first identified in phagocytes. Further studies of its expression have revealed that NOX2 is the most widely distributed NOX isoform in humans (Bedard and Krause, 2007). p22-phagocyte oxidase ($p22^{phox}$) is a membrane partner protein and is required for the activation of NOX1-4 (Brandes et al., 2014, Ambasta et al., 2004). Other partner proteins of the NOX family include RAC1, $p67^{phox}$/NOX activator 1 (NOXA1) and $p47^{phox}$/NOX organiser 1 (NOXO1). The activation of NOX2 requires the

translocation of other cytosolic subunits (Groemping and Rittinger, 2005). Phosphorylated $p47^{phox}$ interacts with $p22^{phox}$ and organises translocation of other cytosolic subunits (Bedard and Krause, 2007, Groemping et al., 2003). The fully assembled and activated NOX2 complex allows the generation of $O_2^{\bullet-}$ through the transfer of an electron from reduced nicotinamide adenine dinucleotide phosphate (NADPH) in the cytosol to oxygen in the extracellular space (Sumimoto et al., 1996).

NOX1 is most highly expressed in the colon epithelium, but it is also expressed in other tissues, including endothelial cells (Ago et al., 2005, Kobayashi et al., 2004) and the prostate (Bánfi et al., 2000). Similarly to NOX2, NOX1 requires $p22^{phox}$ for activation. NOX1 also requires small G-protein RAC1, $p47^{phox}$ and $p67^{phox}$ in order to be activated (Cheng et al., 2006).

NOX3 is primarily expressed in the octonia of the inner ear but is known to be expressed in lower levels in other tissues (Bánfi et al., 2004a). The regulation of NOX3 is less well known, ROS generation requires $p22^{phox}$ and is enhanced by $p47^{phox}$ and $p67^{phox}$ (Ueno et al., 2005).

NOX4 was originally identified as being highly expressed in the kidney, amongst other tissues (Cheng et al., 2001). Unlike NOX1, NOX2 and NOX3, NOX4 only requires $p22^{phox}$ for activation and is constitutively activated. Insulin like growth factor-1 (IGF-1), bone morphogenetic protein-2 (BMP-2), transforming growth factor-β (TGFβ) and toll like receptor 4 (TLR4) are examples of growth factors and receptors that have been shown to activate NOX4 without the requirement of regulatory subunits (Lee et al., 2007, Maloney et al., 2009, Liu et al., 2010, Mandal et al., 2011, Edderkaoui et al., 2011). Stimulation of IGF-1 receptor has been shown to induce

NOX4-generated ROS in pancreatic tumour cells, contributing to cell survival (Lee et al., 2007).

NOX5 is expressed in a variety of tissues including the bone marrow, lymph nodes, ovary, pancreas, placenta, spleen, stomach, testis, uterus, vascular smooth muscle and various foetal tissues (Cheng et al., 2001). DUOX1 and DUOX2 are expressed mainly in the thyroid and the respiratory epithelia (Donkó et al., 2005). NOX5, DUOX1 and DUOX2, unlike NOX1-4 do not require $p22^{phox}$ or the cytosolic subunits for activation (Bánfi et al., 2004b, Kawahara et al., 2005b). Their activation is dependent on intracellular calcium levels, via binding to the calcium binding site in the EF hand region in the N-terminal domain, resulting in a conformational change and subsequent ROS production (Bánfi et al., 2004b, Bedard et al., 2012). DUOX1 and DUOX2 contain a peroxidase-like domain.

NOX-generated ROS production downstream of activated signalling cascades is tightly regulated, through the activity of antioxidants and ROS-scavenging enzymes. Unfortunately, deregulation of NOX ROS occurs, and this results in elevated production of ROS, which has been implicated in many diseases, including cardiovascular disease (Shah, 2015), retinal degeneration (Usui et al., 2009), diabetic kidney disease (Gorin and Block, 2013), asthma (van der Vliet, 2011), Alzheimer's and Parkinson's diseases (Gao et al., 2012).

The important role of NOX proteins is well established and documented downstream of various signalling transduction cascades. NOX-generated ROS often act as secondary signalling molecules downstream of growth factor stimulation (Sundaresan et al., 1995). It is not surprising that the activity of NOX proteins can be deregulated by the aberrant tyrosine kinase activity as a result of oncogenic signalling,

for example, FLT3-ITD in AML (Stanicka et al., 2015). Increased NOX-derived ROS in cancer has two roles; stimulation of cell survival and genomic instability, the two most influential characteristics of cancer progression (Gough and Cotter, 2011). Elevated levels of NOX-derived ROS are involved in the transformation and progression of many common cancers including: bladder, breast, colon and rectal, kidney, leukaemia, lung, melanoma, oesophagus, ovarian, pancreatic, prostate, stomach and thyroid (Table 1.2.). In these cancers, NOX proteins have been shown to drive oncogenesis through proliferation, cell survival, metastasis, invasion, angiogenesis and increased genomic instability (Block and Gorin, 2012).

Cancer type	NADPH oxidase	References
Bladder	NOX1	(Shimada et al., 2009)
	NOX4	(Shimada et al., 2011)
Breast	NOX1	(Desouki et al., 2005, Choi et al., 2010)
	NOX5	(Juhasz et al., 2009)
Colon and rectal	NOX1	(Juhasz et al., 2009, Fukuyama et al., 2005)
	NOX4	(Bauer et al., 2012)
Kidney	NOX1	(Block et al., 2010)
	NOX4	(Block et al., 2010, Block et al., 2007)
Leukaemia	NOX2	(Juhasz et al., 2009, Prata et al., 2008)
	NOX4	(Stanicka et al., 2015, Prata et al., 2008, Naughton et al., 2009)
	NOX5	(Kamiguti et al., 2005)
Lung	NOX4	(Han et al., 2016)
	DUOX1/2	(Luxen et al., 2008)
Melanoma	NOX2	(Aydin et al., 2017)
	NOX4	(Brar et al., 2002)
	NOX5	(Juhasz et al., 2009)
Oesophagus	NOX5	(Fu et al., 2006)

Ovarian	NOX1	(Desouki et al., 2005)
	NOX4	(Juhasz et al., 2009, Xia et al., 2007, Graham et al., 2010)
Pancreatic	NOX4	(Vaquero et al., 2004)
Prostate	NOX1	(Arnold et al., 2007, Lim et al., 2005)
	NOX2	(Kumar et al., 2008)
	NOX4	(Kumar et al., 2008)
	NOX5	(Brar et al., 2003, Huang et al., 2012)
	DUOX1/2	(Pettigrew et al., 2012)
Stomach	NOX1	(Kawahara et al., 2005a, Tominaga et al., 2007)
Thyroid	NOX4	(Weyemi et al., 2010)

Table 1.2. NOX isoforms expression in common cancer types.

1.2.1.1.3. Other enzymes

In addition to mitochondria and NOX proteins, there are several other sources of ROS including cyclooxygenases (COXs), lipoxygenases, xanthine oxidases, nitric oxide synthases and cytochrome P450 enzymes. Elevated production of ROS from these enzyme systems is also linked to cancer (Moloney and Cotter, 2017).

1.2.1.2. Regulation of ROS

ROS homeostasis is essential for cell survival and normal cell signalling, preventing cells from damage (Figure 1.6.). Detoxification of ROS is achieved by non-enzymatic or enzymatic antioxidants which are involved in scavenging of different types of ROS. Non-enzymatic molecules include glutathione, flavonoids, vitamin A, C and E. Enzymatic antioxidants include superoxide dismutase (SOD), superoxide reductase, catalase, glutathione peroxidase (GPX), glutathione reductase,

peroxiredoxin (PRX) and thioredoxin (TRX). Antioxidants have an important role in the degradation of $O_2^{\bullet-}$ and H_2O_2, preventing oxidative damage and maintaining a reduction-oxidation (redox) balance.

SODs are metalloenzymes located in various cellular compartments and are involved in rapid conversion of $O_2^{\bullet-}$ to H_2O_2. SOD1 (Cu/ZnSOD) is located in the cytosol, SOD2 (MnSOD) is located in the mitochondria and SOD3 (Cu/ZnSOD) is extracellular. SODs utilise metal ions, such as copper (Cu^{2+}), iron (Fe^{2+}), manganese (Mn^{2+}) and zinc (Zn^{2+}) as cofactors (Fukai and Ushio-Fukai, 2011).

Various antioxidants exist to maintain H_2O_2 levels for cellular signalling, by reduction of intracellular H_2O_2 to H_2O. Some of the antioxidants involved in this conversion include: catalase, glutathione peroxidase (GPX), peroxiredoxins (PRX) and thioredoxin (TRX) (Reczek and Chandel, 2015). PRXs and TRXs facilitate in the reduction of peroxynitrites and hydroperoxides to water (H_2O) through oxidation of their cysteine residues (Wood et al., 2003, Cox et al., 2010).

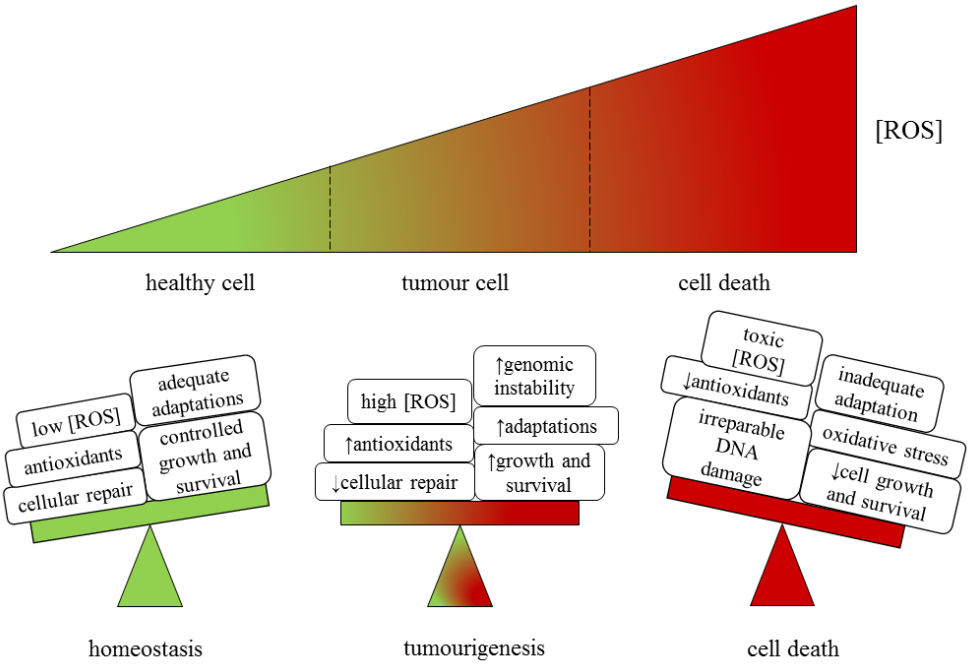

Figure 1.6. Model of ROS effects in cells. Healthy cells have developed adequate adaptations to overcome the damaging effects of ROS. Balanced generation of ROS, sufficient antioxidant activity and cellular repair result in low concentrations of ROS, resulting in limited cell survival and proliferation. Metabolic activity of tumour cells yields high ROS concentrations enhancing cell survival and proliferation leading to DNA damage, decreased cellular repair by faithful DNA damage repair pathways and genetic instability. Elevated ROS levels can cause cellular damage; however, tumour cells readjust with adequate adaptations to conditions, including hypoxia, and also through activation of unfaithful alternative cellular repair pathways. Tumour cells express increased antioxidant activity to remove excessive ROS while maintaining pro-tumourigenic signalling. If ROS levels increase dramatically to toxic ROS concentrations, for example, by ROS-inducing agents such as chemotherapy, oxidative stress results in irreparable damage to the cell, inadequate adaptations and eventually tumour cell death.

As mentioned already, tumour cells produce elevated levels of ROS compared to their normal cell counterparts, which are involved in the initiation and progression of cancer. The overproduction of ROS can be the result of oncogene activation, increased cellular metabolism and diminished tumour suppressor activity. However, the regulation of ROS in tumour cells must be tightly regulated to prevent tumour cell death. An overproduction of ROS results in increased antioxidant levels and

scavenging enzymes. However, antioxidant capacity cannot cope with high concentrations of ROS in cancer and is involved in the maintenance of pro-tumourigenic signalling, allowing the disease to progress and develop resistance to apoptosis (Gorrini et al., 2013). Several mechanisms in which ROS overcome antioxidant functions will be mentioned here. Elevated ROS production in cancer can lead to increased SOD protein expression (Janssen et al., 1999, Miranda et al., 2000), inactivation of H_2O_2 scavenging enzymes (Toledano et al., 2010), inactivation of tumour suppressor gene and protein tyrosine phosphatase (PTP) phosphatase and tensin homolog (PTEN) alongside oxidation and inactivation of many other PTPs (Leslie et al., 2003). Cancer has also been linked to mutations in transcription factors, for example, Nuclear factor (erythroid-derived 2)-like 2 (Nrf2) and also mutations in tumour suppressor genes including p53 (see section 1.3.1.), both of which are involved in increased antioxidant production, all of which contribute to ROS overcoming antioxidant capabilities, resulting in disease progression.

1.3. ROS signalling in cancer

ROS also act as signalling molecules in cancer, contributing to abnormal cell growth, metastasis, resistance to apoptosis, angiogenesis and in some types of cancer, a differentiation block (Sabharwal and Schumacker, 2014, Moloney et al., 2017b). The overproduction of ROS in cancer has been shown to induce a variety of biological effects including enhanced cell proliferation, DNA damage and genetic instability, adaptation, cellular injury and cell death, autophagy and resistance to drugs (Moloney and Cotter, 2017). The outcome is dependent on the genetic background of the cancer, the types of ROS involved ($O_2^{\bullet-}$, H_2O_2, etc.) and the levels and duration of ROS exposure.

1.3.1. Enhanced cell proliferation and cell survival

ROS have a well-established role in cell signalling. An increase in ROS, such as $O_2^{\bullet-}$ and H_2O_2, has been implicated in enhanced cell proliferation (Hole et al., 2013), increased cellular growth, cell survival and in the development of cancer through the regulation of mitogen activated-protein kinase (MAPK)/extracellular signal-regulated kinase 1/2 (ERK1/2) (Irani et al., 1997, Roberts and Der, 2007, Steelman et al., 2008), phosphoinositide-3-kinase (PI3K)/protein kinase B (AKT) (Liu et al., 2006) and protein kinase D (PKD) signalling pathways (Storz and Toker, 2003, Wang et al., 2004b, Liou et al., 2016). Additionally through the negative regulation of phosphatases, PTEN and protein tyrosine phosphatase 1B (PTP1B) (Lee et al., 2002, Salmeen et al., 2003, Wu et al., 2003), regulation of nuclear factor-κB (NF-κB) activating pathways (Duffey et al., 2000, Ahmed et al., 2006, Wang et al., 2007), as well as mutations in transcription factors and tumour suppressor genes including Nrf2

(Padmanabhan et al., 2006, Yoo et al., 2012, No et al., 2014) and p53 (Levine and Oren, 2009, Kruiswijk et al., 2015) (Figure 1.7.).

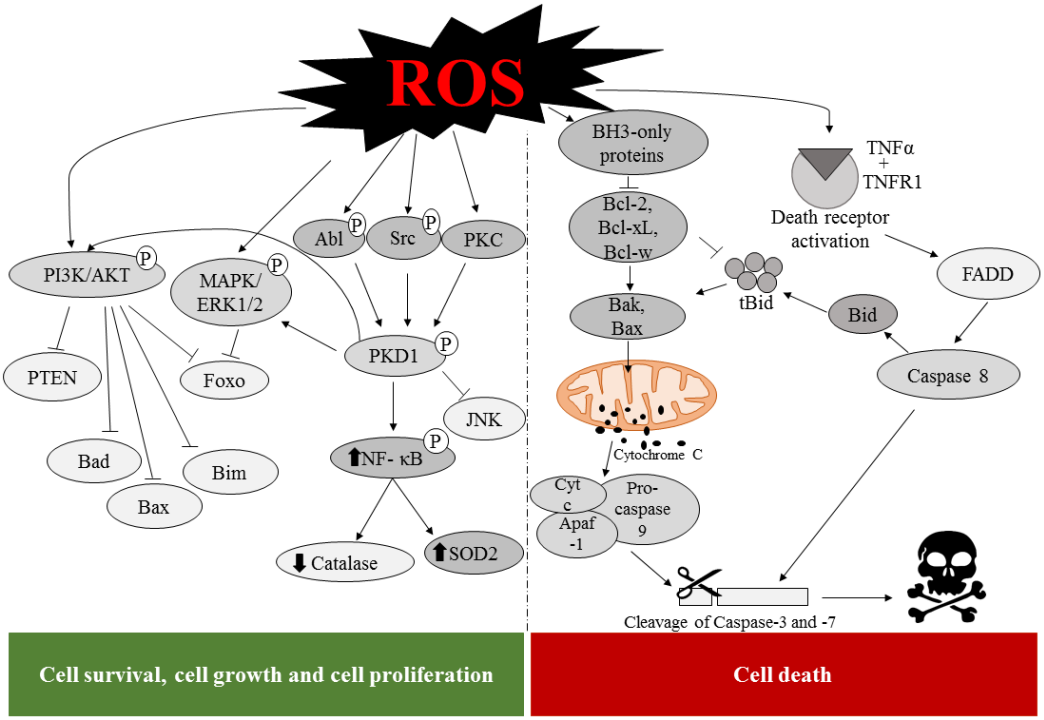

Figure 1.7. ROS-induced cellular signalling in cancer. Elevated ROS production in cancer has been shown to have a role in pro-tumourigenic and anti-tumourigenic signalling. Increased ROS levels contribute to sustained cell survival and proliferation through many pathways including PI3K/AKT, MAPK/ERK1/2 and PKD and inactivation of their downstream targets including Bad, Bax, Bim, Foxo (Brunet et al., 1999, Pastorino et al., 1999, Limaye et al., 2005, Xin and Deng, 2005, Qi et al., 2006, Kawamura et al., 2007) and PTEN. Elevated ROS production has also been linked to inhibition of the JNK pathway. However, toxic levels of ROS in the cell is known to cause cell death initiated by intrinsic apoptotic signalling in the mitochondria or extrinsic apoptotic signalling by death receptor pathways. Toxic ROS levels cause damage to the mitochondrial membrane resulting in the release and translocation of cytochrome c to the cytoplasm. Cytochrome c forms a complex with apoptotic protease activating factor-1 (Apaf-1) and pro-caspase 9 which induces the cleavage of caspase-3 and 7 resulting in apoptosis. Binding of TNFα ligand to TNFR1 death receptor triggers the activation of the initiator caspase 8 resulting in cleavage of caspase 3. Caspase 8 activation also induces cleavage of Bcl-2 BH3 domain-only death agonist protein (Bid) to tBid feeding back into the release of cytochrome c in the intrinsic apoptotic pathway.

1.3.2. DNA damage and genetic instability

Genomic instability has been suggested to be a major driving force of oncogenesis and can account for genetic diversity in many cancers (Loeb et al., 2003, Sieber et al., 2003). The initiation and progression of various cancers is associated with the accumulation of multiple mutated genes, resulting in abnormal cell growth, cell survival and in some cases a block in cell differentiation. Tumour cells require some form of genetic instability to allow the tumour cell to evolve and drive tumourigenesis (Sieber et al., 2003). The overproduction of ROS is associated with an increase in DNA damage, and this may be important in terms of genetic instability (Hole et al., 2011). DNA damage causes oxidation of DNA, resulting in a variety of alterations to DNA including deletions, insertions and base pair mutations and double strand breaks (dsbs), which are one of the most deleterious lesions resulting in deletions and translocations (Cooke et al., 2003, Pelicano et al., 2004). Insufficient repair of DNA damage and dsbs by non-homologous end joining (NHEJ) and homologous recombination are also involved in the generation of genomic instability (Jayavelu et al., 2016b). DNA damage and genetic instability in FLT3-ITD expressing AML is discussed in greater detail in section 1.4.3.

1.3.3. Adaptation

Cells employ a variety of adaptation mechanisms in response to ROS and oxidative stress. The antioxidant system in cells is a form of defence against elevated ROS production as mentioned previously in section 1.2.1.2. In order to maintain a redox balance, increased ROS levels leads to up-regulation of antioxidant system activity. However, as already mentioned this adaptation in tumour cells is very limited.

Increased activity of antioxidants such as SOD2/MnSOD or inactivation of scavenging enzymes including PRX1 are both observed in the development and progression of cancers (Janssen et al., 1999, Miranda et al., 2000, Toledano et al., 2010).

Tumour cells acquire adaptations under hypoxic conditions. Hypoxia arises in primary or metastatic tumours as a result of a deficiency in O_2 supply to the tumours. Prolonged exposure to hypoxia in normal cells results in cell death. Tumour cells adapt to hypoxia through a metabolic switch activating glucose metabolism, a phenomenon known as the Warburg effect, and this contributes to an aggressive phenotype (Dang and Semenza, 1999, Harris, 2002). Tumour cells utilise glycolysis regardless of sufficient O_2 supply (Dang, 2012). Previous studies show tumour cells adapt to glucose-deprivation through the increase of glycolysis to prevent H_2O_2 induced cell death (Aykin-Burns et al., 2009).

1.3.4. Cell death

Toxic levels of ROS in cells are known to induce cell cycle arrest, apoptosis and senescence (Figure 1.7.) (Moon et al., 2010, Moloney and Cotter, 2017). A disproportional increase in ROS can be achieved with chemotherapy, elevated ROS generation by immune cells or by depletion of antioxidant proteins within cells (Liou and Storz, 2010). Activation of the c-Jun N-terminal protein kinase (JNK) pathway by elevated ROS production can result in apoptosis initiated by intrinsic apoptotic signalling in the mitochondria or extrinsic apoptotic signalling by death receptor pathways (Carmody and Cotter, 2001, Dhanasekaran and Reddy, 2008, Pelicano et al., 2003). Inactivating JNK pathway mutations have been observed in various cancers suggesting that this pathway may be implicated in apoptotic signalling (Kennedy and

Davis, 2003). Activation of caspases is one of the most understood hallmarks of apoptosis and ultimately results in cleavage of poly ADP ribose polymerase (PARP), DNA fragmentation and cell death (Groeger et al., 2009). Elevated ROS can directly affect caspase function in the intrinsic- and extrinsic-apoptotic pathways. Overproduction of ROS may also effect the activity of apoptotic effectors including the B-cell lymphoma 2 (Bcl-2) family of proteins and cytochrome c (Groeger et al., 2009).

1.3.5. Autophagy

Autophagy is the controlled lysosomal pathway involved in the degradation and recycling of proteins and organelles within a cell that regulates cellular homeostasis (Poillet-Perez et al., 2015). It is one of the first defences against oxidative stress damage and has been found to be up-regulated in response to elevated ROS levels (Li et al., 2012). Impaired autophagy is observed in various pathologies including cancer, Crohn's disease, diabetes and neurodegenerative disorders including, Alzheimer's and Parkinson's diseases (Tal et al., 2009, Quan et al., 2012). Deregulated autophagy has also been found to have a role both in tumour progression (Aita et al., 1999, Liang et al., 1999, Choi et al., 2013, Laddha et al., 2014) and tumour suppression (Morselli et al., 2009, Debnath, 2011, Komatsu et al., 2010) in response to elevated ROS production. The relationship between elevated ROS levels and autophagy in cancer is quite complex.

1.3.6. Resistance to drugs

Elevated ROS production in cancer has major implications for drug therapy. As mentioned previously, increased ROS production results in pro-tumourigenic signalling, enhanced cell proliferation and survival, genetic instability and DNA damage and also metabolic adaptations, all of which contribute to drug resistance and further progression of cancer. DNA oxidation and dsbs generated by the overproduction of ROS results in the accumulation of multiple mutations, contributing to an increased risk of tumour cells developing resistance to therapies used. DNA damage-driven drug resistance to the frequently used protein tyrosine kinase inhibitors, midostaurin and imatinib, is observed in both AML and CML (Stanicka et al., 2015, Skorski, 2002, Skorski, 2007, Nowicki et al., 2004).

1.3.7. Current strategy for targeting ROS in cancer therapy

The pro-tumourigenic and anti-tumourigenic signalling effects of ROS can be manipulated in the treatment of cancer to prevent ROS production or to induce tumour cell death.

1.3.7.1. Increasing ROS levels to drive oxidative stress-induced tumour cell death

Anti-tumourigenic signalling of ROS can be targeted as a therapy in cancer, by the increased production of ROS levels to toxic levels and exhaustion of the antioxidant system capacity causing programmed cell death. Chemotherapy is widely used in the treatment of cancer and is known to increase ROS production resulting in irreparable damage and cell death. Examples of chemotherapy drugs used include, anthracyclines, cisplatin, bleomycin, arsenic trioxide (Pelicano et al., 2004).

Daunorubicin, an anthracycline, is used in the treatment of AML, acute lymphoblastic leukaemia (ALL) and acute promyelocytic leukaemia (APL). It reacts with cytochrome P450 reductase (Goodman and Hochstein, 1977, Pan et al., 1981) in the presence of reduced NADPH to form semiquinone radical intermediates (Bachur et al., 1977, Bates and Winterbourn, 1982) that react with O_2 to form $O_2^{\bullet-}$ (Bachur et al., 1977, Bachur et al., 1978, Bustamante et al., 1990, Benchekroun et al., 1993). This leads to increased activation of neutral sphingomyelinase enzyme and increased ceramide, resulting in activation of the JNK pathway leading to apoptosis (Mas et al., 1999, Gouazé et al., 2001). Doxorubicin is another widely used anthracycline in the treatment of a broad spectrum of cancers, including breast and oesophageal carcinomas, endometrial carcinomas, bile duct, pancreatic, gastric, liver, Hodgkin's and non-Hodgkin's lymphoma, osteosarcoma, Kaposi's sarcoma and soft tissue sarcomas (Singal and Iliskovic 1998, Buzdar et al., 1985). It causes increased production of ROS and activation of the tumour suppressor p53, resulting in tumour cell death (Wang et al., 2004a, Lotem et al., 1996). Chemotherapy may be used in combination with radiotherapy, amongst other treatments including immunotherapy, hormone therapy and surgery. Sulindac, a nonsteroidal anti-inflammatory drug (NSAID), has been shown to elevate ROS production in the treatment of colon and lung cancer, resulting in damage to the mitochondrial membrane and tumour cells becoming more sensitive to H_2O_2-induced cell death (Marchetti et al., 2009).

As mentioned previously, tumour cells adapt to oxidative stress through increased glucose metabolism resulting in increased ROS generation. Adaptations resulting in increased glucose metabolism are involved in cell survival, inhibiting apoptosis through the redox inactivation of cytochrome c (Vaughn and Deshmukh, 2008). Glucose inhibition using 2 deoxy-glucose (2DG) causes elevated ROS

production and results in cell death in pancreatic and prostate cancer (Ahmad et al., 2008, Coleman et al., 2008).

Previous work in our laboratory has reported how an isoellipticine derivative, 7-hydroxyisoellipticine induces apoptosis in AML cells (Russell et al., 2014). More recently, we have shown a more potent isoellipticine derivative, 7-formyl-10-methylisoellipticine, induces increased mitochondrial ROS production and cytotoxicity in AML. This significantly delays the tumour growth *in vivo*, with no cytotoxic effects to any organs (Russell et al., 2016).

1.3.7.2. Suppressing ROS levels to prevent tumour cell proliferation

Inhibition of ROS production in tumour cells could well result in suppressed pro-tumourigenic signalling. Reduction in ROS levels would lead to decreased cell survival and proliferation, fewer metabolic adaptations and lower levels of DNA damage and genetic instability.

Metformin, used in the treatment of type 2 diabetes is a known inhibitor of complex I of the mitochondrial ETC and has been found to reduce cancer incidence and mortality (El-Mir et al., 2000, Owen et al., 2000, Wheaton et al., 2014, Noto et al., 2012). Metformin has been shown to have pro-apoptotic effects in pancreatic cancer, through the increased protein expression of MnSOD/SOD2 and decreased levels of NOX2 and NOX4 proteins (Cheng and Lanza-Jacoby, 2015).

Studies have shown, inhibition of NOX-generated ROS results in decreased pro-tumourigenic effects in various cancers. Suppressed NOX4-generated ROS production in pancreatic cancer treated with flavoprotein inhibitor diphenyleneiodonium (DPI) resulted in apoptosis via the AKT/apoptosis signal-

regulating kinase 1 (ASK1) pathway (Mochizuki et al., 2006). Recent studies in our laboratory have shown, inhibition of the protein tyrosine kinase FLT3-ITD, as well as inhibition of $p22^{phox}$ and NOX4 activity in AML cells, results in decreased cell survival, as well as a decrease in DNA damage and genomic instability. This identifies NOX as a potential target in the treatment of FLT3-ITD expressing AML (Stanicka et al., 2015).

Treatment with antioxidants is thought to dampen ROS production in cancer through scavenging systems. Studies have shown that the overexpression of antioxidant SOD3 reduced breast cancer metastasis *in vivo*, implicating antioxidants in the reduction of ROS in cancer therapy (Teoh-Fitzgerald et al., 2014). However, antioxidants have also been linked to increased incidence of cancer. Vitamin A and E and also carotene have been linked to an increased risk of cancer (Omenn et al., 1996, Klein et al., 2011). These mixed results show the complexity of antioxidants in the treatment of cancer.

1.4. NOX-driven ROS formation in cell transformation of FLT3-ITD-positive AML

1.4.1. Oncogenic kinases as drivers of ROS formation in myeloid leukaemia

Disease progression in leukaemia is caused by the accumulation of mutated genes resulting in resistance to apoptosis, abnormal cell growth and differentiation (Blume-Jensen and Hunter, 2001). Many genetic mutations have been identified in myeloid leukaemia, yet the mechanism in which these mutations lead to genetic instability remains unclear. Tumour cells must acquire some form of genetic instability as the normal rate of mutation is not sufficient for the oncogenic transformation (Loeb et al., 2003). Reactive oxygen species (ROS), for example, H_2O_2, are considered to play an important function in leukaemia (Rhee, 2006). Increasing evidence has shown that genetic alterations in the genes associated with the myeloid malignancies is linked to an increase in reactive oxygen species (ROS), which is associated with an increase in DNA damage.

More than 90% of chronic myelogenous leukaemia (CML) cases develop from a chromosomal abnormality known as the Philadelphia chromosome (Achkar et al., 2010), which results from a reciprocal translocation between chromosomes 9 and 22 (Rowley, 1973), generating the chimeric kinase BCR-ABL (Shtivelman et al., 1985). BCR-ABL is known to activate downstream pro-survival pathways, for example, PI3K/AKT, JAK/STAT and Raf/MEK/ERK, resulting in resistance to apoptosis and proliferation (Steelman et al., 2004). BCR-ABL expressing cells have been shown to generate increased levels of ROS compared to untransformed cells (Kim et al., 2005). Various sources of ROS have been examined in CML including leakage from the

mitochondrial electron transport chain and NADPH oxidase-generated ROS, particularly NOX4. Naughton et al., demonstrated NOX4-generated ROS contribute significantly to total endogenous ROS upon BCR-ABL induction (Naughton et al., 2009). Treatment of CML cells with the BCR-ABL inhibitors, imatinib and nilotinib showed a significant decrease in ROS. This coincides with a post-translational down-regulation of the small membrane-bound protein $p22^{phox}$, a key component of the NOX complex (Ambasta et al., 2004). Treatment of BCR-ABL expressing cells with NOX inhibitors, DPI or VAS2870, resulted in a reduction in ROS levels. Inhibition of both the PI3K/AKT and Raf/MEK/ERK pathways in combination resulted in $p22^{phox}$ down-regulation. BCR-ABL induced, NOX4-generated ROS are dependent on PI3K/AKT and Raf/MEK/ERK activation and glycogen synthase kinase-3 β (GSK3β) inhibition (Landry et al., 2013). Mitochondrial ROS also appear to contribute to total ROS in CML cells.

FLT3-ITD is the most frequent FLT3 mutation present in acute myeloid leukaemia (AML) patients and has been associated with a poor outcome (Stirewalt and Radich, 2003, Small, 2008). In fact, FLT3 is the most frequently mutated gene in AML (Gilliland and Griffin, 2002). FLT3-ITD mutation result in ligand independent constitutive activation of the FLT3 receptor both at the plasma membrane and the endoplasmic reticulum (Choudhary et al., 2009, Moloney et al., 2017b). Constitutive auto-phosphorylation of FLT3-ITD activates downstream pro-survival signalling pathways including PI3K/AKT, JAK/STAT and Raf/MEK/ERK (Choudhary et al., 2005a), which are known to promote survival, proliferation and transformation (Hayakawa et al., 2000, Brandts et al., 2005). Recent findings have identified that in order for PI3K/AKT and Raf/MEK/ERK pro-survival pathways to be activated they must be located downstream of FLT3-ITD at the plasma membrane, and signal

transducer and activator of transcription 5 (STAT5) is located downstream of FLT3-ITD at the ER (Choudhary et al., 2009). FLT3-ITD expressing cell lines have been shown to produce increased levels of ROS, DNA oxidation and double strand breaks (dsbs) compared to FLT3-wild type (FLT3-WT) expressing cell lines (Godfrey et al., 2012, Sallmyr et al., 2008b). NOX-generated ROS have been identified as the primary source of ROS in FLT3-ITD expressing AML cells. Mutated FLT3 cells have been shown to produce increased levels of NOX2 and NOX4 and their partner protein $p22^{phox}$, compared to wild-type FLT3 cells. Stimulation of FLT3-WT expressing cells with FLT3 ligand results in an increase in $p22^{phox}$ protein levels and endogenous H_2O_2 (Stanicka et al., 2015). There is no significant difference in mitochondrial ROS in FLT3-ITD and FLT3-WT cells (Stanicka et al., 2015). Thus, it can be said that NOX-generated ROS are a potential target for treatment of leukaemia.

Adaption to higher concentrations of ROS by stimulation of survival mechanisms and antioxidant systems may well give cells a mechanism for the induction of resistance to drugs. This coincides with the high relapse risk associated with FLT3-ITD expressing AML cases.

1.4.2. ROS-mediated alteration of transforming signal transduction: Role of PTP oxidation

Protein phosphorylation of tyrosine residues plays a fundamental role in diverse cellular functions including proliferation, growth, metabolism, and differentiation. Protein-tyrosine kinase (PTK)-mediated signal transduction is regulated by protein-tyrosine phosphatases (PTPs), and failure of regulation of either protein family can contribute to unfavourable diseases like cancer. The human PTP

superfamily consists of more than 100 members. Many of these enzymes are identified by the unique consensus signature motif HCX_5R involved in the catalytic function. Despite their sequence and structural similarity, PTPs exhibit a wide range of substrate specificity (Alonso and Pulido, 2016, Tonks, 2013).

Several members of the PTP superfamily were found to be altered by genetic aberration, promoter methylation, or gene overexpression in AML. Protein tyrosine phosphatase non-receptor 11 (PTPN11) (also known as Src homology region 2-containing protein tyrosine phosphatase 2 (SHP-2)) positively regulates FLT3 ligand (FL)-mediated FLT3 receptor signalling (Muller et al., 2008), and not surprisingly, activating mutations (commonly found SHP-2 E76K (glutamic acid substituted with a lysine at amino acid 76) mutant) were identified in AML (Tartaglia et al., 2003, Nabinger et al., 2013). Phosphatase PTEN negatively regulates PI3K signalling downstream of the FLT3 receptor and is also mutated, though rarely in AML (Patel et al., 2012). Several recent findings claim a role for deregulated gene expression of dual-specificity phosphatases, such as phosphatase of regenerating liver 2 and 3 (PRL2 and PRL3) and dual-specificity phosphatase 6 (DUSP6), in AML cases in the presence and absence of a FLT3 mutation (Park et al., 2013, Zhou et al., 2011, Arora et al., 2012). Recently, suppressor of T cell signalling proteins 1 and 2 (STS1 and STS2) (also known as ubiquitin-associated and SH3 domain containing protein 3B and 3A (UBASH3B and UBASH3A)), which belong to a PTP subfamily with histidine-based catalysis (Alonso and Pulido, 2016), were identified to be directly regulating the FLT3 receptor tyrosine phosphorylation in haematopoietic stem cells (Zhang et al., 2015). However, their potential role in regulating constitutively activated FLT3-ITD phosphorylation or FLT3 signalling in AML remains unknown. Other examples include the transmembrane PTP protein tyrosine phosphatase receptor type D

(PTPRD/PTPδ), which is down-regulated by promoter methylation and may be a tumour suppressor in paediatric AML (Song et al., 2016), and CDC25, which is mutated in familial platelet disorder with predisposition to AML (Yoshimi et al., 2014).

PTPs can modulate signal transduction in many ways, both negatively and positively. For example, they prevent the nonspecific activation of PTKs, for example, by averting the ligand-independent activation of RTKs. In other contexts, PTPs can promote signalling by activation of Rous sarcoma oncogene cellular homolog (Src) family kinases or of the RAS pathway (Tonks, 2013). PTP activity is regulated by several mechanisms (Hertog et al., 2008), and one such regulatory process is the reversible oxidation of the catalytic cysteine by ROS. H_2O_2 is considered an important ROS species in the PTP oxidation process. Upon oxidation, the active-site thiol moiety (–SH) is converted to a sulphenyl moiety (–SOH), which further reacts to more stable reaction products, like sulphenylamides or disulphides, in intramolecular reactions. The widely presumed role of H_2O_2 in PTP oxidation may in fact be indirect (Winterbourn and Hampton, 2008), and other oxidants, such as lipid peroxides, can also effectively oxidise PTPs (Östman et al., 2011, Conrad et al., 2010). PTP oxidation is typically transient, and reduction back to the active state is accomplished by interaction with cellular antioxidants like glutathione (GSH) and thioredoxin (Östman et al., 2011). Reversible PTP inactivation facilitates the efficient RTK signal transduction in the cells on ligand/growth factor stimulation (Holmstrom and Finkel, 2014). Emerging reports claim, however, that PTPs are also important targets of pathologically generated ROS, and that in such circumstances, ROS-mediated PTP inactivation could contribute to diseases like cancer. In support that such processes play a role in leukaemia, an early study indicated that high ROS levels

in BCR-ABL-transformed cells were associated with low levels of overall PTP activity, and treatment with antioxidants reversed these effects (Sattler et al., 2000). As outlined above, apart from BCR-ABL, other myeloid leukaemia-specific PTK oncoproteins including FLT3-ITD also cause constitutive formation of elevated levels of ROS, and their possible consequences for PTP deregulation deserve attention.

The transmembrane PTP protein tyrosine phosphatase receptor type J (PTPRJ; also known as density-enhanced phosphatase-1 (DEP-1) or CD148) was previously identified as bona fide PTP negatively regulating FLT3 receptor signalling in myeloid cells (Arora et al., 2011). DEP-1 regulates FL-induced FLT3 receptor signalling by associating with (Böhmer et al., 2013) and dephosphorylating FLT3 directly, thereby attenuating the activation of FLT3. When the role of DEP-1 in the regulation of the FLT3-ITD oncoprotein was analysed, DEP-1 was discovered to be oxidised and partially inactivated because of high levels of sustained ROS generation, leading to elevated FLT3 activity. This promotes downstream signalling pathways, including STAT5 and RAS/ERK1/2 activation, and causally contributes to cellular transformation (Godfrey et al., 2012). Recently, investigation of the relevant ROS sources convincingly indicated that NOX4 messenger RNA (mRNA) and protein levels are elevated in FLT3-ITD-positive AML cells and that NOX4 expression is transcriptionally regulated by STAT5 directly (Jayavelu et al., 2016a). The *NOX4* promoter possesses STAT binding elements, and STAT5 was found by chromatin immunoprecipitation (ChIP) assays to bind to these elements in a FLT3-ITD-dependent manner. General interference with ROS formation by different means including down-regulation of NOX4 with RNA interference (RNAi) or treatments with potential small molecule NOX4 inhibitors caused a pronounced decrease in ROS levels, rescued DEP-1 PTP activity, and attenuated transforming FLT3-ITD-driven

signalling and cell transformation *in vitro* and *in vivo*. Double depletion of DEP-1 and NOX4 partially rescued the effect of NOX4 depletion on transformation *in vitro*, suggesting that DEP-1 reactivation is essential for the inhibitory effect of NOX4 depletion. Interestingly, murine haematopoietic stem cells transduced with a combination of FLT3-ITD and other potent oncogenic drivers (Homeobox A9 (Hoxa9)/Meis homeobox1 (Meis1) or MLL-AF9), and with genetic inactivation or down-regulation of *NOX4*, did not grow in the absence of cytokines *in vitro*, and were impaired in their capacity to elicit a myeloproliferative disease in sub-lethally irradiated recipient mice *in vivo*, respectively (Jayavelu et al., 2016a). These findings revealed an important role played by NOX4-dependent ROS formation in oxidation of DEP-1, a bona fide PTP of FLT3, as a transforming event in FLT3-ITD harbouring aggressive AML (Figure 1.8.). It will be interesting to know whether NOX4-dependent, oxidative inactivation of DEP-1 is a selective mechanism or reflects a more general attenuation of PTPs in FLT3-ITD cells. Although NOX4 may indeed be of interest as a therapeutic target in FLT3-ITD subtype AML, there are still several other potential sources of ROS formation whose investigation is warranted.

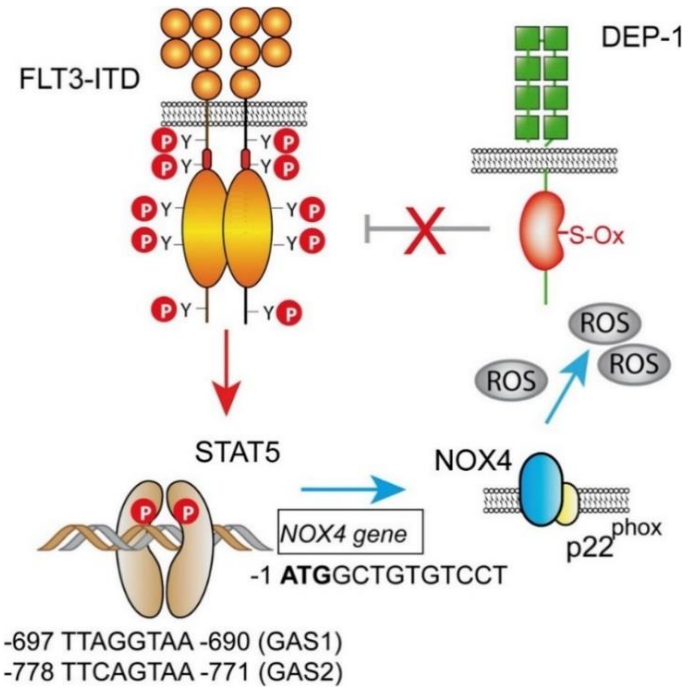

Figure 1.8. Role of ROS formation in leukaemic cell transformation by the oncoprotein FLT3-ITD. FLT3-ITD causes elevated ROS levels in AML cells. This involves activation of STAT5, which can directly bind to the promoter of NADPH oxidase 4 (NOX4), leading to elevated transcription. Increased NOX4 levels cause elevated formation of ROS, which oxidise the catalytic cysteine of density-enhanced phosphatase-1 (DEP-1; a transmembrane protein-tyrosine phosphatase, also known as PTPRJ or CD148). In contrast to its activity in normal cells, the oxidised and thereby (reversibly) inactivated DEP-1 can no longer dephosphorylate FLT3-ITD, enabling elevated signal transduction and promoting cell transformation.

1.4.3. ROS-mediated DNA damage and potential implications for leukaemia biology

Genomic instability has been suggested to be the main cause of genetic diversity in cancer (Sieber et al., 2003). FLT3-ITD mutation initiates a cycle of genomic instability- increased production of ROS leads to enhanced DNA damage (DNA oxidation and double strand breaks (dsbs)) and compromised DNA error repair, by alternative, less well-defined, end joining pathways, causing an aggressive phenotype of AML (Sallmyr et al., 2008b).

As mentioned ROS contribute to the initiation, promotion and progression of cancers, including leukaemia. Oxidative DNA damage can cause a wide range of DNA alterations such as base pair mutations, insertions and deletions (Cooke et al., 2003). Dsbs are one of the most dangerous lesions resulting in translocations and deletions. Alternative mechanisms involved in the generation of genomic instability include unfaithful or insufficient repair of DNA damage (Pelicano et al., 2004). There are two DNA repair systems responsible for DNA dsb repair: a precise homologous recombination and a less precise non-homologous end-joining (NHEJ) (Sallmyr et al., 2008b). In cancer, alternative end-joining (AEJ) plays a significant role and results in severe errors in DNA damage. Increased expression of the unfaithful AEJ repair pathway and down-regulation of the faithful NHEJ pathway is associated with FLT3-ITD and BCR-ABL oncogenic signalling (Fan et al., 2010). It has also been shown that increased repair of FLT3-ITD stimulated DNA damage contributes to drug resistance, which coincides with the high relapse rate associated with FLT3-ITD expressing AML cases.

FLT3-ITD expressing cells have been shown to generate increased levels of ROS, resulting in excessive DNA damage in comparison to FLT3-WT expressing cells, and have been shown to activate alternative unfaithful pathways of DNA repair, leading to an increase in levels of unrepaired DNA damage (Sallmyr et al., 2008b). $p22^{phox}$ and $p22^{phox}$ dependent NOX isoforms, particularly NOX4, have been shown to be the primary source of ROS in FLT3-ITD expressing cells (Woolley et al., 2012). A significant amount of research has been carried out to investigate the effects of FLT3-ITD generated NOXs on genomic instability in AML, examining nuclear levels of H_2O_2. Inhibition of FLT3-ITD, NOX and $p22^{phox}$ (by siRNA) resulted in a significant decrease in nuclear H_2O_2. NOX4 and $p22^{phox}$ have been shown to colocalise

to the nucleus, thus reinforcing the idea that NOX activity contributes to genomic instability in AML (Stanicka et al., 2015). FLT3-ITD expressing cells produce a 100% increase in H_2O_2 compared to FLT-WT, as quantified by flow cytometry using endogenous H_2O_2 specific probe Peroxy Orange 1 (PO1), and a 25% increase in nuclear H_2O_2, in FLT3-ITD compared to WT. There was no significant difference in mitochondrial generated ROS between ITD- and WT-expressing cells (Stanicka et al., 2015).

Phosphorylated histone H2A, member X (ϒH2AX) is one of the most widely used measures of DNA dsbs (Kuo and Yang, 2008). 8-hydroxy-2' deoxyguanosine (8-OHdG) is the predominant form of ROS-induced DNA lesion and therefore is widely used as a marker of oxidative stress (Roszkowski et al., 2011). FLT3-ITD expressing cells, MV4-11, showed a 50% increase in dsbs compared to the FLT3-WT expressing cell line, HL-60. 32D cells, a murine immortalised myeloblast-like cell line transfected with FLT3-ITD and FLT3-WT plasmids showed a similar result with a 75% increase in levels of dsbs in 32D/FLT3-ITD cells compared to 32D/FLT3-WT cells. 32D/FLT3-ITD cells possess 100% more oxidative stress, as assessed by levels of 8-OHdG compared to WT (Stanicka et al., 2015). A study has shown that inhibition of FLT3 using PKC412 resulted in a decrease in protein levels of NOX4 and its partner protein $p22^{phox}$, coinciding with a decrease in total endogenous H_2O_2. FLT3-ITD expressing cells treated with PKC412 showed a significant decrease in dsbs and inhibited the homologous repair of DNA damage. On the other hand, PKC412 had no effect on dsbs or DNA repair pathway in FLT3-WT expressing cells (Seedhouse et al., 2006). The decrease in dsbs in FLT3-ITD expressing cells coincides with a 35% decrease in DNA oxidation using the marker 8-OHdG. Thus these findings highlight the importance and involvement of the FLT3-ITD oncogene in genomic instability.

Knockdown of $p22^{phox}$ and $p22^{phox}$ dependent NOX isoforms in FLT3-ITD expressing cells, MV4-11, resulted in a decrease in endogenous and nuclear H_2O_2 accompanied by a 30% decrease in the number of dsbs and DNA oxidation following $p22^{phox}$ knockdown. $p22^{phox}$ knockdown in FLT3-WT expressing cells showed an increase in endogenous H_2O_2 and dsbs in comparison to scramble control. FLT3-ITD expressing cells have higher $p22^{phox}$ protein levels compared to wild-type cells, thus reinforcing the oncogenic effects of the FLT3-ITD mutation in AML. $p22^{phox}$ is necessary for NOX-generated ROS to oxidatively damage DNA. Interestingly, NOX4 knockdown had a greater effect than $p22^{phox}$ knockdown resulting in a 30% decrease in endogenous H_2O_2 levels and dsbs. NOX inhibition using DPI also resulted in a 30% decrease in dsb marker, ϒH2AX, in 32D/FLT3-ITD cells. Hence, the NOX4/$p22^{phox}$ complex produces DNA-damaging H_2O_2 in FLT3-ITD cells, MV4-11. ϒH2AX levels were not altered following NOX1 knockdown. However, NOX2 knockdown resulted in a 20% decrease in endogenous H_2O_2 and a 30% decrease in dsbs (Stanicka et al., 2015). 32D/FLT3-WT expressing cells, when stimulated with FLT3 ligand, results in an increase in $p22^{phox}$ protein levels, a 40% increase in endogenous H_2O_2 and a 20% increase in nuclear H_2O_2. The increase in $p22^{phox}$ protein levels coincides with a 50% increase in the number of dsbs, demonstrating the DNA damaging properties of FLT3-induced H_2O_2.

The BCR-ABL mutation in CML is involved in a similar cycle of genomic instability to the FLT3-ITD mutation. The oncogenic effects of BCR-ABL leads to increased levels of NOX ROS production leading to enhanced DNA damage and compromised DNA repair (Nowicki et al., 2004, Naughton et al., 2009). Similar to FLT3-ITD, levels of DNA damage are much higher in BCR-ABL transformed cells compared to non-transformed cells, and the rate of DNA repair by unfaithful end

joining systems is much higher (Skorski, 2007). The accumulation of DNA damage and genetic abnormalities contributes to resistance against drugs that are commonly used in the treatment of CML, including imatinib (Skorski, 2002, Koptyra et al., 2006) (Figure 1.9.).

Unfortunately, ROS-mediated damage in AML and CML has major implications in the treatment of leukaemia. It is increasingly more difficult to treat leukaemia due to the accumulation of genetic abnormalities leading to resistance to protein tyrosine kinases inhibitors, for example, PKC412 and imatinib, and this furthers the progression of the malignancy. For detailed information on ROS-mediated damage and genomic instability in leukaemia, the reader is referred to the following reviews (Jayavelu et al., 2016b, Sallmyr et al., 2008b).

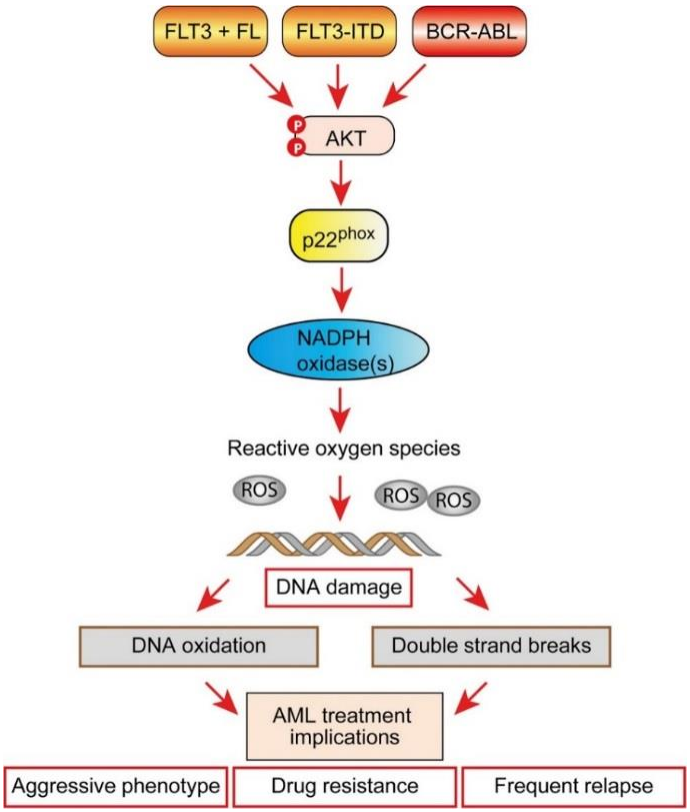

Figure 1.9. Oncoprotein-driven ROS formation in myeloid cells causes DNA damage. FLT3-ITD, but also ligand-activated FLT3 or the BCR-ABL oncoprotein, can drive oxidative DNA damage through a signalling chain involving AKT activation, elevated expression of $p22^{phox}$, and activation of $p22^{phox}$-interacting NADPH oxidases. DNA damage, involving DNA oxidation and generation of double-strand breaks, contributes to genetic instability and the accumulation of mutations associated with aggressive phenotypes, drug resistance, and relapse.

1.5. Objectives

Increased ROS production is becoming a well-recognised hallmark of various cancers, resulting in pro-tumourigenic and anti-tumourigenic signalling. Elevated ROS levels downstream of the FLT3-ITD mutation contributes to pro-tumourigenic signalling in acute myeloid leukaemia (AML) through sustained cell survival and proliferation, a differentiation block resulting in the accumulation of immature haematopoietic progenitor cells or 'blasts', as well as DNA damage and genetic instability contributing to drug resistance. As with many cancer studies, the main goal is to identify targets for selective and effective therapies and to overcome drug resistance. The aims of this study were firstly to investigate the effect of subcellular localisation of the FLT3-ITD oncogene on NOX4- and $p22^{phox}$-generated H_2O_2 in AML. We also wished to examine the pro-survival signalling pathways activated downstream of FLT3-ITD at the plasma membrane and endoplasmic reticulum, responsible for the production of NOX4-generated ROS. Previous studies in our laboratory have identified NOX4 as a major contributor of endogenous H_2O_2 in FLT3-ITD-expressing AML cell lines where it is located in the nuclear membrane, contributing to DNA damage and genetic instability. The final aim of this study was to investigate the expression, localisation and regulation of the NOX4 28 kDa splice variant, NOX4D, in FLT3-ITD-expressing AML. NOX4D has previously been shown to localise to the nucleus in various cell types and is implicated in the generation of ROS and DNA damage.

Chapter 2. Materials and Methods

2.1. Cell culture and treatments

Human patient-derived leukaemic cell lines MV4-11 (homozygous for the FLT3-ITD mutation), MOLM13 (heterozygous for the FLT3-ITD mutation) and K562 were all purchased from DSMZ (Braunschweig, Germany). 32D, a murine immortalised myeloblast-like cell line, stably transfected with FLT3-WT and FLT3-ITD (Mizuki et al., 2000), were a kind gift from Prof. Hubert Serve from Goethe University Frankfurt and Prof. Frank D. Böhmer from the Universitatsklinkium Jena in Germany. The cell lines were maintained in Roswell Park Memorial Institute (RPMI) 1640 medium (Sigma-Aldrich, Dublin, Ireland) supplemented with 10% Foetal Bovine Serum (FBS) (Thermo Scientific/Bio-Sciences, Dublin, Ireland), 2mM L-glutamine (Thermo Scientific/Bio-Sciences, Dublin, Ireland) and 1% penicillin/streptomycin (Sigma-Aldrich, Dublin, Ireland) in a humidified incubator at 37°C with 5% CO_2. For 32D cells, 10% WEHI-conditioned medium was added as a source of interleukin-3 (IL-3). The WEHI conditioned medium was harvested from a 48 h culture of WEHI, a macrophage-like, derived from a BALB/c mouse treated for tumour induction cell line, which produce and secrete IL-3. Prior to carrying out experiments that involved a comparison of 32D/FLT3-ITD and 32D/FLT3-WT, the cells were washed twice with phosphate buffered saline (PBS) and IL-3-starved overnight in 10% FBS medium as recommended previously (Choudhary et al., 2009, Sallmyr et al., 2008a, Songyang et al., 1997).

All cell lines, except for 32D cells were maintained between 0.1-1.5 x 10^6 cells/ml and were sub-cultured every 2-3 days. 32D cells were maintained between 0.2-1.0 x 10^6 cells/ml and were sub-cultured every 2 days. Cell counts were obtained using a haemocytometer under a light microscope. Cell viability was determined by

trypan blue exclusion (#T8154, Sigma-Aldrich, Dublin, Ireland).

HEK 293-T cells were maintained in Dulbecco's Modified Eagle's Medium (DMEM), supplemented with 10% FBS, 10 mM L-glutamine and 1% penicillin/streptomycin in a humidified incubator at 37°C with 5% CO_2.

2.2. Primary AML patient samples

Blood samples from newly diagnosed untreated *de novo* AML patients were obtained in accordance with the Declaration of Helsinki and with approval of the institutional review board of the University Hospital Jena, Germany. Mononuclear cells were purified as previously described (Godfrey et al., 2012). FLT3 mutational analysis was done by standard polymerase chain reaction (PCR) methods to group the patients into FLT3-WT or FLT3-ITD. Primary AML patient blood samples were a kind gift from Dr. Sebastian Scholl from Jena University Hospital, Germany.

2.3. Reagents and chemicals

Protein	Reagent/ inhibitor	Supplier	Cat #	Vehicle	Conc.	Dura-tion
FLT3-ITD	PKC412	Tocris	2992	DMSO	50-250 nM	24 h
FLT3-ITD	AC220	Selleck-chem	S1526	DMSO	5-30 nM	12 h
Glycosylation	Tunicamycin	Sigma	T7765	DMSO	1-10 µg/ml	16 h
Receptor trafficking	Brefeldin A	Sigma	B7651	Ethanol	1-10 µg/ml	16 h
PI3K/AKT	LY294002	CST	9901	DMSO	20-50 µM	16 h
ERK1/2	U0126	Sigma	U120	DMSO	10-100 µM	16 h
STAT5	Pimozide	Millipore	573110	DMSO	5-20 µM	16 h
GSK3β	SB216763	Tocris	1616	DMSO	1-5 µM	16 h
GSK3β	Lithium chloride	Sigma	L9650	Water	10-50 mM	16 h
COX	Diclofenac	Sigma	D6899	Water	1-50 µM	2 h
Mitochondrial ROS	Rotenone	Tocris	3616	DMSO	1-50 µM	1 h
20S proteasome	Lactacystin	Millipore	426100	DMSO	5 µM	16 h

Table 2.1. List of inhibitors and modulators used throughout the course of this thesis. Tocris: Tocris Bioscience (Bristol, UK), Selleckchem: Selleckchem from Stratech (Suffolk, UK), Sigma: Sigma-Aldrich (Dublin, Ireland), CST: Cell Signaling Technology (Boston, MA, USA), Millipore: Merck Millipore (Cork, Ireland). In all cases, if not shown, inhibitor and modulator concentrations were chosen based on their greatest effect with a negligible decrease in cellular viability. All treatment time-points chosen were as optimised in previous studies.

2.4. Antibodies

Gene	Supplier	Cat #	Host	Dilution WB	Dilution IF
AKT	CST	9272	Rabbit polyclonal	1/1000	
Phospho-AKT ser473	CST	9271	Rabbit polyclonal	1/1000	
β-actin	Sigma	A5441	Mouse monoclonal	1/5000	
Calreticulin	Abcam	Ab22683	Mouse monoclonal	1/1000	
ERK1/2	CST	4696	Mouse monoclonal	1/1000	
Phospho-ERK1/2 thr202/tyr204	CST	9106	Mouse monoclonal	1/1000	
Flt-3	Santa Cruz	SC480	Rabbit polyclonal		1/100
GAPDH	CST	5174	Rabbit monoclonal	1/1000	
GSK3β	CST	9315	Rabbit monoclonal	1/1000	
Phospho-GSK3β ser9	CST	9336	Rabbit polyclonal	1/1000	
HA	Cambridge Bioscience	MMS-101R	Mouse monoclonal	1/1000	
HDAC1	CST	5356	Mouse monoclonal	1/1000	
Histone H3	Abcam	Ab1220	Mouse monoclonal	1/5000	
KDEL	Abcam	Ab12223	Mouse monoclonal	1/1000	1/100
Lamin A/C	CST	2032	Rabbit polyclonal	1/1000	
NOX4	Novus Bio	NB110-58849	Rabbit polyclonal	1/1000	
NOX4	Abcam	Ab109225 (UOTR1 B492)	Rabbit monoclonal	1/1000	
NOX4	Prof. Ajay Shah	In-house antibody	Rabbit polyclonal	1/1000	
NUP98	Abcam	Ab179911 (13C1)	Mouse monoclonal	1/500	
$p22^{phox}$	Santa Cruz	SC20781	Rabbit polyclonal	1/1000	

STAT5	BD	610191	Mouse monoclonal	1/1000
Phospho-STAT5 tyr694/699	Millipore	04-886	Rabbit monoclonal	1/1000
α-tubulin	Sigma	T5168	Mouse monoclonal	1/5000
Vinculin	Biozol	BZL03106	Mouse monoclonal	1/10000

Table 2.2. List of antibodies used throughout the course of this thesis. WB: Western Blotting, IF: Immunofluorescence, CST: Cell Signaling Technology (Boston, MA, USA), Sigma: Sigma-Aldrich (Dublin, Ireland), Abcam (Cambridge, UK), Santa Cruz: Santa Cruz Biotechnology Inc. (Dublin, Ireland), Cambridge Bioscience (Cambridge, UK), Novus Bio: Novus Biologicals (Abingdon, UK), BD: BD Biosciences Europe (Oxford, UK), Millipore: Merck Millipore (Cork, Ireland), Biozol: Biozol Diagnostics (Eching, Germany).

2.5. RT-qPCR primers

2.5.1. Qiagen QuantiTect Primer Assays

Gene	Qiagen primer	Product size	Ref Seq ID#
β-actin (ACTB)	QT00095431	146 bp	NM_001101
Beta-2-microglobulin (B2M)	QT00088935	98 bp	NM_004048 XM_005254549 XM_006725182
Proteasome (prosome/macropain) subunit, beta type, 2 (PSMB2)	QT00082999	64 bp	NM_001199779 NM_001199780 NM_002794
$p22^{phox}$/Cytochrome b-245, alpha polypeptide	QT00082481	106 bp	NM_000101
NOX4	QT00057498	77 bp	NM_001143836 NM_001143837 NM_016931 NR_026571 NM_001291926 NM_001291927 NM_001291929 NM_001300995 XM_006718848 XM_006718849 XM_006718852 XM_006718853

Table 2.3.1. List of Qiagen QuantiTect primers used throughout the course of this thesis. All primers are from Qiagen (West Sussex, UK).

2.5.2. Eurofins Primers

Gene	Eurofins primer	Sequence (5'→3')	RefSeq ID#	Ref
NOX 4	NOX4_4	fwd: 5' TCTGTTGTGGACCCAATTCA 3' rev: 5' AGCTGATTGATTCCGCTGAG 3'	XM_011 542857.2	(Reddy et al., 2011)

Table 2.3.2. Forward and reverse sequence of NOX4_4 Eurofins primers used to amplify NOX4 (186 bp) throughout the course of this thesis. NOX4_4 primers are from Eurofins (Wolverhampton, UK).

2.6. Flow cytometry

2.6.1. Measurement of intracellular H_2O_2

Total intracellular hydrogen peroxide (H_2O_2) was measured by incubating cells with 5 μM of cell-permeable H_2O_2-probe Peroxy Orange 1 (PO1) (Tocris Bioscience, cat# 4944) added to the medium for 1 h at 37°C in the dark. Cells were then briefly washed with PBS and immediately viewed under the microscope or quantified by flow cytometry using FACSCalibur (BD Bioscience, Europe) and Cellquest Pro software (Becton Dickinson). The probe was excited using the FL2-H (red) flow cytometry laser. Healthy populations of cells were gated and the mean fluorescent intensity of 10,000 events was recorded. The viability/healthiness of the cells was estimated, based on their size and granularity using the forward scatter-height (FSC-H) and side scatter-height (SSC-H) lasers. The geometric mean fluorescence of three biological (N=3) and three technical (n=3) replicates of viable cells was calculated. The fluorescence of the vehicle control (control) cells was set to 100% and the fluorescence of treated cells was expressed as a percentage of the control.

2.6.2. Flow cytometry analysis

The fluorescence of control/32D/FLT3-WT cells was set to 100% in all experiments to rule out variations in experimental set up, for example, experiments being carried out on different days, different passages of cells, any slight variation in probe incubation times, etc., and also variations in instrument settings, such as differences in gating, calibration, etc. The relative mean fluorescence of treated/32D/FLT3-ITD cells was expressed as a percentage of control/32D/FLT3-WT cells in each of the biological and technical replicates. For simplicity, one control set

to 100% is presented in the bar chart showing relative mean FLT3/PO1 fluorescence of treated cells expressed as percentage of control. This control is representative of individual controls (DMSO/Ethanol/water) for each of the drug concentrations tested. The relative mean FLT3/PO1 fluorescence of treated cells was expressed as a percentage of the individual matched controls and statistical significance was analysed. The relative mean FLT3/PO1 fluorescence is not being compared between the different drug concentrations. Flow cytometric statistical significance was analysed by Student's t-test using GraphPad, Prism 6. Values of $p<0.05$ were considered statistically significant.

2.7. Immunofluorescence

2.7.1. Fixed cell immunofluorescence

MV4-11 cells were cytospun onto glass slides at 500 rpm for 2 min with a Shandon CytoSpin 11 Cytocentrifuge (Shandon). Cells were fixed for 10 min using 4% paraformaldehyde (PFA)/PBS, washed in PBS and permeabilised with 0.2% Triton-X-100 for 5 min at room temperature. Following two 5 min-washings with PBS, the antigens were blocked for 30 min with 5% FBS/PBS. The cells were incubated with 50 µl of KDEL and FLT3 antibody solutions (1/100 in 5% FBS/PBS) for 1 h at room temperature in a humidity chamber followed by two 5 min-washings with PBS. 50 µl of goat anti-rabbit Alexa fluor 488 (Abcam, cat# Ab150077) or goat anti-mouse Alexa fluor 594 (Abcam, cat# Ab150116) secondary antibody solutions (1/100 in 5% FBS/PBS) were added onto the slides and incubated for 1 h at room temperature. The slides were subsequently washed thoroughly with PBS, followed by water and finally mounted on the coverslips using 5 µl of mowiol (Sigma-Aldrich,

Dublin, Ireland). The slides were dried overnight at room temperature. As controls, fixed cells were incubated with 50 µl of goat anti-rabbit Alexa fluor 488 (Abcam, cat# Ab150077) or goat anti-mouse Alexa fluor 594 (Abcam, cat# Ab150116) secondary antibody solutions (1/100 in 5% FBS/PBS). Eliminating the primary antibody in solution served as a negative control.

2.7.2. Live cell immunofluorescence

Labelling of plasma membrane FLT3-ITD– Live cell immunofluorescence of FLT3-ITD at the plasma membrane of MV4-11, 32D/FLT3-ITD and 32D/FLT3-WT cells was performed on ice. Following centrifugation at 1,000 rpm for 5 min, cells were incubated with anti-FLT3 primary antibody (1/100 in 5% FBS/PBS containing approximately 0.01% Sodium Azide) for 1 h. Following three by 5 min-washings with PBS, the cells were incubated with anti-rabbit Alexa fluor 488 (1/100 in 5% FBS/PBS) for 1 h. Secondary antibody only controls were used. Cells were washed three by 5 min-washings with PBS and viewed under the microscope in ice cold PBS and quantified by flow cytometry using FACSCalibur (BD Biosciences, Europe) and Cellquest Pro software (Becton Dickinson). Healthy populations of cells were gated and the mean fluorescent intensity of 10,000 events was determined.

2.7.3. Microscopy

Mounted slides were viewed on a Leica DM LB2 microscope with Nikon Digital Sight DS-U2 camera, using 40x and 100x objectives. Digital images were captured using the software NIS-Elements version 3.0, Nikon, Japan.

2.8. Western blotting

2.8.1. Whole cell lysis

Following the treatments of indicated durations or siRNA transfections, cells were washed with ice-cold PBS and centrifuged at 1,000 rpm for 5 min at 4°C. Following careful removal of PBS, cells were incubated in radio immunoprecipitation assay (RIPA) lysis buffer [Tris-HCl (50 mM; pH 7.4), 1% NP-40, 0.25% sodium deoxycholate, NaCl (150 mM), EGTA (1mM), sodium orthovanadate (1 mM), sodium fluoride (1 mM), cocktail protease inhibitors (Roche, Welwyn, Hertforshire, UK) and phenylmethylsulfonyl fluoride (1mM)] for 35-45 min at 4°C in vortex, followed by centrifugation at 14,000 rpm for 15 min to remove cell debris. In all cases equivalent amounts of protein (50-100 μg per lane), as determined by the Bio-Rad Protein Assay (Bio-Rad, Hemel, Hempstead, UK) were resuspended in 4X Protein Sample Loading Buffer (LI-COR, cat# P/N 928-40004) containing β-mercaptoethanol (Sigma-Aldrich, Dublin, Ireland) and loaded into 12% (w/v) sodium dodecyl sulphate-polyacrylamide gel electrophoresis (SDS-PAGE). The proteins were stacked at 90 V for 10-15 min and resolved at 120 V using SDS-PAGE. The proteins were then transferred from the SDS-polyacrylamide gel to the nitrocellulose membrane at 100 V for 1 h (Schleicher and Schuell, Dassel, Germany). Total protein levels were analysed using Ponceau or REVERT total protein stain (LI-COR, cat# P/N 926-11011 as per manufacturer's instructions and imaged on a LI-COR Odyssey infrared imaging system (LI-COR Biosciences UK Ltd, Cambridge, UK)). The membranes were incubated for 1 h at room temperature with 5% (w/v) non-fat dry milk or 5% (w/v) bovine serum albumin (BSA) solutions, based on the manufacturer's recommendations, to block non-specific protein binding. The membranes were then incubated overnight at 4°C with the appropriate primary antibodies diluted in blocking solution. Following incubation with

primary antibody, the membranes were washed two times with TBST for 5 min each time. The membrane was then incubated in the secondary antibody (dilution 1:10,000) coupled with Alexa Fluor 680 or 800 (LI-COR Biosciences UK Ltd, Cambridge, UK) diluted in the blocking solution for 1 h at room temperature, followed by two TBST washes and one TBS wash for 5 min each time. In all analyses of whole cell lysate western blots, we normalised for differences in protein loading using REVERT total protein stain or loading controls (β-actin, α-tubulin or Vinculin). Antibody reactive bands were detected using a LI-COR Odyssey infrared imaging. All experiments were carried out in triplicate (N=3 biological samples per condition). Western blots shown in results are representative images of three or more independent experiments, using different samples each time. Densitometry was performed using Image Studio Lite Version 5.0 (LI-COR Biosciences UK Ltd, Cambridge, UK).

2.8.2. Subcellular fractionation

Subcellular fractionation was performed to detect the localisation of NOX4D in FLT3-ITD expressing AML cells, MV4-11 and 32D/FLT3-ITD and BCR-ABL expressing CML cells, K562 using a subcellular protein fractionation kit (Thermo Scientific). According to the manufacturer's protocol, extracts from subcellular compartments generally have less than 15% contamination between fractions, which is sufficient purity for most experiments studying protein localisation. Subcellular fractionation is a very useful technique but has many steps requiring optimisation and careful pipetting of fractions following each extraction step. Manufacturer's instructions were modified to ensure optimal amounts of protein were obtained from each fractionation step. In brief, for MV4-11, 32D/FLT3-ITD and 32D/FLT3-WT

cells, we assumed $1x10^6$ cells were equivalent to 1 µl packed cell volume and for K562 cells, $1x10^6$ cells were equivalent to 2 µl packed cell volume. For the cytoplasmic fraction, one sixth of the recommended quantity of buffer was added followed by gentle mixing for 6-7 min. In the membrane extraction step, one eighth of the recommended quantity of buffer was added. Finally, for the nuclear extraction, one fifth of the recommended quantity of buffer was added for soluble nuclear and chromatin bound nuclear extractions. RIPA lysis buffer was used as an alternative to the nuclear extraction buffers provided. RIPA buffer was added at a volume of 10 µl per initial 10 µl packed cell volume. Soluble nuclear- and chromatin bound nuclear-extraction buffers provided in the kit were used for the majority of experiments as they were found to obtain better protein concentrations than that of RIPA lysis buffer. In all analyses of subcellular fractionation western blots, we normalised for differences in protein loading of membrane and soluble nuclear fractions using ER membrane marker, calreticulin, and nuclear membrane marker, NUP98. Antibody reactive bands were detected using a LI-COR Odyssey infrared imaging. All experiments were carried out in triplicate (N=3 biological samples per condition). Western blots shown in results are representative images of three or more independent experiments, using different samples each time. Densitometry was performed using Image Studio Lite Version 5.0 (LI-COR Biosciences UK Ltd, Cambridge, UK).

2.9. Small interfering RNA (siRNA) and small hairpin (shRNA) transfections

The siRNA transfection of MV4-11 cells was performed using the Nucleofector Kit L (Amaxa, Cologne, Germany) and AmaxaNucleofector Technology according to the company's protocol. The predesigned siRNA used for silencing was $p22^{phox}$ (ID: S3786 (A)). For the negative control, the siRNA used was Silencer Select Negative Control #1 siRNA (Control). All were purchased from Ambion, Warrington, UK. Cells were seeded at 0.5×10^6/ml 16 h before the transfection. Before the procedure siRNA solutions were prepared in 50 µl of the nucleofection buffer provided. Approximately 2×10^6 cells were cytospun at 1,000 rpm for 5 min at room temperature and resuspended in 50 µl of the same nucleofection buffer. The solutions of cells and siRNA were combined and immediately transferred into the certified nucleofection cuvette. The cuvette was inserted into the nucleofection cuvette holder and the correct nucleofection program was applied (Q-001). The contents of the cuvette were immediately diluted in the fresh medium (0.5 ml) and added drop wise onto the 6-well plate with more of fresh medium in it (1.5 ml). The final density of cells in the well following the transfection was 1×10^6/ml. The plate was transferred to a humidified incubator (37°C with 5% CO_2) for 24 h. NOX4 siRNA and shRNA in 32D/FLT3-ITD cells was carried out by our collaborator as previously decribed (Jayavelu et al., 2016a).

2.10. NOX4 overexpression transfections

For NOX4 overexpression in HEK 293-T cells, cells were transfected using calcium phosphate. Briefly, cells were seeded 5 h prior to transfection to allow confluency of 70%. 4 µg of pCMV3-C-HA encoding full length cDNA clone of *Homo sapiens* NOX4 (#HG15189-CY; Sino Biological, UK) was added to $CaCl_2$. The DNA/$CaCl_2$ mixture was then added dropwise to 2X Hanks' balanced salt solution (HBSS) at a ratio of 1:1. Samples were allowed to stand for 1-2 min after which the solution was distributed to the pre-seeded cells in a dropwise manner. Cells were then incubated overnight to allow the transfection to proceed, after which cells were reseeded for experimental purposes and lysed 48 h later.

2.11. Total RNA isolation and RT-qPCR

Total RNA was isolated from whole cells using RNeasy Mini Kit (Qiagen, West Sussex, UK) following manufacturer's protocol. All samples were treated for DNase using RNase free DNase set (Qiagen) and 1 µg complementary DNA (cDNA) was synthesised using QuantiTect Reverse Transcription Kit (Qiagen) according to manufacturer's instructions. The cDNA product was then diluted 1:5 with RNase free water (Sigma) and RT-PCR was performed using SYBR Green JumpStart *Taq* ReadyMix (Sigma-Aldrich) in a 384 well plate (Starstedt AG & Co.). Plates were run using the Applied Biosystems 7900HT Fast Real-Time PCR System (Life Technologies Ltd., Paisley, UK) and each set of reactions included both a non-reverse transcription control and a no template sample negative control (data not shown). The protocol consisted of a cycling profile of 30s at 95°C, 60s at 60°C, and 30s at 72°C

for 40 cycles. Qiagen QuantiTect Primer assays were used for housekeeping genes, NOX4 and $p22^{phox}$ (Table 2.3.1.). NOX4 primers (Eurofins) were used (Table 2.3.2.), as designed by (Reddy et al., 2011). Melt curve analysis confirmed that a single PCR product was present for all genes amplified by Qiagen QuantiTect Primer Assays except for NOX4. Primer efficiency was checked for each primer-set using a representative test sample prepared as the experimental sample (untreated cDNA from MV4-11 cells). A serial dilution was used to evaluate the slope of the log (relative concentration) versus Ct and primer efficiency was calculated by the equation m = (1/log E), where m = slope of the line and E = the efficiency (Mygind et al. 2002). All primer sets were between 86% and 105% efficient and within 20% efficiency of each other, as is recommended (Schmittgen and Livak, 2008). NOX4 melt curve analysis identified a variety of PCR products following amplification with Eurofins NOX4 primer, primer efficiency was tested and subsequent gene sequencing was carried out by GATC Biotech, London, United Kingdom. Relative changes in gene expression were quantified using the comparative Ct ($\Delta\Delta$Ct) method as described by (Livak and Schmittgen, 2001, Schmittgen and Livak, 2008). The Ct value of the gene of interest was normalised to an average of the three endogenous housekeeping genes (ACTB, B2M and PSMB2). This was then compared to the normalised control sample - i.e. the equivalent dimethyl sulfoxide (DMSO; for tunicamycin and PKC412)/Ethanol control (for brefeldin A). All experiments were carried out in triplicate (PKC412) or quadruplicate (tunicamycin and brefeldin A) (N=3 or N=4 biological samples per condition and n=3 technical replicates per biological sample). Alterations in mRNA expression of target genes was defined as fold difference in the expression level in cells after treatment, relative to that of the control.

2.11.1. Agarose gel electrophoresis of RT-qPCR product

Approximately 20 µl of the gene sequences amplified by RT-qPCR were resuspended in 5X DNA loading buffer (Bioline, cat# BIO-37045) and run on 2% agarose gel containing SYBR Safe DNA gel stain (Invitrogen, cat# S33102) at 100 V for 1 h. The ladder used was BioLabs Quick-load 100 bp DNA ladder (New England BioLabs, cat# N0467).

2.12. Analysis of cell number and cell viability

Cells were incubated in 1 ml of RPMI 1640 medium in 24-well plates at 37°C for indicated time points with the indicated concentration of drugs used, equivalent volumes of DMSO (for all drugs unless otherwise stated), ethanol (for brefeldin A) and sterile H_2O (for LiCl and diclofenac) were added to cells as controls. Numbers and viability of the cells were determined by counting with a haemocytometer after staining with trypan blue (#T8154, Sigma-Aldrich, Ireland, Dublin). All experiments were carried out in duplicate (N=2 biological samples per condition).

2.13. Haematoxylin staining

MV4-11 cells were cytospun onto glass slides at 500 rpm for 2 min with a Shandon CytoSpin 11 Cytocentrifuge (Shandon). Slides were fixed using ethanol, methanol/acetone (1:1) or 4% PFA/PBS. *Ethanol fixation*- slides were immersed in 100% ethanol for 15 min, 70% ethanol for 5 min, 50% ethanol for 5 min and 25% ethanol for 5 min. *Methanol/acetone fixation*- the glass slides were immersed in ice-

cold methanol/acetone and incubated at -20°C for 10-15 min. *4% PFA/PBS fixation*-slides were fixed with 4% PFA/PBS for 5 min at room temperature followed by brief wash with PBS to remove excess 4% PFA/PBS. Following fixation, slides were left to dry and stained for 3-4 min with haematoxylin (GH5232, Sigma-Aldrich, Dublin, Ireland) and washed gently under running tap water for 5 min. Slides were dehydrated and coverslips were mounted using distyrene plasticizer xylene (DPX) (100503-834, VWR) and left to dry in a fume hood overnight before imaging.

2.14. Statistical analysis

Image Studio Lite Version 5.0 (LI-COR Biosciences UK Ltd, Cambridge, UK) was used to analyse all western blots. Values in all graphs are representative of mean ± standard deviation (SD) and are representative of at least three independent experiments. Statistical significance was analysed using the appropriate test (see individual figure legends) using GraphPad, Prism 6. Values of $p<0.05$ were considered statistically significant.

Chapter 3. Subcellular localisation of FLT3-ITD and ROS generation

3.1. Abstract

Internal tandem duplication of the juxtamembrane domain of FMS-like tyrosine kinase 3 (FLT3-ITD) receptor is the most prevalent FLT3 mutation accounting for 15-35% of acute myeloid leukaemia (AML) patients. FLT3-ITD mutation results in ligand-independent constitutive activation of the receptor at the plasma membrane and 'impaired trafficking' of the receptor in compartments of the endomembrane system, such as the endoplasmic reticulum (ER). FLT3-ITD expressing cells have been shown to generate increased levels of reactive oxygen species (ROS), in particular NADPH oxidase (NOX)-generated ROS which act as pro-survival signals. The purpose of this study was to investigate FLT3-ITD production of ROS at the plasma membrane and ER in the FLT3-ITD expressing AML cell line MV4-11. Receptor trafficking inhibitors, tunicamycin and brefeldin A, induce ER retention of FLT3-ITD, resulting in a decrease in protein levels of NOX4 and its partner protein $p22^{phox}$. This demonstrates the critical importance of FLT3-ITD localisation for the generation of pro-survival ROS. NOX- and mitochondrial-generated ROS contribute to total endogenous hydrogen peroxide (H_2O_2) in AML as quantified by flow cytometry using the cell-permeable H_2O_2-probe Peroxy Orange 1 (PO1). ER retention of FLT3-ITD resulted in NOX4 deglycosylation and decreased $p22^{phox}$ at both RNA and protein levels.

3.2. Introduction

Constitutively active mutations in receptor tyrosine kinases (RTKs) are frequently observed in human cancers (Blume-Jensen and Hunter, 2001, Köthe et al., 2013). FMS-like tyrosine kinase 3 (FLT3) is a type III RTK expressed in approximately 90% of acute myeloid leukaemia (AML) cases and regulates early steps of haematopoiesis (Stirewalt and Radich, 2003, Gilliland and Griffin, 2002). Internal tandem duplication (ITD) of the juxtamembrane domain is the most prevalent mutation of FLT3 present in 15-35% of AML patients, resulting in ligand-independent constitutive activation of the receptor at the plasma membrane and impaired trafficking of the receptor in compartments of its biosynthetic route, such as the endoplasmic reticulum (ER) (Gilliland and Griffin, 2002, Smith et al., 2012, Schmidt-Arras et al., 2009, Jayavelu et al., 2016b). AML patients with the FLT3-ITD mutation have a poor prognosis (Thiede et al., 2002, Small, 2008). Ligand-independent constitutive activation of FLT3 stimulates autophosphorylation of the receptor and downstream signalling pathways including PI3K/AKT, ERK and STAT5 resulting in abnormal cell growth, resistance to apoptosis and a differentiation block (Choudhary et al., 2005a, Brandts et al., 2005, Hayakawa et al., 2000, Mizuki et al., 2000). Our group demonstrated that cells expressing FLT3-ITD produce higher levels of pro-survival reactive oxygen species (ROS) in comparison to cells expressing wild-type FLT3 (Sallmyr et al., 2008a, Godfrey et al., 2012, Woolley et al., 2012, Stanicka et al., 2015).

Increased production of ROS has been linked to various pathophysiological states including leukaemia (Hole et al., 2011). Little is known about how FLT3-ITD generates such a stress. NADPH oxidases (NOXs) are one of the known sources of

ROS in FLT3-ITD expressing cells (Stanicka et al., 2015). There are seven NOX isoforms NOX1-5 and dual oxidase 1-2 (DUOX1-2), varying in structure, subcellular localisation, biochemical characteristics and regulatory subunit requirements ($p22^{phox}$, $p47^{phox}$, $p67^{phox}$ and RAS-related C3 Botulinum Toxin substrate 1/2 (RAC1/2)). NOX1-4 require $p22^{phox}$ to produce functionally active NOX (Brandes et al., 2014, Ambasta et al., 2004). NOX2 and NOX4 have been shown previously to be expressed in leukaemia (Jayavelu et al., 2016a, Block and Gorin, 2012). Other sources of ROS include mitochondrial ROS, cyclooxygenase (COX), xanthine oxidase, cytochrome P450 enzymes and lipoxygenases (Holmstrom and Finkel, 2014, Finkel, 2011, Gough and Cotter, 2011).

Previous studies have looked at the molecular mechanisms through which FLT3-ITD initiates aberrant signalling of pro-survival pathways (PI3K, ERK, STAT5) at the plasma membrane and ER using receptor trafficking inhibitors, tunicamycin and brefeldin A (Choudhary et al., 2009). However, the molecular mechanism describing how mislocalised activation of FLT3-ITD and aberrant signalling of downstream pathways leads to the production of ROS and sources of ROS remains unknown. To analyse the role of the cellular localisation of FLT3-ITD in the generation of ROS and its signalling outcome, we utilised a panel of inhibitors of glycosylation/receptor trafficking and ROS production, FLT3-ITD and the 20S proteasome, alongside ROS specific antibodies, probes and RT-qPCR. Experiments were carried out in the FLT3-ITD AML expressing MV4-11 cell line.

Receptor trafficking inhibitors, tunicamycin and brefeldin A, induce ER retention of FLT3-ITD, resulting in a decrease in protein levels of NOX4 and its partner protein $p22^{phox}$. This is as a result of NOX4 deglycosylation and decreased

p22^{phox} RNA levels and protein degradation. Our data demonstrates the critical importance of FLT3-ITD localisation for the generation of pro-survival ROS.

3.3. Results

3.3.1. Haematoxylin staining of fixed and permeabilised MV4-11 cells

Fixation of cells using 4% PFA/PBS and permeabilisation using 0.2% Triton-X-100 is the most commonly used fixative in immunofluorescence protocols. We analysed the effect of different fixation and permeabilisation protocols: ethanol, methanol/acetone and 4% PFA/PBS and 0.2% Triton-X-100 on the morphology of MV4-11 cells (Figure 3.1.). Although the cells morphology changed following fixation with 4% PFA/PBS and permeabilisation with 0.2% Triton-X-100, we found this to be the optimal fixation/permeabilisation for immunofluorescence colocalisation studies.

a)

b)

c)

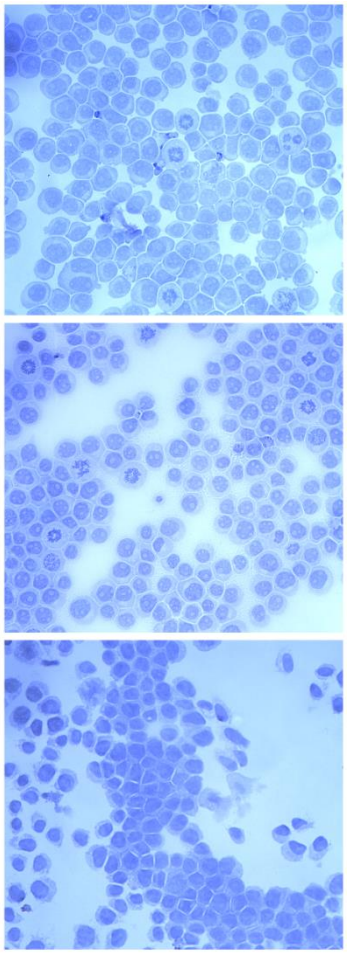

Figure 3.1. Haematoxylin staining of fixed and permeabilised MV4-11 cells. Cells were fixed and permeabilised using ethanol *(a)*, methanol/acetone *(b)* and 4% PFA/PBS and 0.2% Triton-X-100 *(c)* followed by incubation with haematoxylin for 3-4 min.

3.3.2. FLT3-ITD expression colocalises to the plasma membrane and endoplasmic reticulum of MV4-11 cell line

FLT3-ITD is the most common mutation expressed in 15-35% of AML cases (Stirewalt and Radich, 2003). In order to study the role of the FLT3-ITD mutation in redox signalling in AML, we chose the MV4-11 human cell line as our model. MV4-11 cell line is a well-established model of patient derived AML that expresses homozygous FLT3-ITD.

FLT3-WT receptor in its unstimulated form is found at the plasma membrane, unphosphorylated with an inactive tyrosine kinase domain (Köthe et al., 2013, Grafone et al., 2012). Upon interaction with FL, the receptor autophosphorylates and undergoes a conformational change resulting in activation of the tyrosine kinase domain (Levis and Small, 2003). FLT3-ITD is the most prevalent FLT3 mutation resulting in ligand-independent constitutive activation of the receptor at the plasma membrane and impaired trafficking of the receptor in intracellular compartments, such as the ER (Choudhary et al., 2009, Jayavelu et al., 2016b, Moloney et al., 2017b). Immunofluorescence studies confirmed the colocalisation of FLT3-ITD to the ER (Figure 3.2.) and plasma membrane (Figure 3.7.) in MV4-11 cells.

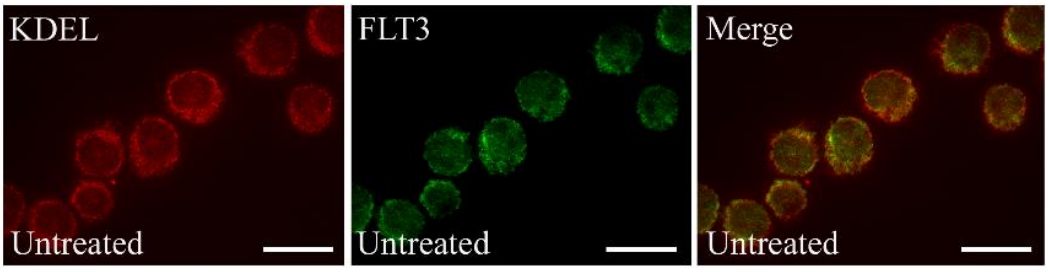

Figure 3.2. FLT3 is localised to the endoplasmic reticulum in MV4-11 cells. Colocalisation of FLT3 with ER marker KDEL in untreated MV4-11 cells. The scale bar represents 30µm.

3.3.3. FLT3-ITD expressing cells express significantly higher levels of the FLT3 receptor at the plasma membrane compared to FLT3-WT expressing cells

In addition to the FLT3-ITD AML expressing MV4-11 cell line, we also employed an overexpression of the FLT3 system. FLT3-WT or mutated FLT3-ITD plasmids were stably transfected into 32D cells. 32D is a murine immortalised myeloblast-like cell line that is grown in IL-3 supplemented medium. Post transfection, due to strong cytokine-like FLT3-ITD signalling, 32D/FLT3-ITD cells became IL-3 independent (Mizuki et al., 2000, Fenski et al., 2000). Both wild-type and mutated FLT3 receptor have been found to colocalise to the plasma membrane (Choudhary et al., 2009). FLT3-ITD has been found to be activated independently of FLT3 ligand stimulation and is constitutively activated. We analysed the expression of the FLT3 receptor at the plasma membrane of 32D/FLT3-WT- and 32D/FLT3-ITD-expressing cells by fluorescently labelling the FLT3 receptor at the plasma membrane in live cells. 32D/FLT3-ITD cells were found to express a 250-fold increase in FLT3 expression at the plasma membrane compared to their wild-type counterpart (Figure 3.3.).

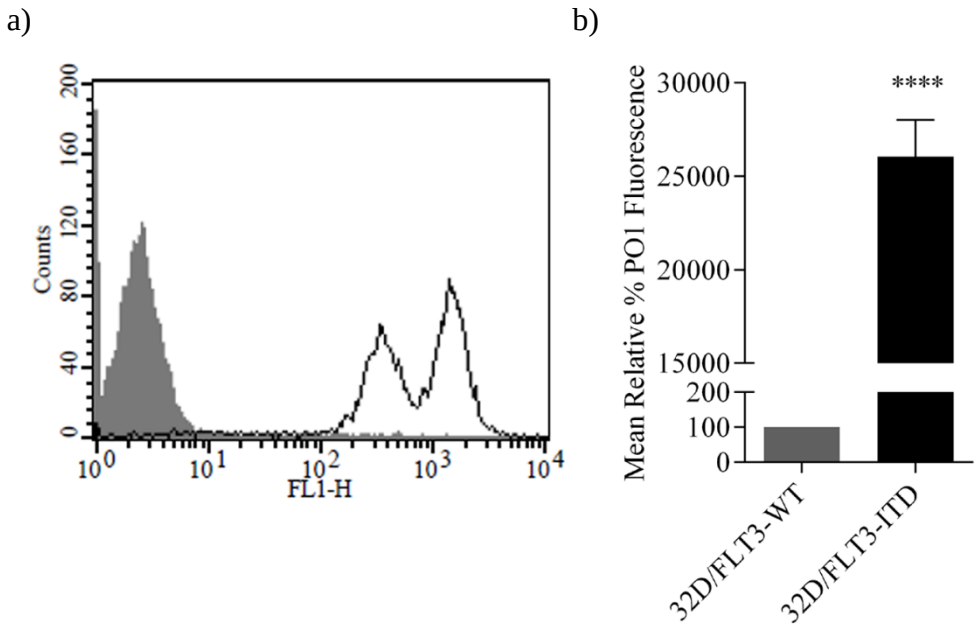

Figure 3.3. 32D/FLT3-ITD cells express significantly higher levels of FLT3 at the plasma membrane compared to 32D/FLT3-WT cells. Flow cytometric analysis of FLT3 fluorescence at the plasma membrane of 32D cells stably transfected with FLT3-WT and FLT3-ITD *(a)*. Bar chart shows relative mean FLT3 fluorescence at the plasma membrane of 32D/FLT3-ITD cells expressed as a % of 32D/FLT3-WT cells *(b)*. Results are presented as mean ± SD from three independent experiments. Asterisks indicate statistically significant differences (****$p<0.0001$) as analysed by Student's t-test.

3.3.4. Receptor trafficking inhibitors, tunicamycin and brefeldin A, induce ER retention of FLT3-ITD

We have shown that FLT3-ITD colocalises to the ER and plasma membrane of MV4-11 cells. In order to analyse the role of cellular localisation of FLT3-ITD in the generation of ROS and its signalling outcome, cells were treated with tunicamycin and brefeldin A to inhibit glycosylation of FLT3-ITD, resulting in impaired trafficking of the FLT3-ITD receptor to the plasma membrane. Tunicamycin prevents glycosylation of plasma membrane receptors, retaining receptors in intracellular compartments, by blocking the formation of protein N-glycosidic linkages and consequently blocking the first step of glycoprotein synthesis (Helenius and Aebi,

2004, Bassik and Kampmann, 2011). Brefeldin A inhibits mature and complex glycosylation of plasma membrane receptors through inhibition of guanine-nucleotide exchange factors that are required for ADP-ribosylation factor (ARF) GTPases, resulting in disruption of the structure and function of the Golgi apparatus (Fujiwara et al., 1988). We show that treatment of MV4-11 cells with tunicamycin and brefeldin A result in retention of FLT3-ITD in a compartment of the biosynthetic route, such as the ER (Figure 3.4.). We found the optimal concentration with the largest decrease in mean relative FLT3 fluorescence at the plasma membrane with the least effect on cell viability to be 5 µg/ml tunicamycin (Figure 3.5.) and 10 µg/ml brefeldin A (Figure 3.6.). We demonstrated that both of these treatments resulted in a decrease of 50-60% of FLT3-ITD expression at the plasma membrane when compared to vehicle control (tunicamycin; DMSO and brefeldin A; Ethanol) as quantified by flow cytometry (Figure 3.7.).

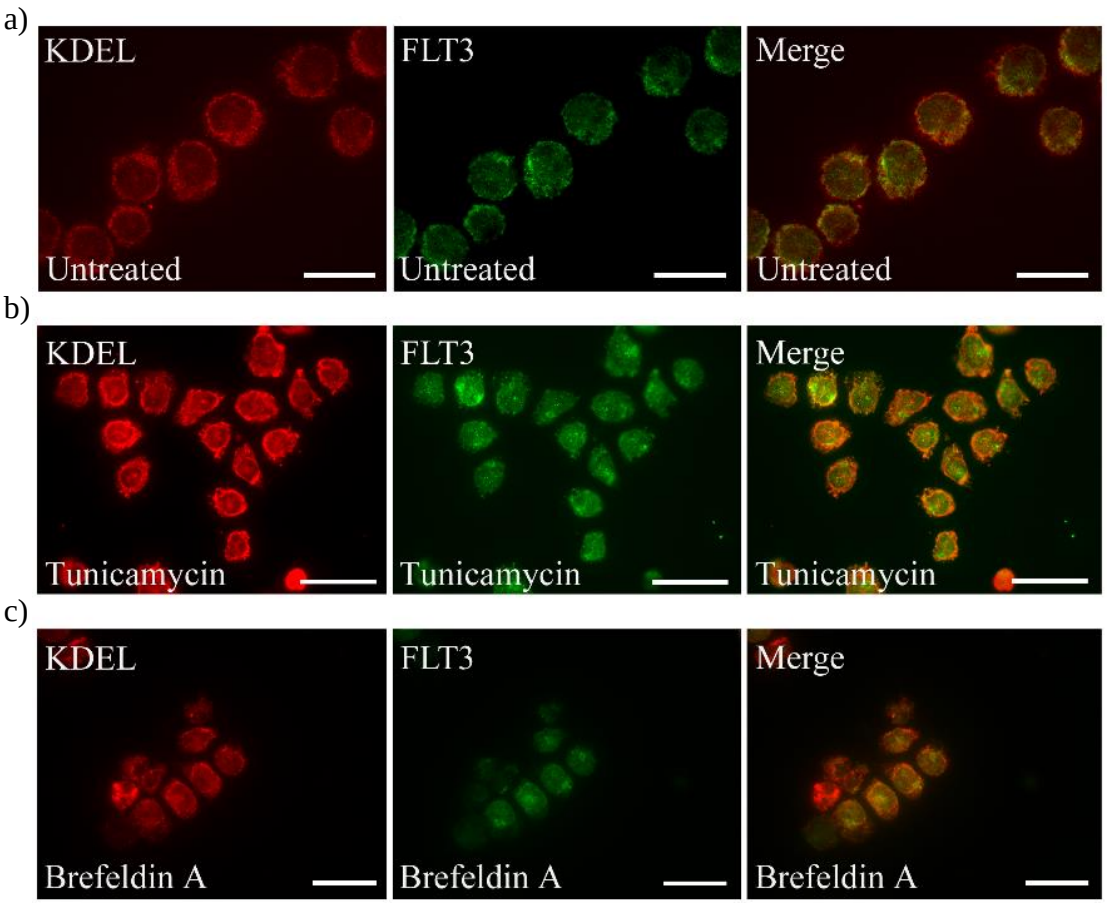

Figure 3.4. FLT3 localises to the endoplasmic reticulum following treatment with tunicamycin and brefeldin A. Colocalisation of FLT3 with ER marker KDEL in MV4-11 cell line. Untreated (*a*), tunicamycin treated (5 µg/ml overnight) (*b*) and brefeldin A treated (10 µg/ml overnight) (*c*). The scale bar represents 30µm.

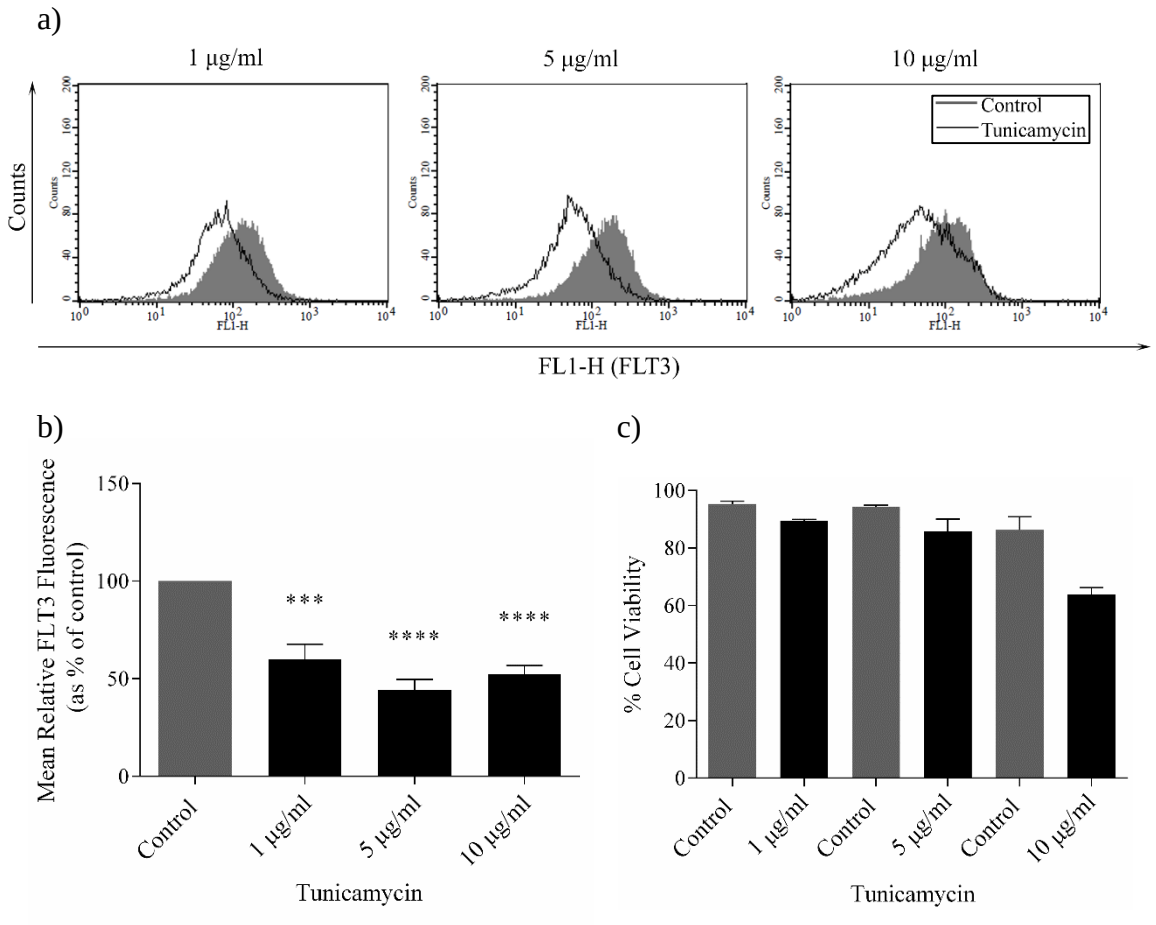

Figure 3.5. Tunicamycin induced ER retention of FLT3-ITD in MV4-11 cells. % FLT3 fluorescence at the plasma membrane of MV4-11 cells following treatment with receptor trafficking inhibitor tunicamycin. Flow cytometric analysis of mean relative FLT3 fluorescence at the plasma membrane using 1 µg/ml - 10 µg/ml range tunicamycin concentrations in MV4-11 cells treated overnight (*a)*. Bar chart shows relative mean FLT3 fluorescence of treated cells expressed as % of control *(b)*. Results are presented as mean ± SD from three independent experiments. Asterisks indicate statistically significant differences (***p<0.001, ****p<0.0001) as analysed by Student's t-test. Bar chart of % cell viability following treatment with the indicated concentrations of tunicamycin compared to vehicle controls (N=2) *(c)*.

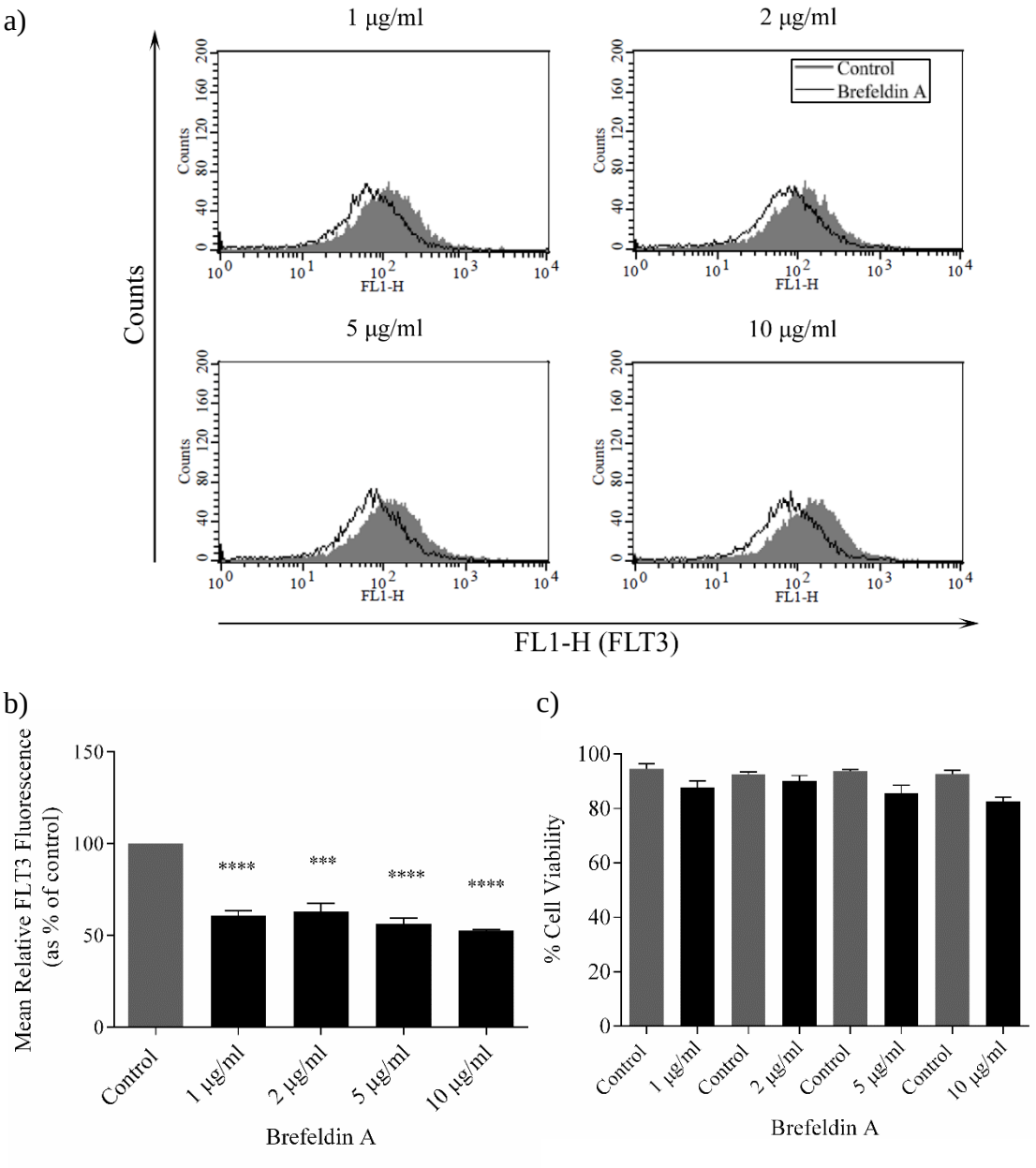

Figure 3.6. Brefeldin A induced ER retention of FLT3-ITD in MV4-11 cells. % FLT3 fluorescence at the plasma membrane of MV4-11 cells following treatment with receptor trafficking inhibitor brefeldin A. Flow cytometric analysis of mean relative FLT3 fluorescence at the plasma membrane using 1 µg/ml - 10 µg/ml range brefeldin A concentrations in MV4-11 cells treated overnight (*a*). Bar chart shows relative mean FLT3 fluorescence of treated cells expressed as % of control *(b)*. Results are presented as mean ± SD from three independent experiments. Asterisks indicate statistically significant differences (***p<0.001, ****p<0.0001) as analysed by Student's t-test. Bar chart of % cell viability following treatment with the indicated concentrations of brefeldin A compared to vehicle controls (N=2) *(c)*.

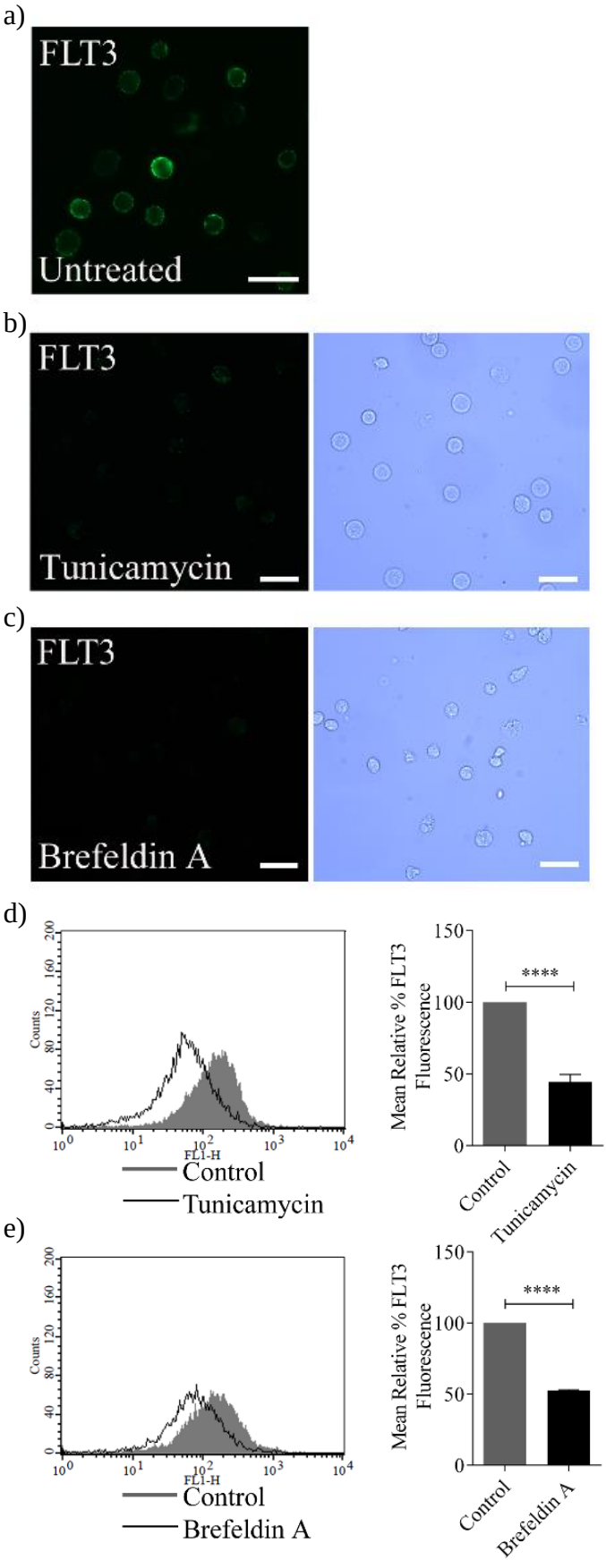

Figure 3.7. Tunicamycin and brefeldin A induce ER retention of FLT3-ITD in MV4-11 cells. Live cell immunofluorescence of FLT3 at the plasma membrane in MV4-11 cell line, untreated (*a*), tunicamycin treated (5 µg/ml overnight) (*b*) and brefeldin A treated (10 µg/ml overnight) (*c*). Phase contrast pictures were taken to show the presence of cells with a decrease in FLT3 fluorescence at the plasma membrane. The scale bar represents 30µm. Flow cytometric analysis of mean relative FLT3 fluorescence at the plasma membrane in MV4-11 cell line treated with tunicamycin (*d*) and brefeldin A (*e)*. Bar charts show relative mean FLT3 fluorescence of treated cells expressed as % of control. Results are presented as mean ± SD from three independent experiments. Asterisks indicate statistically significant differences (****p<0.0001) as analysed by Student's t-test.

3.3.5. $p22^{phox}$ has many hydrophobic regions and boiling of cell lysates results in $p22^{phox}$ protein aggregation

$p22^{phox}$ is a partner protein of NOX1-4 and is required for NOX activation. We prepared unboiled and boiled samples of equal protein concentrations from the same MV4-11 cell lysates and carried out western blot analysis. We observed that $p22^{phox}$ protein levels were undetectable in boiled cell lysates compared to unboiled cell lysates (Figure 3.8. a). Firstly, we investigated if protein aggregation was an issue. Denaturation of the proteins in cell lysates resulted in protein aggregation evident by the presence of proteins at the top of the gel and membrane (Figure 3.8. b and c). Moreover, to validate $p22^{phox}$ protein aggregation following boiling of cell lysates, we examined the amino acid sequence for $p22^{phox}$ and identified the presence of several hydrophobic amino acids including alanine, glycine, isoleucine, leucine, methionine, phenylalanine, proline and valine (Figure 3.8. d) suggesting that the $p22^{phox}$ protein aggregates following denaturation of cell lysates. Therefore, in future studies investigating $p22^{phox}$ protein levels and the levels and expression of proteins who require $p22^{phox}$ for fully functioning proteins such as NOX4, cell lysates should not be boiled/denatured.

a)

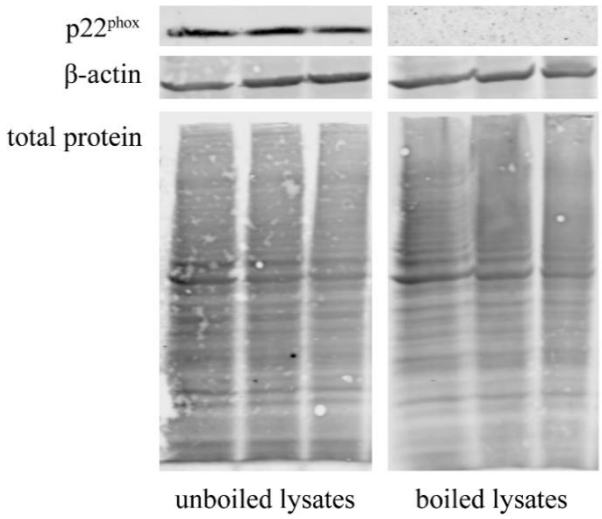

b)

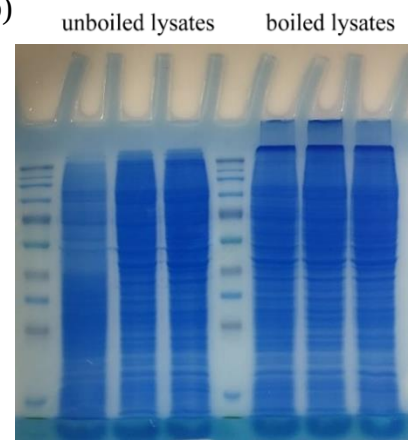

c)

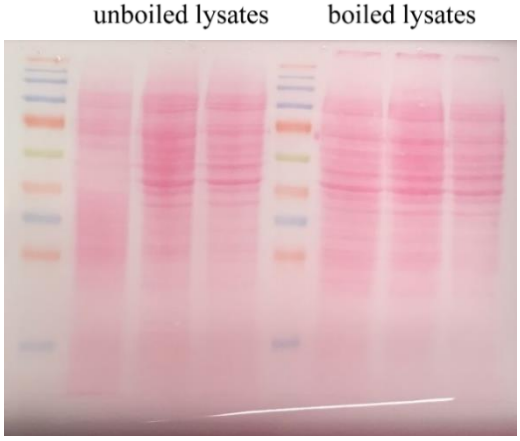

d)

>sp|P13498|CY24A_HUMAN Cytochrome b-245 light chain OS=Homo sapiens GN=CYBA PE=1 SV=3

MGQI**E**W**AM**W**A**NEQ**ALA**S**GLILI**T**GGIVA**T**AG**R**F**TQWY**FGA**YS**IVAGVFV**C**LL**EY**P**R
GKRKK**G**ST**M**ERW**G**QKY**M**T**AVV**K**LFGPF**TRNYY**V**R**AVL**H**LLL**S**VPAGFLLA**T**ILG**TA
C**LAIA**S**GI**Y**LLAAV**R**G**EQWT**PI**E**P**K**P**RER**P**Q**IGG**T**I**KQ**PP**SN**PPP**R**PPA**E**A**RKK**P**S
EEE**GGP**Q**V**N**PIPV**TDE**VV**

Figure 3.8. Boiling of MV4-11 cell lysates results in p22^{phox} protein aggregation. Western blot analysis of p22^{phox} protein levels in unboiled and boiled cell lysates *(a)*. β-actin and total protein (REVERT total protein stain) are shown as loading controls. Western blots are representative of three independent experiments. Analysis of total protein levels in unboiled cell lysates (lanes 2-4) and boiled cell lysates (Lane 6-8) by means of staining the gel with Coomassie brilliant blue overnight *(b)* and incubating the nitrocellulose membrane with Ponceau *(c)*. p22^{phox} amino acid sequence *(d)*. The hydrophobic amino acids are represented in bold. Alanine (A), glycine (G), isoleucine (I), leucine (L), methionine (M), phenylalanine (F), proline (P), valine (V).

3.3.6. Impaired trafficking of the FLT3-ITD receptor to the plasma membrane results in a decrease in protein levels of NOX4 and its partner protein $p22^{phox}$

FLT3-ITD expressing cell lines have been shown to express higher levels of endogenous ROS in comparison to FLT3-WT receptor cell line (Sallmyr et al., 2008a, Stanicka et al., 2015). The mechanism in which FLT3-ITD driven pro-survival ROS leads to the aggressive form of AML remains unknown. We examined the effect of ER retention of FLT3-ITD on $p22^{phox}$ and NOX4 protein levels. $p22^{phox}$ and NOX4 protein levels decreased significantly following treatment with both receptor trafficking inhibitors, tunicamycin and brefeldin A (Figure 3.9.). This suggests that for FLT3-ITD to produce NOX-generated pro-survival ROS it has to be located at the plasma membrane. This is supported by previous work from our laboratory showing that ligand-stimulated FLT3-WT results in an increase in $p22^{phox}$ protein levels (Stanicka et al., 2015).

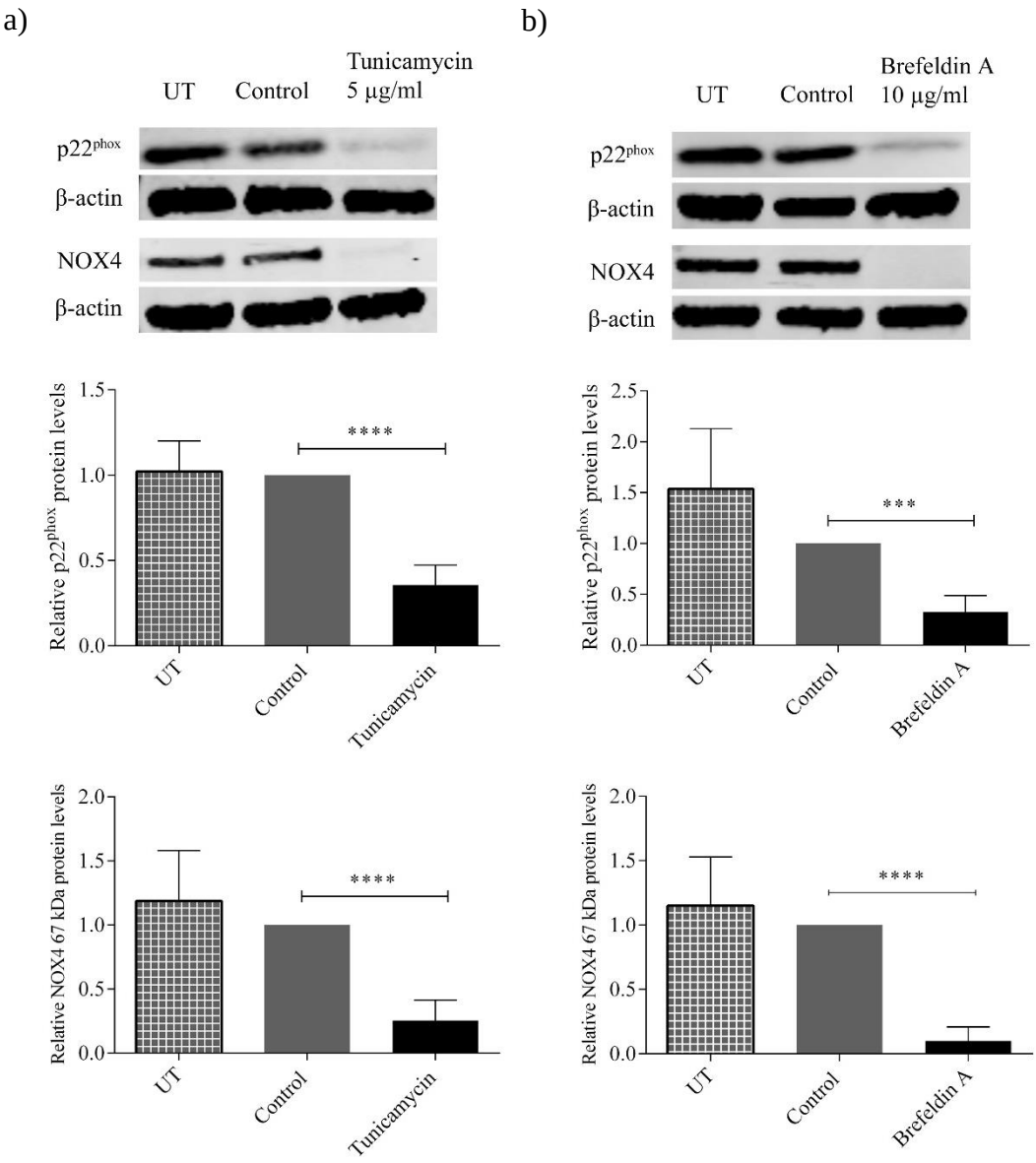

Figure 3.9. Plasma membrane FLT3-ITD is required for p22^{phox} and NOX4 expression at the protein level. p22^{phox} and NOX4 protein levels following ER induced retention of FLT3-ITD. Western blot analysis of p22^{phox} and NOX4 protein levels in untreated (UT), vehicle control (control) and following treatment with tunicamycin (5 µg/ml) *(a)* and brefeldin A (10 µg/ml) *(b)* overnight. β-actin is shown as a loading control. Bar charts show relative mean p22^{phox} and NOX4 protein levels following treatment with tunicamycin (5 µg/ml) *(a)* and brefeldin A (10 µg/ml) *(b)* overnight as quantified by densitometry. The data are expressed as % of control, where the ratio in the control was defined as 1. Results are presented as mean ± SD from four independent experiments. Asterisks indicate statistically significant differences (***$p<0.001$, ****$p<0.0001$) as analysed by Student's t-test.

3.3.7. p22^{phox} knockdown had no effect on NOX4 protein levels

We have shown that impaired trafficking of the mutated FLT3 receptor to the plasma membrane results in decreased p22^{phox} and NOX4 protein levels (Figure 3.9.). p22^{phox} is a partner protein and is required for functionally active NOX1-4 (Ambasta et al., 2004). Specific p22^{phox} knockdown allowed us to investigate the effects of p22^{phox} on NOX4 protein expression. Knockdown of p22^{phox} had no effect on NOX4 protein levels (Figure 3.10.).

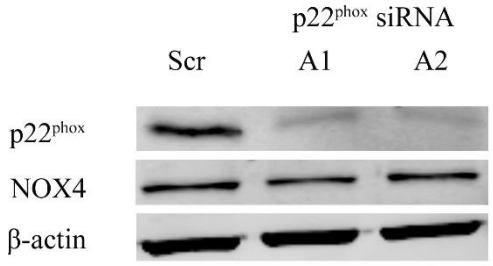

Figure 3.10. Knockdown of p22^{phox} in FLT3-ITD expressing MV4-11 cells had no effect on NOX4 protein levels. p22^{phox} siRNA knockdown effect on NOX4 protein levels. Western blot analysis of p22^{phox} and NOX4 protein levels in MV4-11 cells following treatment with p22^{phox} siRNA compared with the non-targeting scrambled (Scr) siRNA treated control. β-actin is shown as a loading control. Western blot is representative of three independent experiments.

3.3.8. NOX-generated ROS contribute to total pro-survival ROS in AML

Our group has shown previously that knocking down p22^{phox} resulted in almost 20% decrease in total and nuclear H_2O_2, and knocking down NOX4 resulted in approximately 30% decrease of total cellular H_2O_2 and 20% decrease of nuclear H_2O_2 (Stanicka et al., 2015). Given that ER retention of FLT3-ITD resulted in a significant decrease in p22^{phox} and NOX4 protein levels (Figure 3.9.), we decided to investigate the effect of ER retention of FLT3-ITD on total endogenous H_2O_2 using the probe

Peroxy Orange 1 (PO1). This revealed that tunicamycin treated cells resulted in approximately 35% decrease and brefeldin A treated cells resulted in approximately 25% decrease of total endogenous H_2O_2 as quantified by flow cytometry. (Figure 3.11.)

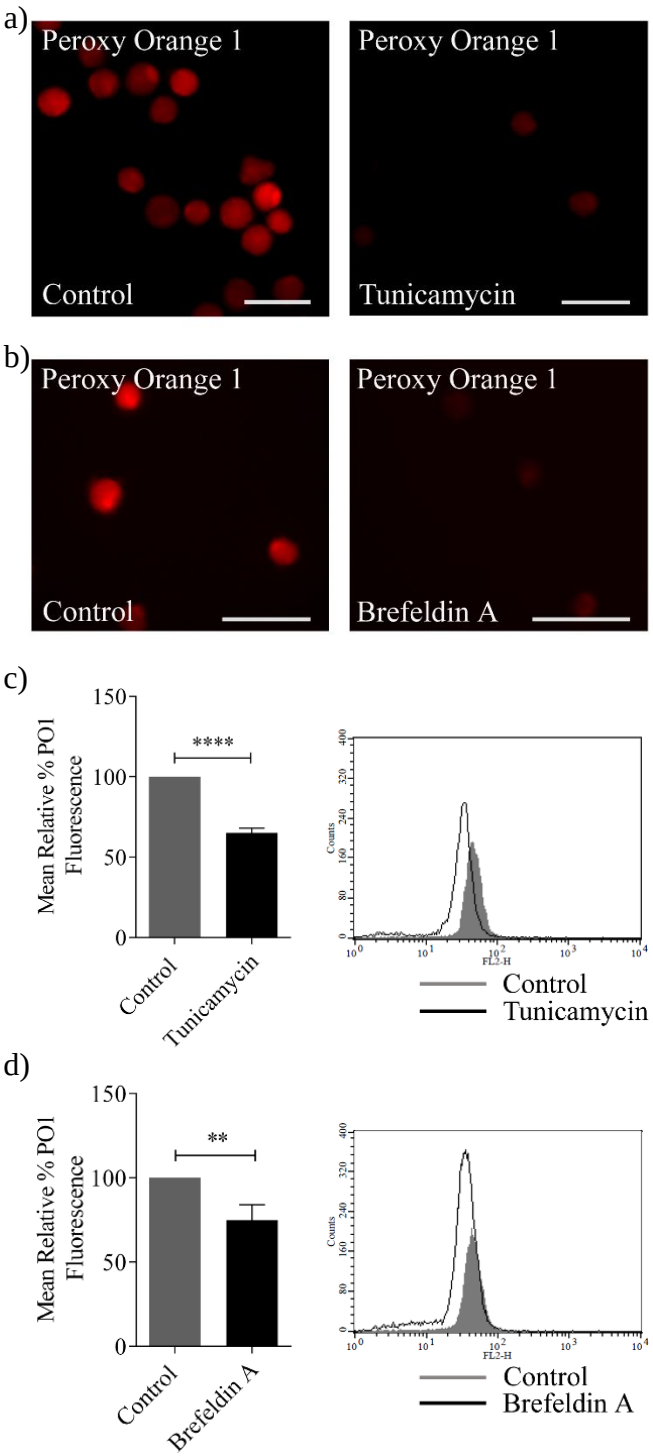

Figure 3.11. Production of NOX4-generated ROS from FLT3-ITD at the plasma membrane contributes to total endogenous H_2O_2 in MV4-11 cells. Cellular H_2O_2 levels following retention of FLT3-ITD in compartments of the endomembrane system. Live cell immunofluorescence of total cellular H_2O_2 levels in vehicle control (control) and tunicamycin treated (5 µg/ml overnight) (*a*) and brefeldin A treated (10 µg/ml overnight) (*b*) MV4-11 cells as measured by H_2O_2-probe, Peroxy Orange 1 (PO1). The scale bar represents 30µm. Flow cytometric analysis of mean relative PO1 fluorescence in MV4-11 cell line treated with tunicamycin overnight (*c*), and brefeldin A overnight (*d*). Bar charts show relative mean PO1 fluorescence of treated cells expressed as % of control. Results are presented as mean ± SD from three independent experiments. Asterisks indicate statistically significant differences (**p<0.01, ****p<0.0001) as analysed by Student's t-test.

3.3.9. Cyclooxygenase-generated ROS do not contribute to total endogenous H_2O_2 in AML; while mitochondrial-generated ROS contribute to total endogenous H_2O_2 in AML.

$p22^{phox}$ and NOX4 contribute to approximately 25-35% total endogenous H_2O_2 (Figure 3.11.). We investigated other potential sources of ROS that may contribute to total endogenous H_2O_2 in FLT3-ITD expressing AML MV4-11 cells. We used cyclooxygenase inhibitor, diclofenac, and mitochondrial ROS inhibitor, rotenone, and measured their effect on total endogenous H_2O_2 using PO1. Quantification by flow cytometry revealed that cyclooxygenase-generated ROS do not contribute significantly to total endogenous H_2O_2 (Figure 3.12.). However, inhibition of mitochondrial-generated ROS, using rotenone at high concentrations (50 µM), resulted in approximately 30% decrease of total endogenous H_2O_2. (Figure 3.13.)

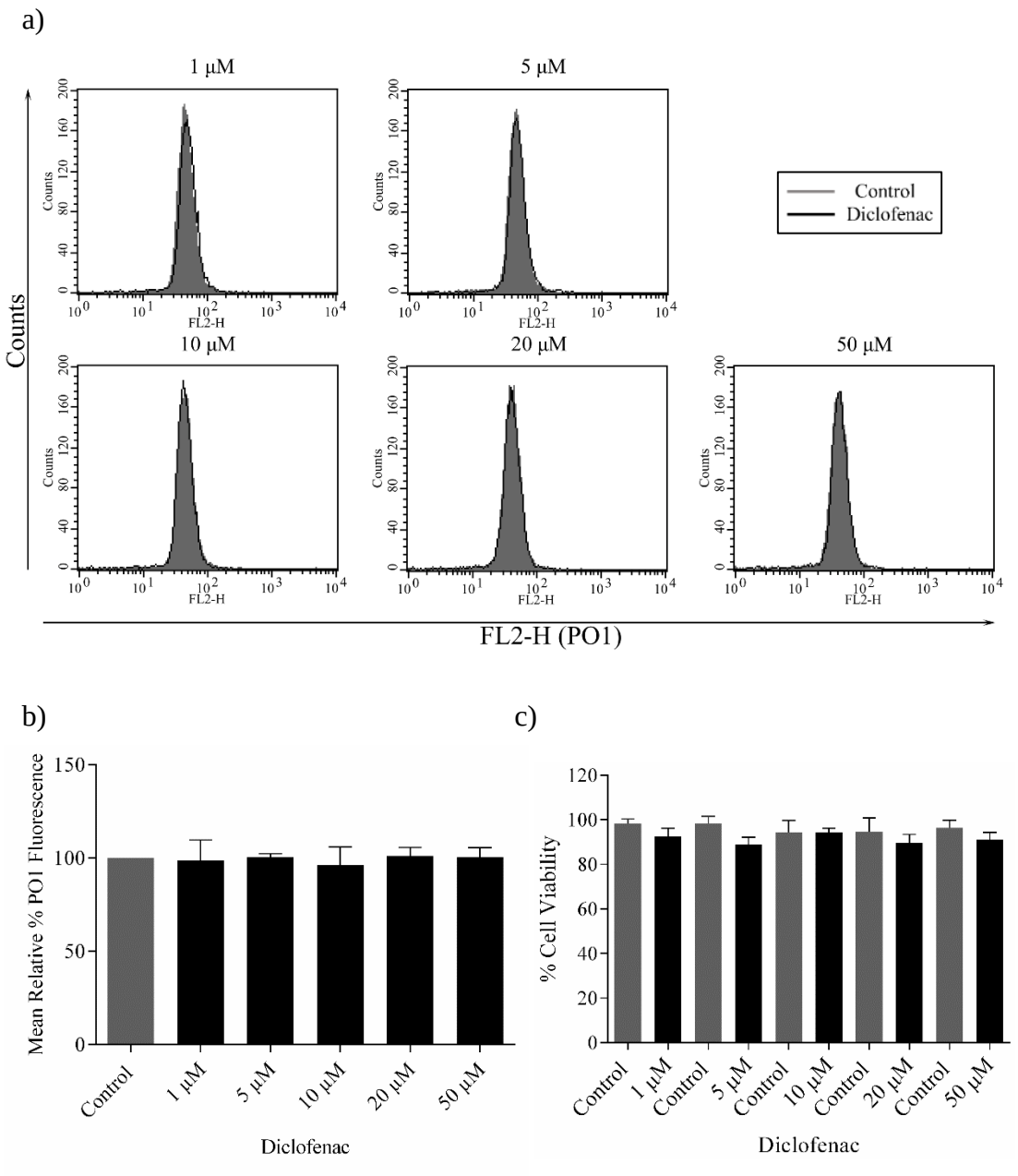

Figure 3.12. Cyclooxygenase-generated ROS do not contribute to total endogenous H_2O_2 in MV4-11 cells. Cellular H_2O_2 levels following inhibition of cyclooxygenase-generated ROS using diclofenac. Flow cytometric analysis of mean relative PO1 fluorescence using 1 µM - 50 µM range diclofenac concentrations in MV4-11 cells for 2 h *(a)*. Bar chart shows relative mean PO1 fluorescence of treated cells expressed as % of control *(b)*. Results are presented as mean ± SD from three independent experiments. Bar chart of % cell viability following treatment with the indicated concentrations of diclofenac compared to vehicle controls (N=2) *(c)*.

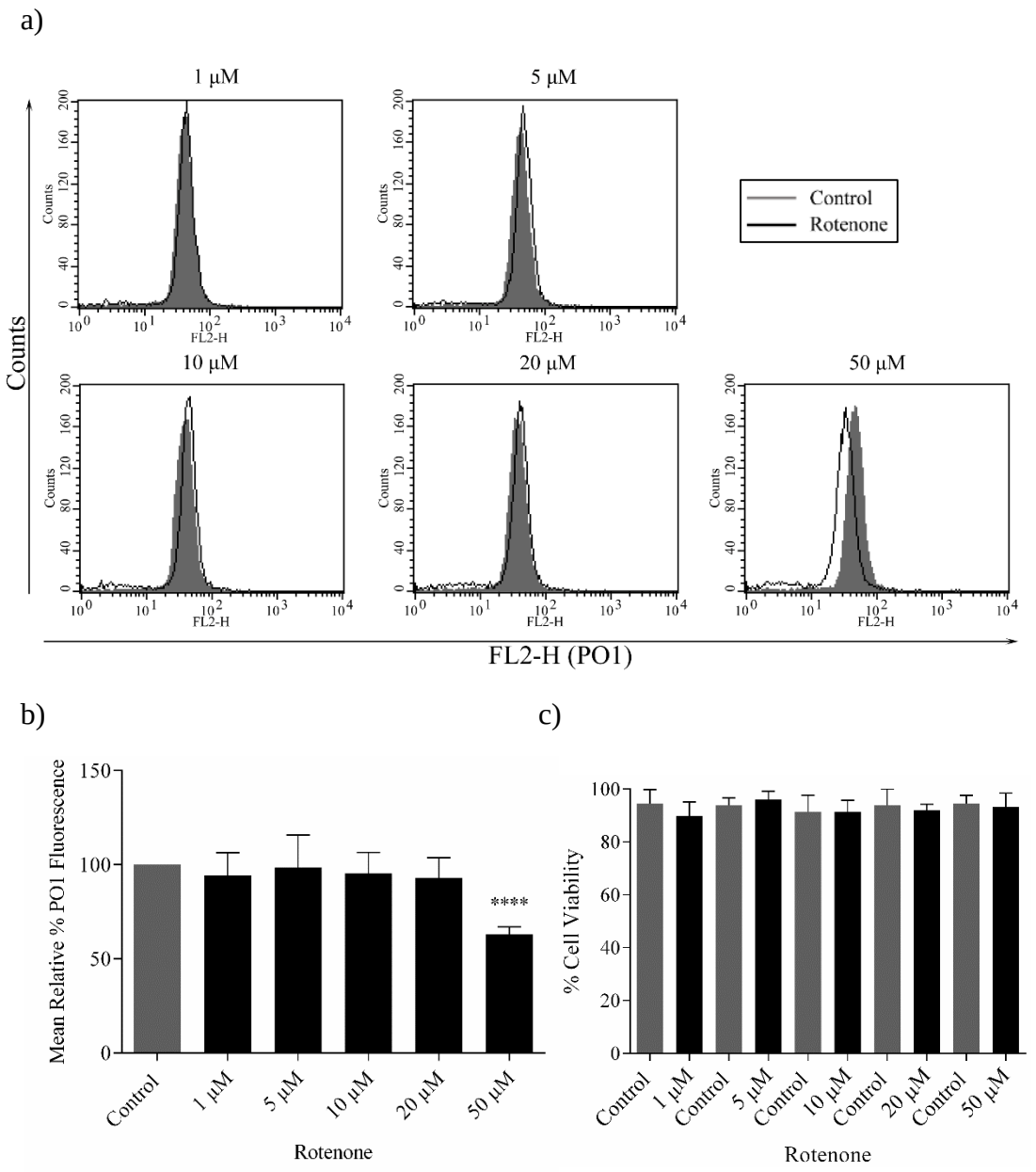

Figure 3.13. Mitochondrial-generated ROS contribute to total endogenous H_2O_2 in MV4-11 cells. Cellular H_2O_2 levels following inhibition of mitochondrial-generated ROS using rotenone. Flow cytometric analysis of mean relative PO1 fluorescence using 1 µM - 50 µM range rotenone concentrations in MV4-11 cells for 1 h *(a)*. Bar chart shows relative mean PO1 fluorescence of treated cells expressed as % of control *(b)*. Results are presented as mean ± SD from three independent experiments. Asterisks indicate statistically significant differences (****p<0.0001) as analysed by Student's t-test. Bar chart of % cell viability following treatment with the indicated concentrations of rotenone compared to vehicle controls (N=2) *(c)*.

3.3.10. Inhibition of FLT3-ITD in MV4-11 cells reduces total endogenous H_2O_2

We have shown that impaired trafficking of the mutated FLT3 receptor to the plasma membrane in MV4-11 cells resulted in a decrease of 25-35% total endogenous H_2O_2 (Figure 3.11.). To study the molecular events downstream of FLT3-ITD at the plasma membrane and ER, we employed a small tyrosine kinase inhibitor (TKI) of FLT3, PKC412, recently approved by FDA for the treatment of AML patients expressing the FLT3-ITD mutation (Rydapt, 2017, Stone et al., 2017). Inhibition of the FLT3 receptor in MV4-11 cells using PKC412 resulted in a decrease of 45-50% of total endogenous H_2O_2 (Figure 3.14.).

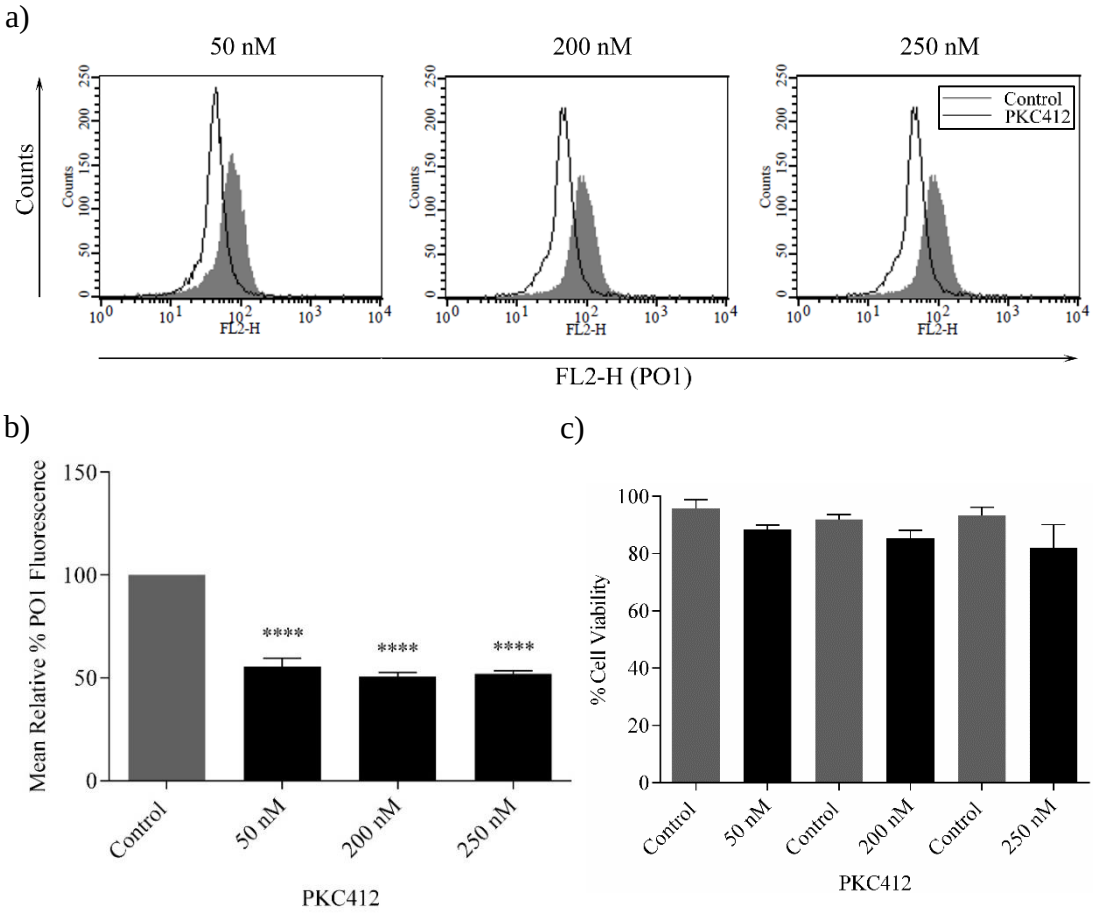

Figure 3.14. Inhibition of the FLT3 receptor in FLT3-ITD expressing MV4-11 cells reduces total endogenous H_2O_2. Levels of cellular H_2O_2 following FLT3-ITD inhibition. Flow cytometric analysis of mean relative PO1 fluorescence in MV4-11 cell line treated with PKC412 (50 nM, 200 nM and 250 nM) for 24 h *(a)*. Bar chart shows relative mean PO1 fluorescence of PKC412 treated cells expressed as % of control *(b*). Results are presented as mean ± SD from three independent experiments. Asterisks indicate statistically significant differences (****p<0.0001) as analysed by Student's t-test. Bar chart of % cell viability following treatment with the indicated concentrations of PKC412 compared to vehicle controls (N=2) *(c)*.

3.3.11. Impaired trafficking of the FLT3-ITD receptor to the plasma membrane and FLT3-ITD inhibition results in decreased $p22^{phox}$ mRNA levels

Given that ER retention of FLT3-ITD results in a significant decrease in NOX4 and $p22^{phox}$ protein levels in MV4-11 cells (Figure 3.9.), we investigated whether this effect was mediated at the transcriptional or at the translational level. In order to examine the effects of tunicamycin and brefeldin A on $p22^{phox}$ and NOX4 at mRNA level, we employed and tested Qiagen QuantiTect Primer Assays to amplify β-actin (ACTB), Beta-2-microglobulin (B2M), Proteasome (prosome/macropain) subunit, beta type, 2 (PSMB2), $p22^{phox}$/Cytochrome b-245, alpha polypeptide and NOX4. Primer efficiency was first examined for each QuantiTect Primer Assay set as described in Section 2.11. All primer sets were between 86% and 105% efficient (Figure 3.15.) and within 20% efficiency of each other, as is recommended (Schmittgen and Livak, 2008). However, the Qiagen QuantiTect NOX4 Primer Assay failed to amplify the NOX4 mRNA transcript in MV4-11 cells. We tested four predesigned NOX4 primer sets, yet only one primer set successfully amplified NOX4 in MV4-11 cells, NOX4_4 (fourth primer set). As a result this NOX4 primer set (NOX4_4), previously shown to amplify the NOX4 mRNA transcript in MV4-11 cells were employed (Reddy et al., 2011). By comparison of both sets of primers we identified that FLT3-ITD expressing MV4-11 cells express the NOX4 transcript variant X3 (Figure 3.16.). Qiagen QuantiTect NOX4 Primer Assay does not amplify this transcript hence the failure to detect NOX4 using these primers.

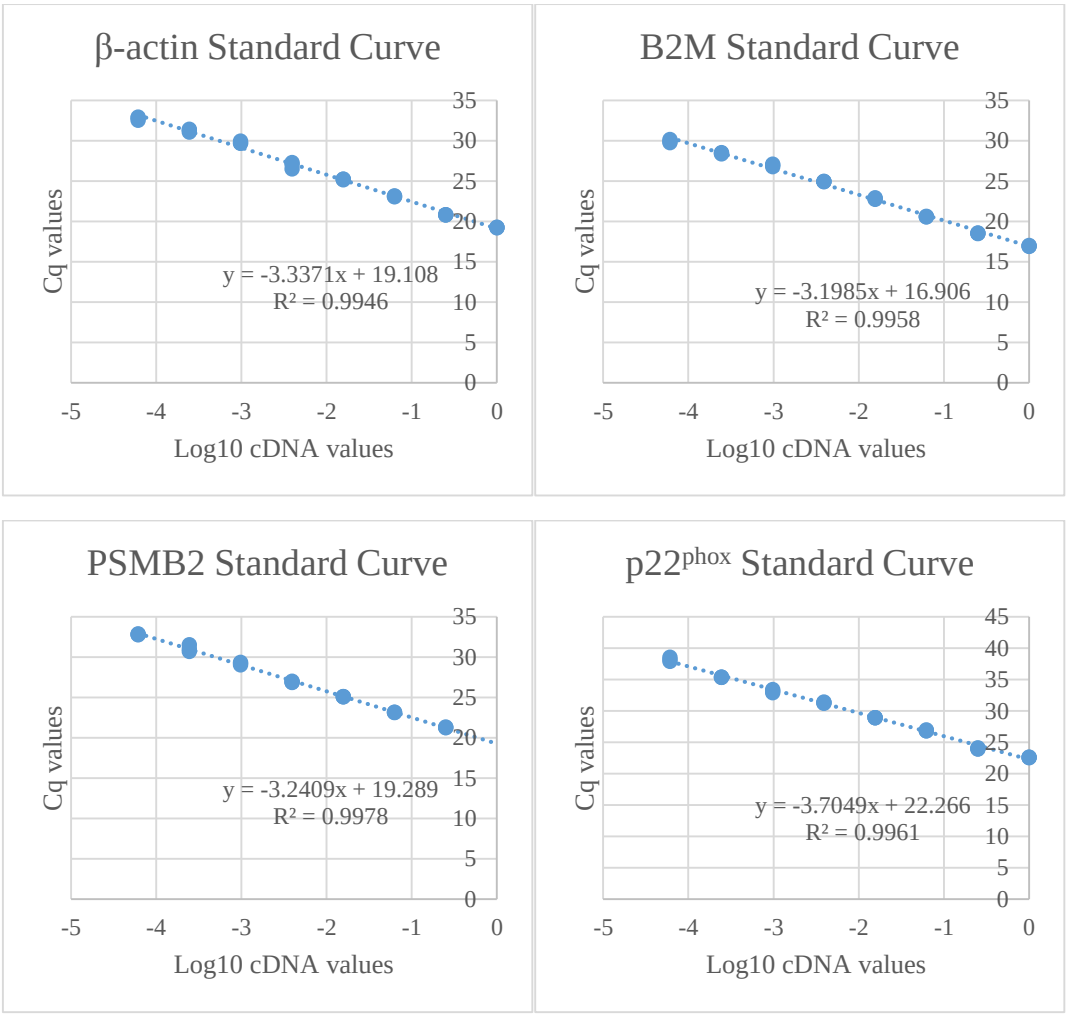

Gene	R^2 value	Slope	Amplification Factor	Primer Efficiency (%)
β-actin	0.9946	-3.3371	1.99	99.37
B2M	0.9958	-3.1985	2.05	105.42
PSMB2	0.9978	-3.2409	2.03	103.5
$p22^{phox}$	0.9961	-3.7049	1.86	86.17

Figure 3.15. RT-qPCR primer efficiency plots. Mean quantification cycle (Cq) values of each set of serial dilution plotted against the logarithm of cDNA template (from untreated MV4-11 cells) concentration.

a)

Gene	Qiagen Primer set	Product size	Ref Seq ID#	Transcript variant, mRNA
NOX4	QT00057498	77 bp	NM_001143836	*Homo sapiens* NOX4, transcript variant NOX4B, mRNA
			NM_001143837	*Homo sapiens* NOX4, transcript variant 3, mRNA
			NM_016931	*Homo sapiens* NOX4, transcript variant 1, mRNA
			NM_026571	Replaced by NM_001291926
			NM_001291926	*Homo sapiens* NOX4, transcript variant 4, mRNA
			NM_001291927	*Homo sapiens* NOX4, transcript variant 5, mRNA
			NM_001291929	*Homo sapiens* NOX4, transcript variant 6, mRNA
			NM_001300995	*Homo sapiens* NOX4, transcript variant 8, mRNA
			XM_006718848	Record removed
			XM_006718849	Predicted: *Homo sapiens* NOX4, transcript variant X2, mRNA
			XM_006718852	Record removed
			XM_006718853	Record removed

b)

>XM_011542857.2 PREDICTED: Homo sapiens NADPH oxidase 4 (NOX4), transcript variant X3, mRNA

TGGAGAAACAACCTAGAAAATGCACCAACAAATGGGGCACAATAACTACTCTGAGAGAGAGTGGCACACA
GTGGACGCAAAGAAGAGGTTCCTGATGCAGCTGGGAAGAGTCTACATGGGCCTCTAGCAGGAGAAGATAC
TGGTCTTGAGTTTGGAGACTAAGTAAGCATCTCCAGTTCATCTGGCTCTCCATGAATGTCCTGCTTTTCT
GGAAAACCTTCTTGCTGTATAACCAAGGGCCAGAGTATCACTACCTCCACCAGATGTTGGGGCTAGGATT
GTGTCTAAGCAGAGCCTCAGCATCTGTTCTTAACCTCAACTGCAGCCTTATCCTTTTACCCATGTGCCGA
ACACTCTTGGCTTACCTCCGAGGATCACAGAAGGTTCCAAGCAGGAGAACCAGGAGATTGTTGGATAAAA
GCAGAACATTCCATATTACCTGTGGTGTTACTATCTGTATTTTCTCAGGCGTGCATGTGGCTGCCCATCT
GGTGAATGCCCTCAACTTCTCAGTGAATTACAGTGAAGACTTTGTTGAACTGAATGCAGCAAGATACCGA
GATGAGGATCCTAGAAAACTTCTCTTCACAACTGTTCCTGGCCTGACAGGGGTCTGCATGGTGGTGGTGC
TATTCCTCATGATCACAGCCTCTACATATGCAATAAGAGTTTCTAACTATGATATCTTCTGGTATACTCA
TAACCTCTTCTTTGTCTTCTACATGCTGCTGACGTTGCATGTTTCAGGAGGGCTGCTGAAGTATCAAACT
AATTTAGATACCCACCCTCCCGGCTGCATCAGTCTTAACCGAACCAGCTCTCAGAATATTTCCTTACCAG
AGTATTTCTCAGAACATTTTCATGAACCTTTCCCTGAAGGATTTTCAAAACCGGCAGAGTTTACCCAGCA
CAAATTTGTGAAGATTTGTATGGAAGAGCCCAGATTCCAAGCTAATTTTCCACAGACTTGGCTTTGGATT
TCTGGACCTTTGTGCCTGTACTGTGCCGAAAGACTTTACAGGTATATCCGGAGCAATAAGCCAGTCACCA
TCATTTCGGTCATGAGTCATCCCTCAGATGTCATGGAAATCCGAATGGTCAAAGAAAATTTTAAAGCAAG
ACCTGGTCAGTATATTACTCTACATTGTCCCAGTGTATCTGCATTAGAAAATCATCCATTTACCCTCACA
ATGTGTCCAACTGAAACCAAAGCAACATTTGGGGTTCATCTTAAAATAGTAGGAGACTGGACAGAACGAT
TTCGAGATTTACTACTGCCTCCATCTAGTCAAGACTCCGAAATTCTGCCCTTCATTCAATCTAGAAATTA
TCCCAAGCTGTATATTGATGGTCCTTTTGGAAGTCCATTTGAGGAATCACTGAACTATGAGGTCAGCCTC
TGCGTGGCTGGAGGCATTGGAGTAACTCCATTTGCATCAATACTCAACACCCTGTTGGATGACTGGAAAC
CATACAAGCTTAGAAGACTATACTTTATTTGGGTATGCAGAGATATCCAGTCCTTCCGTTGGTTTGCAGA
TTTACTCTGTATGTTGCATAACAAGTTTTGGCAAGAGAACAGACCTGACTATGTCAACATCCAGCTGTAC
CTCAGTCAAACAGATGGGATACAGAAGATAATTGGAGAAAAATATCATGCACTGAATTCAAGACTGTTTA
TAGGACGTCCTCGGTGGAAACTTTTGTTTGATGAAATAGCAAAATATAACAGAGGAAAAACAGTTGGTGT
TTTCTGTTGTGGACCCAATTCACTATCCAAGACTCTTCATAAACTGAGTAACCAGAACAACTCATATGGG
ACAAGATTTGAATACAATAAAGAGTCTTTCAGCTGAAAACTTTTGCCATGAAGCAGGACTCTAAAGAAGG
AATGAGTGCAATTTCTAAGACTTTGAAACTCAGCGGAATCAATCAGCTGTGTTATGCCAAAGAATAGTAA
GGTTTTCTTATTTATGATTATTTAAAATGGAAATGTGAGAATGTGGCAAGATGACCGTCACATTACATGT
TTAATCTGGAAACCAAAGAGACCCTGAAGAATATTTGATGTGATGATTCACTTTTCAGTTCTCAAATTAA
AAGAAAACTGTTAGATGCACACTGTTGATTTTCATGGTGGATTCAAGAACTCCCTAGTGAGGAGCTGAAC
TTGCTCAATCTAAGGCTGATTGTCGTGTTCCTCTTTAAATTGTTTTTGGTTGAACAAATGCAAGATTGAA
CAAAATTAAAAATTCATTGAAGCTGAAATTCCA

Figure 3.16. Hs_NOX4_1_SG QuantiTect Primer Assay does not amplify *Homo sapiens* NADPH oxidase 4 (NOX4), transcript variant X3, mRNA sequence (Ref Seq ID# XM_011542857.2); NOX4_4 primers (Eurofins) amplify NOX4, transcript variant X3. Table of Hs_NOX4_1_SG_QuantiTect Primer Assay (QT00057498) detected transcripts *(a)*. NOX4_4 primers (Eurofins) (yellow) amplify *Homo sapiens* NOX4, transcript variant X3, mRNA sequence expressed in MV4-11 cells *(b)*.

The integrity of isolated RNA was examined by separation of 5 µg of isolated RNA on 1% SYBR Safe agarose gel. RNA integrity was confirmed if distinct, sharp bands for 28S and 18S ribosomal RNA (rRNA) were distinguishable, with no smearing of the sample or additional bands (Figure 3.17. a). Amplification of the intended transcript variants was confirmed by the appearance of a single band at the appropriate size following amplification (Figure 3.17. b).

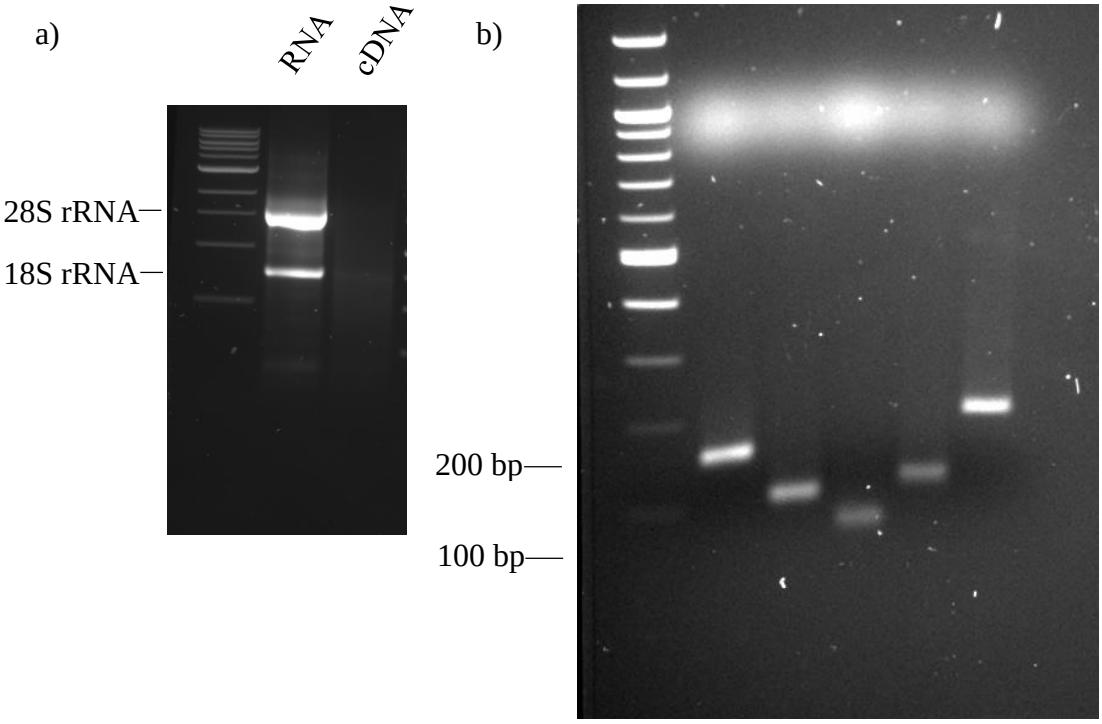

Figure 3.17. Integrity of RNA and confirmation of amplified RT-qPCR products. 5 µg of isolated RNA and 1 µg cDNA were separated on 1% SYBR Safe agarose gel with 28S and 18S rRNA bands indicated *(a)*. RT-qPCR products run on 2% SYBR Safe agarose gel. Amplification of the intended target transcripts. Lane 1-5: β-actin, B2M, PSMB2, $p22^{phox}$ (all from Qiagen) and NOX4 (Eurofins) *(b)*.

The NOX4_4 Eurofins primer set melt curve analysis identified a variety of PCR products following amplification. Primer efficiency was tested and identified the primer set to be inefficient (Figure 3.18. a). On the other hand, subsequent gene

sequencing was carried out by GATC Biotech and confirmed the amplification and expression of NOX4 transcript variant X3 in FLT3-ITD expressing MV4-11 cells (Figure 3.18. b). Due to issues with NOX4 primer inefficiency we decided not to continue with NOX4 mRNA studies.

a)

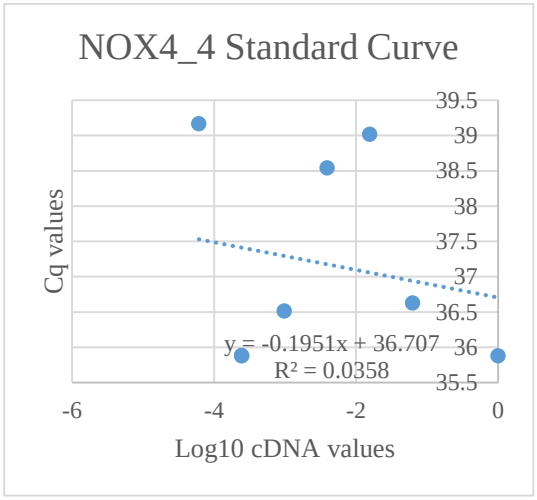

Gene	R^2 value	Slope
NOX4	0.0358	-0.1951

b)

Download GenBank Graphics

PREDICTED: Homo sapiens NADPH oxidase 4 (NOX4), transcript variant X3, mRNA
Sequence ID: XM_011542857.2 Length: 2273 Number of Matches: 1

Range 1: 1815 to 1935 GenBank Graphics Next Match Previous Match

Score	Expect	Identities	Gaps	Strand
224 bits(121)	3e-55	121/121(100%)	0/121(0%)	Plus/Plus

```
Query  1     TATGGGACAAGATTTGAATACAATAAAGAGTCTTTCAGCTGAAAACTTTTGCCATGAAGC  60
             ||||||||||||||||||||||||||||||||||||||||||||||||||||||||||||
Sbjct  1815  TATGGGACAAGATTTGAATACAATAAAGAGTCTTTCAGCTGAAAACTTTTGCCATGAAGC  1874

Query  61    AGGACTCTAAAGAAGGAATGAGTGCAATTTCTAAGACTTTGAAACTCAGCGGAATCAATC  120
             ||||||||||||||||||||||||||||||||||||||||||||||||||||||||||||
Sbjct  1875  AGGACTCTAAAGAAGGAATGAGTGCAATTTCTAAGACTTTGAAACTCAGCGGAATCAATC  1934

Query  121   A  121
             |
Sbjct  1935  A  1935
```

Figure 3.18. RT-qPCR primer efficiency plot for NOX4_4 primers. **Inefficient NOX4_4 primers amplified NOX4, transcript variant X3 in MV4-11 cells.** Mean quantification cycle (Cq) values of each set of serial dilution plotted against the logarithm of cDNA template (from untreated MV4-11 cells) concentration *(a)*. BLAST alignment of NOX4_4 product compared to NCBI database *(b)*. 'Query' is the sequence of the sample amplified, and the 'Sbjct' is NADPH oxidase 4 (NOX4), transcript variant X3 mRNA sequence in the NCBI database. The two sequences are an exact match.

Following confirmation of the amplification of the intended transcripts (Figure 3.17. b), we examined the effect of impaired trafficking of FLT3-ITD to the plasma membrane on p22^{phox} regulation at the transcriptional level. p22^{phox} mRNA levels decreased approximately 60% following treatment with tunicamycin and approximately 75% following treatment with brefeldin A (Figure 3.19.). Taken together these results suggest that p22^{phox} is regulated at the transcriptional level following treatment with both receptor trafficking inhibitors.

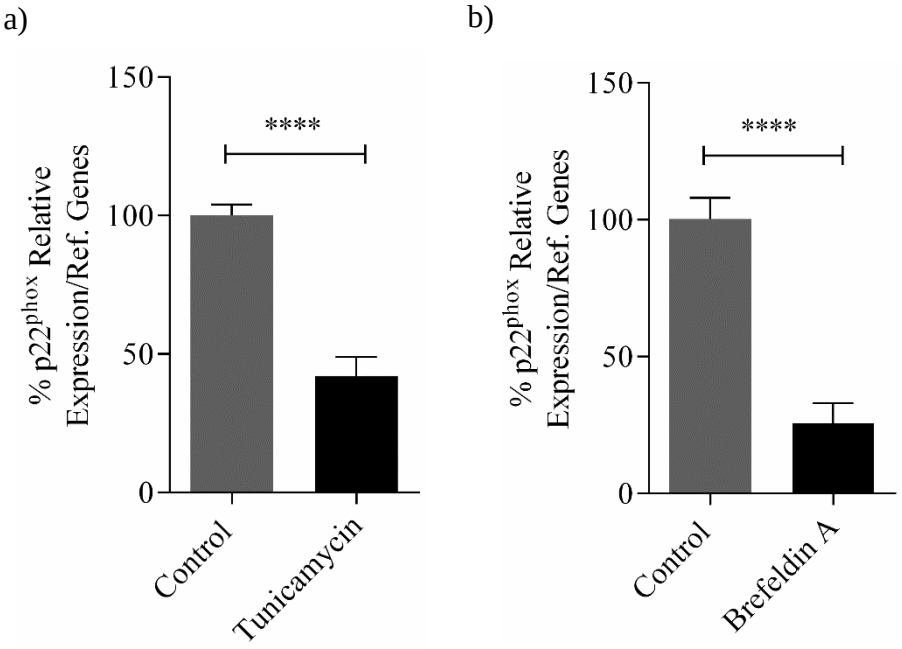

Figure 3.19. Treatment of MV4-11 cells with tunicamycin and brefeldin A results in a decrease in p22^{phox} RNA expression. p22^{phox} RNA expression following treatment with receptor trafficking inhibitors tunicamycin (5 µg/ml overnight) *(a)* and brefeldin A (10 µg/ml overnight) *(b)* in MV4-11 cells. Results are presented as mean ± SD from four independent experiments. Asterisks indicate statistically significant differences (****p<0.0001) as analysed by Student's t-test.

Previous studies in our laboratory have reported p22^{phox} to be regulated at the post-translational level following inhibition of FLT3-ITD using PKC412 (Woolley et al., 2012). Therefore, we examined the effect of FLT3-ITD inhibition via PKC412 on p22^{phox} mRNA levels. FLT3-ITD inhibition resulted in approximately 40% decrease

in p22^{phox} mRNA levels (Figure 3.20.). Collectively p22^{phox} is regulated at both RNA and protein levels following inhibition of FLT3-ITD in MV4-11 cells.

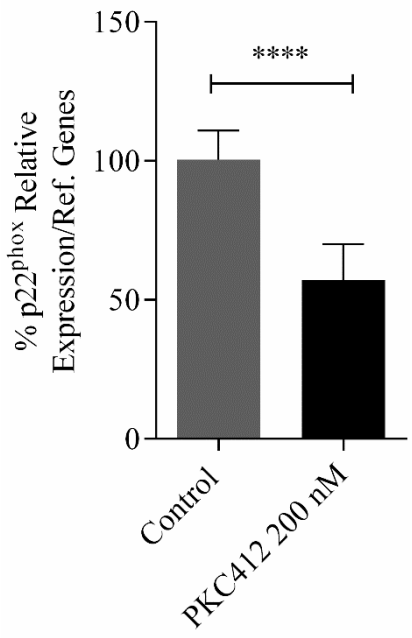

Figure 3.20. FLT3-ITD inhibition results in a decrease in p22^{phox} RNA expression. p22^{phox} RNA expression following treatment with PKC412 200 nM for 24 h in MV4-11 cells. Results are presented as mean ± SD from three independent experiments. Asterisks indicate statistically significant differences (****p<0.0001) as analysed by Student's t-test.

3.3.12. Serine protease inhibitor 4-(2-Aminoethyl) benzenesulfonyl fluoride hydrochloride (AEBSF) inhibits NOX4 protein levels

We have shown previously that ER retention of FLT3-ITD resulted in decreased p22^{phox} mRNA levels (Figure 3.19.). We decided to investigate if p22^{phox} was also regulated at the translational level, as well as investigating the effect of impaired FLT3-ITD receptor trafficking on the regulation of NOX4 at the translational level. At the beginning of this study, some western blotting issues were encountered. NOX4, β-actin and α-tubulin proteins were not detected in freshly prepared MV4-11 cell lysates (Figure 3.21. a) compared to previously prepared MV4-11 cell lysates (Figure 3.21. b). It was crucial to solve this issue for future western blotting studies.

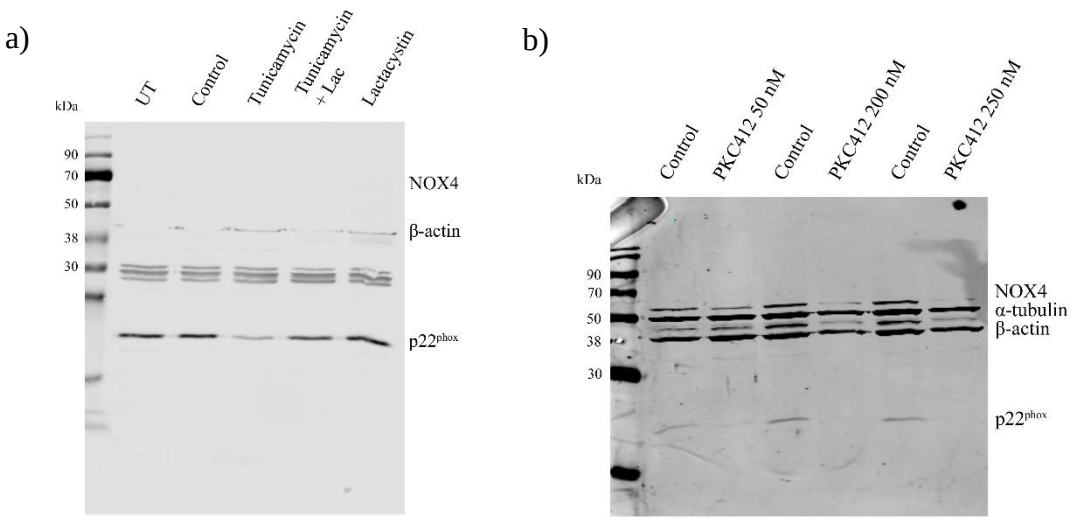

Figure 3.21. Failure to detect NOX4, β-actin and α-tubulin protein levels in freshly prepared MV4-11 cell lysates. Western blot analysis of $p22^{phox}$, NOX4 and β-actin protein levels in fresh lysates: untreated (UT), vehicle control (control), following treatment with tunicamycin (5 µg/ml) and tunicamycin in combination with 20S proteasome inhibitor lactacystin (5 µM) overnight *(a)*. β-actin is shown as a loading control. Western blot analysis of $p22^{phox}$, NOX4, β-actin and α-tubulin protein levels in previously prepared lysates (positive control): vehicle control (control) and following treatment with indicated concentrations of PKC412 for 24 hr *(b)*. β-actin and α-tubulin are shown as loading controls.

Using NOX4-expressing lysates as a positive control, we investigated total protein levels in the SDS-PAGE gel stained with Coomassie brilliant blue and the nitrocellulose membrane stained with Ponceau. Decreased levels of proteins ranging from 38 kDa to 90 kDa in weight were detected in freshly prepared lysates compared to our positive controls. The decreased protein levels corresponds to the molecular weights of NOX4, β-actin and α-tubulin (Figure 3.22.).

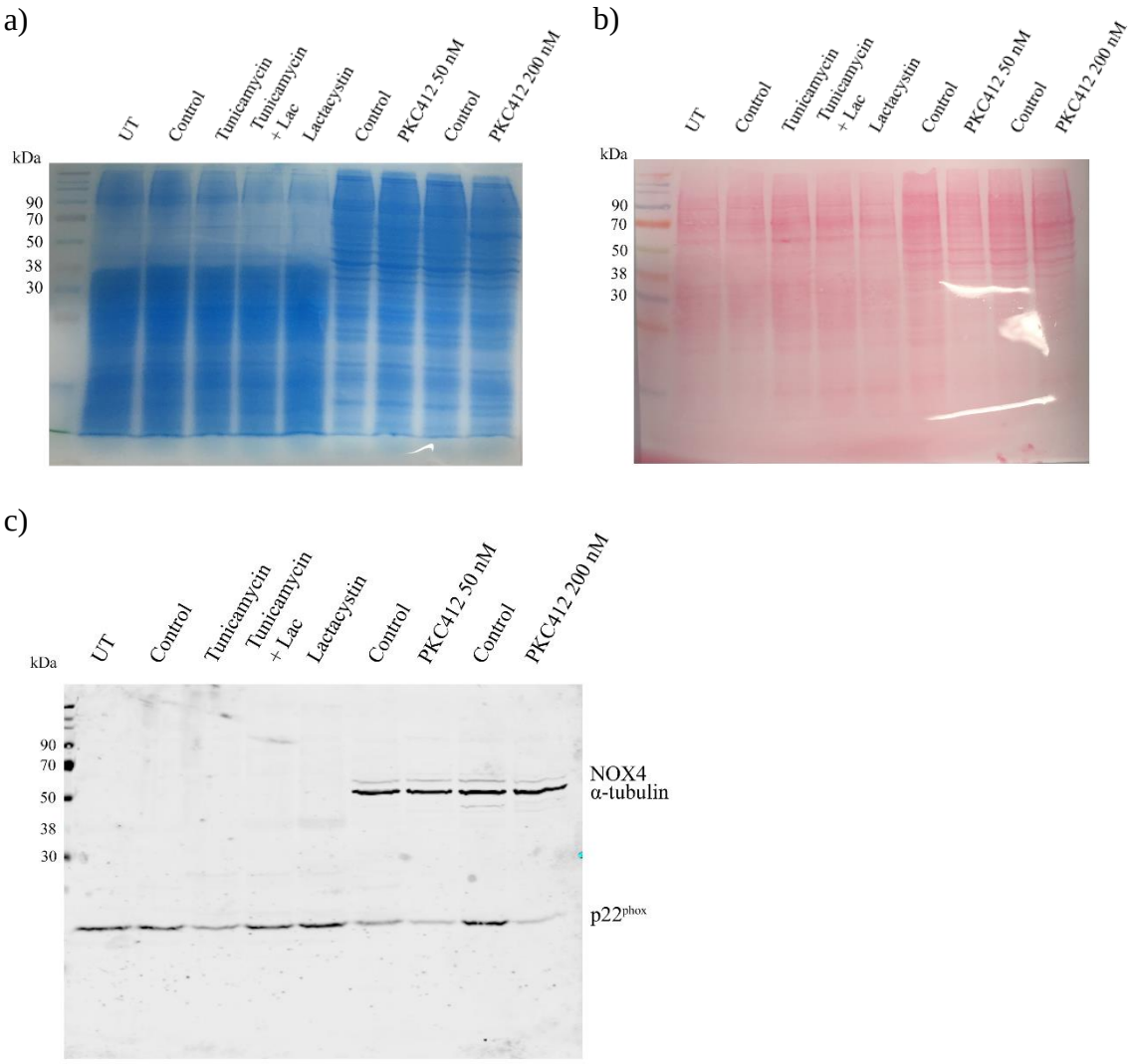

Figure 3.22. Decreased levels of protein bands ranging from 38 kDa to 90 kDa in size detected in freshly prepared lysates. Analysis of total protein levels in freshly prepared lysates (Lane 2-6) and previously prepared lysates (Lane 7-10 (positive control)) by means of staining the gel with Coomassie brilliant blue overnight *(a)* and incubating the nitrocellulose membrane with Ponceau *(b).* Western blot analysis of $p22^{phox}$, NOX4 and α-tubulin protein levels in freshly prepared lysates compared to positive control lysates *(c).*

Next we investigated if the proteins were aggregating in the stacking gel and if the cells were lysing efficiently with RIPA buffer. We demonstrated that protein aggregation was not an issue due to the absence of protein in the stacking gel of the SDS-PAGE gel (Figure 3.23. a). We validated cells were lysed instantly and efficiently

by the lack of protein in pellets following cell lysis with RIPA buffer (Figure 3.23. b and c). Following the purchase and lysing of new MV4-11 cells, the issue still remained. We therefore turned our attention to components in the RIPA lysis buffer. We focused on protease inhibitors due to the lack of protein detection between 38 kDa and 90 kDa molecular weight marker in the new vial of cells (Figure 3.23. d-f).

a)

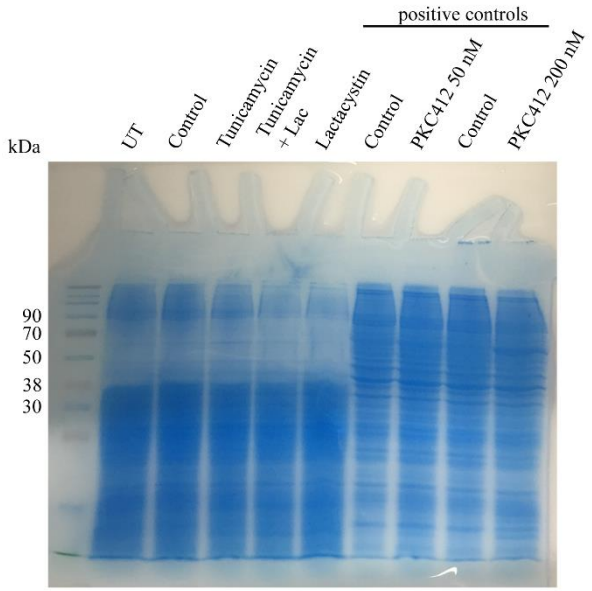

b)

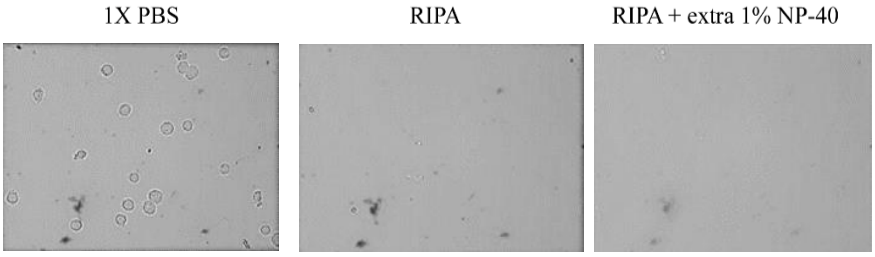

c)

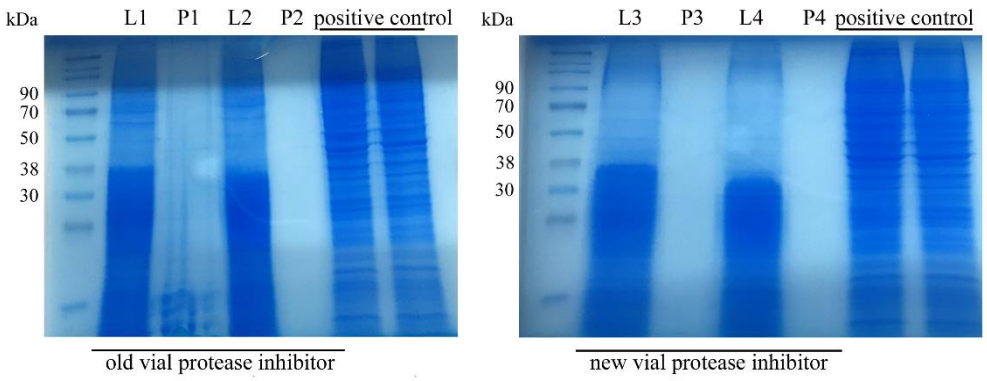

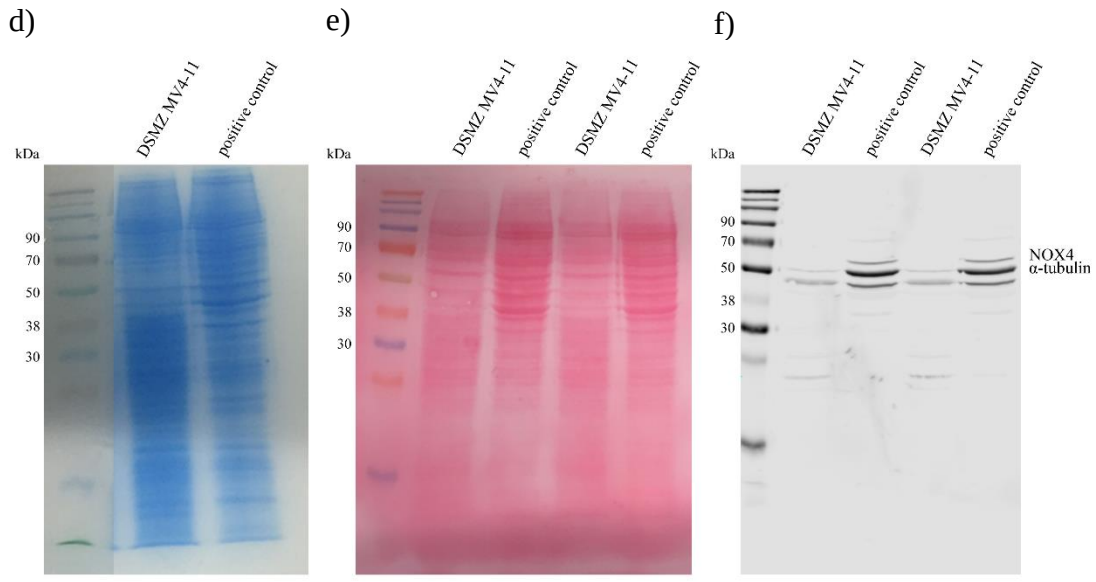

Figure 3.23. RIPA buffer lysed MV4-11 cells efficiently. Analysis of total protein levels in freshly prepared and positive control MV4-11 cell lysates in the stacking and resolving gels of the SDS-PAGE gel following staining overnight with Coomassie brilliant blue *(a)*. Phase contrast imaging of MV4-11 cells in 1X PBS, RIPA buffer and RIPA plus an extra 1% NP-40 *(b)*. Staining of the SDS-PAGE gel containing lysates prepared with old (L1 and L2) and new (L3 and L4) vial of cocktail protease inhibitors and pellet extractions with old (P1 and P2) and new (P3 and P4) vial of cocktail protease inhibitors overnight with Coomassie brilliant blue *(c)*. Analysis of whole cell lysis of a new vial of MV4-11 cells from DSMZ (Braunschweig, Germany) by means of staining the SDS-PAGE gel with Coomassie brilliant blue overnight *(d)* and incubating the nitrocellulose membrane in Ponceau *(e)*. Western blot analysis of NOX4 and α-tubulin protein levels in new DSMZ MV4-11 cell lysates *(f)*.

Prior to these western blotting issues, one of the protease inhibitors in the RIPA lysis buffer was changed. 4-(2-Aminoethyl) benzenesulfonyl fluoride hydrochloride (AEBSF) is one of the most commonly used serine protease inhibitors and from this study it is demonstrated as having an effect on NOX4 protein levels. Reverting back to Phenylmethylsulfonyl fluoride (PMSF), a serine protease inhibitor and acetylcholinesterase resulted in detection of NOX4, β-actin and α-tubulin proteins (Figure 3.24.). Interestingly, the serine protease inhibitor AEBSF has been identified as a proposed inhibitor of NOXs (Diatchuk et al., 1997, Drummond et al., 2011,

Altenhöfer et al., 2015). Taken together, these findings suggest that the serine protease inhibitor PMSF should be used as an alternative to AEBSF when preparing lysates to study the expression and activity of NOX proteins.

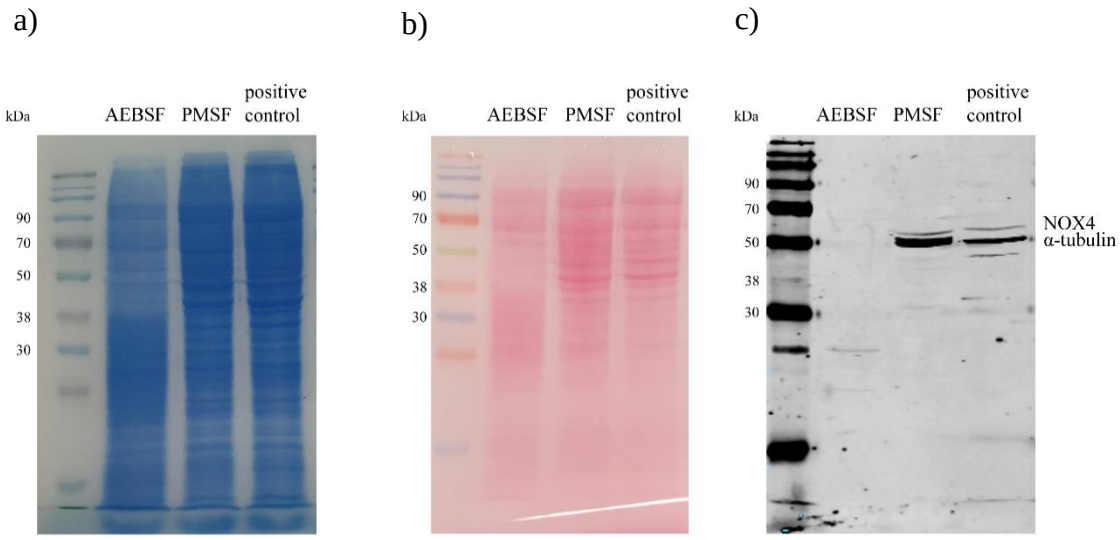

Figure 3.24. Serine protease inhibitor 4-(2-Aminoethyl) benzenesulfonyl fluoride hydrochloride (AEBSF) inhibits NOX4 protein levels; serine protease inhibitor and acetylcholinesterase Phenylmethylsulfonyl fluoride (PMSF) should be used as an alternative when preparing cell lysates. Analysis of whole cell lysis of MV4-11 cells using serine protease inhibitors, AEBSF and PMSF alongside a positive control lysate by means of staining the SDS-PAGE gel with Coomassie brilliant blue overnight *(a)* and incubating the nitrocellulose membrane with Ponceau *(b)*. Western blot analysis of NOX4 and α-tubulin protein levels using RIPA buffer containing AEBSF and PMSF *(c)*.

3.3.13. Inhibition of FLT3-ITD cell surface expression results in proteasomal degradation of $p22^{phox}$ and deglycosylation of NOX4

Our group has shown that inhibition of FLT3-ITD using PKC412 results in proteasomal degradation of $p22^{phox}$ by the ubiquitin proteasome pathway (Woolley et al., 2012). Given that $p22^{phox}$ and NOX4 protein levels decrease significantly following treatment with tunicamycin and brefeldin A (Figure 3.9.), we decided to

investigate whether impaired trafficking of FLT3-ITD resulted in regulation of $p22^{phox}$ and NOX4 at the translational level. To this end, we treated cells with tunicamycin and brefeldin A in the presence of 20S proteasome inhibitor, lactacystin. ER retention of FLT3-ITD resulted in NOX4 deglycosylation and $p22^{phox}$ degradation by the proteasome. Inhibition of the 20S proteasome prevented proteasomal degradation of $p22^{phox}$ (Figure 3.25. a and b). Interestingly, this increase in $p22^{phox}$ protein levels to basal level did not coincide with an increase in endogenous H_2O_2 (Figure 3.26. a and b).

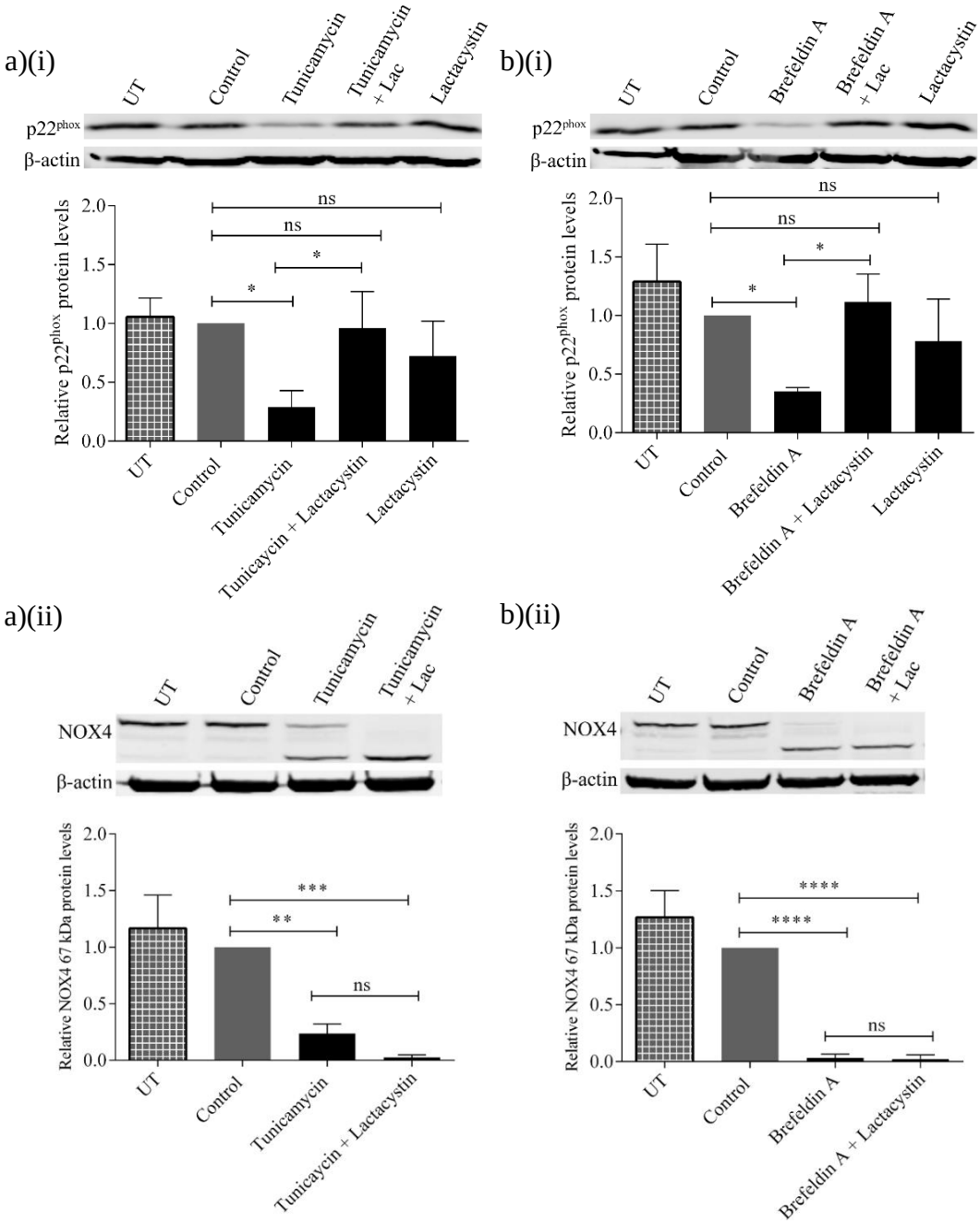

Figure 3.25. Tunicamycin and brefeldin A induce ER retention of FLT3-ITD, resulting in NOX4 deglycosylation and p22^{phox} proteasomal degradation. p22^{phox} and NOX4 protein levels following ER retention of FLT3-ITD and inhibition of the 20S proteasome. Western blot analysis of p22^{phox} and NOX4 protein levels in untreated (UT), vehicle control (control), following treatment with tunicamycin (5 µg/ml) *(a)* and brefeldin A (10 µg/ml) *(b)* overnight and also in combination with 20S proteasome inhibitor lactacystin (5 µM) overnight. β-actin is shown as a loading control. Bar charts show relative mean p22^{phox} and NOX4 protein levels following treatment with tunicamycin (5 µg/ml) *(a)* and brefeldin A (10 µg/ml) *(b)* overnight and in combination with lactacystin (5 µM) as quantified by densitometry. The data are expressed as % of control, where the ratio in the control was defined as 1. Results are presented as mean ± SD from three independent experiments. Asterisks indicate statistically significant differences (*p<0.05, **p<0.01, ***p<0.001, ****p<0.0001) as analysed by one-way ANOVA with multiple comparisons.

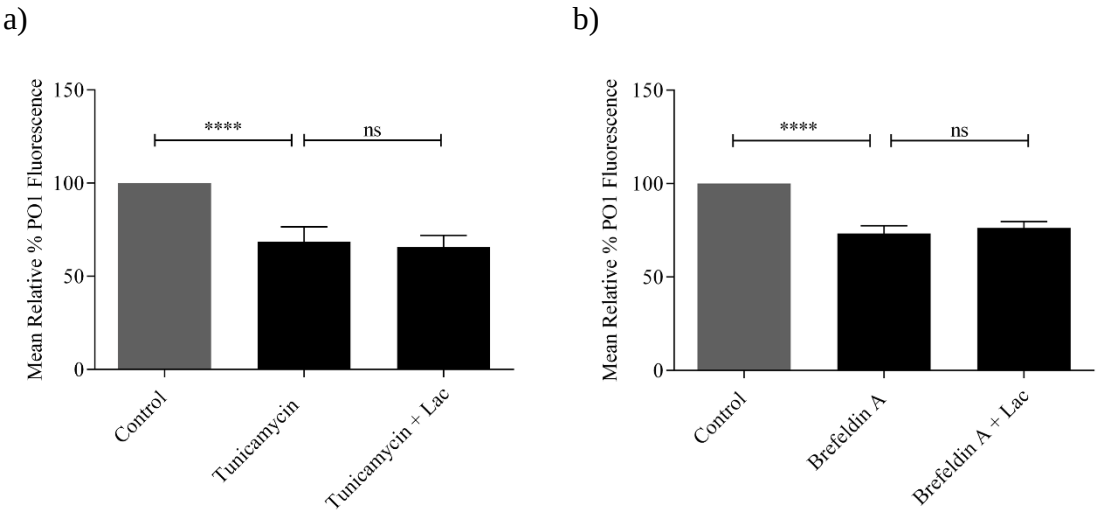

Figure 3.26. Prevention of p22^{phox} degradation had no effect on total endogenous H_2O_2 levels in MV4-11 cells. Cellular H_2O_2 levels following retention of FLT3-ITD in compartments of the endomembrane system and inhibition of the 20S proteasome. Flow cytometric analysis of mean relative PO1 fluorescence in MV4-11 cell line treated with lactacystin and tunicamycin overnight (*a*), and brefeldin A overnight (*b*). Bar charts show relative mean PO1 fluorescence of treated cells expressed as % of control. Results are presented as mean ± SD from three independent experiments. Asterisks indicate statistically significant differences (****$p<0.0001$) as analysed by Student's t-test.

3.4. Discussion

Oncogenic kinases act as drivers of ROS production in myeloid leukaemia (Behrend et al., 2003). Mutations in tyrosine kinases are commonly found in cancer and act as primary or secondary mediators of oncogenic signalling (Blume-Jensen and Hunter, 2001). FLT3-ITD is the most prevalent FLT3 mutation expressed in 15-35% of AML cases. Constitutive activation of FLT3-ITD at the plasma membrane and ER is associated with a poor prognosis (Kayser et al., 2009). The FLT3-WT and FLT3-ITD receptors have been shown to colocalise to the plasma membrane, however, the mutated FLT3 receptor has been associated with an inferior outcome resulting in disease development and progression. Here we analysed the expression of the FLT3 receptor at the plasma membrane of FLT3-ITD-expressing cells and found that they express 250-fold increase of FLT3 protein and cell surface expression compared to their wild-type counterpart (Figure 3.3.). This validates that the localisation of the mutated FLT3 receptor to the plasma membrane of FLT3-ITD-expressing cells is associated with oncogenic signalling and disease progression.

A number of studies have investigated the function of ROS, specifically NOX4-generated ROS in AML. Our group has shown that NADPH oxidases (NOX), in particular NOX4 and $p22^{phox}$, a small membrane subunit of the NOX complex, are major sources of ROS in AML (Woolley et al., 2012, Stanicka et al., 2015). However, the molecular mechanism describing how mislocalised activation of FLT3-ITD and the aberrant signalling of downstream pathways (PI3K/AKT, ERK/MAPK and STAT5) leads to the production of ROS remains unknown.

NOX-derived ROS have been shown to have numerous effects in leukaemia including a differentiation block, cell proliferation and resistance to apoptosis (Naughton et al., 2009, Reddy et al., 2011). Leukaemic oncogenes have been widely

documented in the regulation of the expression of the NOX family and their partner protein, $p22^{phox}$ (Jayavelu et al., 2016a, Naughton et al., 2009, Landry et al., 2013, Hurtado-Nedelec et al., 2013). $p22^{phox}$ is a membrane-bound protein and is an essential component required for fully functioning NOX1-4 (Ambasta et al., 2004). Our group demonstrated that cells expressing FLT3-ITD produce higher levels of pro-survival reactive oxygen species (ROS) in comparison to FLT3-wild type (Stanicka et al., 2015).

In this study, we investigated the role of trafficking of the oncogenic FLT3-ITD receptor and its effect on the production of ROS utilising receptor trafficking inhibitors, tunicamycin and brefeldin A. We found that tunicamycin and brefeldin A cause ER retention of FLT3-ITD (Figure 3.4. - Figure 3.7.) by inhibiting glycosylation of the FLT3-ITD receptor (Choudhary et al., 2009, Moloney et al., 2017b). $p22^{phox}$ and NOX4 protein levels decrease significantly following ER retention of FLT3-ITD (Figure 3.9.) suggesting that $p22^{phox}$ and NOX4 protein expression is dependent on FLT3-ITD being present at the plasma membrane. Importantly, to our knowledge, this is the first study that finds FLT3-ITD cellular organisation to play an essential role in the production of NOX4-generated pro-survival ROS and $p22^{phox}$ stability.

$p22^{phox}$ is a partner protein of NOX4 and is required for NOX4 activation (Ambasta et al., 2004). We found that $p22^{phox}$ knockdown in MV4-11 cells had no significant effect on NOX4 protein levels (Figure 3.10.). However, previous studies demonstrated that NOX4 knockdown in human umbilical vein endothelial cells (HUVECs) had no effect on $p22^{phox}$ at mRNA level yet resulted in a substantial decrease in $p22^{phox}$ protein levels (Kuroda et al., 2005). These observations suggested that NOX4 forms a complex with $p22^{phox}$ resulting in the stabilisation of $p22^{phox}$ at the protein level.

Plasma membrane FLT3-ITD and endoplasmic reticulum FLT3-ITD contribute to total endogenous H_2O_2 in FLT3-ITD expressing AML (Figure 3.14.). Here, we show that a decrease in $p22^{phox}$ and NOX4 protein levels following ER retention of FLT3-ITD correlates with a decrease in endogenous H_2O_2 (Figure 3.11.). This data suggests that $p22^{phox}$- and NOX4-generated H_2O_2 contribute to total endogenous H_2O_2 in FLT3-ITD AML. Also we found that mitochondrial-generated ROS contribute to endogenous H_2O_2 in FLT3-ITD expressing AML (Figure 3.13.). Interestingly, we have shown that cyclooxygenase-generated ROS do not contribute to total pro-survival ROS in FLT3-ITD expressing AML (Figure 3.12.).

Tunicamycin and brefeldin A inhibit glycosylation of many proteins. For this reason they are not suitable for the treatment of FLT3-ITD expressing AML cases. They have however previously been used to examine the effects of cellular localisation of oncogenic FLT3-ITD and its effect on pro-survival signalling pathways (Choudhary et al., 2009). In this study, a mutant of FLT3-ITD was created that contained a deletion of the extracellular ligand-binding domain of FLT3-ITD (FLT3-ITD ΔECD). This mutation eliminated many potential sites of glycosylation, resulting in glycosylation-independent trafficking of the FLT3-ITD receptor. The findings in this study not only support the current study, highlighting a crucial role for FLT3-ITD at the plasma membrane activating oncogenic signalling, but it also endorses the use of receptor trafficking inhibitors, such as tunicamycin and brefeldin A, as a method to investigate the effect of subcellular localisation of FLT3-ITD on the generation of ROS. This study will be discussed in further detail in the next chapter.

Our group has previously shown that inhibition of FLT3-ITD results in decreased $p22^{phox}$ protein levels as a result of protein degradation by the ubiquitin

proteasome pathway (Woolley et al., 2012). We have shown that inhibition of FLT3-ITD results in regulation of $p22^{phox}$ at both RNA and protein levels (Figure 3.20.).

We have demonstrated that ER retention of FLT3-ITD results in regulation of $p22^{phox}$ at the transcriptional level (Figure 3.19.) and proteasomal degradation of $p22^{phox}$ (Figure 3.25.). Receptor trafficking inhibitors, tunicamycin and brefeldin A inhibit glycosylation. NOX4 is glycosylated at two asparagines, amino acid position 133 and 230 (Goyal et al., 2005). Treatment of FLT3-ITD AML expressing cells with these inhibitors results in deglycosylation of NOX4 (Figure 3.25.). Degradation of $p22^{phox}$ was prevented following treatment with the 20S proteasome inhibitor lactacystin (Figure 3.25.). Interestingly, $p22^{phox}$ function was not recovered, as we observed by no significant increase in endogenous H_2O_2 (Figure 3.26.).

In conclusion, we propose that FLT3-ITD at the plasma membrane is responsible for the activation and expression of $p22^{phox}$- and NOX4-generated pro-survival ROS in FLT3-ITD expressing AML cells. $p22^{phox}$ is essential for the maintenance of pro-survival signalling in AML. For FLT3-ITD to generate its oncogenic effects it has to be located at the plasma membrane. ER retention of FLT3-ITD results in NOX4 deglycosylation and decreased mRNA levels and proteasomal degradation of $p22^{phox}$. This study presents FLT3-ITD at the plasma membrane as a potential therapeutic target, in preventing downstream ROS-driven oncogenic effects. The production of $p22^{phox}$- and NOX4-generated pro-survival H_2O_2 downstream of FLT3-ITD at the plasma membrane is studied in further detail in Chapter 4.

Further studies have identified glycan biosynthesis as a therapeutic target for cancer (Contessa et al., 2010). Inhibition of N-glycosylation of RTKs including FLT3-ITD and c-KIT has been shown to have anti-leukaemic activity in AML using 2-

deoxy-glucose and fluvastatin. Loss of surface expression of FLT3-ITD and c-KIT results in the induction of apoptotic cell death, mitigation of resistance to TKIs including the most potent FLT3 inhibitor currently in clinical trials, quizartinib, and also restores sensitivity to chemotherapy drug cytarabine (Williams et al., 2012). More recently, our collaborators have demonstrated the synergistic killing of FLT3-ITD expressing AML MV4-11 cell line and primary cells through combined inhibition of FLT3-ITD tyrosine kinase activity and N-glycosylation using low doses of tunicamycin (Tsitsipatis et al., 2017). Taken together these studies confirm FLT3-ITD surface expression as a promising therapeutic target in AML.

Chapter 4. Mislocalised activation of FLT3-ITD initiates aberrant signalling from pro-survival pathways

4.1. Abstract

Aberrant activation of oncogenic kinases at intracellular locations is frequently observed in cancer. Internal tandem duplication of the juxtamembrane domain of FMS-like tyrosine kinase 3 receptor (FLT3-ITD) is the most prevalent mutation in acute myeloid leukaemia (AML), resulting in constitutive activation of the FLT3 receptor at the plasma membrane and 'impaired trafficking' of the receptor in compartments of its biosynthetic route, such as the endoplasmic reticulum (ER). We have shown that NADPH oxidase (NOX)-and $p22^{phox}$-generated reactive oxygen species (ROS) are located downstream of FLT3-ITD at the plasma membrane where they are contributing to cell survival and proliferation, a differentiation block and disease progression. The mechanism describing how mislocalised activation of FLT3-ITD at the plasma membrane leads to the production of NOX4- and $p22^{phox}$- pro-survival ROS remains unknown. The purpose of this study was to investigate which pro-survival pathways are activated downstream of FLT3-ITD at the plasma membrane and are responsible for the production of NOX4- and $p22^{phox}$-generated hydrogen peroxide (H_2O_2) in AML. Receptor trafficking inhibitors, tunicamycin and brefeldin A inhibit surface expression of FLT3-ITD. FLT3-ITD at the plasma membrane is responsible for the activation of AKT and ERK1/2 signalling and inhibition of the GSK3β pro-survival pathway. We found that PI3K/AKT signalling only occurs when FLT3-ITD is expressed at the plasma membrane and is required for the production of NOX4- and $p22^{phox}$-generated ROS. Taken together these findings and previous findings indicate that FLT3-ITD at the plasma membrane is responsible for the production of NOX4- and $p22^{phox}$-generated H_2O_2 and presents FLT3-ITD at the plasma membrane as a potential therapeutic target in AML.

4.2. Introduction

In the previous chapter, we began to elucidate the importance of FLT3-ITD subcellular localisation on the production of NOX4- and $p22^{phox}$-generated ROS in AML. FLT3-ITD expressing cells have been shown to produce elevated levels of H_2O_2 compared to their wild-type counterpart and the elevated production of ROS are known to contribute to enhanced cell proliferation and cell survival, differentiation block as well as drug resistance and disease progression. We showed that FLT3-ITD expressing cells express significantly higher levels of the FLT3 receptor at the plasma membrane compared to FLT3-WT expressing cells, presenting FLT3-ITD at the plasma membrane as a mediator of oncogenic signalling. We have suggested that FLT3-ITD at the plasma membrane is responsible for the production of $p22^{phox}$-generated H_2O_2, and in this chapter, we further investigate the production of NOX4-generated H_2O_2 downstream of FLT3-ITD at the plasma membrane. This study therefore aimed to examine the mechanism by which mislocalised activation of FLT3-ITD at the plasma membrane leads to the activation and production of $p22^{phox}$- and NOX4-generated H_2O_2. From this, we aimed to get a further understanding of the localisation and regulation of pro-survival pathways activated downstream of FLT3-ITD in MV4-11 cells.

Different types of tumour cells express elevated levels of ROS compared to their normal counterparts. The overproduction of ROS has been shown to induce a variety of biological effects including enhanced cell proliferation and cell survival, DNA damage and genetic instability, adaptation, cellular injury and apoptosis, autophagy and drug resistance (Moloney and Cotter, 2017). ROS have a well-established role in cell signalling, where an increase in ROS such as $O_2^{\bullet-}$ and H_2O_2 has

been implicated in enhanced cell proliferation and cell survival, increased cellular growth and the development of cancer through the regulation of MAPK/ERK1/2, PI3K/AKT and PKD signalling pathways to name a few. Increased ROS also function through negative regulation of phosphatases, such as PTEN and PTP1B, regulation of NF-κB activating pathways, as well as mutations in transcription factors and tumour suppressor genes including Nrf2 and p53 (Moloney and Cotter, 2017).

Growth factors and KRAS stimulated pathways have been shown to activate the MAPK/ERK1/2 pathway in cancer, and this has a role in increased cellular proliferation (Khavari and Rinn, 2007, Roberts and Der, 2007). H_2O_2 is produced as a by-product of oestrogen metabolism in breast tumour cells and is responsible for the activation of ERK1/2 signalling pathway, resulting in increased proliferation (Irani et al., 1997, Reddy and Glaros, 2007) and the activation of the pro-survival PI3K/AKT signalling pathway (Burdick et al., 2003, Park et al., 2009). ERK1/2 has additional roles other than proliferation. It has a role in cell survival, anchorage-independent growth and motility in a variety of cancers including breast, leukaemia, melanoma and ovarian cancer (Roberts and Der, 2007, McCubrey et al., 2007, Steelman et al., 2008). PKD1 has also been shown to promote cell survival through activation of ERK1/2 and down-regulation of the pro-apoptotic c-Jun N terminal protein kinase (JNK) pathway (Singh and Czaja, 2007). Other members of the PKD family are implicated in various other cancers; PKD2 and PKD3 are found to be highly expressed in breast cancer (Hao et al., 2013), increased expression of PKD1 and PKD3 found in prostate carcinoma tissue compared to normal prostate tissue (Chen et al., 2008a). PKD2 is also highly expressed in both high- and low-grade gliomas (Azoitei et al., 2011). The regulation of ROS function in cell survival is cell specific (Chan et al., 2008, Lee et al., 2005, Rygiel et al., 2008).

The AKT pathway functions in cell survival through the phosphorylation and inactivation of its target proteins including pro-apoptotic Bcl-2-associated death promoter (Bad), Bcl-2-like protein 4 (Bax), Bcl-2-like 11 (Bim) and forkhead transcription factor (Foxo) transcription factors (Brunet et al., 1999, Kawamura et al., 2007, Limaye et al., 2005, Pastorino et al., 1999, Qi et al., 2006, Xin and Deng, 2005). Epidermal growth factor (EGF)-derived H_2O_2 production has been shown to activate AKT in ovarian cancer (Liu et al., 2006). H_2O_2 acts by oxidising and inactivating the phosphatases PTEN and PTP1B, negative regulators of PI3K/AKT signalling, resulting in cell survival (Lee et al., 2002, Salmeen et al., 2003). Inactivation of PTEN is frequently found in a variety of cancers including breast, endometrial cancers, glioblastomas, melanoma and prostate cancer (Wu et al., 2003).

Previous studies have investigated the effects of subcellular localisation of FLT3-ITD on the activation of pro-survival pathways in 32D cells stably transfected with the FLT3-ITD mutation (Choudhary et al., 2009). In this study they employed tunicamycin and brefeldin A to inhibit surface expression of FLT3-ITD alongside a mutant created of FLT3-ITD, which contained a deletion of the extracellular ligand-binding domain (FLT3-ITD ΔECD) thus eliminating any glycosylation sites. Both the receptor trafficking inhibitors and FLT3-ITD ΔECD identified the MAPK/ERK1/2 and PI3K/AKT pro-survival signalling pathways to be activated downstream of FLT3-ITD at the plasma membrane and STAT5 signalling pathway to be activated downstream of FLT3-ITD at the endoplasmic reticulum (Choudhary et al., 2009). These findings endorse the receptor trafficking inhibitors tunicamycin and brefeldin A as a method to investigate the effect of subcellular localisation of FLT3-ITD on the activation of pro-survival pathways and the generation of pro-survival ROS.

4.3. Results

4.3.1. FLT3-ITD at the plasma membrane is responsible for the activation of AKT signalling and inhibition of GSK3β signalling

In the previous chapter, we began to elucidate the importance of FLT3-ITD localisation to the plasma membrane on the production of NOX4- and $p22^{phox}$-generated ROS in AML. However, the mechanism in which FLT3-ITD at the plasma membrane contributes to the production of NOX and $p22^{phox}$-generated H_2O_2 is unclear. FLT3-ITD-induced up-regulation of ROS production in AML has been linked to enhanced cell survival and proliferation, a differentiation block and genetic instability. Constitutive activation of FLT3 switches on downstream pro-survival signalling pathways such as PI3K/AKT, MAPK/ERK1/2 and STAT5. Previous studies in our laboratory have identified the PI3K/AKT and GSK3β signalling pathways to be activated as a result of BCR-ABL induced up-regulation of NOX4-generated ROS in CML (Naughton et al., 2009, Landry et al., 2013). Therefore, we investigated the outcome of treating MV4-11 cells with tunicamycin and brefeldin A on AKT and GSK3β pro-survival pathways. Impaired trafficking of the FLT3-ITD receptor to the plasma membrane resulting in ER retention of FLT3-ITD revealed a decrease in AKT and GSK3β phosphorylation, as well as a decrease in total AKT and GSK3β (Figure 4.1.). Thus suggesting that the AKT and GSK3β cell signalling pathways are located downstream of FLT3-ITD at the plasma membrane.

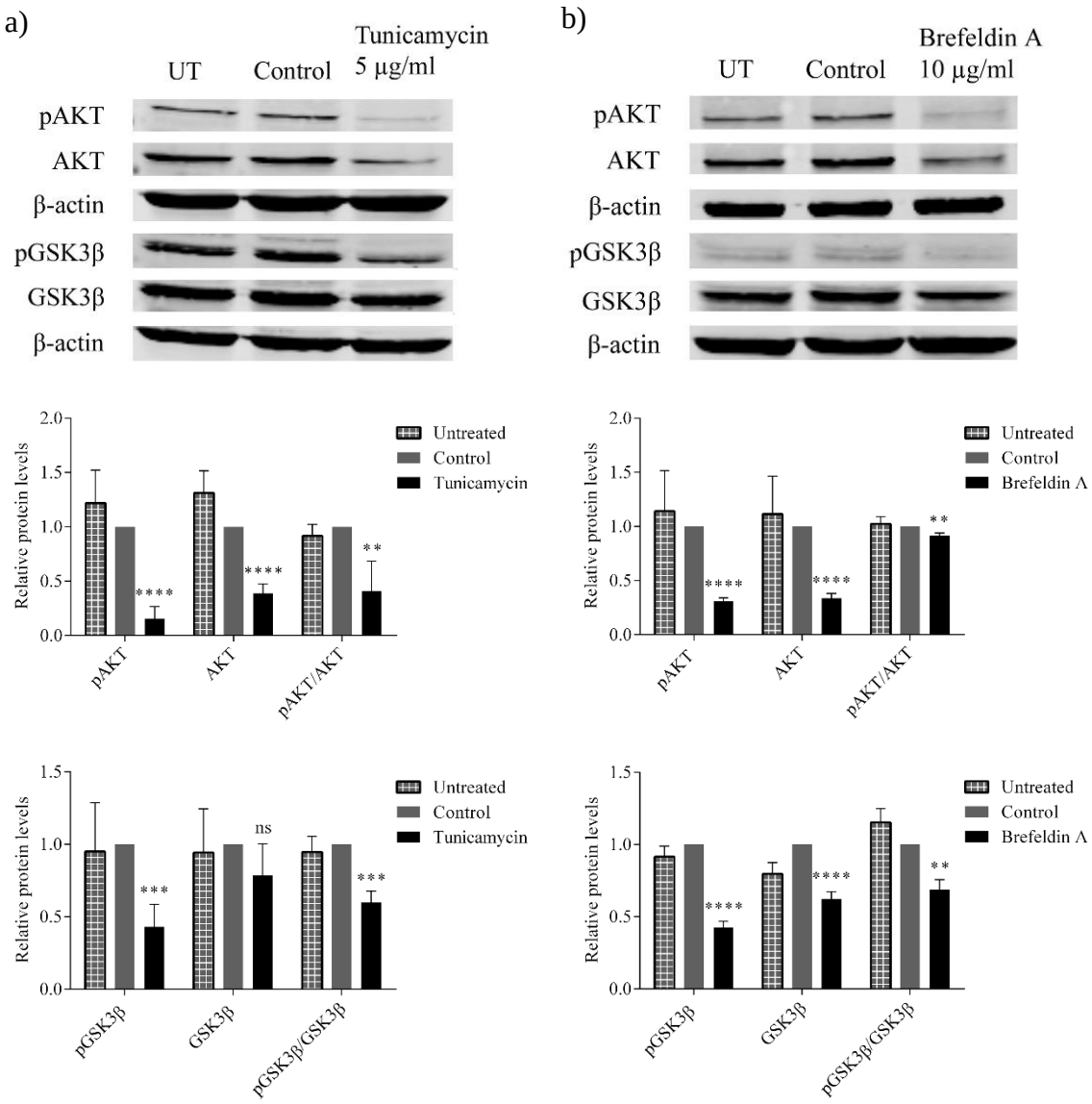

Figure 4.1. FLT3-ITD at the plasma membrane is responsible for the activation of AKT signalling and inhibition of GSK3β signalling. Western blot analysis of AKT and GSK3β signalling in untreated (UT), vehicle control (control), and following treatment with tunicamycin (5 µg/ml) overnight *(a)*; in untreated (UT), vehicle control (control) and following treatment with brefeldin A (10 µg/ml) overnight *(b)*. β-actin is shown as a loading control. Bar charts show relative mean pAKT, AKT, pAKT/AKT, pGSK3β, GSK3β and pGSK3β/GSK3β protein levels following treatment with tunicamycin (5 µg/ml) *(a)* and brefeldin A (10 µg/ml) *(b)* overnight as quantified by densitometry. The data are expressed as % of control, where the ratio in the control was defined as 1. Results are presented as mean ± SD from three independent experiments. Asterisks indicate statistically significant differences (**p<0.01, ***p<0.001, ****p<0.0001) as analysed by Student's t-test.

4.3.2. PI3K/AKT pathway needs to be activated in order for FLT3-ITD at the plasma membrane to produce its oncogenic effects

Given that both AKT and GSK3β are switched on downstream of ligand-independent constitutively activated FLT3-ITD receptor, we investigated which signalling pathways are responsible for the aberrant production of NOX4- and $p22^{phox}$-generated pro-survival ROS. The PI3K/AKT inhibitor LY294002 and GSK3β inhibitors SB216763 and lithium chloride (LiCl) were used in this study.

We found the optimal LY294002 concentration with a significant decrease in AKT phosphorylation and a minimal effect on cell viability to be 50 μM (Figure 4.2.).

SB216763 is described as an inhibitor of GSK3β, and GSK3β is inhibited when it is phosphorylated. In disagreement with this, SB216763 was found to decrease pGSK3β (Ser9) levels significantly in MV4-11 cells suggesting that it is acting as an activator of GSK3β (Figure 4.3. b). It is possible that SB216763 could have different effects in other cell types. However, based on our findings, we advise careful consideration and assessment of pGSK3β levels when using this drug. We found the optimal SB216763 concentration with the largest decrease in GSK3β phosphorylation and minimal effect on cell viability to be 5 μM (Figure 4.3.).

Lithium chloride (LiCl) is widely used as a GSK3β inhibitor (Cohen and Goedert, 2004). Inhibition of GSK3β using LiCl caused a significant increase in GSK3β phosphorylation (Figure 4.4.) in MV4-11 cells, indicative of inhibition of the pathway with minimal effect on cell viability.

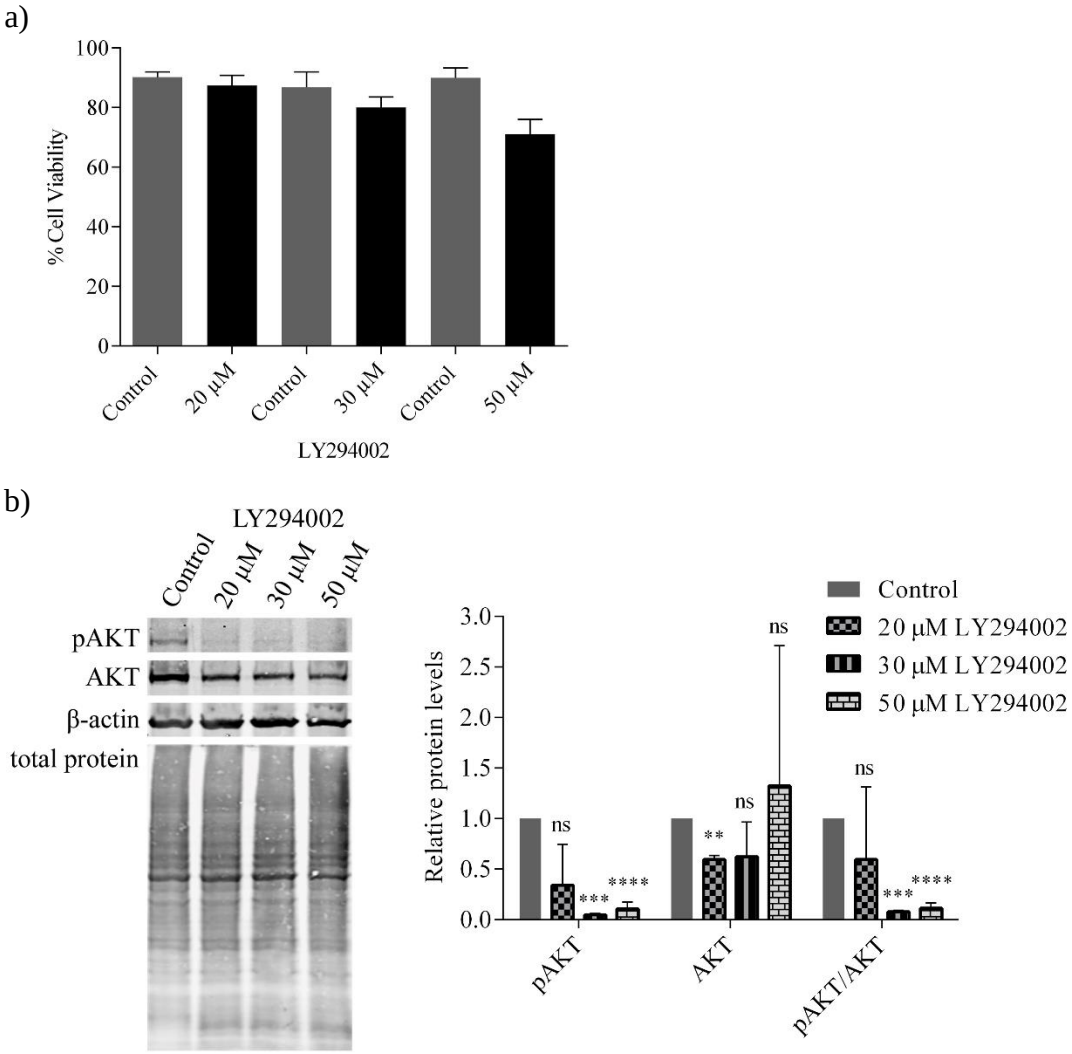

Figure 4.2. Inhibition of PI3K/AKT signalling in MV4-11 cells using LY294002. Bar chart of % cell viability following treatment with the indicated concentrations of LY294002 compared to vehicle controls (N=2) *(a)*. Western blot analysis of AKT signalling in vehicle control (control), and following treatment with LY294002 (20 µM, 30 µM and 50 µM) for 16 h *(b)*. β-actin and total protein (REVERT total protein stain) are shown as loading controls. Bar chart shows relative mean pAKT, AKT and pAKT/AKT protein levels following treatment with LY294002 (20 µM, 30 µM and 50 µM) for 16 h as quantified by densitometry. The data are expressed as % of control, where the ratio in the control was defined as 1. Results are presented as mean ± SD from three independent experiments. Asterisks indicate statistically significant differences (**p<0.01, ***p<0.001, ****p<0.0001) as analysed by Student's t-test.

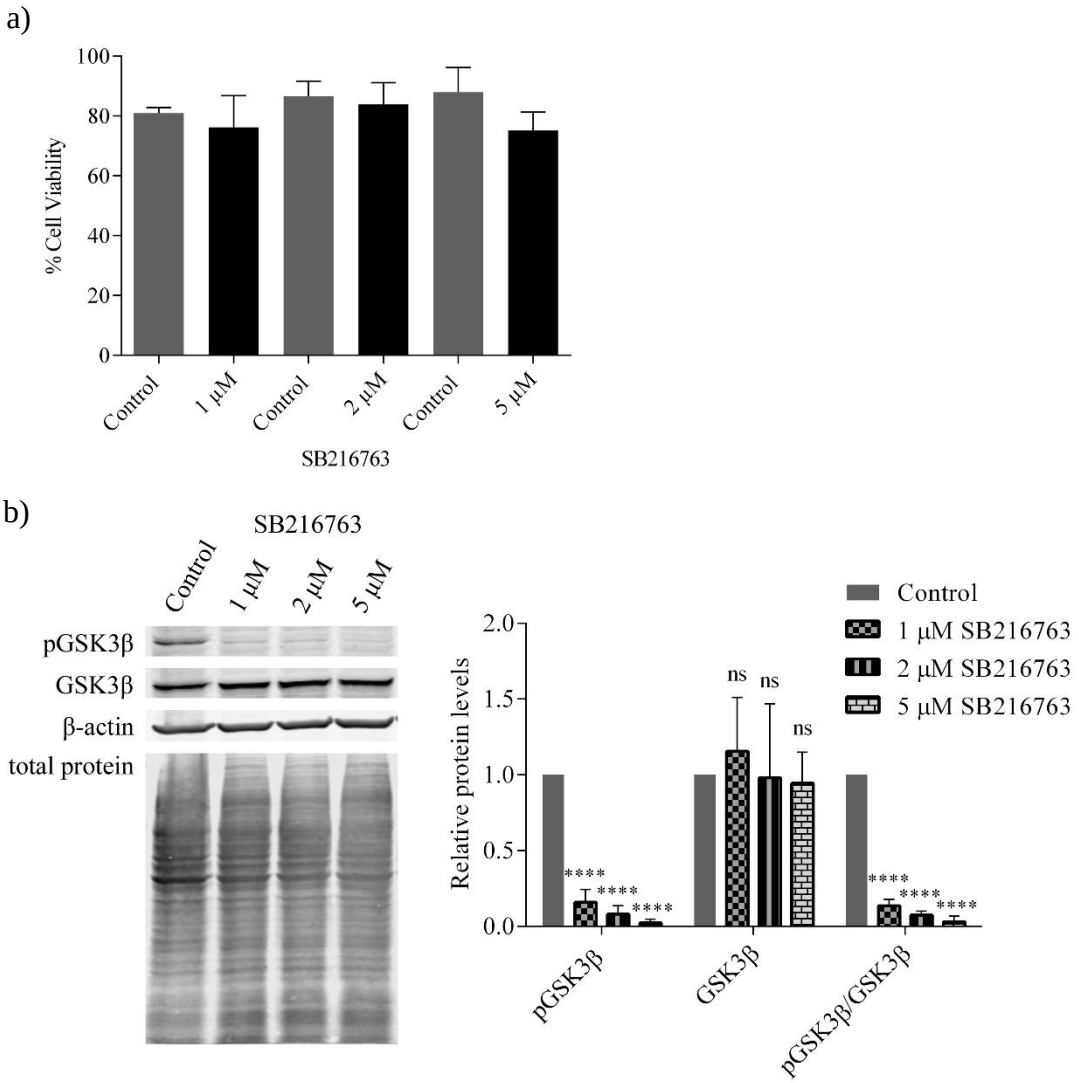

Figure 4.3. Activation of GSK3β signalling in MV4-11 cells using SB216763. Bar chart of % cell viability following treatment with the indicated concentrations of SB216763 compared to vehicle controls (N=2) *(a)*. Western blot analysis of GSK3β signalling in vehicle control (control), and following treatment with SB216763 (1 µM, 2 µM and 5 µM) for 16 h *(b)*. β-actin and total protein (REVERT total protein stain) are shown as loading controls. Bar chart shows relative mean pGSK3β, GSK3β and pGSK3β/GSK3β protein levels following treatment with SB216763 (1 µM, 2 µM and 5 µM) for 16 h as quantified by densitometry. The data are expressed as % of control, where the ratio in the control was defined as 1. Results are presented as mean ± SD from three independent experiments. Asterisks indicate statistically significant differences (****$p<0.0001$) as analysed by Student's t-test.

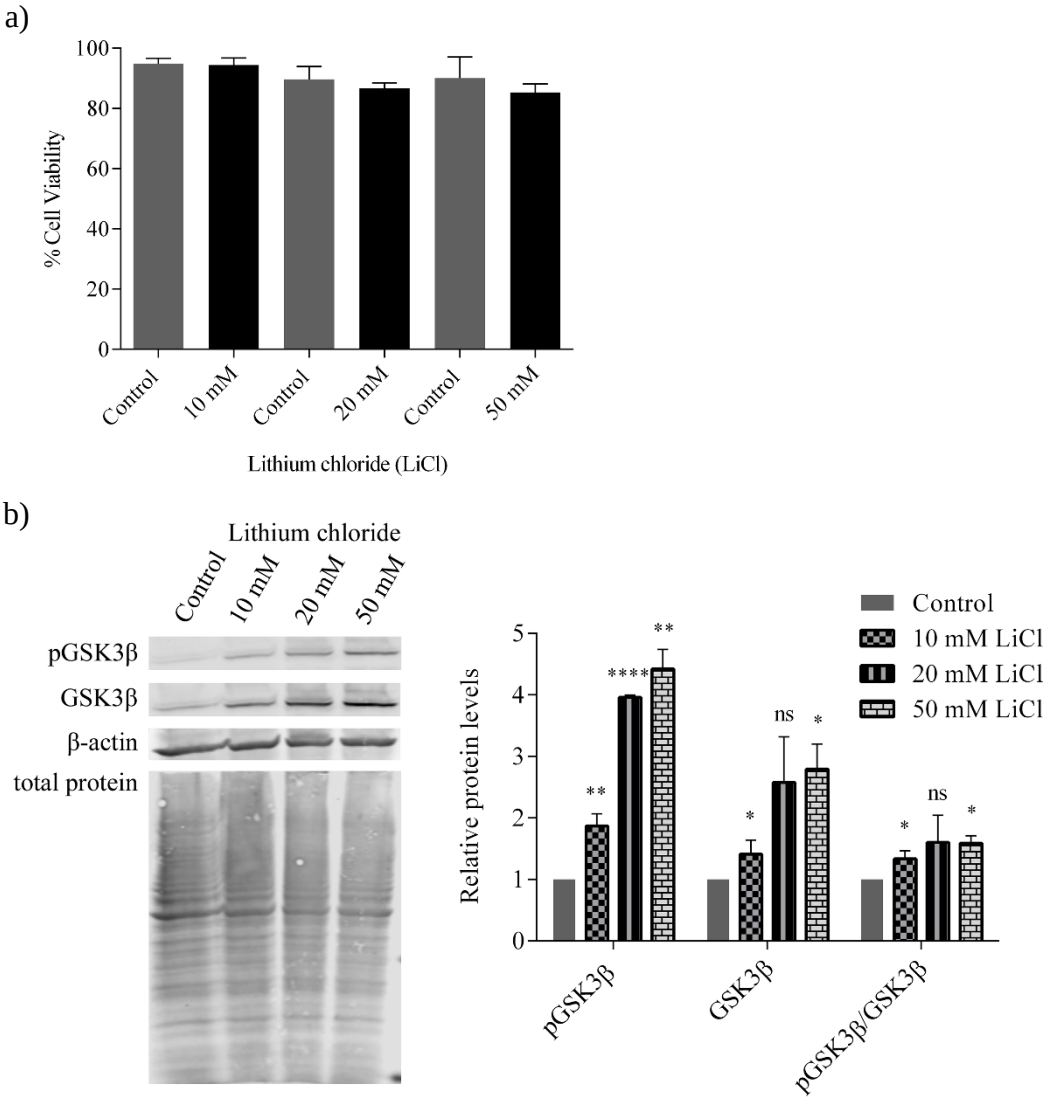

Figure 4.4. Inhibition of GSK3β signalling in MV4-11 cells using lithium chloride (LiCl). Bar chart of % cell viability following treatment with the indicated concentrations of LiCl compared to vehicle controls (N=2) *(a)*. Western blot analysis of GSK3β signalling in vehicle control (control), and following treatment with LiCl (10 mM, 20 mM and 50 mM) for 16 h *(b)*. β-actin and total protein (REVERT total protein stain) are shown as loading controls. Bar chart shows relative mean pGSK3β, GSK3β and pGSK3β/GSK3β protein levels following treatment with LiCl (10 mM, 20 mM and 50 mM) for 16 h as quantified by densitometry. The data are expressed as % of control, where the ratio in the control was defined as 1. Results are presented as mean ± SD from three independent experiments. Asterisks indicate statistically significant differences (*p<0.05, **p<0.01, ****p<0.0001) as analysed by Student's t-test.

Inhibition of the AKT pathway using the PI3K inhibitor, LY294002 (LY), resulted in a significant decrease in $p22^{phox}$ and NOX4 protein levels (Figure 4.5. (i) a and Figure 4.5. (ii) a). Activation of GSK3β using SB216763 (SB) was found to have no noticeable effect on NOX4 and $p22^{phox}$ protein levels (Figure 4.5. (i) b and Figure 4.5. (ii) b) whereas inhibition of GSK3β using LiCl caused a significant increase in NOX4 protein levels. Interestingly, $p22^{phox}$ protein levels decreased significantly following treatment with 50 mM LiCl (Figure 4.5. (i) c and Figure 4.5. (ii) c). Thus, AKT needs to be phosphorylated and activated in order for FLT3-ITD at the plasma membrane to produce its oncogenic effects.

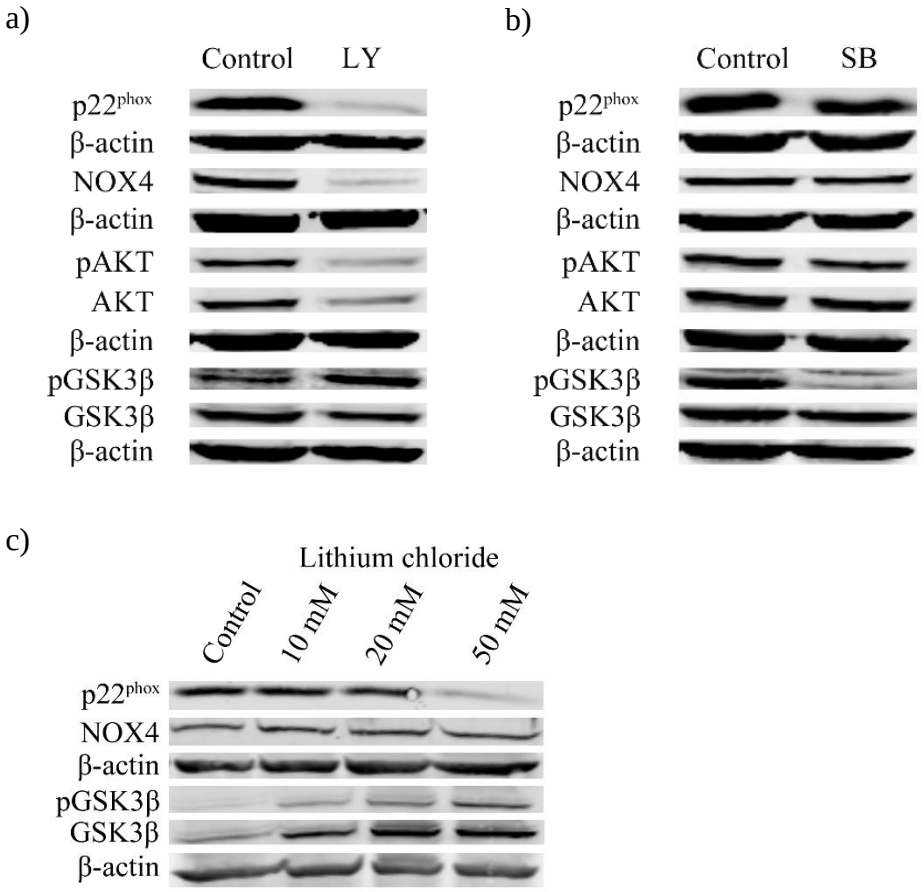

Figure 4.5. (i) NOX4- and $p22^{phox}$-generated pro-survival ROS require AKT activation. Western blot analysis of $p22^{phox}$ and NOX4 protein levels in MV4-11 cells following treatment with PI3K/AKT inhibitor LY294002 (LY; 50 μM) *(a)*, GSK3β activator SB216763 (SB; 5 μM) *(b)* and GSK3β inhibitor lithium chloride (10 mM, 20 mM and 50 mM) *(c)* for 16 h. β-actin is shown as a loading control. Western blots are representative of three independent experiments.

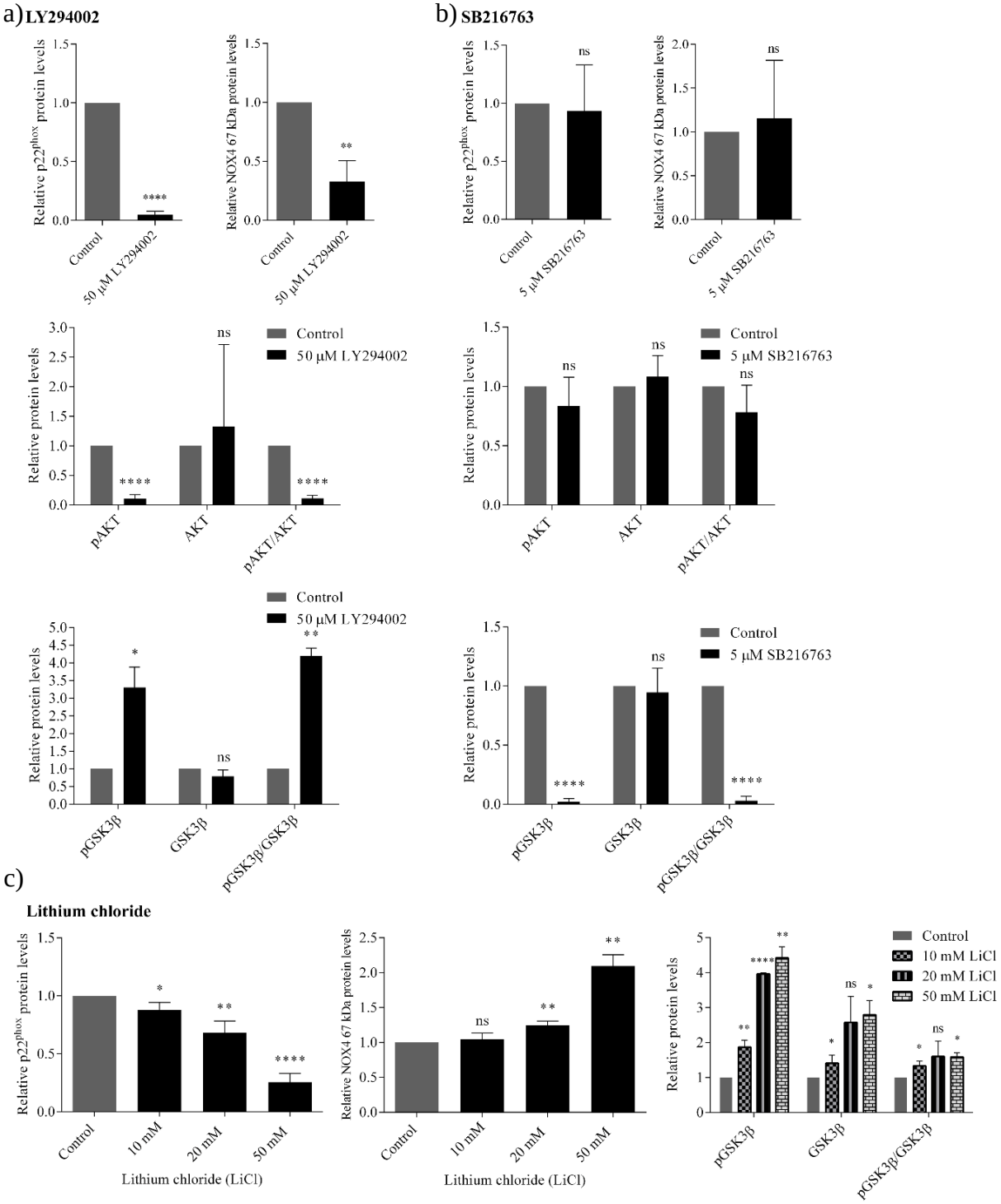

Figure 4.5. (ii) NOX4- and p22^{phox}-generated pro-survival ROS require AKT activation. Bar charts show relative mean p22^{phox}, NOX4, pAKT, AKT, pAKT/AKT, pGSK3β, GSK3β and pGSK3β/GSK3β protein levels following treatment with LY294002 (50 µM) *(a)*, SB216763 (5 µM) *(b)* and LiCl (10 mM, 20 mM and 50 mM) *(c)* for 16 h as quantified by densitometry. The data are expressed as % of vehicle control (control), where the ratio in the control was defined as 1. Results are presented as mean ± SD from three independent experiments. Asterisks indicate statistically significant differences (*p<0.05, **p<0.01, ****p<0.0001) as analysed by Student's t-test.

Given that inhibition of PI3K/AKT signalling in MV4-11 cells resulted in increased GSK3β phosphorylation, indicative of GSK3β inhibition (Figure 4.5.), we investigated the effect of combined AKT inhibition and GSK3β activation on NOX4 and $p22^{phox}$ protein levels in MV4-11 cells. 50 µM LY294002 (Figure 4.2.) and 5 µM SB216763 (Figure 4.3.) were identified as the optimal concentrations. Treatment of MV4-11 cells with LY294002 in combination with SB216763 had no synergistic effects on NOX4 and $p22^{phox}$ protein levels (Figure 4.6. (i) b and Figure 4.6. (ii)).

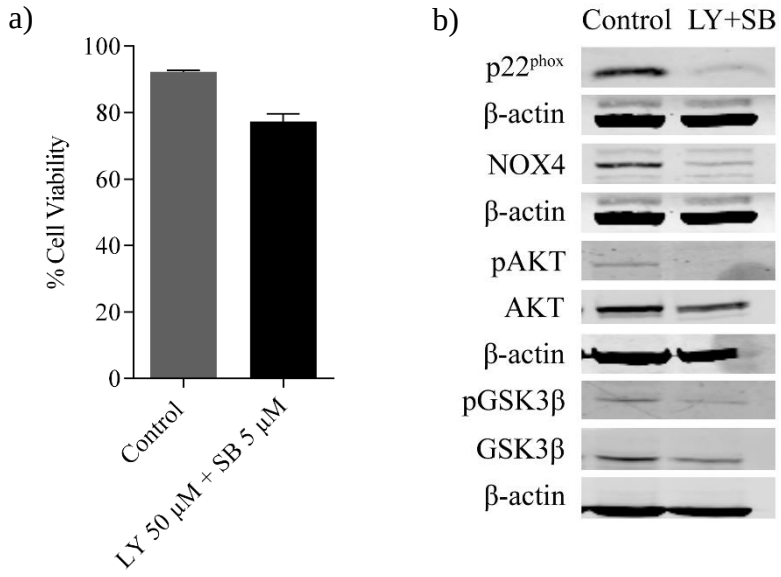

Figure 4.6. (i) Inhibition of AKT signalling and activation of GSK3β signalling in combination had no synergistic effects on NOX4 and $p22^{phox}$ protein levels in MV4-11 cells. Bar chart of % cell viability following treatment with the indicated concentrations of LY294002 and SB216763 in combination for 16 h compared to vehicle control (N=2) *(a)*. Western blot analysis of $p22^{phox}$ and NOX4 protein levels in MV4-11 cells following treatment with LY294002 and SB216763 in combination (LY+SB; 50 µM + 5 µM) *(b)* for 16 h. β-actin is shown as a loading control. Western blots are representative of three independent experiments.

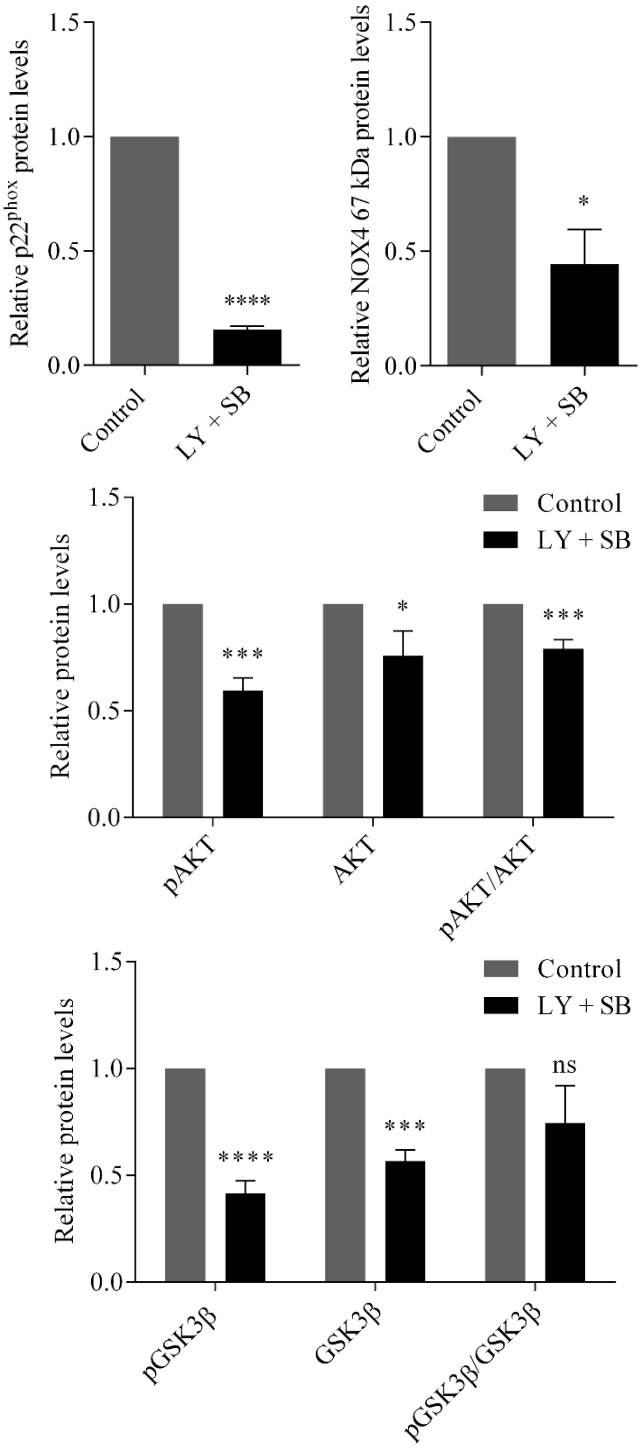

Figure 4.6. (ii) Inhibition of AKT signalling and activation of GSK3β signalling in combination had no synergistic effects on NOX4 and p22^{phox} protein levels in MV4-11 cells. Bar charts show relative mean p22^{phox}, NOX4, pAKT, AKT, pAKT/AKT, pGSK3β, GSK3β and pGSK3β/GSK3β protein levels following treatment with LY294002 (50 µM) and SB216763 (5 µM) for 16 h as quantified by densitometry. The data are expressed as % of vehicle control (control), where the ratio in the control was defined as 1. Results are presented as mean ± SD from three independent experiments. Asterisks indicate statistically significant differences (*p<0.05, ***p<0.001, ****p<0.0001) as analysed by Student's t-test.

In the previous chapter, we have demonstrated that inhibition of FLT3-ITD cell surface expression resulted in a significant decrease in $p22^{phox}$ protein levels (Figure 3.9. and Figure 3.25.). MV4-11 cells were treated with tunicamycin and brefeldin A in the presence of 20S proteasome inhibitor, lactacystin, which prevented $p22^{phox}$ degradation (Figure 3.25.). However, endogenous H_2O_2 levels were not restored suggesting $p22^{phox}$ function was not restored (Figure 3.26.). We identified PI3K/AKT signalling to be activated and GSK3β signalling to be inhibited downstream of FLT3-ITD at the plasma membrane (Figure 4.1.). Treatment of MV4-11 cells with tunicamycin and brefeldin A in the presence of lactacystin had no effect on AKT and GSK3β signalling, both AKT and GSK3β remained dephosphorylated (Figure 4.7.).

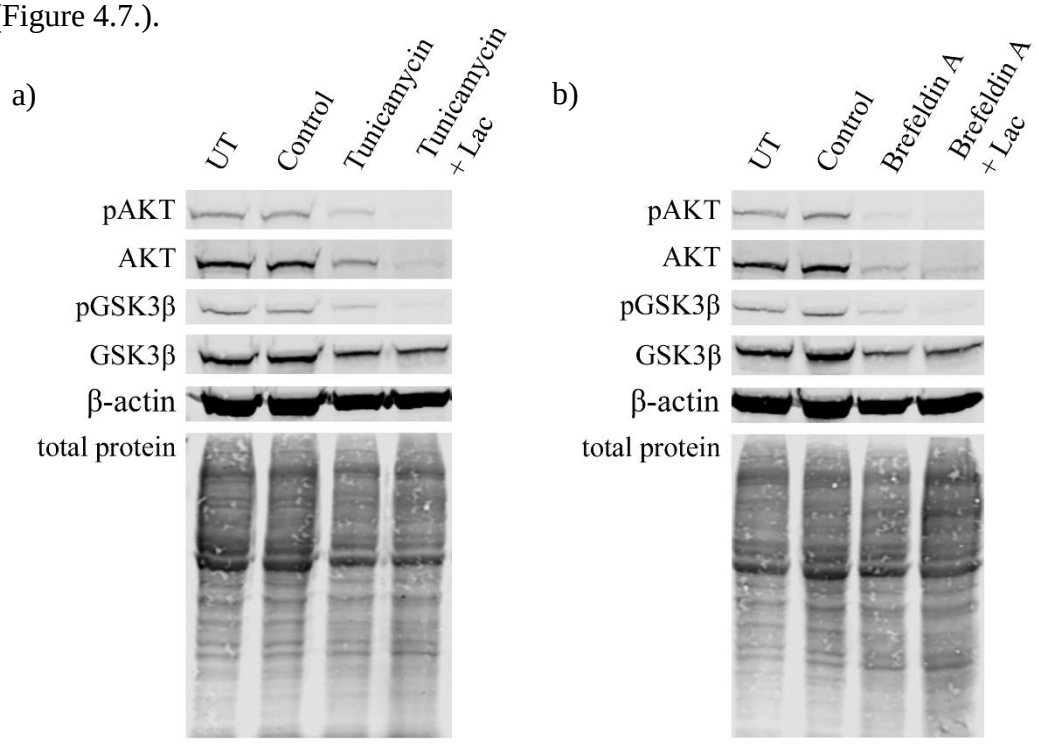

Figure 4.7. Tunicamycin and brefeldin A induce ER retention of FLT3-ITD, resulting in decreased phosphorylation of AKT and GSK3β. pAKT, AKT, pGSK3β and GSK3β protein levels following ER retention of FLT3-ITD and inhibition of the 20S proteasome. Western blot analysis of pAKT, AKT, pGSK3β and GSK3β protein levels in untreated (UT), vehicle control (control), following treatment with tunicamycin (5 μg/ml) *(a)* and brefeldin A (10 μg/ml) *(b)* overnight and also in combination with 20S proteasome inhibitor lactacystin (5 μM) overnight. β-actin and total protein (REVERT total protein stain) are shown as loading controls. Western blots are representative of three independent experiments.

Inhibition of FLT3-ITD using PKC412, a drug recently approved by the FDA for the treatment of FLT3-ITD expressing AML (Rydapt, 2017, Stone et al., 2017), resulted in a significant decrease in $p22^{phox}$, NOX4, pAKT and pGSK3β protein levels as expected (Figure 4.8.).

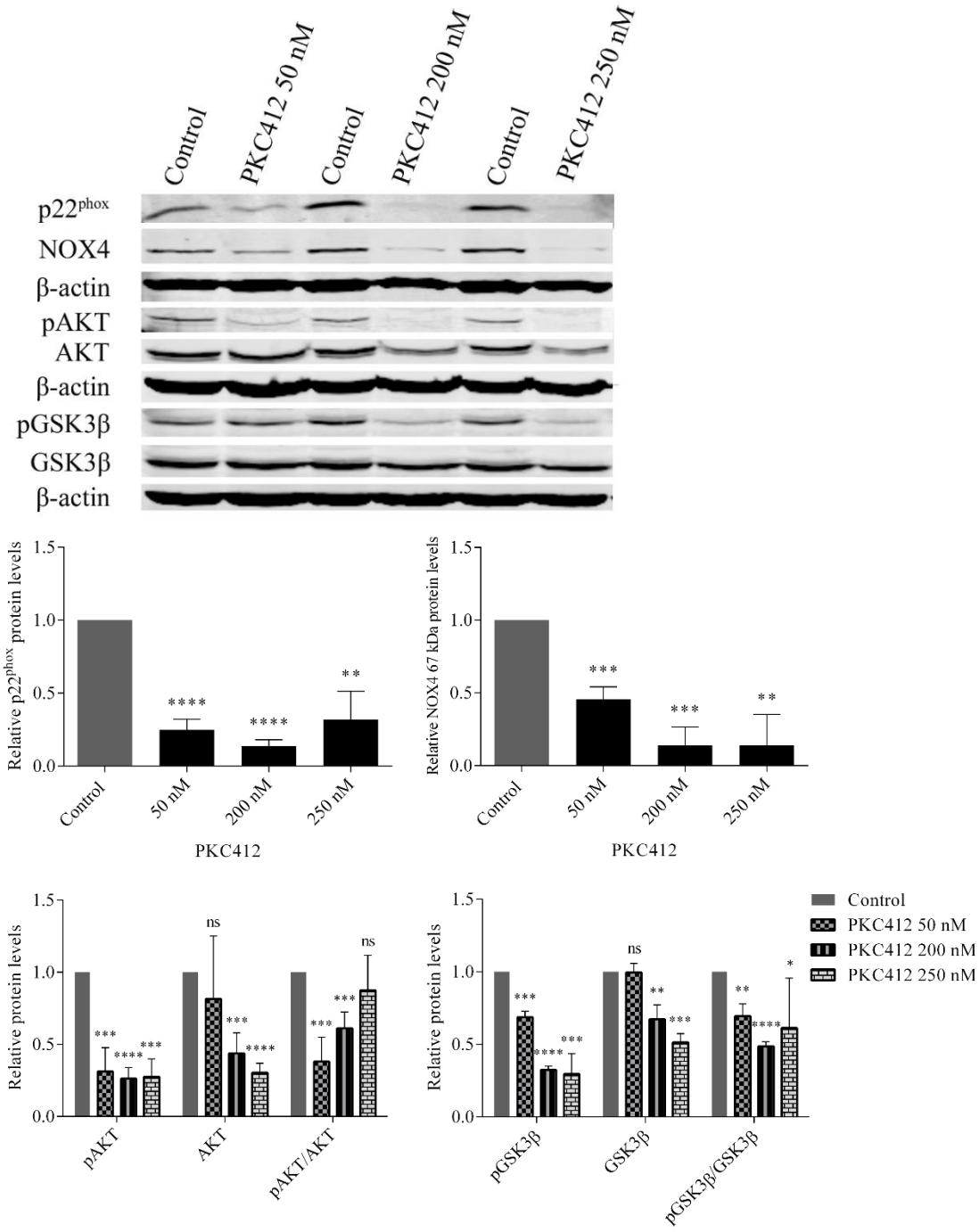

Figure 4.8. Inhibition of FLT3-ITD using PKC412 resulted in a decrease in p22^{phox}, NOX4, pAKT and pGSK3β protein levels in MV4-11 cells. Western blot analysis of p22^{phox}, NOX4, pAKT, AKT, pGSK3β and GSK3β protein levels in vehicle control (control), and following treatment with PKC412 (50 nM, 200 nM and 250 nM) for 24 h in MV4-11 cells. β-actin is shown as a loading control. Bar charts show relative mean p22^{phox}, NOX4, pAKT, AKT, pAKT/AKT, pGSK3β, GSK3β and pGSK3β/GSK3β protein levels following treatment with PKC412 (50 nM, 200 nM and 250 nM) for 24 h as quantified by densitometry. There was a separate control for each drug concentration. The data are expressed as % of control, where the ratio in the control was defined as 1. Results are presented as mean ± SD from three independent experiments. Asterisks indicate statistically significant differences (*p<0.05, **p<0.01, ***p<0.001, ****p<0.0001) as analysed by Student's t-test.

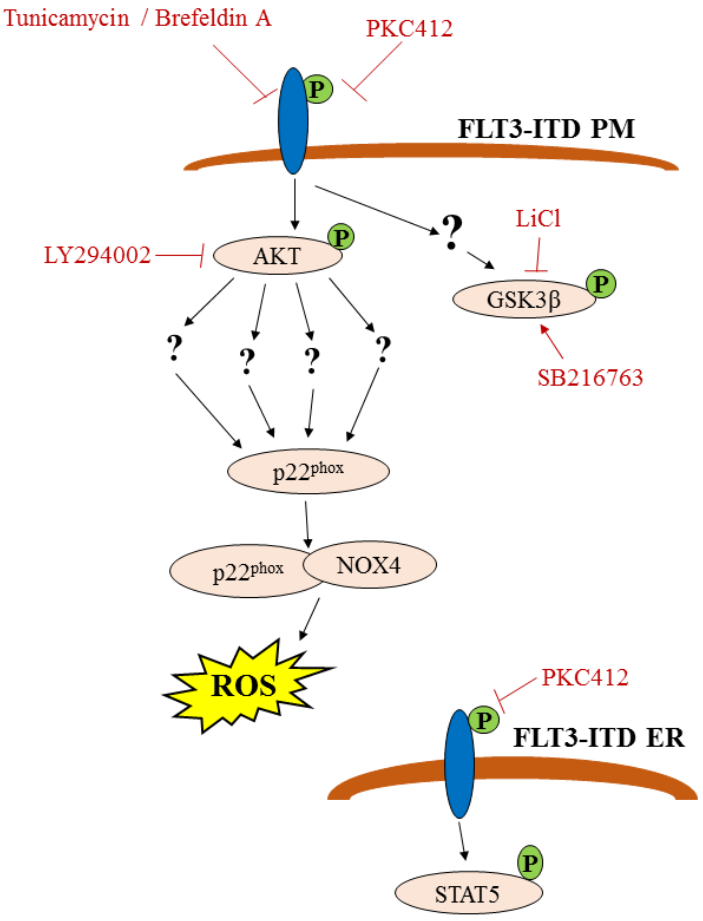

Figure 4.9. A schematic of the proposed mechanism in which FLT3-ITD at the plasma membrane and its downstream pro-survival pathways lead to the production of NOX4 pro-survival ROS in FLT3-ITD-expressing AML cells. FLT3-ITD at the plasma membrane is responsible for the phosphorylation and activation of the AKT signalling pathway and the production of $p22^{phox}$- and NOX4-generated H_2O_2.

4.3.3. Constitutive activation of the FLT3 receptor switches on downstream pro-survival signalling pathways such as AKT, GSK3β, ERK1/2 and STAT5

Previous studies in our laboratory have reported that FLT3-ITD-expressing cells produce elevated levels of ROS compared to FLT3-WT-expressing cells (Stanicka et al., 2015). Increased ROS levels are linked to increased transformation potential and activation of aberrant signalling cascades contributing to cell survival and disease progression. However, the cellular mechanisms describing the activation and regulation of these aberrant signalling pathways downstream of the FLT3-ITD mutation remains unclear. Therefore, we decided to analyse and further our knowledge on the role of cellular organisation of FLT3-ITD in controlling the outcome of enhanced cell survival. Firstly, we investigated which pro-survival pathways were activated downstream of FLT3-ITD in MV4-11 AML cells. Inhibition of the FLT3 receptor using TKI, PKC412, resulted in significantly decreased phosphorylation of AKT, GSK3β, ERK1/2 and STAT5 (Figure 4.10.). Together these data suggest that constitutive activation of FLT3 switches on downstream pro-survival signalling pathways including AKT, GSK3β, ERK1/2 and STAT5.

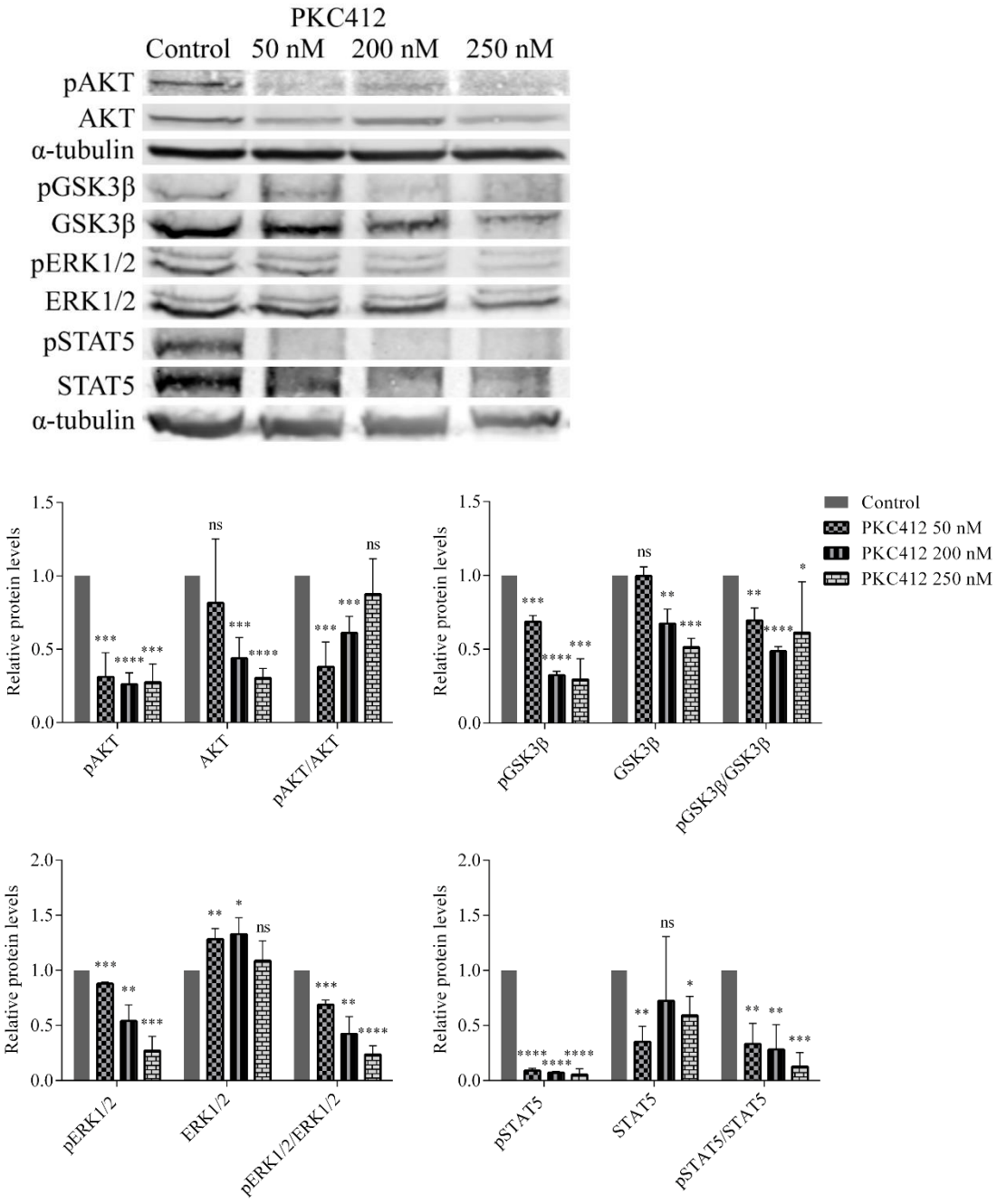

Figure 4.10. Inhibition of FLT3-ITD using PKC412 resulted in a decrease in pAKT, pGSK3β, pERK1/2 and pSTAT5 protein levels in MV4-11 cells. Western blot analysis of AKT, GSK3β, ERK1/2 and STAT5 signalling in vehicle control (control), and following treatment with PKC412 (50 nM, 200 nM and 250 nM) for 24 h. α-tubulin is shown as a loading control. Bar charts show relative mean pAKT, AKT, pAKT/AKT, pGSK3β, GSK3β, pGSK3β/GSK3β, pERK1/2, ERK1/2, pERK1/2/ERK1/2, pSTAT5, STAT5 and pSTAT5/STAT5 protein levels following treatment with PKC412 (50 nM, 200 nM and 250 nM) for 24 h as quantified by densitometry. The data are expressed as % of control, where the ratio in the control was defined as 1. Results are presented as mean ± SD from three independent experiments. Asterisks indicate statistically significant differences (*$p<0.05$, **$p<0.01$, ***$p<0.001$, ****$p<0.0001$) as analysed by Student's t-test.

4.3.4. FLT3-ITD at the plasma membrane is responsible for the activation of ERK1/2 signalling and FLT3-ITD at the endoplasmic reticulum is responsible for the activation of STAT5 signalling

Previous studies have endorsed the use of tunicamycin and brefeldin A, as a method to investigate the effect of subcellular localisation of FLT3-ITD on the initiation of aberrant signalling cascades (Choudhary et al., 2009). Both receptor trafficking inhibitors prevent cell surface expression of FLT3-ITD in MV4-11 cells (Figure 3.4. - Figure 3.7.). Impaired trafficking of FLT3-ITD to the plasma membrane resulted in decreased pAKT, pGSK3β and pERK1/2 protein levels (Figure 4.11. (i) and Figure 4.11. (ii)). Thus suggesting that the AKT, GSK3β and ERK1/2 signalling pathways are located downstream of FLT3-ITD at the plasma membrane. Interestingly, in contrast to the activation of GSK3β signalling and the inactivation of AKT and ERK1/2 signalling, phosphorylation of STAT5 increased following ER retention of FLT3-ITD in MV4-11 cells when compared to the vehicle control (Figure 4.11. (i) and Figure 4.11. (ii)). This increase in pSTAT5 has been shown to coincide with an increase in the expression of STAT5 target genes including Pim-1 and Pim-2 in 32D/FLT3-ITD cells (Choudhary et al., 2009). These findings support the current study that STAT5 signalling is activated downstream of FLT3-ITD at the endoplasmic reticulum in MV4-11 cells.

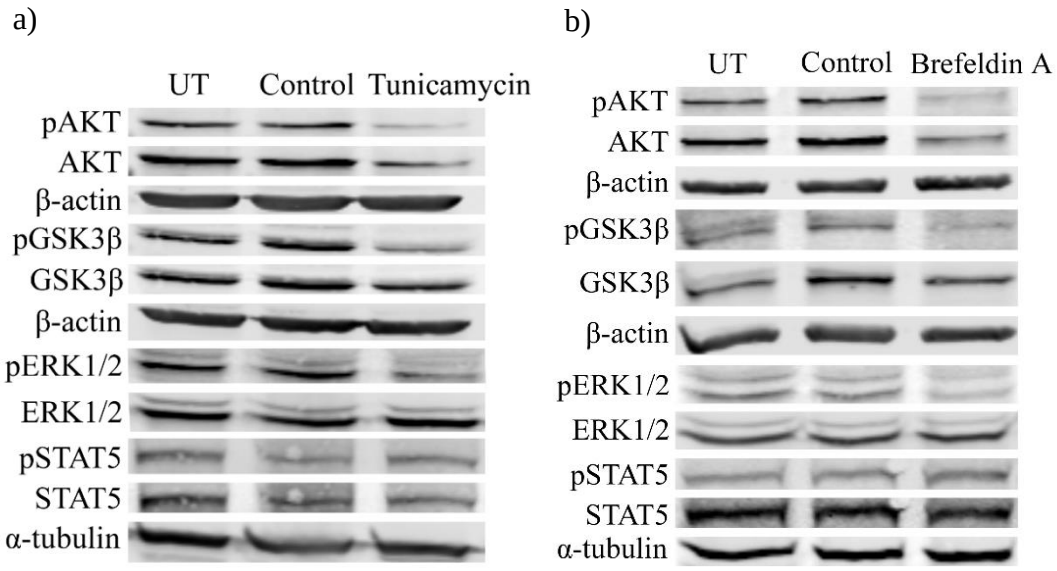

Figure 4.11. (i) PI3K/AKT and ERK1/2 are activated and GSK3β signalling is inhibited downstream of FLT3-ITD at the plasma membrane and STAT5 signalling is activated downstream of FLT3-ITD at the endoplasmic reticulum in MV4-11 cells. Western blot analysis of AKT, GSK3β, ERK1/2 and STAT5 signalling in untreated (UT), vehicle control (control), and following treatment with tunicamycin (5 µg/ml) overnight *(a)*; in untreated (UT), vehicle control (control) and following treatment with brefeldin A (10 µg/ml) overnight *(b)*. β-actin and α-tubulin are shown as loading controls. Western blots are representative of three independent experiments.

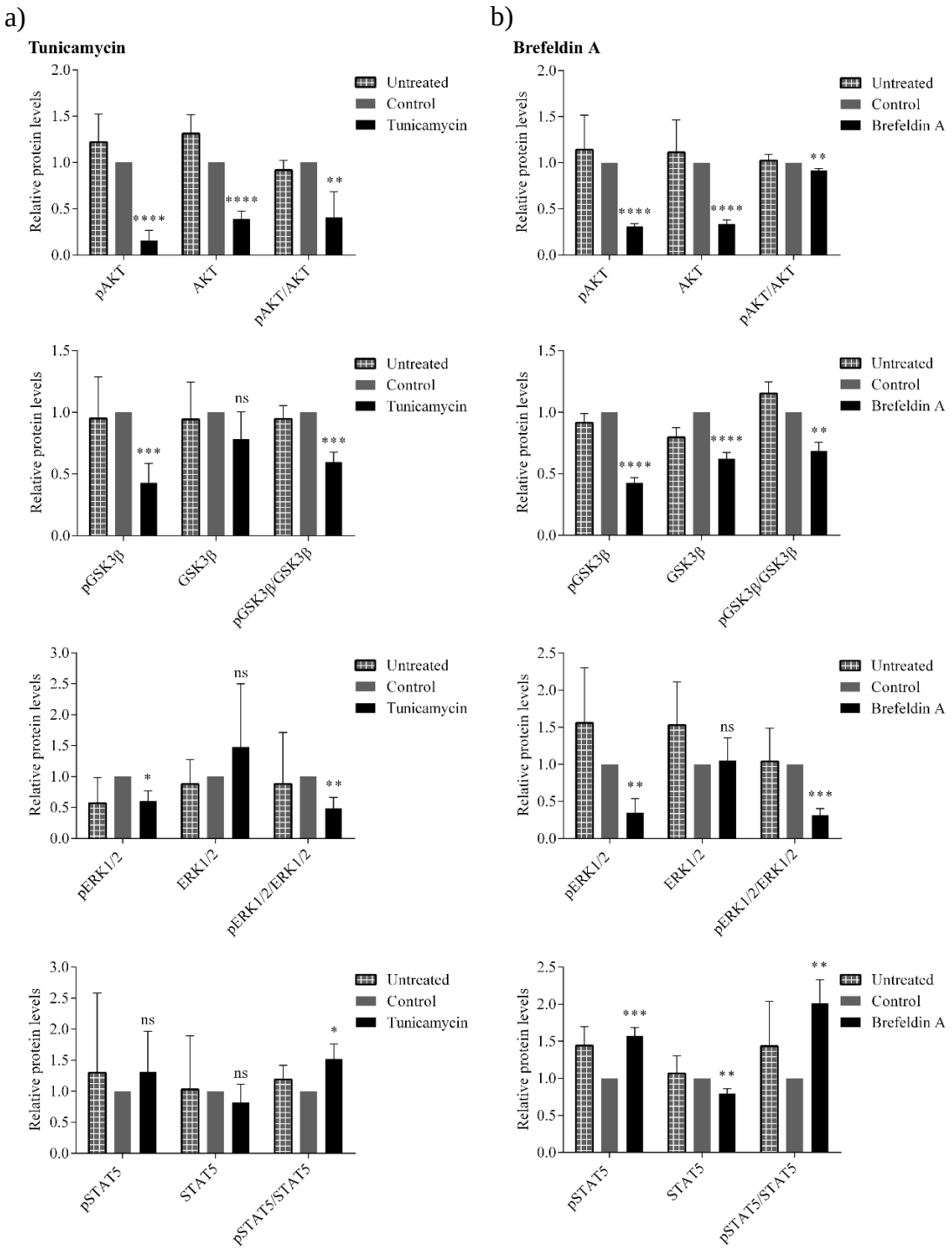

Figure 4.11. (ii) PI3K/AKT and ERK1/2 are activated and GSK3β signalling is inhibited downstream of FLT3-ITD at the plasma membrane and STAT5 signalling is activated downstream of FLT3-ITD at the endoplasmic reticulum in MV4-11 cells. Bar charts show relative mean pAKT, AKT, pAKT/AKT, pGSK3β, GSK3β, pGSK3β/GSK3β, pERK1/2, ERK1/2, pERK1/2/ERK1/2, pSTAT5, STAT5 and pSTAT5/STAT5 protein levels following treatment with tunicamycin (5 µg/ml) *(a)* and brefeldin A (10 µg/ml) *(b)* overnight as quantified by densitometry. The data are expressed as % of vehicle control (control), where the ratio in the control was defined as 1. Results are presented as mean ± SD from three independent experiments. Asterisks indicate statistically significant differences (*p<0.05, **p<0.01, ***p<0.001, ****p<0.0001) as analysed by Student's t-test.

4.3.5. GSK3β pathway is inhibited downstream of ERK1/2 signalling in FLT3-ITD expressing AML

Previous studies have demonstrated that PI3K/AKT signalling phosphorylates and inactivates GSK3β signalling downstream of the JAK2 V617F and BCR-ABL oncoproteins in myelodysplastic syndromes and CML. In a previous study it was determined that inhibition of the PI3K/AKT/GSK3β signalling pathway downstream of JAK2 V617F and BCR-ABL resulted in down-regulation of DNA damage-induced Chk1 activation, as well as G2/M arrest-enhancing the induction of apoptosis (Kurosu et al., 2013). Interestingly, we have found that inhibition of PI3K/AKT signalling using PI3K inhibitor, LY294002, resulted in significantly increased phosphorylation and inhibition of GSK3β signalling (Figure 4.5. a and Figure 4.12.). This finding suggests that GSK3β signalling is not inhibited downstream of PI3K/AKT signalling in FLT3-ITD expressing AML.

We have identified ERK1/2 signalling to be activated and GSK3β signalling to be inhibited downstream of FLT3-ITD at the plasma membrane (Figure 4.11. (i) and Figure 4.11. (ii)). Therefore, we investigated the effect of ERK1/2 inhibition using ERK1/2 inhibitor, monoethanolate (U0126) on GSK3β signalling. ERK1/2 inactivation resulted in a significant decrease in GSK3β phosphorylation, indicative of activation of GSK3β signalling (Figure 4.13.). Thus, GSK3β signalling is inhibited downstream of ERK1/2 signalling in MV4-11 cells.

Although we have shown STAT5 signalling to be phosphorylated and activated downstream of FLT3-ITD at the endoplasmic reticulum, we questioned the effect of STAT5 inhibition using STAT5 inhibitor, pimozide, on GSK3β signalling in MV4-11 cells. Interestingly, we have found that inhibition of STAT5 signalling using

STAT5 inhibitor, pimozide, resulted in significantly increased phosphorylation and inhibition of GSK3β signalling (Figure 4.14.).

Together these findings demonstrated that the GSK3β pathway is inhibited downstream of FLT3-ITD-induced ERK1/2 signalling at the plasma membrane (Figure 4.15.)

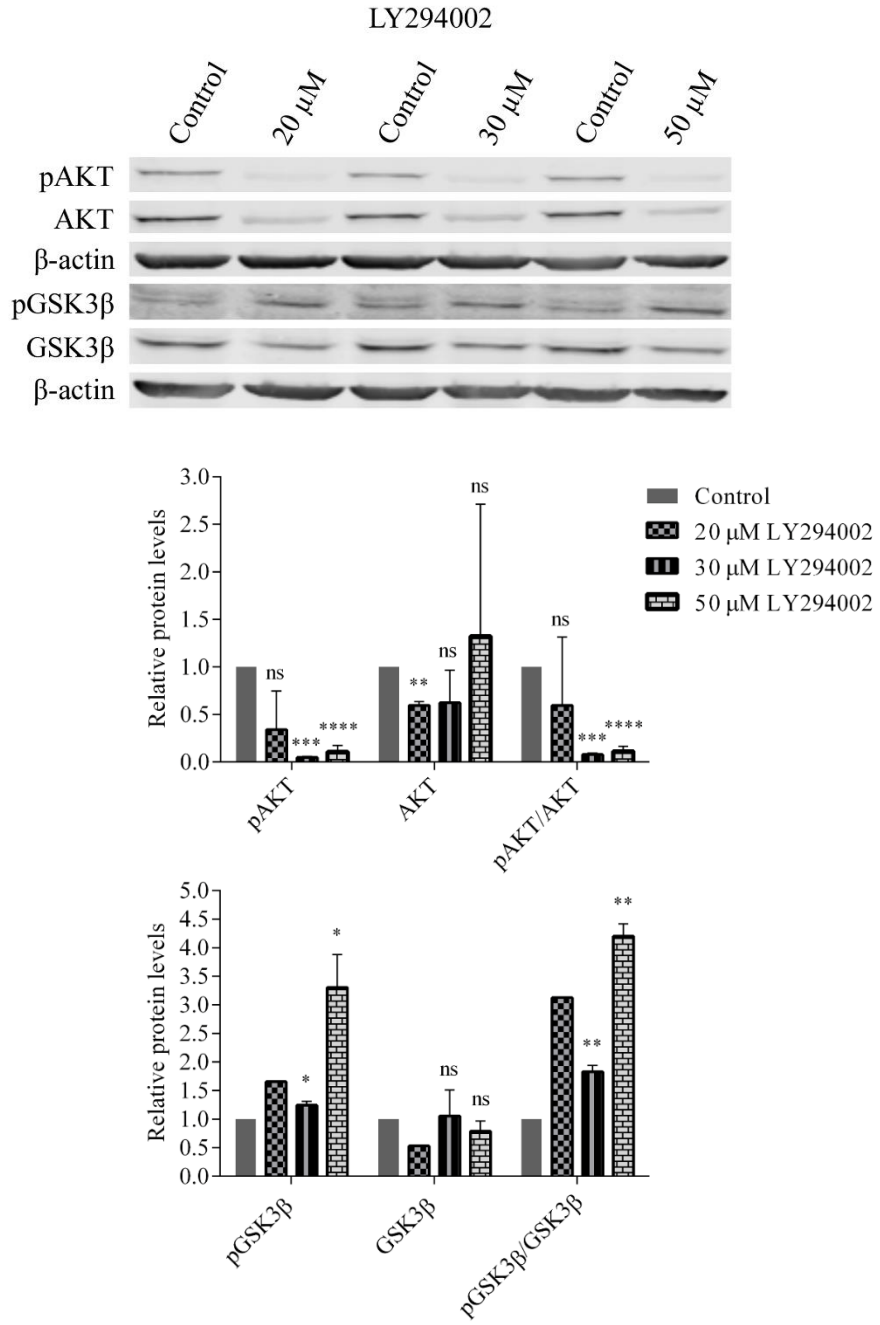

Figure 4.12. Inhibition of AKT signalling results in increased inhibition of GSK3β signalling in MV4-11 cells. Western blot analysis of AKT signalling and GSK3β signalling in vehicle control (control), and following treatment with LY294002 (20 μM, 30 μM and 50 μM) for 16 h. β-actin is shown as a loading control. Bar charts show relative mean pAKT, AKT, pAKT/AKT, pGSK3β, GSK3β and pGSK3β/GSK3β protein levels following treatment with LY294002 (20 μM, 30 μM and 50 μM) for 16 h as quantified by densitometry. The data are expressed as % of control, where the ratio in the control was defined as 1. There was a separate control for each drug concentration. Results are presented as mean ± SD from three independent experiments (except for relative mean pGSK3β, GSK3β and pGSK3β/GSK3β protein levels following treatment with 20 μM LY294002 (N=1)). Asterisks indicate statistically significant differences (*p<0.05, **p<0.01, ***p<0.001, ****p<0.0001) as analysed by Student's t-test.

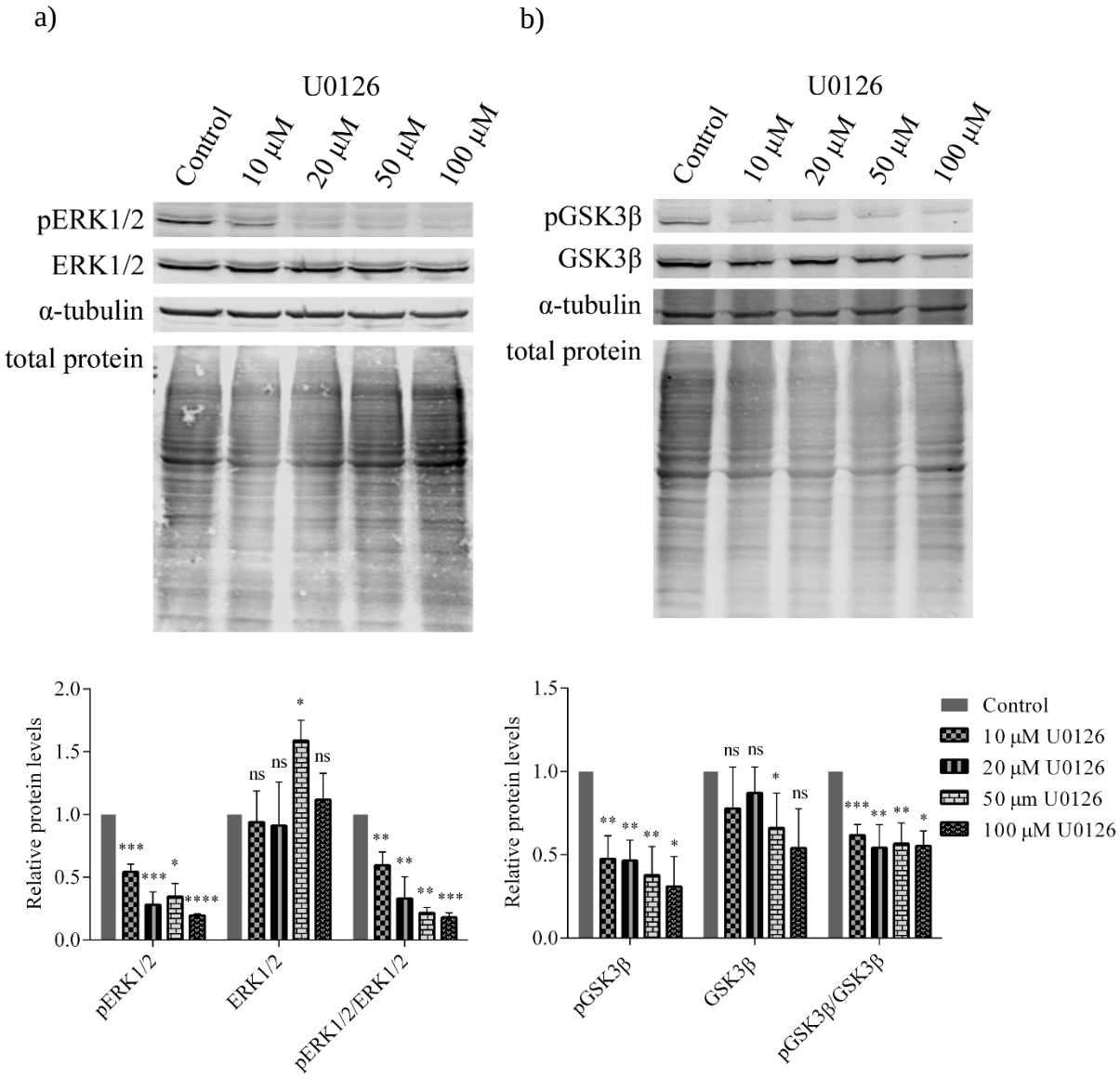

Figure 4.13. GSK3β signalling is located downstream of ERK1/2 signalling in FLT3-ITD expressing MV4-11 cells. Western blot analysis of ERK1/2 signalling *(a)* and GSK3β signalling *(b)* in vehicle control (control), and following treatment with U0126 (10 μM, 20 μM, 50 μM and 100 μM) for 16 h. α-tubulin and total protein (REVERT total protein stain) are shown as loading controls. Bar charts show relative mean pERK1/2, ERK1/2, pERK1/2/ERK1/2, pGSK3β, GSK3β and pGSK3β/GSK3β protein levels following treatment with U0126 (10 μM, 20 μM, 50 μM and 100 μM) for 16 h as quantified by densitometry. The data are expressed as % of control, where the ratio in the control was defined as 1. Results are presented as mean ± SD from three independent experiments. Asterisks indicate statistically significant differences (*p<0.05, **p<0.01, ***p<0.001, ****p<0.0001) as analysed by Student's t-test.

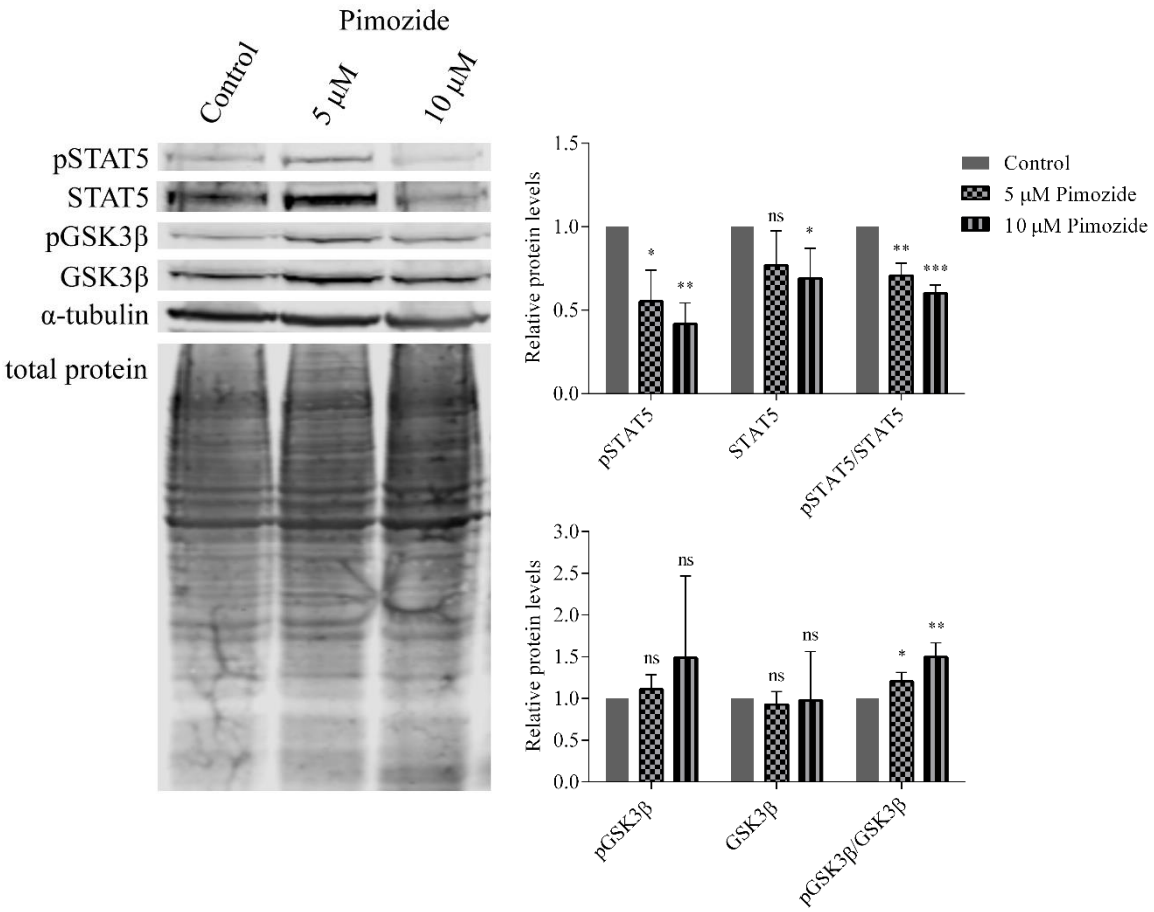

Figure 4.14. Inhibition of STAT5 signalling results in increased inhibition of GSK3β signalling in MV4-11 cells. Western blot analysis of STAT5 signalling and GSK3β signalling in vehicle control (control), and following treatment with pimozide (5 μM and 10 μM) for 16 h. α-tubulin and total protein (REVERT total protein stain) are shown as loading controls. Bar charts show relative mean pSTAT5, STAT5, pSTAT5/STAT5, pGSK3β, GSK3β and pGSK3β/GSK3β protein levels following treatment with pimozide (5 μM and 10 μM) for 16 h as quantified by densitometry. The data are expressed as % of control, where the ratio in the control was defined as 1. Results are presented as mean ± SD from three independent experiments. Asterisks indicate statistically significant differences (*$p<0.05$, **$p<0.01$, ***$p<0.001$) as analysed by Student's t-test.

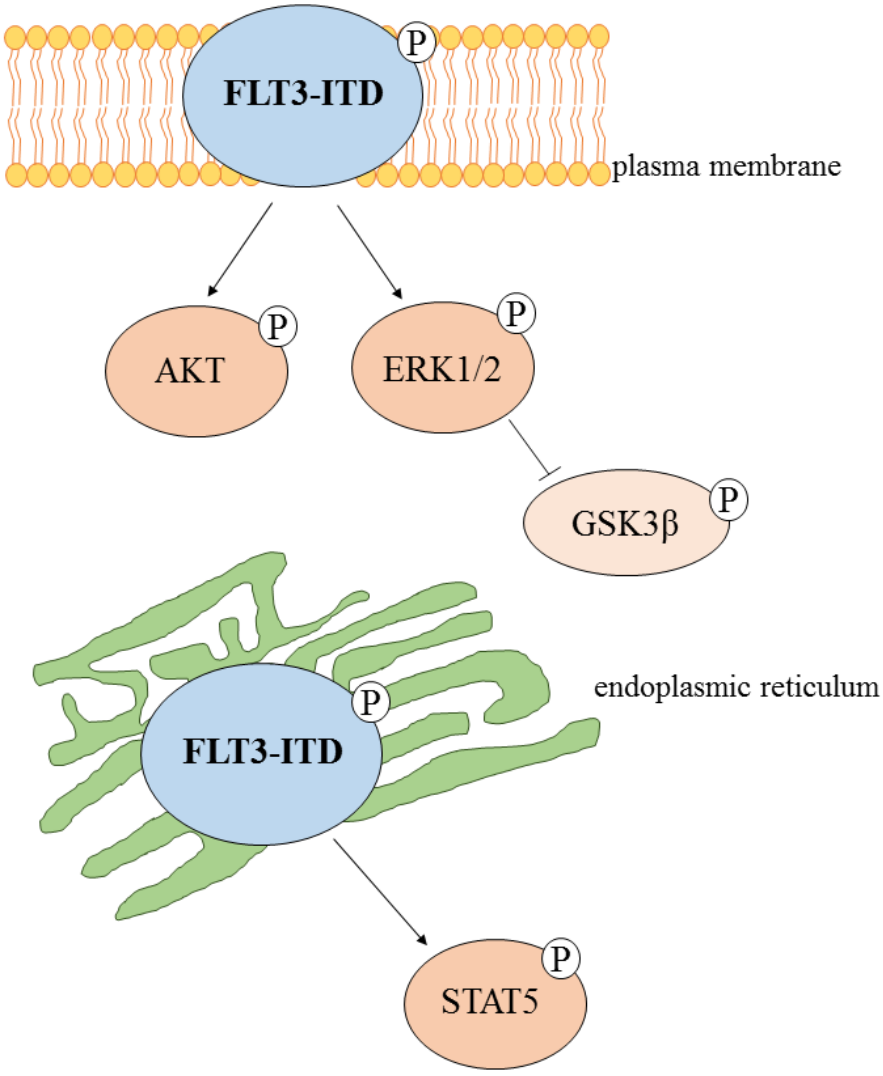

Figure 4.15. A schematic of the pro-survival pathways activated downstream of FLT3-ITD at the plasma membrane and endoplasmic reticulum. FLT3-ITD at the plasma membrane is responsible for the phosphorylation and activation of AKT- and ERK1/2-signalling pathways. Activation of ERK1/2 signalling inhibits GSK3β signalling through phosphorylation of GSK3β on serine 9. FLT3-ITD at the endoplasmic reticulum is responsible for the phosphorylation and activation of STAT5 signalling pathway.

4.4. Discussion

In this study, we validate the importance of FLT3-ITD subcellular localisation on the production of NOX4- and $p22^{phox}$-generated ROS in AML. In the previous chapter, we have suggested that FLT3-ITD at the plasma membrane is responsible for the activation and expression of $p22^{phox}$-generated pro-survival ROS in FLT3-ITD expressing AML cells (Figure 3.9. and Figure 3.11.). The aim of this work was to investigate if FLT3-ITD at the plasma membrane was responsible for the activation of NOX4-generated ROS in FLT3-ITD expressing AML. Secondly, we wished to investigate the mechanism in which mislocalised activation of FLT3-ITD at the plasma membrane initiates the activation of pro-survival signalling pathways resulting in the production of NOX4- and $p22^{phox}$-generated H_2O_2 in MV4-11 cells.

FLT3-ITD expressing cells have been shown to express increased levels of NOX4 and $p22^{phox}$ proteins as well as elevated ROS production compared to FLT3-WT expressing cells (Stanicka et al., 2015). The overproduction of ROS has been shown to induce a variety of biological effects including enhanced cell survival and disease progression through the regulation of pro-survival signalling pathways such as MAPK/ERK1/2, PI3K/AKT, STAT5 and PKD to name a few. Increased ROS levels also function through negative regulation of phosphatases, such as PTEN and PTPRJ/DEP-1, regulation of NF-κB activating pathways, as well as, mutations in transcription factors and tumour suppressor genes including Nrf2 (Moloney and Cotter, 2017).

Previous studies in our laboratory have identified the PI3K/AKT and GSK3β signalling pathways to be activated as a result of BCR-ABL induced up-regulation of NOX-generated ROS in CML, identifying a role for PI3K/AKT and GSK3β signalling in BCR-ABL-induced NOX4 pro-survival signalling in CML (Naughton et al., 2009).

Therefore, we aimed to investigate the effect of ER retention of FLT3-ITD on AKT and GSK3β signalling and examine their effects on the production of NOX4- and $p22^{phox}$-generated H_2O_2 downstream of FLT3-ITD at the plasma membrane. We suggest that FLT3-ITD at the plasma membrane is responsible for the activation of AKT signalling and inhibition of GSK3β signalling (Figure 4.1.). Inhibition of both of these signalling pathways revealed that the PI3K/AKT pathway is responsible for the activation and generation of NOX4-generated ROS in MV4-11 cells (Figure 4.5.). Although the GSK3β pathway is located downstream of FLT3-ITD at the plasma membrane, it has minimal effect on $p22^{phox}$ and NOX4 protein levels (Figure 4.5.). This result demonstrated that PI3K/AKT regulates $p22^{phox}$ and NOX4 expression and may be responsible for the production of pro-survival ROS in FLT3-ITD expressing AML. In the previous chapter we have shown that inhibition of cell surface FLT3-ITD expression results in proteasomal degradation of $p22^{phox}$ using 20S proteasome inhibitor (Figure 3.25.), although $p22^{phox}$ function was not restored (Figure 3.26.). Inhibition of the 20S proteasome had no effect on AKT and GSK3β signalling, AKT and GSK3β remained dephosphorylated as expected (Figure 4.7.). Interestingly, inhibition of AKT signalling resulted in increased inhibition of GSK3β (Figure 4.5. and Figure 4.12.). AKT inactivation and activation of GSK3β signalling in combination had no synergistic effects on NOX4 and $p22^{phox}$ protein levels (Figure 4.6.). Thus, validating PI3K/AKT induced production of NOX4-generated ROS in FLT3-ITD expressing AML.

We also studied which pro-survival pathways were activated downstream of FLT3-ITD and examined the effect of FLT3-ITD subcellular localisation on the regulation and activation of aberrant signalling cascades. Ligand-independent constitutive activation of FLT3 stimulates downstream signalling pathways including

PI3K/AKT, GSK3β, ERK1/2 and STAT5 (Figure 4.8. and Figure 4.10.). We have demonstrated that ER retention of FLT3-ITD results in decreased pAKT, pGSK3β, and pERK1/2 protein levels, however, phosphorylation of STAT5 increased in MV4-11 cells (Figure 4.11.). These findings support previous studies investigating the role of mislocalised activation of FLT3-ITD on the initiation of aberrant signalling cascades in 32D cells expressing the FLT3-ITD mutation (Choudhary et al., 2009). The PI3K/AKT and ERK1/2 signalling pathways are activated and the GSK3β signalling pathway is inhibited downstream of FLT3-ITD at the plasma membrane. STAT5 signalling is activated downstream of FLT3-ITD at the endoplasmic reticulum. Interestingly, we found that inhibition of PI3K/AKT signalling results in further inhibition of the GSK3β pathway (Figure 4.12.). Previous studies have identified the PI3K/AKT pathway to regulate GSK3β signalling through phosphorylation of GSK3β on serine 9 resulting in the inhibition of GSK3β signalling (Kurosu et al., 2013). We identified GSK3β signalling to be inhibited downstream of ERK1/2 activation in FLT3-ITD expressing AML (Figure 4.13.).

Tunicamycin and brefeldin A inhibit glycosylation of many proteins. For this reason they are not suitable for the treatment of FLT3-ITD expressing AML cases. They have however previously been used to examine the effects of cellular localisation of oncogenic FLT3-ITD and its effect on pro-survival signalling pathways (Choudhary et al., 2009). In this study, a mutant of FLT3-ITD was created that contained a deletion of the extracellular ligand-binding domain of FLT3-ITD (FLT3-ITD ΔECD). This mutation eliminated many potential sites of glycosylation, resulting in glycosylation-independent trafficking of the FLT3-ITD receptor. Inhibition of FLT3-ITD ΔECD with PKC412 resulted in a loss of pro-survival signalling, as indicated by a decrease in pERK1/2 and pAKT. Due to the mutation in glycosylation sites recognised by

tunicamycin, treatment with this inhibitor had no effect on trafficking of the receptor and pERK1/2 and pAKT levels remained high. Brefeldin A inhibits glycosylation of receptors indirectly by disruption of the structure and function of the Golgi apparatus. Treatment with brefeldin A therefore successfully inhibited trafficking of the receptor to the plasma membrane and as a result, pERK1/2 and pAKT levels decreased. As further support, they showed that wild-type FLT3, found only at the plasma membrane, in the presence of FLT3 ligand leads to the activation of PI3K and ERK1/2 signalling (Choudhary et al., 2009). These findings not only support the current study, highlighting a crucial role for FLT3-ITD at the plasma membrane in stimulating pro-survival signalling, but it also endorses the use of inhibitors, such as tunicamycin and brefeldin A, as a method to investigate the effect of subcellular localisation of FLT3-ITD on the production of pro-survival ROS.

In conclusion, we propose that FLT3-ITD at the plasma membrane is responsible for the activation and expression of NOX4- and $p22^{phox}$-generated pro-survival ROS in FLT3-ITD expressing AML cells. $p22^{phox}$ is an essential component of NOX1-4 and is required to produce functionally active NOX. For FLT3-ITD to generate its oncogenic effects it has to be located at the plasma membrane. Plasma membrane FLT3-ITD induced activation of PI3K/AKT pro-survival signalling is responsible for the activation and generation of $p22^{phox}$- and NOX4-generated ROS in AML (Figure 4.9.). In terms of activation of other pro-survival signalling pathways, FLT3-ITD at the plasma membrane activates ERK1/2 signalling resulting in the inhibition of GSK3β signalling and FLT3-ITD at the endoplasmic reticulum is responsible for the activation of STAT5 signalling (Figure 4.15.). Together these findings further present FLT3-ITD at the plasma membrane as a potential therapeutic

target in the treatment of AML in preventing downstream pro-tumourigenic driven oncogenic effects.

Chapter 5. Nuclear membrane-localised NOX4D generates pro-survival ROS in FLT3-ITD-expressing AML

5.1. Abstract

Internal tandem duplication of the juxtamembrane domain of FMS-like tyrosine kinase 3 (FLT3-ITD) is the most prevalent genetic aberration present in 15-35% of acute myeloid leukaemia (AML) cases and is associated with a poor prognosis. FLT3-ITD expressing cells have been shown to express elevated levels of NADPH oxidase 4 (NOX4)-generated pro-survival hydrogen peroxide (H_2O_2) contributing to increased levels of DNA oxidation and double strand breaks (dsbs). NOX4 is constitutively active and has been found to have various isoforms expressed at multiple locations within a cell. The purpose of this study was to investigate the expression, localisation and regulation of NOX4 28 kDa splice variant, NOX4D. NOX4D has previously been shown to localise to the nucleus and nucleolus in various cell types and is implicated in the generation of reactive oxygen species (ROS) and DNA damage. Here, we demonstrate that FLT3-ITD expressing-AML patient samples, as well as cell lines that express the NOX4D isoform, result in elevated H_2O_2 levels compared to FLT3-WT expressing cells, as quantified by flow cytometry using the cell-permeable H_2O_2 -probe Peroxy Orange 1(PO1). Cell fractionation indicated that NOX4D is nuclear membrane-localised in FLT3-ITD expressing cells. Treatment of MV4-11 cells with receptor trafficking inhibitors, tunicamycin and brefeldin A, resulted in deglycosylation of NOX4 and NOX4D. Inhibition of the FLT3 receptor revealed that the FLT3-ITD oncogene is responsible for the production of NOX4D-generated H_2O_2 in AML. We found that inhibition of the PI3K/AKT and STAT5 pathways resulted in down-regulation of NOX4D-generated pro-survival ROS. Taken together these findings indicate that nuclear membrane-localised NOX4D-generated

pro-survival H_2O_2 may be contributing to genetic instability in FLT3-ITD expressing AML.

5.2. Introduction

Aberrant signalling of receptor tyrosine kinases (RTKs) is associated with tumour development and transformation (Blume-Jensen and Hunter, 2001, Köthe et al., 2013, Regad, 2015). FMS-like tyrosine kinase 3 (FLT3) is a type III RTK expressed in approximately 90% of acute myeloid leukaemia (AML) and plays a critical role in normal haematopoiesis (Stirewalt and Radich, 2003, Gilliland and Griffin, 2002). Internal tandem duplication (ITD) of sequences in the juxtamembrane domain is the most prevalent genetic aberration of FLT3, with a gain of function mutation, implicated in 15-35% of AML patients (Gilliland and Griffin, 2002, Network, 2013, Jayavelu et al., 2016b). Patients with this mutation have a particularly poor prognosis with a high incidence of relapse (Small, 2008, Konig and Levis, 2015). Constitutive activation of the tyrosine kinase domain of FLT3-ITD results in autophosphorylation and activation of downstream pro-survival cascades including PI3K/AKT, ERK1/2 and STAT5 resulting in the promotion of cell survival, proliferation and transformation in myeloid leukaemia (Brandts et al., 2005, Choudhary et al., 2005a, Choudhary et al., 2009, Choudhary et al., 2007, Mizuki et al., 2000, Hayakawa et al., 2000). It has been demonstrated that AML cells expressing the FLT3-ITD mutation produce higher levels of reactive oxygen species (ROS) and DNA damage compared to their wild-type counterpart (Sallmyr et al., 2008a, Godfrey et al., 2012, Woolley et al., 2012, Stanicka et al., 2015).

ROS have been long implicated in leukaemia cancer pathology due to their ability to induce DNA damage (Rassool et al., 2007, Hole et al., 2011). The NADPH oxidase (NOX) family consisting of NOX1-5 and dual oxidase (DUOX) 1 and 2, are well established producers of ROS (Bedard and Krause, 2007), with NOX2 and NOX4

playing a central role in the increased production of hydrogen peroxide (H_2O_2) in AML (Stanicka et al., 2015, Jayavelu et al., 2016a, Moloney et al., 2017b). NOX proteins vary in structure, subcellular localisation, biochemical characteristics and regulatory subunits ($p22^{phox}$, $p47^{phox}$, $p67^{phox}$ and RAC1/2). p22 phagocyte oxidase ($p22^{phox}$) is a partner protein and is required for functionally active NOX1-4 (Brandes et al., 2014, Ambasta et al., 2004). Among the NOX family members NOX4 is unique. It is constitutively activated, generating H_2O_2, unlike its family members NOX1 and NOX2, which require an agonist for activation (Martyn et al., 2006, Serrander et al., 2007, Takac et al., 2011). Oxidation of protein tyrosine phosphatases (PTPs) occurs in FLT3-ITD expressing AML cells. NOX4-driven ROS formation causes partial inactivation of DEP-1/PTPRJ, a transmembrane PTP responsible for negative regulation of FLT3 signalling, contributing to unfavourable downstream signalling (Jayavelu et al., 2016a).

NOX4 subcellular localisation plays an important role, given its constitutive activity. NOX4 has been reported to be localised in the cytoskeleton (Hilenski et al., 2004), endoplasmic reticulum (ER) (Ambasta et al., 2004, Chen et al., 2008b, Helmcke et al., 2008, Zhang et al., 2011), mitochondria (Block et al., 2009, Case et al., 2013), plasma membrane (Zhang et al., 2011, Lee et al., 2006) and nucleus (Anilkumar et al., 2013, Kuroda et al., 2005, Matsushima et al., 2013) in different cell types. Previous studies in our laboratory have shown that NOX4 and $p22^{phox}$ colocalise to the nuclear membrane by immunofluorescence in FLT3-ITD expressing MV4-11 AML cell line contributing to DNA oxidation and double strand breaks (dsbs), possibly driving genetic instability (Stanicka et al., 2015).

Previous studies identified NOX4 isoforms, expressed at varying levels, in the presence of the prototype in the human lung cancer cell line, A549 cells. The truncated

NOX4 splice variant D (28 kDa) lacks the majority of the transmembrane domain and has been shown to produce higher levels of ROS and DNA damage compared to its prototype (Goyal et al., 2005). NOX4D retains the NADPH and FAD-binding domains required for electron transfer activity and ROS production despite its truncation (Nisimoto et al., 2010). NOX4D is localised to the nucleus and nucleolus in vascular smooth muscle cells (VSMC), A7R5 cells and in many other cells including human aortic vascular smooth muscle cells, human umbilical vein endothelium cells (HUVEC), H9C2 rat cardiomyocytes, human embryonic kidney fibroblasts (HEK), mouse primary cardiac fibroblasts and rat neonatal cardiomyocytes. NOX4D is expected to be soluble rather than membrane-localised (Anilkumar et al., 2013).

To investigate if FLT3-ITD expressing AML cells express NOX4D and in order to identify the localisation of NOX4D, we utilised subcellular fractionation, inhibitors of FLT3-ITD and pro-survival signalling pathways, siRNA, alongside ROS specific probes and antibodies. Experiments were carried out in *de novo* primary AML samples, human patient-derived AML cell line MV4-11 and in the murine haematopoietic 32D cell line stably expressing FLT3-wild type (FLT3-WT) receptor and FLT3-ITD mutation.

We show that FLT3-ITD expressing AML patient samples and cell lines express the NOX4D 28 kDa splice variant. FLT3-ITD expressing AML cells express NOX4D in the nuclear membrane, which may be contributing to genetic instability in AML. NOX4D expression is dependent on the FLT3-ITD mutation. NOX4 partner protein $p22^{phox}$ does not regulate NOX4 or NOX4D protein levels. Inhibition of the PI3K and STAT5 pro-survival pathways results in decreased NOX4D protein levels, alongside a decrease in endogenous H_2O_2 detected using the H_2O_2 specific probe Peroxy Orange 1 (PO1). Inhibition of ERK1/2 signalling had no effect on NOX4D

protein levels, however a decrease in $p22^{phox}$ protein levels alongside a decrease in endogenous H_2O_2 was observed. Inhibition of GSK3β resulted in increased levels of NOX4D, however, a slight decrease in endogenous H_2O_2 was observed. This demonstrates that NOX4D is downstream of FLT3-ITD signalling in AML, located in the nuclear membrane where it may be contributing to DNA damage and disease progression.

5.3. Results

5.3.1. FLT3-ITD expressing AML patient samples express the NOX4 splice variant NOX4D 28 kDa

FLT3-ITD expressing AML cells have been shown previously to express higher levels of total endogenous H_2O_2, DNA oxidation and dsbs compared to FLT3-WT cells (Jayavelu et al., 2016b, Stanicka et al., 2015). NOX4 has been well established as a producer of pro-survival ROS in FLT3-ITD expressing AML, contributing to DNA damage and disease progression (Stanicka et al., 2015, Jayavelu et al., 2016a). As mentioned previously, NOX4 is unique to other members of the NOX family of proteins, as it is constitutively activated. Therefore, NOX4 subcellular localisation plays an important role in cellular regulation. Our group has previously shown that NOX4 and $p22^{phox}$ colocalise to the nuclear membrane in MV4-11 cells (Stanicka et al., 2015). Previous studies identified the presence of NOX4 isoforms, including NOX4 splice variant NOX4D (28 kDa), to be expressed and localised to the nucleus and nucleolus of VSMC where it is contributing to ROS production, DNA damage and genetic instability (Anilkumar et al., 2013). We investigated if FLT3-ITD- and FLT3-WT-expressing AML patient samples expressed the NOX4D isoform. We show that NOX4D is expressed in FLT3-ITD expressing patient samples, but is absent in FLT3-WT patient samples (Figure 5.1.).

a)

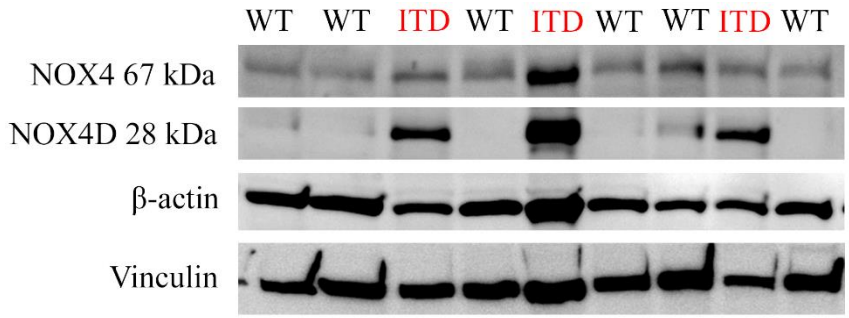

b)

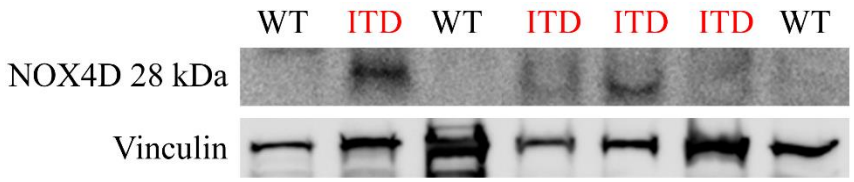

Figure 5.1. FLT3-ITD expressing AML patient samples express the NOX4D 28 kDa isoform. Western blot analysis of NOX4 67 kDa and NOX4D 28 kDa protein levels in FLT3-ITD- and FLT3-WT-expressing patient samples using Abcam NOX4 antibody (cat# Ab109225 (UOTR1B492)). β-actin and Vinculin are shown as loading controls *(a)*. Western blot analysis of NOX4D 28 kDa protein levels in FLT3-ITD- and FLT3-WT-expressing patient samples using Professor Ajay Shah's in-house NOX4 antibody. Vinculin is shown as a loading control *(b)*. Figure courtesy of Dr Ashok Kumar Jayavelu.

5.3.2. Specificity of Abcam NOX4 (Ab109225) antibody

Studies have raised issues with NOX4 antibody specificity in the past, due to difficulties in detecting NOX4 protein levels. Therefore, a key issue concerned the use of the Abcam NOX4 antibody (Ab109225) and the Novus Biologicals NOX4 antibody (NB110-58849) in our study. For this reason, a series of control experiments were first performed to validate the NOX4 antibodies employed in this study.

Previous studies identified the expression of NOX4 isoforms including NOX4 67 kDa and NOX4D 28 kDa to be expressed and localised to the nucleus and nucleolus of VSMC using an in-house NOX4 antibody (Anilkumar et al., 2008, Anilkumar et al., 2013). In this study they demonstrated the specificity of this in-house antibody for NOX4 67 kDa and NOX4D 28 kDa by means of siRNA against NOX4 exon 14 (expressed in NOX4D) and NOX4 exon 3 (not expressed in NOX4D) (Anilkumar et al., 2013). To validate the specificity of the Abcam NOX4 antibody (Ab109225) against NOX4 67 kDa and NOX4D 28 kDa in primary AML samples in this study, we also used Prof. Ajay Shah's in-house antibody to support our finding that NOX4D is expressed in FLT3-ITD expressing patient samples and is absent in FLT3-WT patients (Figure 5.1. b). Specific NOX4 knockdowns using NOX4 targeted siRNA and shRNA in 32D/FLT3-ITD cells resulted in depletion of NOX4 67 kDa protein levels detected using Abcam NOX4 antibody (Figure 5.2.). Together, these experiments validated that the Abcam NOX4 (Ab109225) antibody used in this study was specific for NOX4 67 kDa and NOX4D 28 kDa.

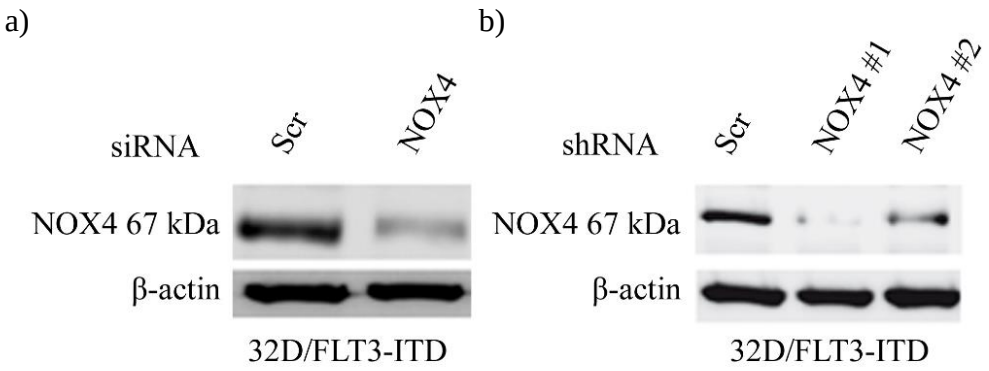

Figure 5.2. Abcam NOX4 (Ab109225) antibody specificity. Western blot analysis of NOX4 67 kDa protein levels in 32D/FLT3-ITD whole cell lysates at 48 h following NOX4 siRNA *(a)* and shRNA transfection *(b)*. Non-targeting scrambled (Scr) siRNA and shRNA were used as negative controls. β-actin is shown as a loading control. Western blots are representative of three independent experiments. Figure courtesy of Dr Ashok Kumar Jayavelu.

5.3.3. FLT3-ITD expressing MV4-11 and 32D/FLT3-ITD cells express the NOX4 splice variant NOX4D 28 kDa in the nuclear membrane

We investigated if FLT3-ITD- and FLT3-WT-expressing AML patient samples expressed the NOX4D isoform (Figure 5.1.) and also examined the expression and localisation of NOX4D 28 kDa in two cell lines: FLT3-ITD-expressing AML MV4-11 cell line and 32D cell line stably transfected with FLT3-WT or FLT3-ITD. Localisation of NOX4D was assessed by means of subcellular fractionation. We show that NOX4D is expressed in FLT3-ITD expressing cells (Figure 5.3. - Figure 5.6.), but is absent in 32D cells transfected with the FLT3-WT receptor (Figure 5.5. and Figure 5.6.). NOX4D is present in the membrane and soluble nuclear fractions of MV4-11 cells (Figure 5.3. and Figure 5.4.) and the membrane, soluble nuclear and chromatin bound nuclear (chr.b.nuclear) fractions of 32D cells stably transfected with

FLT3-ITD (Figure 5.5. and Figure 5.6.). In support of previous work, we have identified the NOX4 prototype (67 kDa) in the soluble nuclear fraction and $p22^{phox}$ in the membrane and soluble nuclear fractions in both MV4-11 cells (Figure 5.3. and Figure 5.4.) and 32D/FLT3-ITD cells (Figure 5.5. and Figure 5.6.) (Stanicka et al., 2015, Woolley et al., 2012). Interestingly, we found NOX4 67 kDa was lacking from the membrane fraction in MV4-11 cells (Figure 5.3. and Figure 5.4.). In contrast NOX4 67 kDa was observed in the membrane fraction of 32D/FLT3-ITD cells (Figure 5.5. and Figure 5.6.). There are therefore clear differences in NOX4 67 kDa subcellular localisation between these cell lines. We are unsure why there are differences between MV4-11 and 32D/FLT3-ITD cells, nonetheless, it was a clear observation.

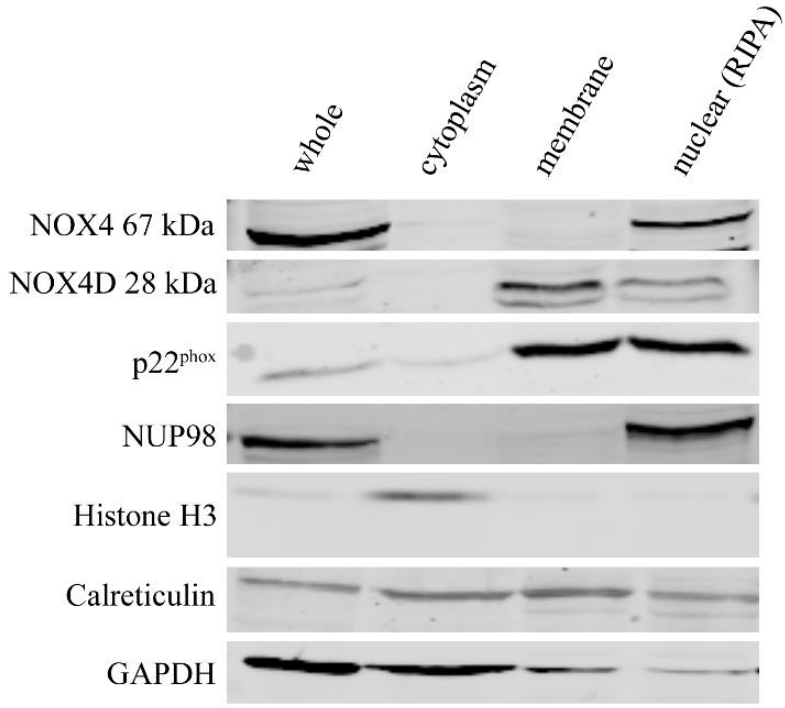

Figure 5.3. FLT3-ITD expressing AML MV4-11 cells express the NOX4D 28 kDa isoform. Subcellular fractionation was carried out in FLT3-ITD expressing AML cell line, MV4-11, using a subcellular fractionation kit and RIPA lysis buffer. Expression of NOX4 67 kDa, NOX4D 28 kDa and $p22^{phox}$ was assessed by means of western blot analysis. Equal loading of samples and verification of the subcellular fractions were demonstrated by probing for nuclear-localised NUP98 and Histone H3, membrane-localised calreticulin and cytosolic-localised GAPDH. Western blots are representative of five independent experiments.

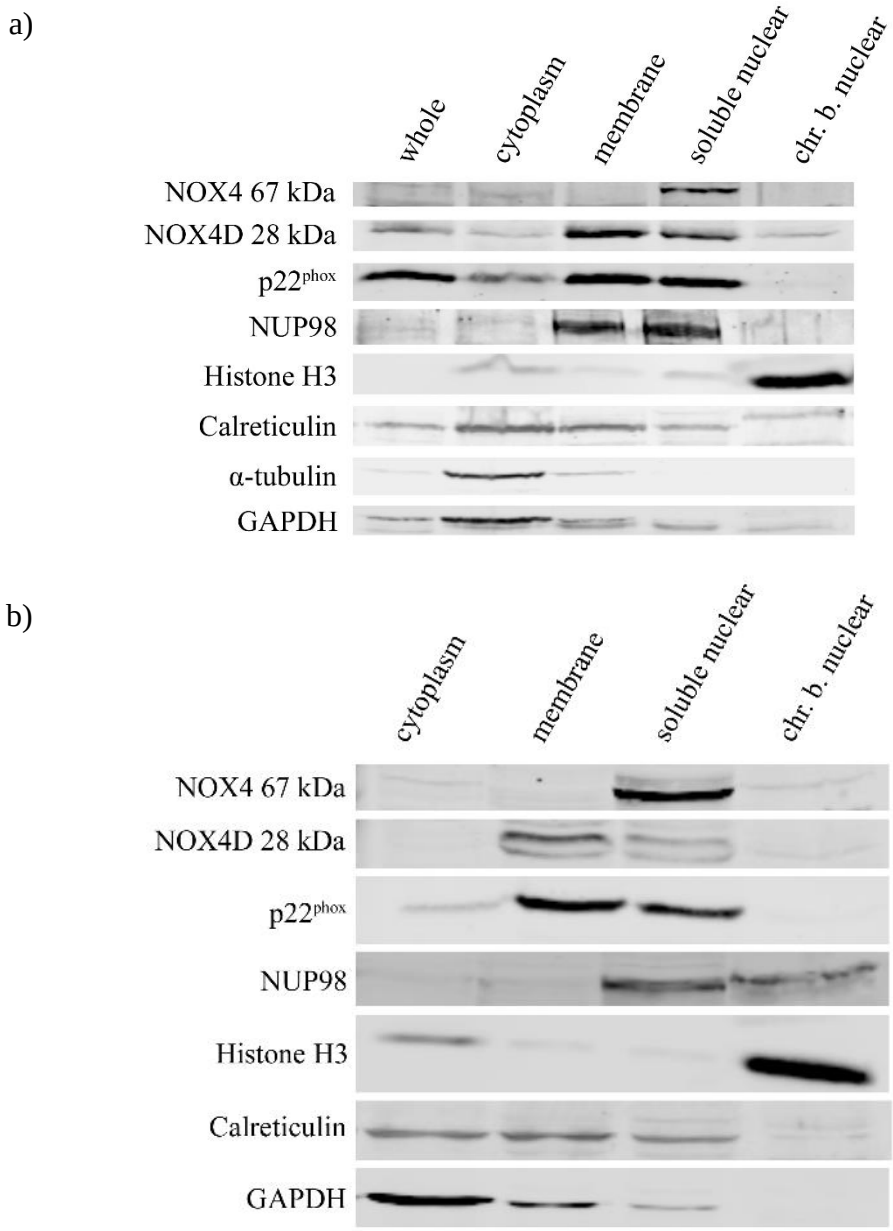

Figure 5.4. FLT3-ITD expressing AML MV4-11 cells express the NOX4D 28 kDa isoform. Subcellular fractionation was carried out in FLT3-ITD expressing AML cell line, MV4-11, using a subcellular fractionation kit. Expression of NOX4 67 kDa, NOX4D 28 kDa and $p22^{phox}$ was assessed by means of western blot analysis *(a and b)*. Subcellular fractionation technique was optimised from *(a)* to *(b)* in order to obtain higher protein concentrations and cleaner fractions. Equal loading of samples and verification of the subcellular fractions were demonstrated by probing for nuclear-localised NUP98 and Histone H3, membrane-localised calreticulin and cytosolic-localised GAPDH and α-tubulin. Western blots are representative of five independent experiments.

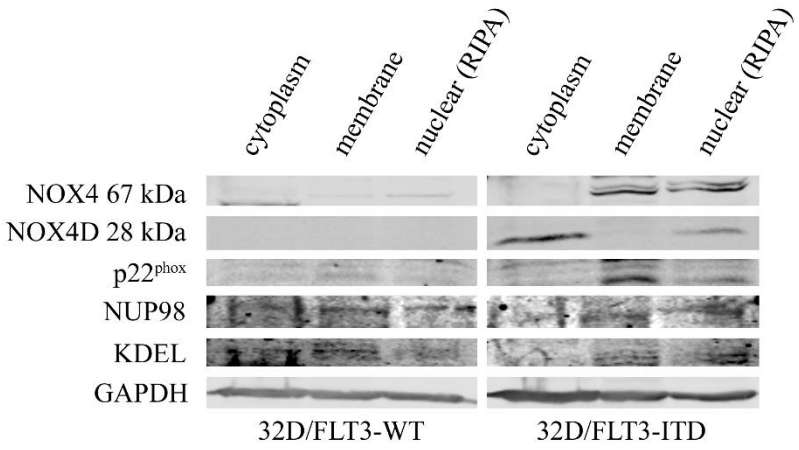

Figure 5.5. FLT3-ITD expressing 32D cells express the NOX4D 28 kDa isoform. Subcellular fractionation was carried out in 32D cells transfected with FLT3-WT or FLT3-ITD using a subcellular fractionation kit and RIPA lysis buffer. Expression of NOX4 67 kDa, NOX4D 28 kDa and $p22^{phox}$ was assessed by means of western blot analysis. Equal loading of samples and verification of the subcellular fractions were demonstrated by probing for nuclear-localised NUP98, membrane-localised KDEL and cytosolic-localised GAPDH. Western blots are representative of five independent experiments.

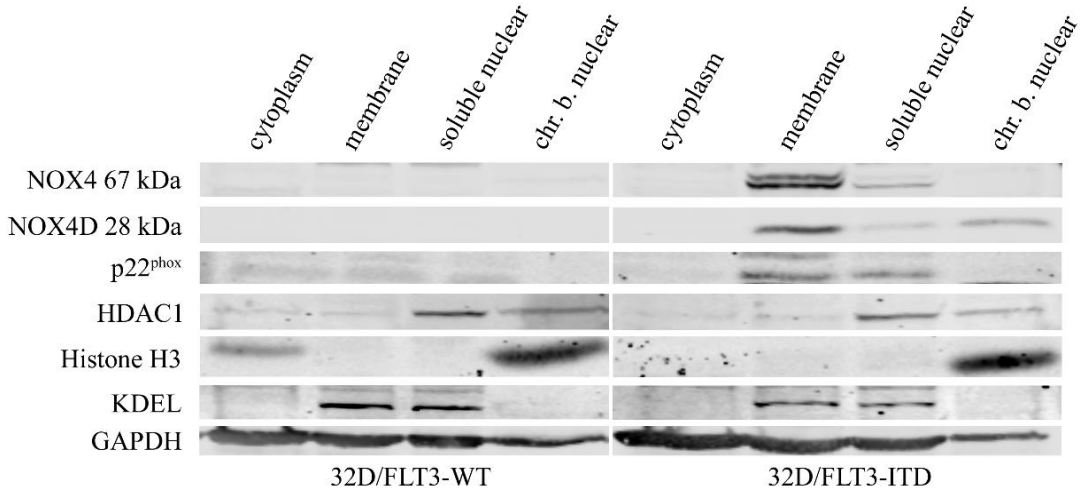

Figure 5.6. FLT3-ITD expressing 32D cells express the NOX4D 28 kDa isoform. Subcellular fractionation was carried out in 32D cells transfected with FLT3-WT or FLT3-ITD using a subcellular fractionation kit. Expression of NOX4 67 kDa, NOX4D 28 kDa and $p22^{phox}$ was assessed by means of western blot analysis. Equal loading of samples and verification of the subcellular fractions were demonstrated by probing for nuclear-localised HDAC1 and Histone H3, membrane-localised KDEL and cytosolic-localised GAPDH. Western blots are representative of five independent experiments.

5.3.4. Specificity of Novus Biologicals NOX4 (NB110-58849) antibody

As mentioned previously, studies have raised issues with NOX4 antibody specificity in the past. Therefore, a key issue concerned the use of the Novus Biologicals NOX4 (NB110-58849) antibody in our study. For this reason, a series of control experiments were first performed to validate the Novus Biologicals (NB110-58849) NOX4 antibody employed in this study.

The Abcam NOX4 (Ab109225) antibody was employed for the primary FLT3-ITD expressing AML patients studies. The remainder of the experiments in this study employed the Novus Biologicals NOX4 antibody (NB110-58849). In order to demonstrate specificity of this antibody for NOX4 67 kDa, HEK-293-T cells were transfected with empty vector (EV)-HA or p-CMV3-C-HA encoding full length cDNA clone of *Homo sapiens* NOX4 (#HG15189-CY; Sino Biological, UK) and were analysed 48 h post transfection by western blot. NOX4 overexpression in HEK 293-T cells resulted in increased NOX4 67 kDa protein expression in the presence of HA protein expression at the corresponding molecular weight compared to HEK 293-T cells transfected with EV (Figure 5.7.). Unexpectedly, an increase in NOX4D 28 kDa protein expression was also observed.

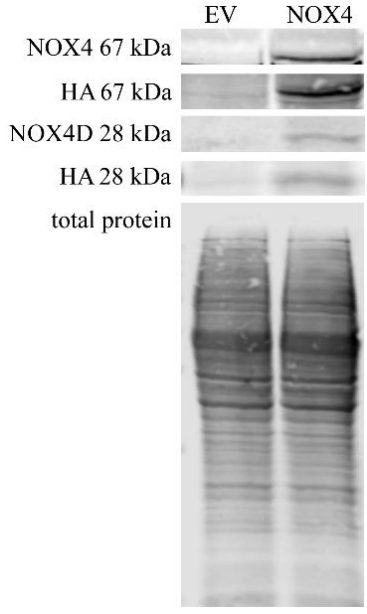

Figure 5.7. Novus Biologicals NOX4 (NB110-58849) antibody specificity. HEK293-T cells were transfected with EV-HA or pCMV3-C-HA encoding full length cDNA clone of *Homo sapiens* NOX4 (#HG15189-CY; Sino Biological, UK) using calcium phosphate. Western blot analysis of NOX4 67 kDa and NOX4D 28 kDa protein levels in HEK 293-T whole cell lysates following transfection with EV-HA or NOX4-HA for 48 h. Total protein (REVERT total protein stain) is shown as a loading control. Western blot is representative of three independent experiments.

5.3.5. 32D cells stably transfected with FLT3-ITD express higher levels of endogenous H_2O_2 compared to FLT3-WT

FLT3-ITD expressing AML cells have been shown to produce elevated levels of ROS and DNA damage compared to their wild-type counterpart (Stanicka et al., 2015). Having confirmed that FLT3-ITD expressing AML patient samples and 32D cells express NOX4D; whereas, FLT3-WT expressing patient samples and 32D cells do not, we investigated the effect of NOX4D expression on total endogenous H_2O_2. We demonstrate that 32D cells stably transfected with FLT3-ITD produced approximately 170% more endogenous H_2O_2 than 32D cells stably transfected with FLT3-WT receptor, as assessed with a H_2O_2 specific probe-PO1 (Figure 5.8.).

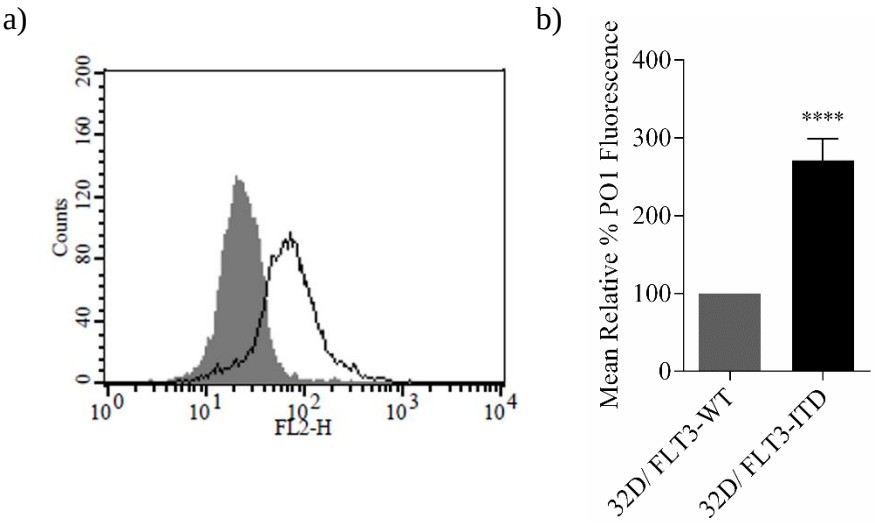

Figure 5.8. 32D cells stably transfected with FLT3-ITD express higher levels of endogenous H_2O_2 compared to FLT3-WT. 32D cells transfected with FLT3-WT and FLT3-ITD were IL-3 starved overnight, followed by ROS visualisation with H_2O_2 specific probe, Peroxy Orange 1 (PO1), for 1 h before flow cytometric analysis *(a)*. Bar chart shows relative mean PO1 fluorescence of 32D/FLT3-ITD cells expressed as a % of 32D/FLT3-WT cells *(b)*. Results are presented as mean ± SD from three independent experiments. Asterisks indicate statistically significant differences (****$p<0.0001$) as analysed by Student's t-test.

5.3.6. p22^{phox} knockdown had no effect on NOX4 67 kDa and NOX4D 28 kDa protein levels

p22^{phox} is a partner protein and is required for functionally active NOX1-4 (Ambasta et al., 2004). Specific p22^{phox} knockdown allowed us to investigate the effects of p22^{phox} on NOX4 67 kDa and NOX4D 28 kDa protein levels. Knockdown of p22^{phox} had no effect on NOX4 67 kDa and NOX4D 28 kDa protein levels (Figure 5.9.).

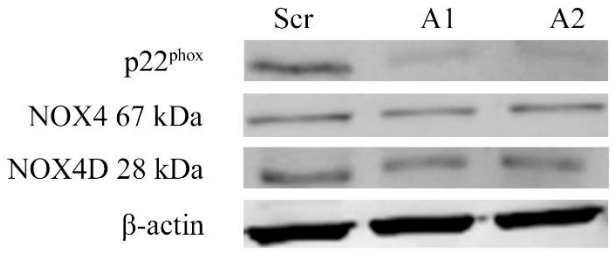

Figure 5.9. Knockdown of p22^{phox} in FLT3-ITD expressing MV4-11 cells had no effect on NOX4 67 kDa and NOX4D 28 kDa protein levels. Western blot analysis of p22^{phox}, NOX4 67 kDa and NOX4D 28 kDa protein levels in MV4-11 whole cell lysates at 24 h following p22^{phox} siRNA transfection compared with the scrambled (Scr) siRNA treated control. A non-targeting scrambled siRNA was utilised as a negative control. β-actin is shown as a loading control. Western blot is representative of three independent experiments.

5.3.7. Inhibition of glycosylation in MV4-11 cell line resulted in NOX4 67 kDa and NOX4D 28 kDa deglycosylation

Previous studies in our laboratory have found NOX4 67 kDa to be glycosylated in FLT3-ITD expressing AML MV4-11 cells (Figure 3.25.) (Moloney et al., 2017b). We investigated if NOX4D 28 kDa is glycosylated in the MV4-11 cell line. Cells were treated with glycosylation inhibitor, tunicamycin and receptor trafficking inhibitor,

brefeldin A. Treatment of MV4-11 cells with glycosylation and receptor trafficking inhibitors resulted in deglycosylation of NOX4D 28 kDa as seen by the presence of a lower molecular weight band marked by asterisks (Figure 5.10.).

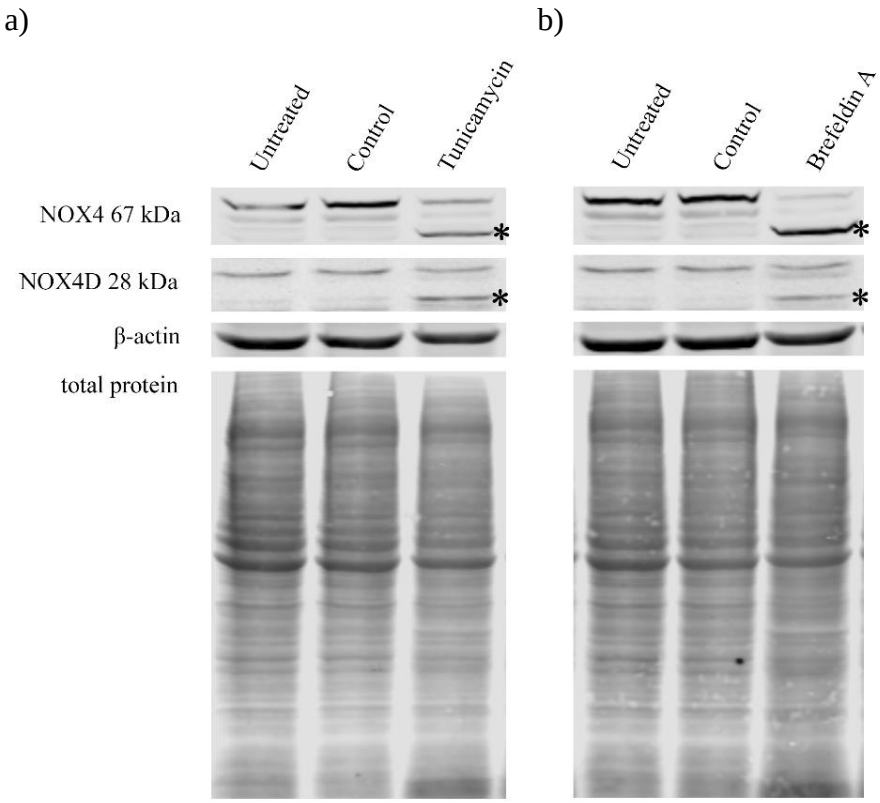

Figure 5.10. NOX4D 28 kDa is glycosylated in FLT3-ITD expressing AML. Western blot analysis of NOX4 67 kDa and NOX4D 28 kDa protein levels in whole cell lysates following treatment with tunicamycin (5 μg/ml) *(a)* and brefeldin A (10 μg/ml) *(b)* overnight. (Asterisks indicate a shift in protein molecular weight). β-actin and total protein (REVERT total protein stain) are shown as loading controls. Western blots are representative of three independent experiments.

5.3.8. Inhibition of FLT3-ITD in MV4-11 cell line and 32D cells transfected with FLT3-ITD causes a decrease in NOX4 67 kDa and NOX4D 28 kDa protein levels as well as reductions in total endogenous H_2O_2

32D cells transfected with FLT3-ITD and FLT3-WT receptor, in addition to MV4-11 cells, were treated with FLT3-ITD inhibitor, PKC412. The inhibition of FLT3 receptor resulted in a decrease in total endogenous H_2O_2 in 32D/FLT3-ITD cells, but not in 32D/FLT3-WT cells. As shown previously in Figure 5.8. 32D/FLT3-ITD cells possess approximately 170% more total endogenous H_2O_2 compared to their wild-type counterpart. Moreover, inhibition of FLT3 resulted in approximately 40% decrease in total endogenous H_2O_2 following treatment with 50 nM and 200 nM PKC412 specifically in 32D cells expressing the FLT3-ITD mutation and not in cells expressing FLT3-WT receptor (Figure 5.11.).

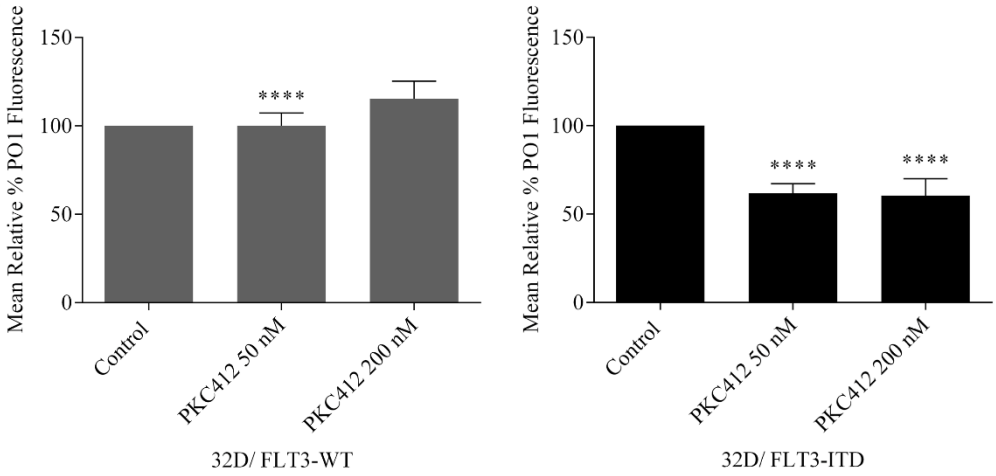

Figure 5.11. Inhibition of the FLT3 receptor following treatment with PKC412, results in a decrease in total endogenous H_2O_2 in 32D/FLT3-ITD cells but not in 32D/FLT3-WT cells. 32D/FLT3-WT and 32D/FLT3-ITD cells were IL-3 starved overnight and treated for 24 h with PKC412 (50 nM and 200 nM), followed by staining with H_2O_2 specific probe PO1 for 1 h before FACS reading. Bar charts show relative mean PO1 fluorescence of treated cells expressed as % of vehicle control (control). Results are presented as mean ± SD from four independent experiments. Asterisks indicate statistically significant differences (****$p<0.0001$) as analysed by Student's t-test.

FLT3-ITD expressing MV4-11 cells were treated with PKC412. Inhibition of the FLT3 receptor in MV4-11 cells resulted in significantly decreased NOX4 67 kDa and NOX4D 28 kDa protein levels in whole cell lysates, significantly decreased $p22^{phox}$ protein levels in the membrane and soluble nuclear fractions (Figure 5.12.) and reduced total endogenous H_2O_2. 50 nM and 200 nM PKC412 treatments resulted in a significant decrease of 45-50% in total endogenous H_2O_2 (Figure 5.13.). The inhibition of FLT3-ITD using AC220, another commonly used and very selective FLT3 receptor inhibitor, resulted in decreased NOX4D 28 kDa protein levels in the nuclear fractions of MV4-11 cells (Figure 5.14. a) and 32D/FLT3-ITD cells (Figure 5.14. b). These results suggest that both FLT3-ITD and NOX4D proteins play a role in the generation of H_2O_2 in MV4-11 and 32D/FLT3-ITD cells and that FLT3-ITD activity is presumably an upstream regulator of NOX4D-generated pro-survival ROS.

In Figure 5.14. Lamin A/C is used as a marker for nuclear fractions. Lamin A/C is cleaved by caspase-6 and serves as a marker of caspase-6 activation. During apoptosis, Lamin A/C is specifically cleaved to a large (40-45 kDa) and a small (28 kDa) fragment. The cleavage of Lamin A/C results in nuclear dysregulation and death.

The Cell Signaling Technology Lamin A/C (2032) antibody employed in this study detects endogenous levels of total full length Lamin A (and Lamin C) (70 kDa), as well as the small (28 kDa) fragment of Lamin A (and Lamin C) resulting from cleavage at aspartic acid 230.

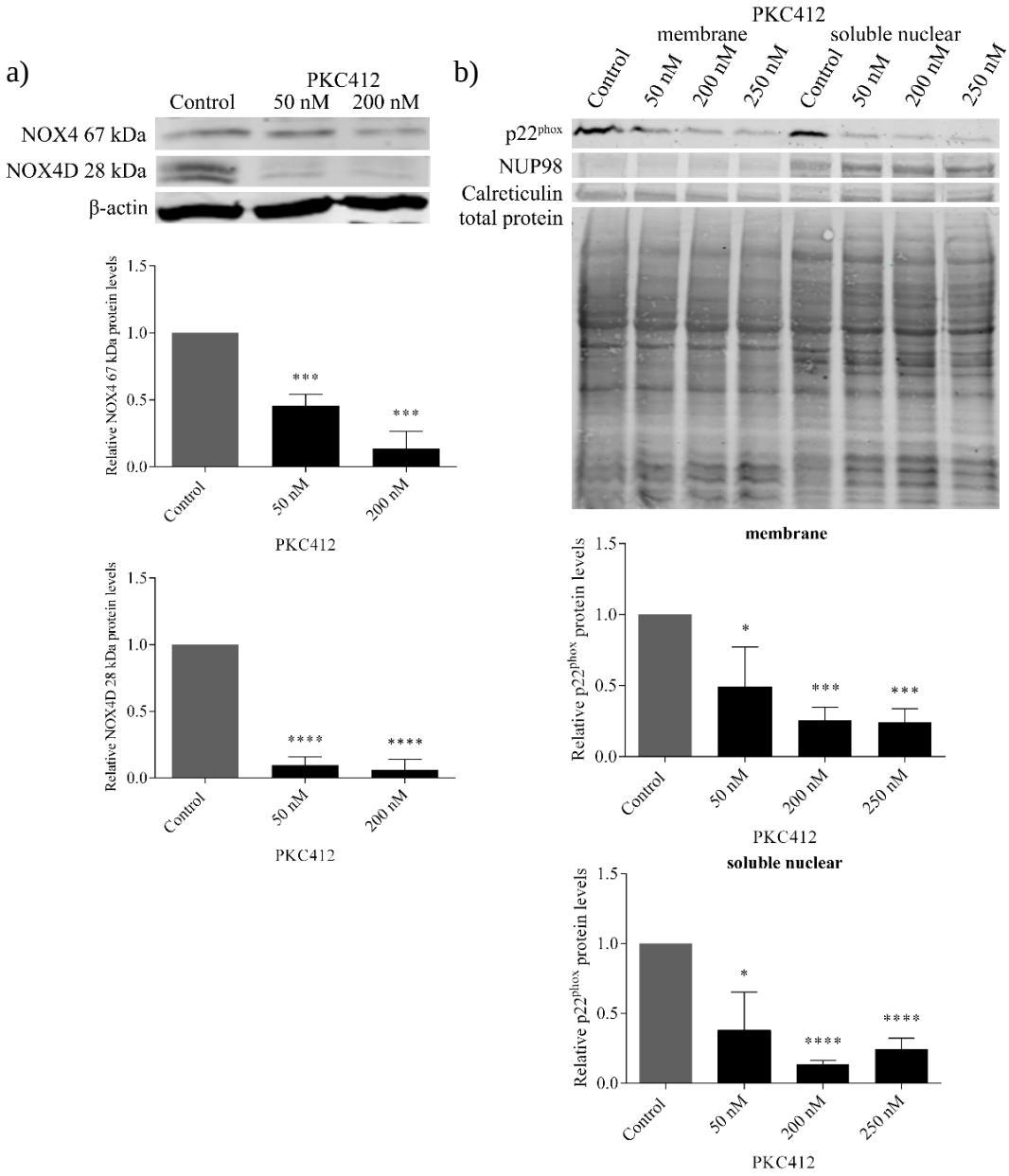

Figure 5.12. Inhibition of the FLT3 receptor using PKC412 in FLT3-ITD expressing MV4-11 cells reduces NOX4 67 kDa, NOX4D 28 kDa and p22^{phox} protein levels. Western blot analysis of NOX4 67 kDa and NOX4D 28 kDa protein levels in MV4-11 whole cell lysates following treatment with PKC412 (50 nM and 200 nM) for 24 h *(a)*. β-actin is shown as a loading control. p22^{phox} protein levels in membrane and soluble nuclear fractions of MV4-11 cells following treatment with PKC412 (50 nM, 200 nM and 250 nM) for 24 h *(b)*. Equal loading of samples is shown by total protein (REVERT total protein stain) and verification of subcellular fractions were assessed by probing for nuclear-localised NUP98 and membrane-localised calreticulin. Bar charts show relative mean NOX4 67 kDa and NOXD 28 kDa protein levels in whole cell lysates *(a)* and p22^{phox} protein levels in membrane and soluble nuclear fractions *(b)* following treatment with PKC412 for 24 h at indicated concentrations as quantified by densitometry. The data are expressed as % of vehicle control (control), where the ratio in the control was defined as 1. Results are presented as mean ± SD from three independent experiments. Asterisks indicate statistically significant differences (*p<0.05, ***p<0.001, ****p<0.0001) as analysed by Student's t-test.

a)

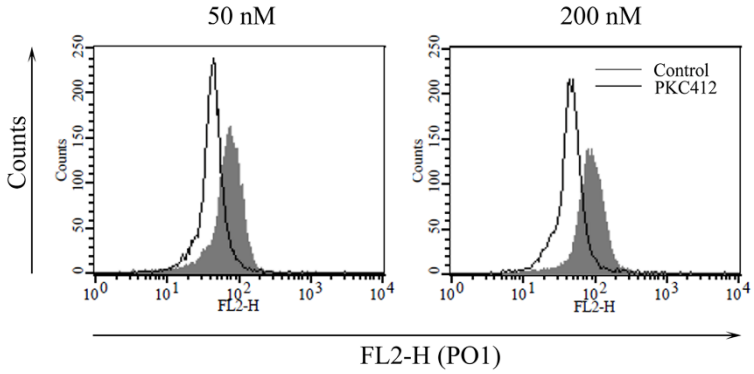

b)

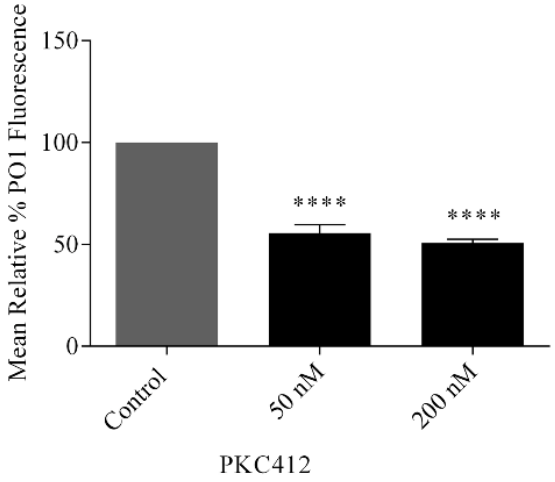

Figure 5.13. Inhibition of the FLT3 receptor in FLT3-ITD expressing MV4-11 cells reduces total endogenous H_2O_2. Flow cytometric analysis of mean relative PO1 fluorescence in MV4-11 cells treated with PKC412 (50 nM and 200 nM) for 24 h *(a)*. Bar chart shows relative mean PO1 fluorescence of treated cells expressed as % of vehicle control (control) *(b)*. Results are presented as mean ± SD from three independent experiments. Asterisks indicate statistically significant differences (****$p<0.0001$) as analysed by Student's t-test.

a)

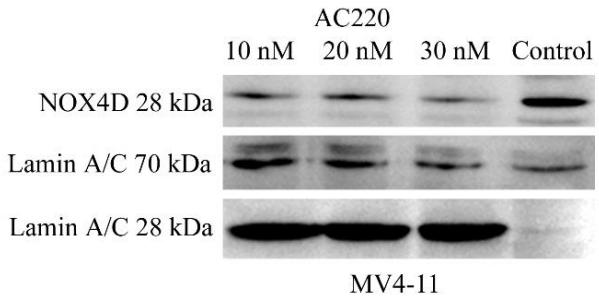

b)

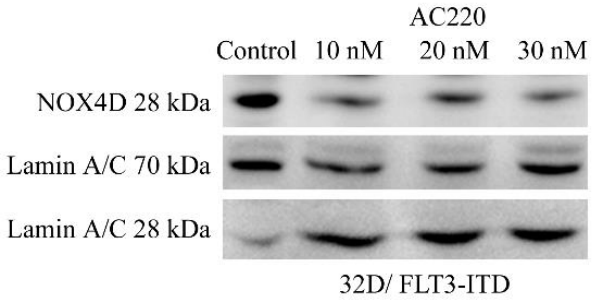

Figure 5.14. Inhibition of the FLT3 receptor using AC220 in FLT3-ITD expressing MV4-11 cells and 32D/FLT3-ITD cells reduces NOX4D 28 kDa protein levels. Western blot analysis of NOX4D 28 kDa protein levels in the nuclear fraction following treatment with AC220 (10 nM, 20 nM and 30 nM) for 12 h in MV4-11 cells *(a)* and 32D cells transfected with FLT3-ITD *(b)*. Equal loading of nuclear fractions was demonstrated by probing for nuclear-localised Lamin A/C. Western blots are representative of three independent experiments. Figure courtesy of Dr Ashok Kumar Jayavelu.

5.3.9. Inhibition of the FLT3 receptor in the MOLM13 cell line causes a decrease in NOX4D 28 kDa protein levels

Patient-derived AML MV4-11 and MOLM13 (heterozygous for the FLT3-ITD mutation) cells both harbour endogenously expressing FLT3-ITD. To further validate the dependence of NOX4D expression on the activation of FLT3-ITD signalling, we treated MOLM13 cells, heterozygous for FLT3-ITD mutation with the selective FLT3-ITD kinase inhibitor, AC220 (5 nM, 10 nM, 20 nM and 30 nM) for 12 h. Inhibition of the FLT3 receptor resulted in decreased NOX4D protein levels (Figure 5.15.).

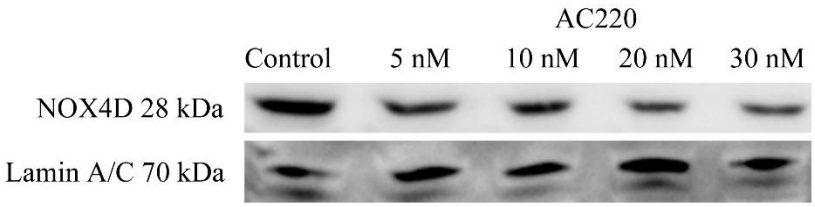

Figure 5.15. Inhibition of the FLT3 receptor using AC220 in MOLM13 cells reduces NOX4D 28 kDa protein levels. Western blot analysis of NOX4D 28 kDa protein levels in the nuclear fraction of MOLM13 cells following treatment with AC220 (5 nM, 10 nM, 20 nM and 30 nM) for 12 h. Equal loading of nuclear fractions was demonstrated by probing for nuclear-localised Lamin A/C. Western blot is representative of three independent experiments. Figure courtesy of Dr Ashok Kumar Jayavelu.

5.3.10. PI3K/AKT pathway is required for FLT3-ITD mediated-NOX4 67 kDa and -NOX4D 28 kDa generation of pro-survival H_2O_2

Constitutively activated FLT3-ITD kinase stimulates aberrant proliferative signalling through downstream signalling pathways including PI3K/AKT, ERK1/2, STAT5 and GSK3β (Figure 4.10.). We have shown previously that NOX4- and $p22^{phox}$-generated pro-survival ROS require AKT activation in MV4-11 cells (Figure 4.5.) (Moloney et al., 2017b). Therefore, we examined the effect of PI3K/AKT inhibition on NOX4D 28 kDa protein levels in membrane and soluble nuclear fractions of MV4-11 cells. Inhibition of AKT signalling (Figure 5.16. (i) a and Figure 5.16. (ii)) using PI3K inhibitor, LY294002, resulted in slight decreases in NOX4 67 kDa and more noticeable decreases in NOX4D 28 kDa and $p22^{phox}$ protein levels in the soluble nuclear fraction (Figure 5.16. (i) b). The observed decreases were statistically significant (Figure 5.16. (ii)). As shown, NOX4D 28 kDa protein levels are weak in the membrane fraction and it is therefore difficult to detect any change. We next examined the effect of AKT inhibition on the generation of total endogenous H_2O_2. AKT inhibition resulted in approximately 25% decrease in total endogenous H_2O_2 following treatment with 20 μM and 30 μM LY294002 and approximately 35% decrease following treatment with 50 μM LY294002 (Figure 5.16. (i) c and d). Thus, activation of the AKT pathway is required for FLT3-ITD to produce NOX4D-generated ROS.

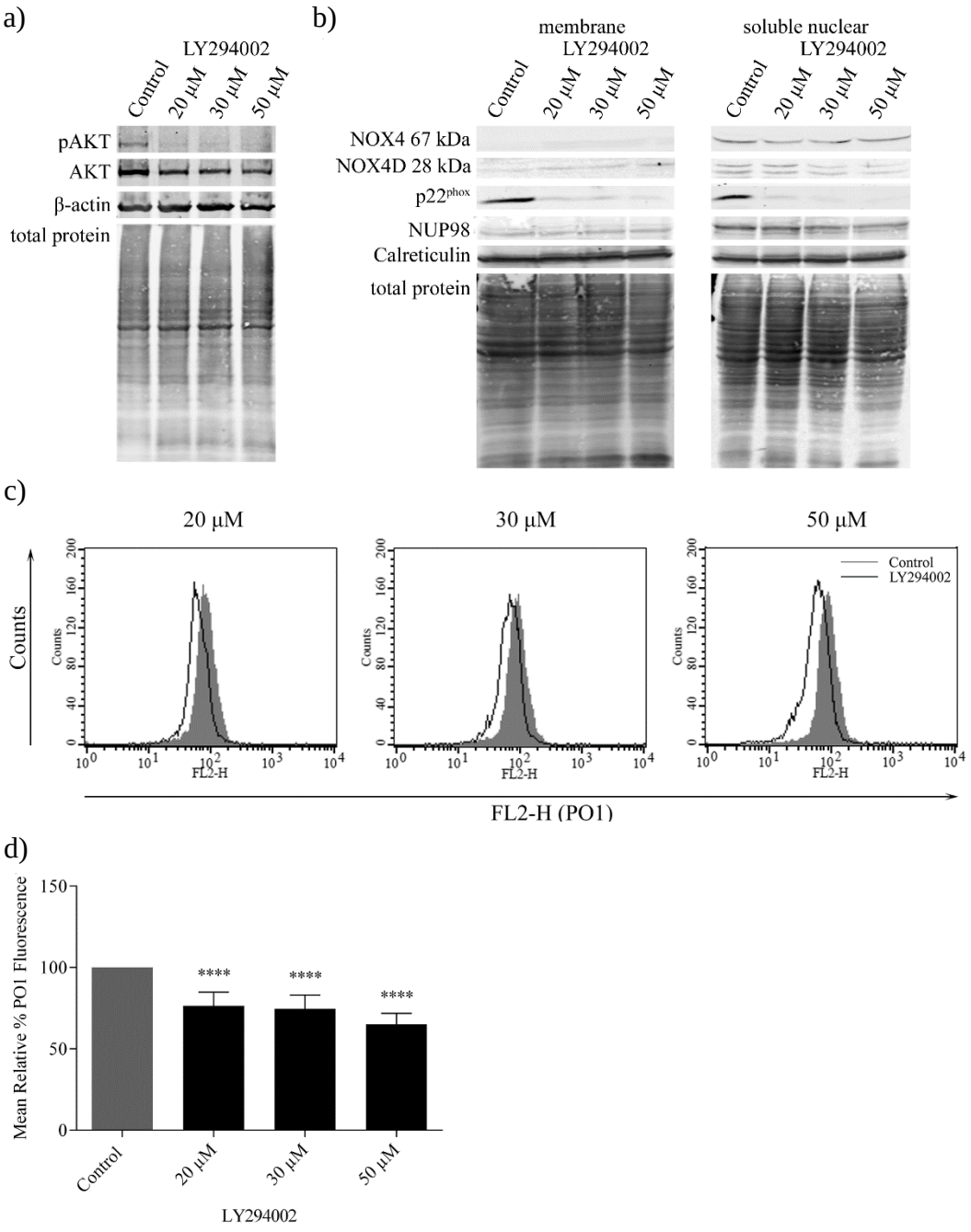

Figure 5.16. (i) NOX4 67 kDa- and NOX4D 28 kDa-generated pro-survival ROS require AKT activation. Western blot analysis of AKT signalling in FLT3-ITD expressing MV4-11 cells following treatment with LY294002 (20 μM, 30 μM and 50 μM) for 16 h *(a)*. β-actin and total protein (REVERT total protein stain) are shown as loading controls. NOX4 67 kDa, NOX4D 28 kDa and $p22^{phox}$ protein levels in membrane and soluble nuclear fractions of MV4-11 cells following treatment with LY294002 for 16 h at indicated concentrations *(b)*. Equal loading of samples is shown by total protein (REVERT total protein stain) and verification of subcellular fractions were assessed by probing for nuclear-localised NUP98 and membrane-localised calreticulin. Western blot analysis is representative of three independent experiments. Flow cytometric analysis of mean relative PO1 fluorescence in MV4-11 cells treated with LY294002 for 16 h at indicated concentrations *(c)*. Bar chart shows relative mean PO1

fluorescence of treated cells expressed as % of vehicle control (control) *(d)*. Results are presented as mean ± SD from three independent experiments. Asterisks indicate statistically significant differences (****$p<0.0001$) as analysed by Student's t-test.

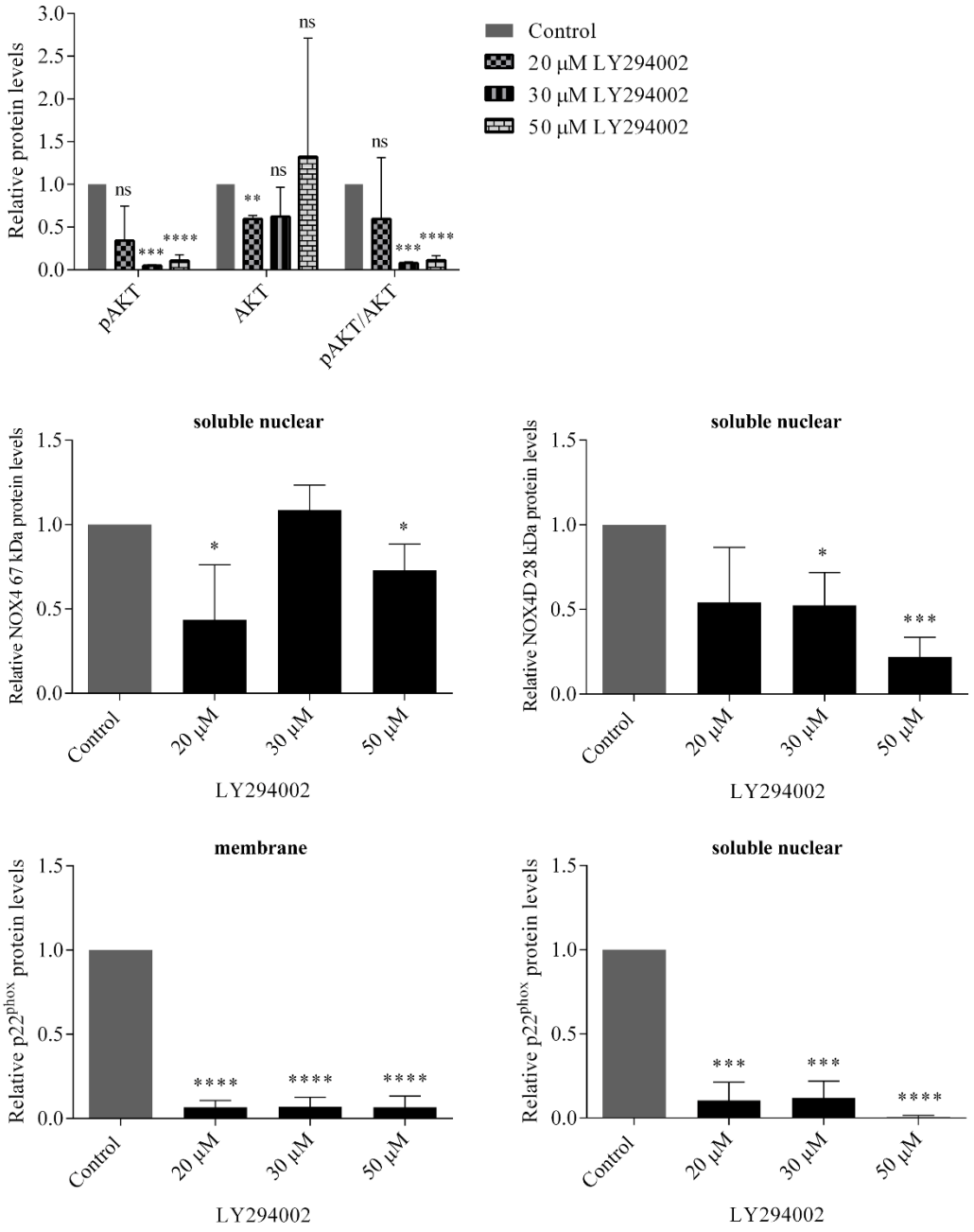

Figure 5.16. (ii) NOX4 67 kDa- and NOX4D 28 kDa-generated pro-survival ROS require AKT activation. Bar charts show relative mean pAKT, AKT and pAKT/AKT protein levels in whole cell lysates and NOX4 67 kDa, NOX4D 28 kDa and $p22^{phox}$ protein levels in membrane and soluble nuclear fractions following treatment with LY294002 (20 µM, 30 µM and 50 µM) for 16 h as quantified by densitometry. The data are expressed as % of vehicle control (control), where the ratio in the control was defined as 1. Results are presented as mean ± SD from three independent experiments. Asterisks indicate statistically significant differences (*$p<0.05$, **$p<0.05$, ***$p<0.001$, ****$p<0.0001$) as analysed by Student's t-test.

5.3.11. NOX4 67 kDa- and NOX4D 28 kDa-generated pro-survival ROS are independent of ERK1/2 signalling however $p22^{phox}$-mediated H_2O_2 production requires ERK1/2 activation

The ERK1/2 pathway is known to be activated downstream of constitutively activated FLT3-ITD. We investigated the effect of ERK1/2 signalling inhibition using U0126 in MV4-11 cells (Figure 5.17. (i) a and Figure 5.17. (ii)) on NOX4D 28 kDa protein levels. Inhibition of ERK1/2 signalling did not cause a significant decrease in NOX4 67 kDa and NOX4D 28 kDa protein levels when compared to control, however, $p22^{phox}$ protein levels decreased significantly following treatment with 100 μM U0126 (Figure 5.17. (i) b and Figure 5.17. (ii)). This suggests that NOX4 67 kDa- and NOX4D 28 kDa-generated pro-survival ROS are independent of ERK1/2 signalling. A decrease of 40-45% in total endogenous H_2O_2 was observed following treatment with 50 μM and 100 μM U0126 (Figure 5.17. (i) c and d).

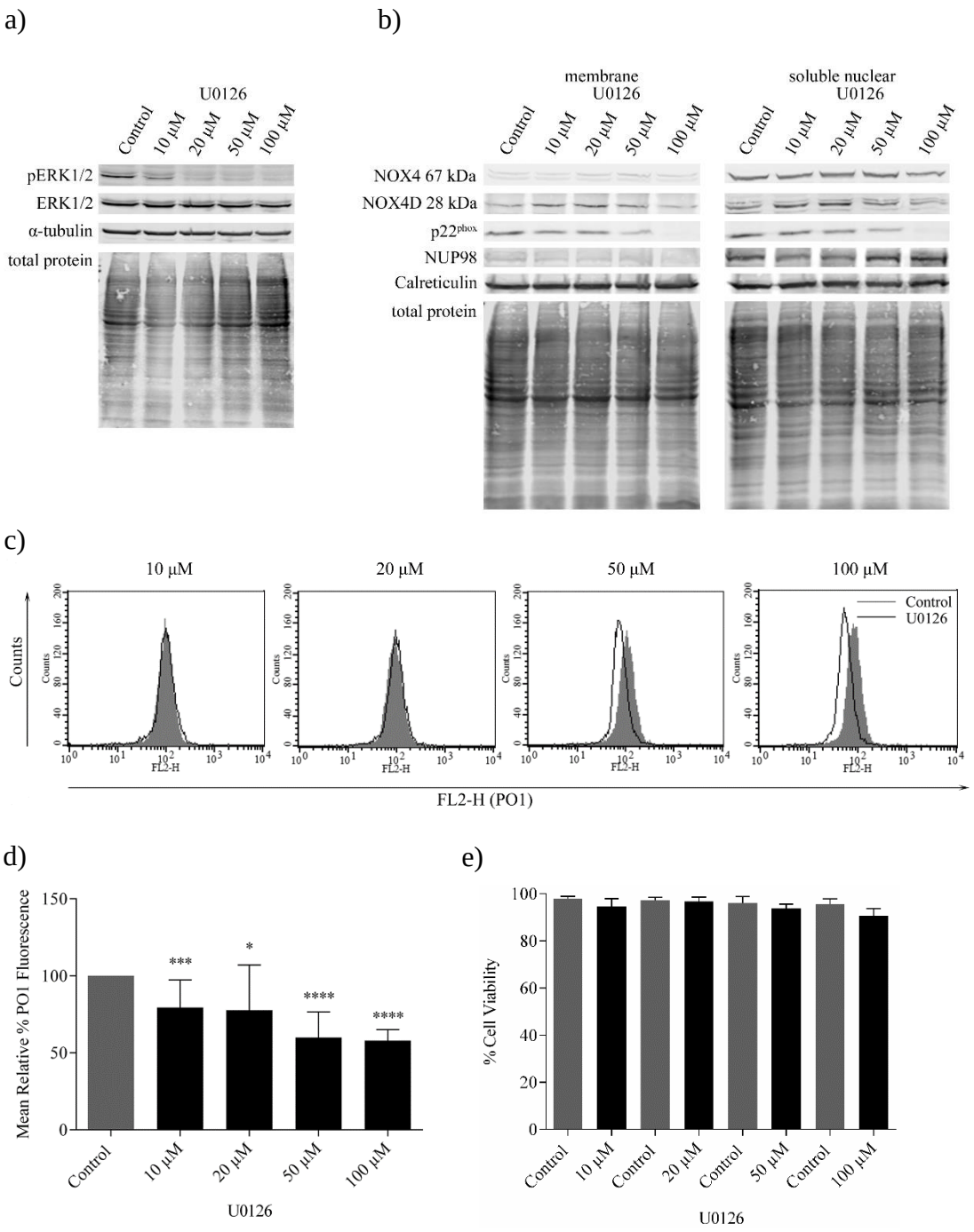

Figure 5.17. (i) NOX4 67 kDa- and NOX4D 28 kDa-generated pro-survival ROS are independent of ERK1/2 signalling. p22^{phox}-generated H_2O_2 requires ERK1/2 activation. Western blot analysis of ERK1/2 signalling in FLT3-ITD expressing MV4-11 cells following treatment with U0126 (10 μM, 20 μM, 50 μM and 100 μM) for 16 h. α-tubulin and total protein (REVERT total protein stain) are shown as loading controls *(a)*. NOX4 67 kDa, NOX4D 28 kDa and p22^{phox} protein levels in membrane and soluble nuclear fractions of MV4-11 cells following treatment with U0126 for 16 h at indicated concentrations *(b)*. Equal loading of samples is shown by total protein (REVERT total protein stain) and verification of subcellular fractions was assessed by probing for nuclear-localised NUP98 and membrane-localised calreticulin. Western blot analysis is representative of three independent experiments. Flow cytometric analysis of mean relative PO1 fluorescence in MV4-11 cells treated with

U0126 for 16 h at indicated concentrations *(c)*. Bar chart shows relative mean PO1 fluorescence of treated cells expressed as % of vehicle control (control) *(d)*. Results are presented as mean ± SD from four independent experiments. Asterisks indicate statistically significant differences (*$p<0.05$, ***$p<0.001$, ****$p<0.0001$) as analysed by Student's t-test. Bar chart of % cell viability following treatment with the indicated concentrations of U0126 compared to vehicle controls (N=2) *(e)*.

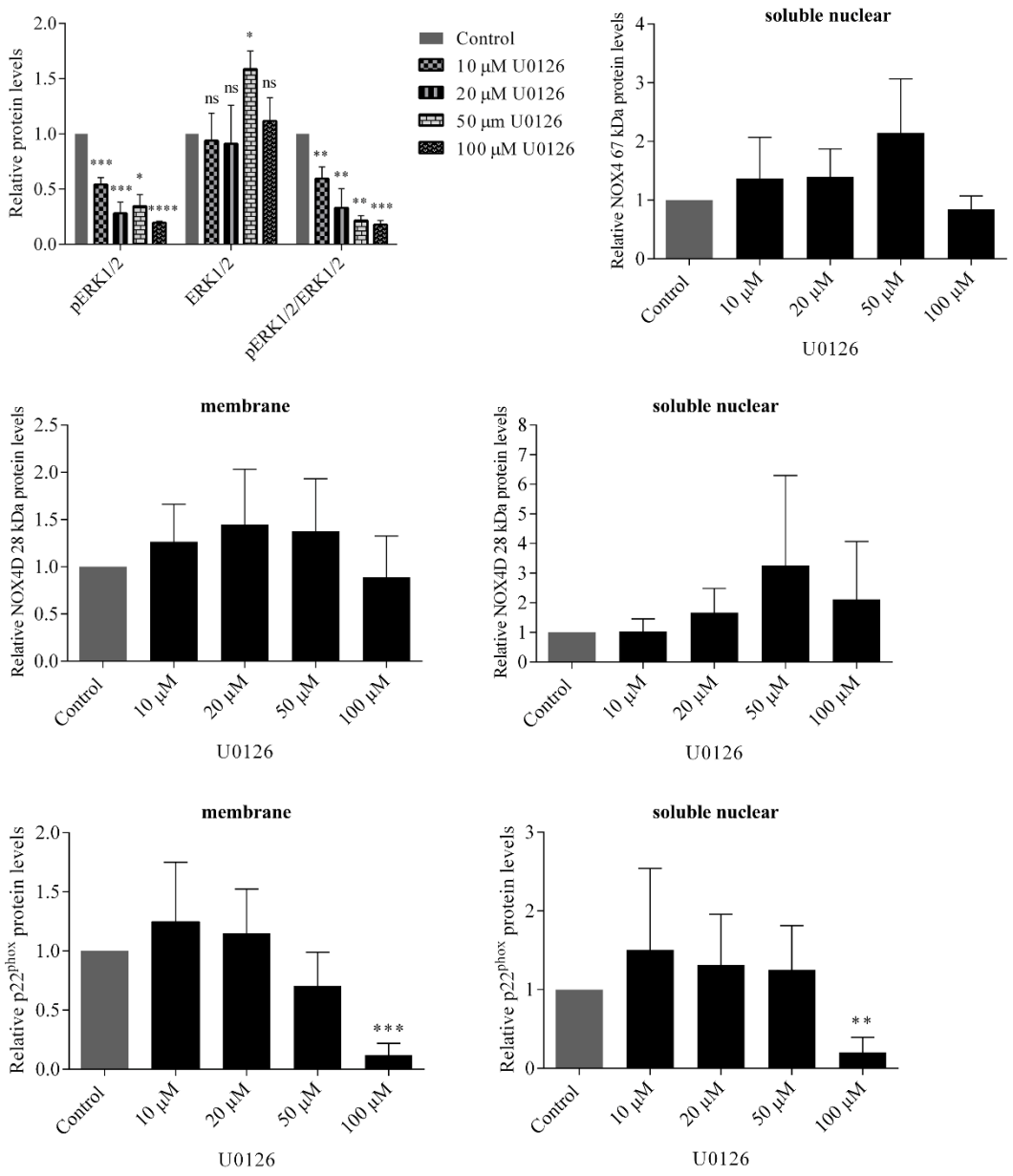

Figure 5.17. (ii) NOX4 67 kDa- and NOX4D 28 kDa-generated pro-survival ROS are independent of ERK1/2 signalling. p22^{phox}-generated H_2O_2 requires ERK1/2 activation. Bar charts show relative mean pERK1/2, ERK1/2 and pERK1/2/ERK1/2 protein levels in whole cell lysates and NOX4 67 kDa, NOX4D 28 kDa and p22^{phox} protein levels in membrane and soluble nuclear fractions following treatment with U0126 (10 µM, 20 µM, 50 µM and 100 µM) for 16 h as quantified by densitometry. The data are expressed as % of vehicle control (control), where the ratio in the control was defined as 1. Results are presented as mean ± SD from three independent experiments. Asterisks indicate statistically significant differences (*p<0.05, **p<0.01, ***p<0.001, ****p<0.0001) as analysed by Student's t-test.

5.3.12. NOX4 67 kDa and NOX4D 28 kDa generate pro-survival ROS downstream of STAT5 signalling

Previous studies have shown that FLT3-ITD drives evident activation of STAT5 signalling compared to FLT3-WT resulting in increased mRNA and protein levels of NOX4 (Jayavelu et al., 2016a, Choudhary et al., 2005b, Grundler et al., 2005). Given that treatment with pimozide clearly reduced NOX4 mRNA in FLT3-ITD expressing MV4-11 cells (Jayavelu et al., 2016a), we investigated the effect of STAT5 inhibition in MV4-11 cells (Figure 5.18. (i) a and Figure 5.18. (ii)) on NOX4D 28 kDa protein levels. Treatment with indicated concentrations of pimozide resulted in a significant decrease in NOX4 67 kDa, NOX4D 28 kDa and $p22^{phox}$ protein levels following treatment with 20 µM pimozide (Figure 5.18. (i) b and Figure 5.18. (ii)). Furthermore, inhibition of STAT5 signalling caused a decrease of 30-40% in total endogenous H_2O_2 at all concentrations (Figure 5.18. (i) c and d), indicating a role for STAT5 signalling in the production of NOX4D-generated pro-survival ROS.

Inhibition of STAT5 signalling had a substantial effect on cell viability at all concentrations, particularly following treatment with 20 µM pimozide (Figure 5.18. (i) e). This can also be seen by the increase in counts (peak) in pimozide treated cells in the flow cytometry histograms (Figure 5.18. (i) c) in order to record 10,000 viable cell counts.

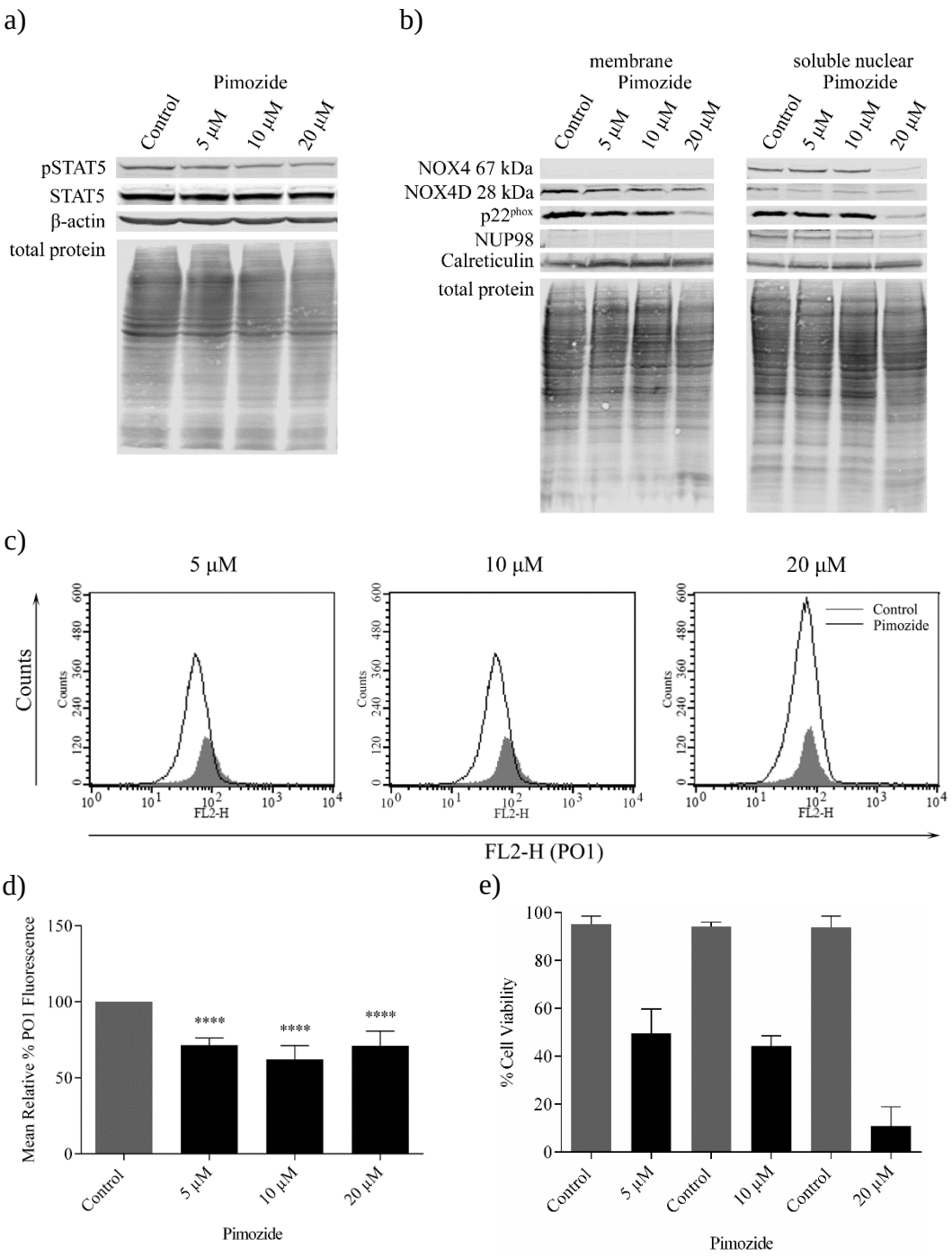

Figure 5.18. (i) NOX4 67 kDa and NOX4D 28 kDa generate H_2O_2 downstream of STAT5 activation. Western blot analysis of STAT5 signalling in FLT3-ITD expressing MV4-11 cells following treatment with pimozide (5 μM, 10 μM and 20 μM) for 16 h *(a)*. β-actin and total protein (REVERT total protein stain) are shown as loading controls. NOX4 67 kDa, NOX4D 28 kDa and $p22^{phox}$ protein levels in membrane and soluble nuclear fractions of MV4-11 cells following treatment with pimozide for 16 h at indicated concentrations *(b)*. Equal loading of samples is shown by total protein (REVERT total protein stain) and verification of subcellular fractions were assessed by probing for nuclear-localised NUP98 and membrane-localised calreticulin. Western blot analysis is representative of three *(a)* or four *(b)* independent experiments. Flow cytometric analysis of mean relative PO1 fluorescence in MV4-11 cells treated with pimozide for 16 h at indicated concentrations

(c). Bar chart shows relative mean PO1 fluorescence of treated cells expressed as % of vehicle control (control) *(d)*. Results are presented as mean ± SD from three independent experiments. Asterisks indicate statistically significant differences (****$p<0.0001$) as analysed by Student's t-test. Bar chart of % cell viability following treatment with the indicated concentrations of pimozide compared to vehicle controls (N=2) *(e)*.

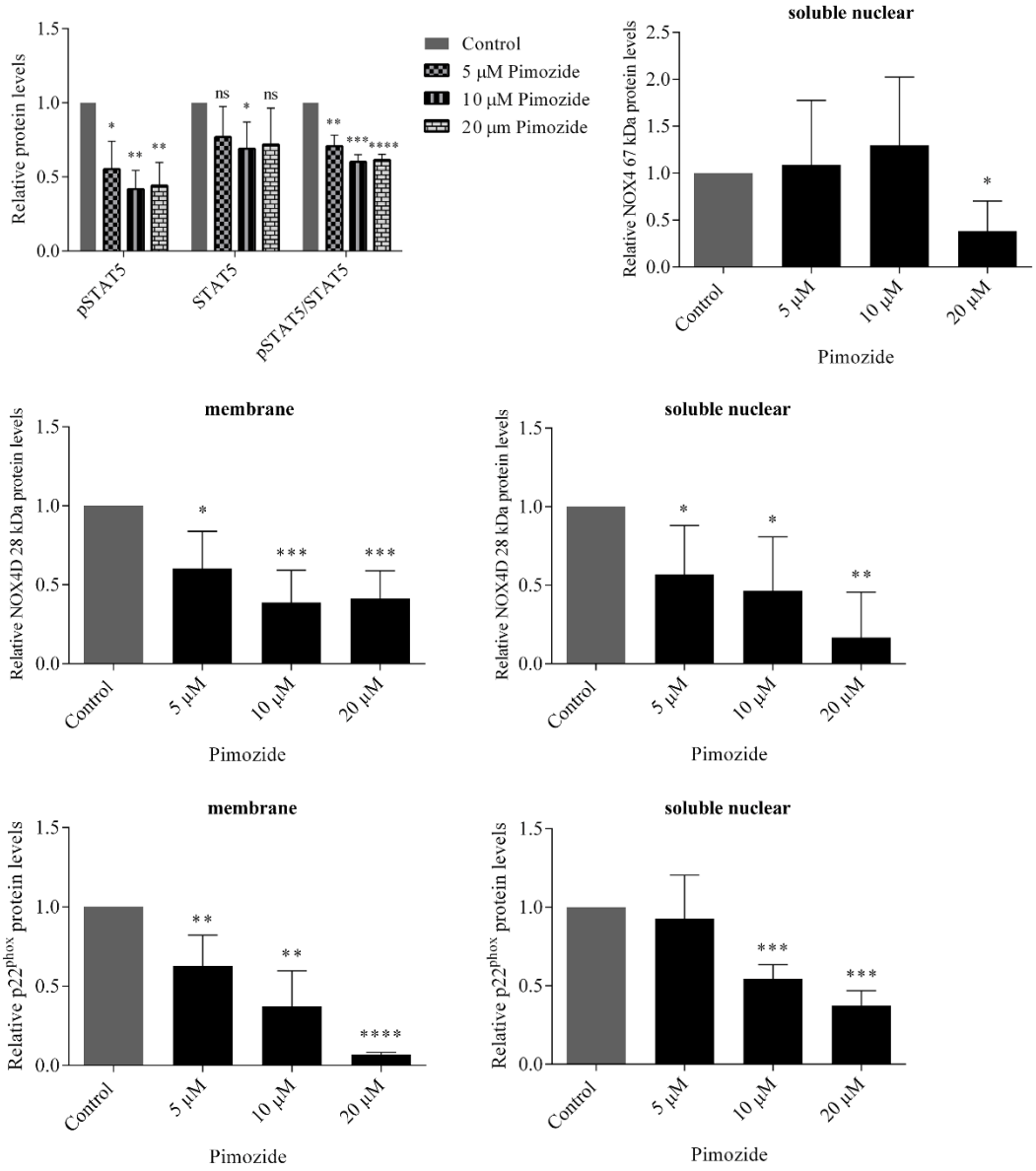

Figure 5.18. (ii) NOX4 67 kDa and NOX4D 28 kDa generate H_2O_2 downstream of STAT5 activation. Bar charts show relative mean pSTAT5, STAT5 and pSTAT5/STAT5 protein levels in whole cell lysates and NOX4 67 kDa, NOX4D 28 kDa and $p22^{phox}$ protein levels in membrane and soluble nuclear fractions following treatment with pimozide (5 μM, 10 μM and 20 μM) for 16 h as quantified by densitometry. The data are expressed as % of vehicle control (control), where the ratio in the control was defined as 1. Results are presented as mean ± SD from three (pSTAT5, STAT5 and pSTAT5/STAT5) or four (NOX4 67 kDa, NOX4D 28 kDa and $p22^{phox}$) independent experiments. Asterisks indicate statistically significant differences (*$p<0.05$, **$p<0.01$, ***$p<0.001$, ****$p<0.0001$) as analysed by Student's t-test.

5.3.13. Inhibition of GSK3β signalling in MV4-11 cell line increases NOX4D 28 kDa protein levels and decreases $p22^{phox}$ protein levels

Previous studies in our laboratory have demonstrated that PKC412-mediated $p22^{phox}$ down-regulation at protein level requires GSK3β activation, establishing a role for GSK3β signalling in post-translational regulation of NOX4 partner protein $p22^{phox}$ (Woolley et al., 2012). SB216763, a drug described as an inhibitor of GSK3β (Dash et al., 2011, Tao et al., 2013) was found to decrease pGSK3β (Ser9) protein levels significantly in MV4-11 cells, therefore resulting in the activation of GSK3β signalling (Figure 5.19. (i) a and Figure 5.19. (ii)).Treatment of MV4-11 cells with indicated concentrations of SB216763 showed no obvious effect on NOX4 67 kDa, NOX4D 28 kDa and $p22^{phox}$ protein levels in membrane and soluble nuclear fractions (Figure 5.19. (i) b and Figure 5.19. (ii)). However, activation of GSK3β signalling increased total endogenous H_2O_2 by 45-50% following treatment with 1 µM and 2 µM SB216763 and approximately 40% following treatment with 5 µM SB216763 (Figure 5.19. (i) c and d). Lithium chloride (LiCl) is widely used as a GSK3β inhibitor (Cohen and Goedert, 2004). Inhibition of GSK3β using LiCl caused an increase in pGSK3β (Ser9) protein levels (Figure 5.20. (i) a and Figure 5.20. (ii)) in MV4-11 cells, indicative of inhibition of the pathway. This increase coincided with a significant increase in NOX4D 28 kDa protein levels in membrane and soluble nuclear fractions. Interestingly, $p22^{phox}$ protein levels decreased significantly following treatment with 50 mM LiCl in both membrane and soluble nuclear fractions (Figure 5.20. (i) b and Figure 5.20. (ii)). Inhibition of GSK3β activation had little or no effect on total endogenous H_2O_2 levels (Figure 5.20. (i) c and d).

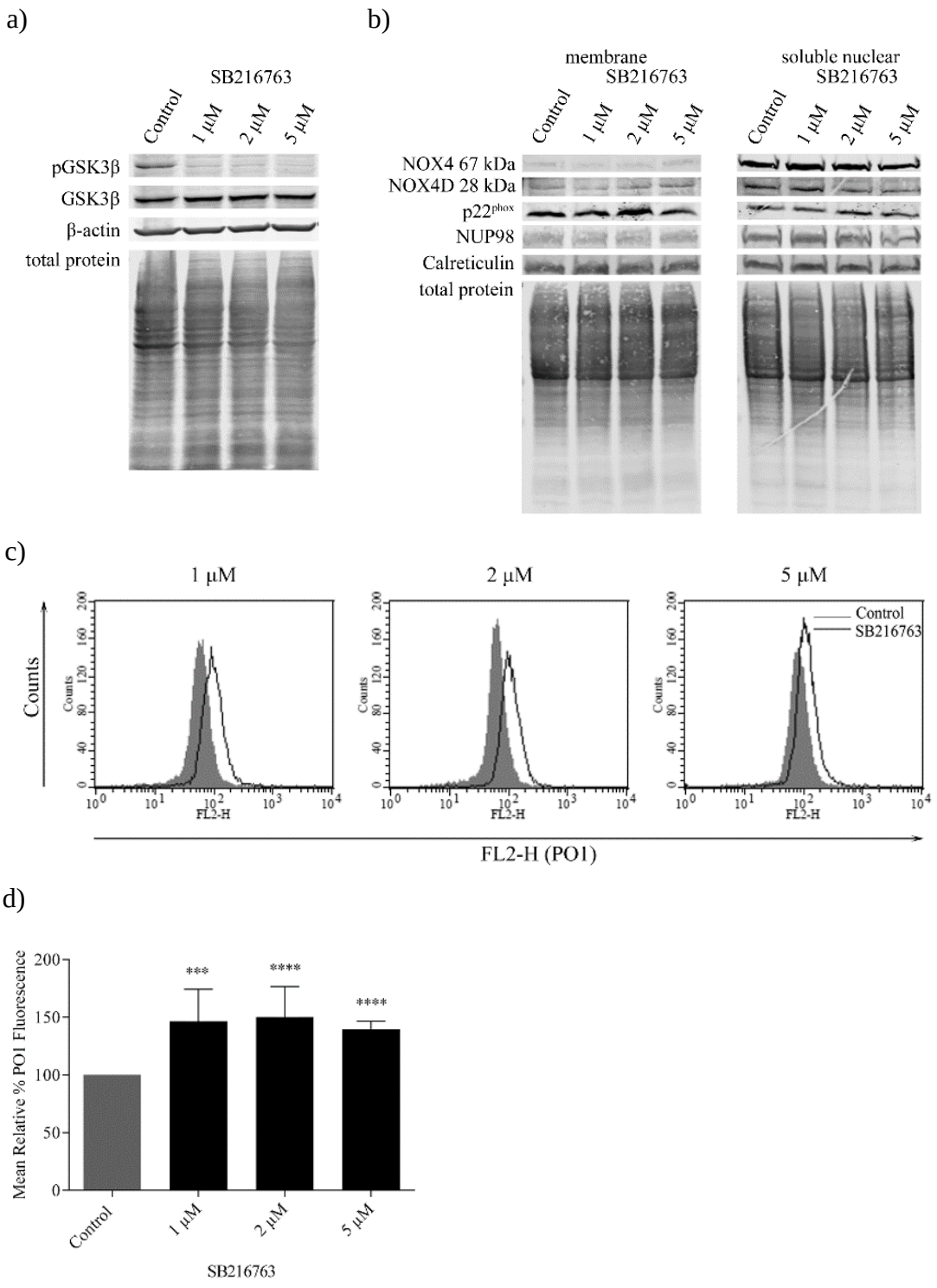

Figure 5.19. (i) GSK3β activation had no noticeable effect on NOX4 67 kDa and NOX4D 28 kDa protein levels. Western blot analysis of GSK3β signalling in FLT3-ITD expressing MV4-11 cells following treatment with SB216763 (1 μM, 2 μM and 5 μM) for 16 h *(a)*. β-actin and total protein (REVERT total protein stain) are shown as loading controls. NOX4 67 kDa, NOX4D 28 kDa and $p22^{phox}$ protein levels in membrane and soluble nuclear fractions of MV4-11 cells following treatment with SB216763 for 16 h at indicated concentrations *(b)*. Equal loading of samples is shown by total protein (REVERT total protein stain) and verification of subcellular fractions were assessed by probing for nuclear-localised NUP98 and membrane-localised calreticulin. Western blot analysis is

representative of three *(a)* or four *(b)* independent experiments. Flow cytometric analysis of mean relative PO1 fluorescence in MV4-11 cells treated with SB216763 for 16 h at indicated concentrations *(c)*. Bar chart shows relative mean PO1 fluorescence of treated cells expressed as % of vehicle control (control) *(d)*. Results are presented as mean ± SD from three independent experiments. Asterisks indicate statistically significant differences (***$p<0.001$, ****$p<0.0001$) as analysed by Student's t-test.

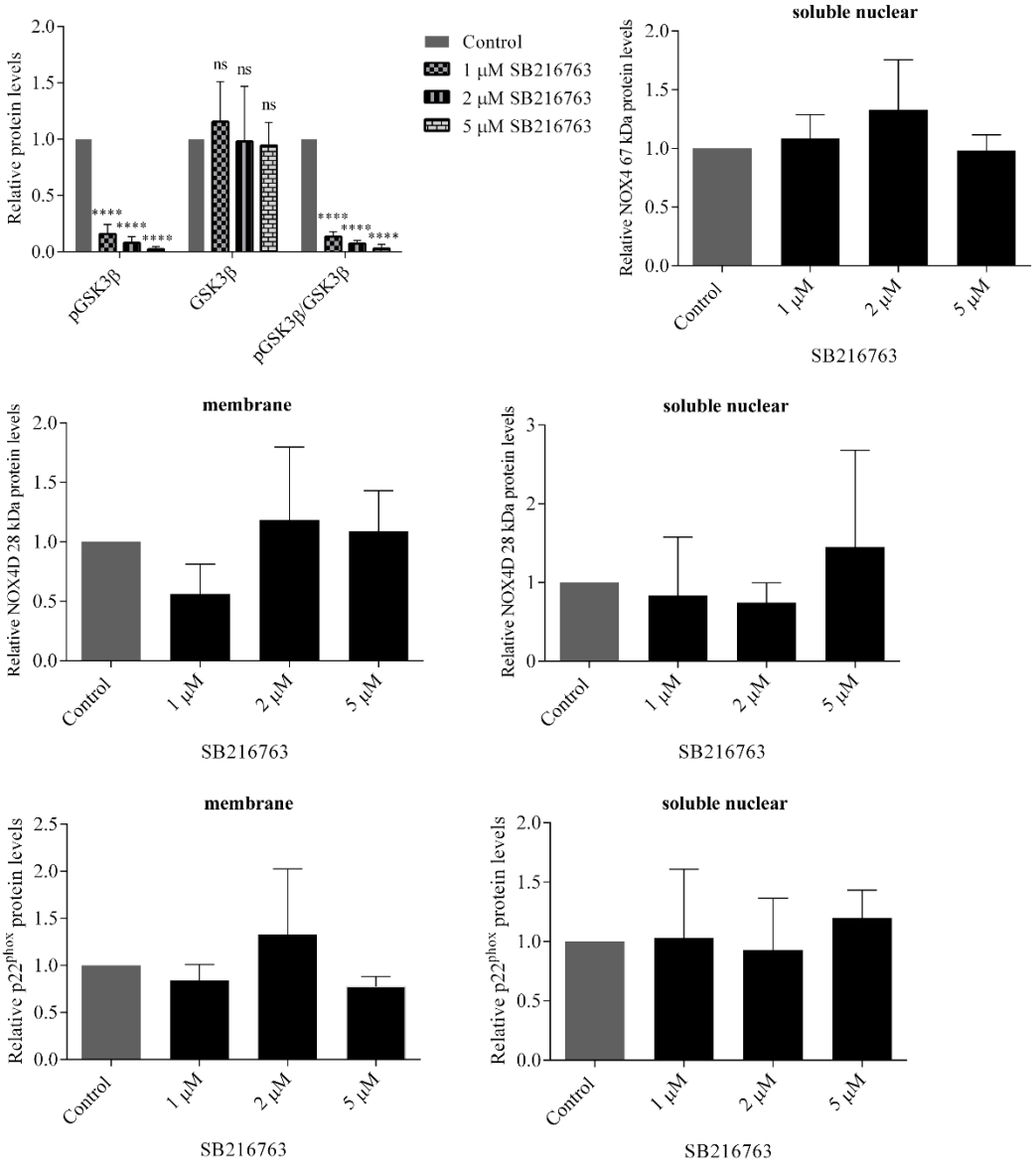

Figure 5.19. (ii) GSK3β activation had no noticeable effect on NOX4 67 kDa and NOX4D 28 kDa protein levels. Bar charts show relative mean pGSK3β, GSK3β and pGSK3β/GSK3β protein levels in whole cell lysates and NOX4 67 kDa, NOX4D 28 kDa and $p22^{phox}$ protein levels in membrane and soluble nuclear fractions following treatment with SB216763 (1 µM, 2 µM and 5 µM) for 16 h as quantified by densitometry. The data are expressed as % of vehicle control (control), where the ratio in the control was defined as 1. Results are presented as mean ± SD from three (pGSK3β, GSK3β and pGSK3β/GSK3β) or four (NOX4 67 kDa, NOX4D 28 kDa and $p22^{phox}$) independent experiments. Asterisks indicate statistically significant differences (****$p<0.0001$) as analysed by Student's t-test.

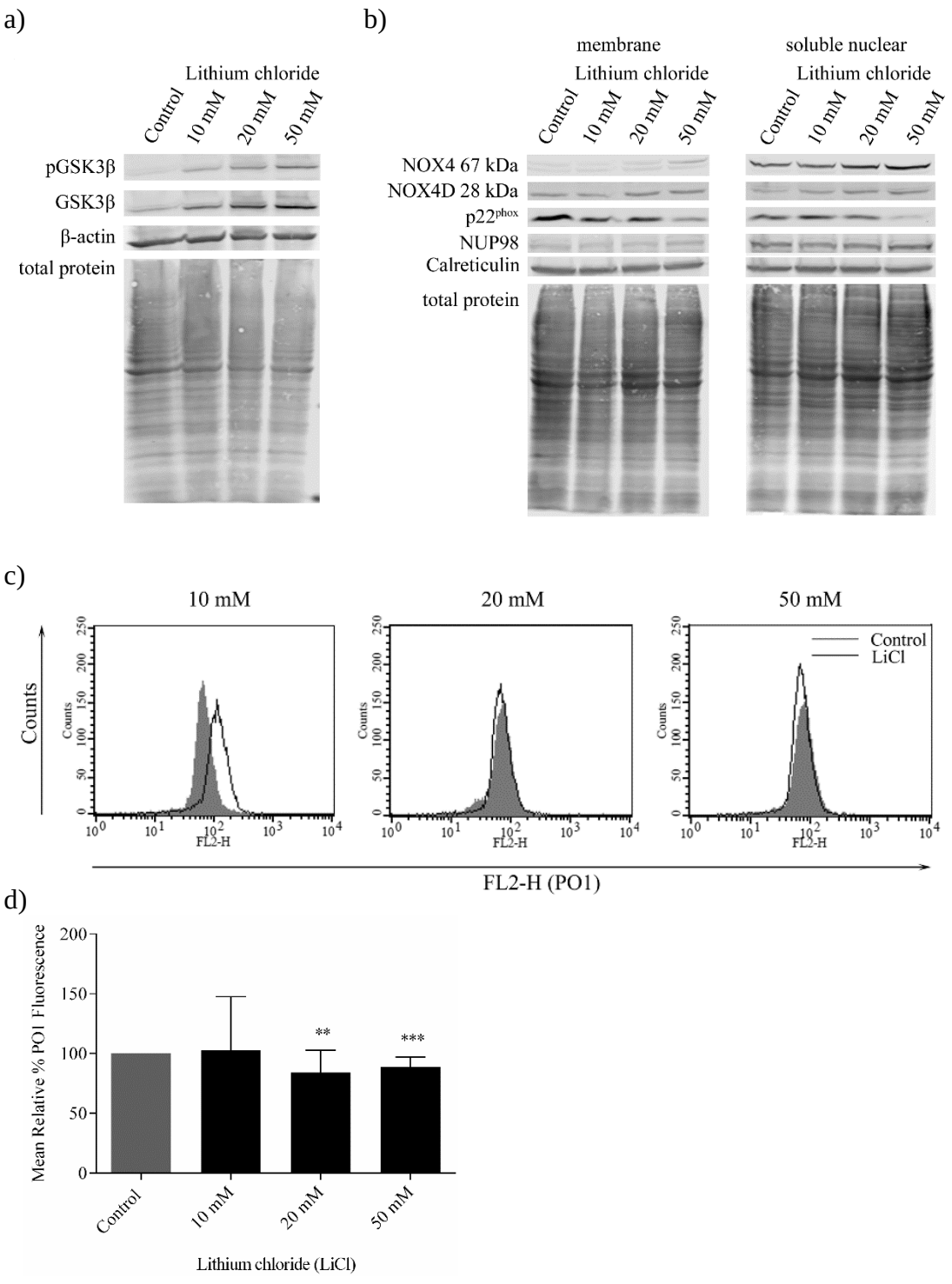

Figure 5.20. (i) Inhibition of GSK3β signalling results in elevated NOX4D 28 kDa protein levels. Western blot analysis of GSK3β signalling in FLT3-ITD expressing MV4-11 cells following treatment with lithium chloride (10 mM, 20 mM and 50 mM) for 16 h *(a)*. β-actin and total protein (REVERT total protein stain) are shown as loading controls. NOX4 67 kDa, NOX4D 28 kDa and $p22^{phox}$ protein levels in membrane and soluble nuclear fractions of MV4-11 cells following treatment with lithium chloride for 16 h at indicated concentrations *(b)*. Equal loading of samples is shown by total protein (REVERT total protein stain) and verification of subcellular fractions were assessed by probing for nuclear-localised NUP98 and membrane-localised calreticulin. Western blot analysis is representative

of three independent experiments. Flow cytometric analysis of mean relative PO1 fluorescence in MV4-11 cells treated with lithium chloride for 16 h at indicated concentrations *(c)*. Bar chart shows relative mean PO1 fluorescence of treated cells expressed as % of vehicle control (control) *(d)*. Results are presented as mean ± SD from four independent experiments. Asterisks indicate statistically significant differences (**$p<0.01$, ***$p<0.001$) as analysed by Student's t-test.

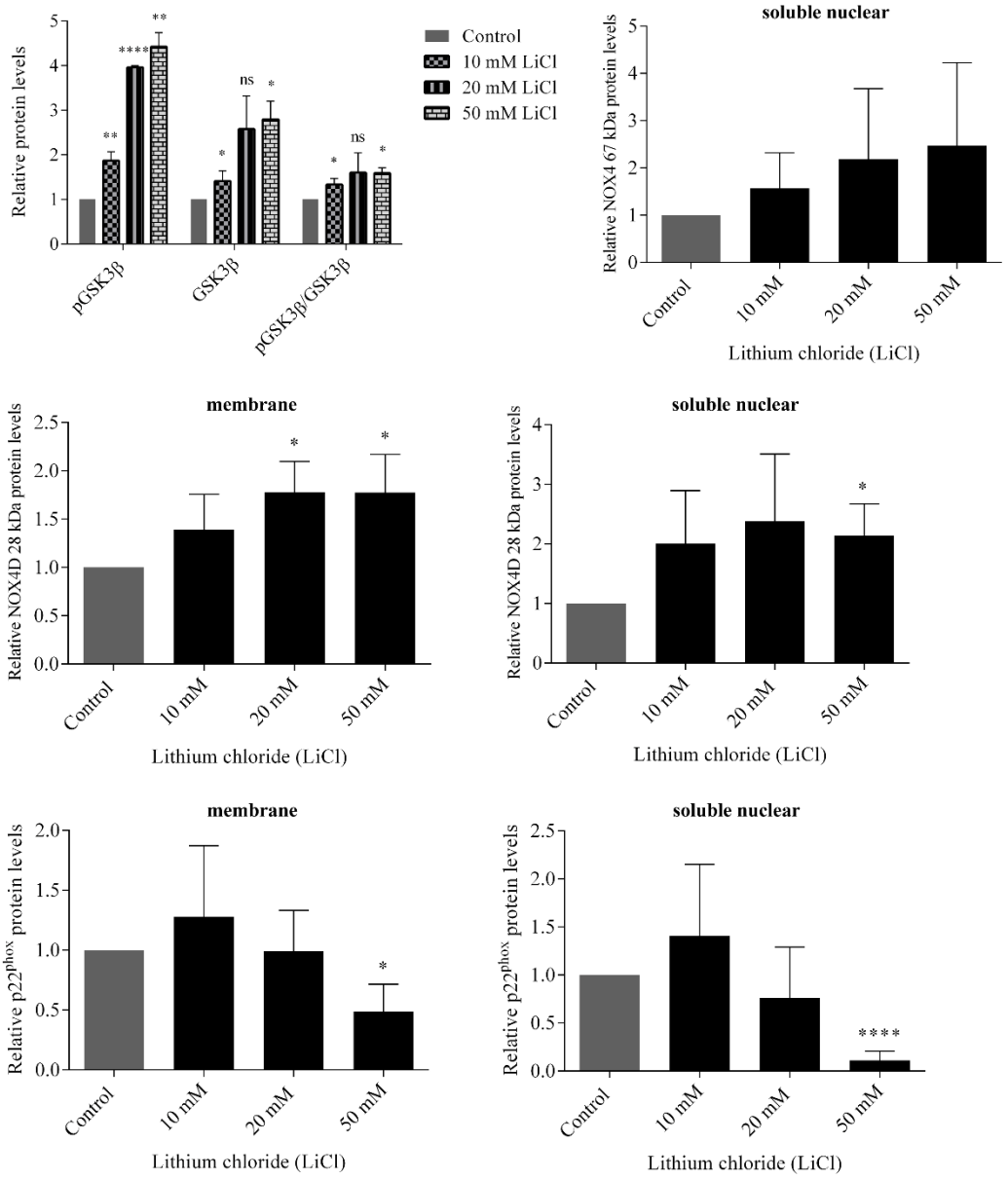

Figure 5.20. (ii) Inhibition of GSK3β signalling results in elevated NOX4D 28 kDa protein levels. Bar charts show relative mean pGSK3β, GSK3β and pGSK3β/GSK3β protein levels in whole cell lysates and NOX4 67 kDa, NOX4D 28 kDa and $p22^{phox}$ protein levels in membrane and soluble nuclear fractions following treatment with lithium chloride (LiCl) (10 mM, 20 mM and 50 mM) for 16 h as quantified by densitometry. The data are expressed as % of vehicle control (control), where the ratio in the control was defined as 1. Results are presented as mean ± SD from three independent experiments. Asterisks indicate statistically significant differences (*$p<0.05$, **$p<0.01$, ****$p<0.0001$) as analysed by Student's t-test.

5.3.14. FLT3-ITD-driven NOX4D-generated H_2O_2 in AML

Together with previous findings we have identified that ligand-independent constitutive activation of the FLT3 receptor, FLT3-ITD, activates PI3K/AKT, ERK1/2 and STAT5 signalling and inhibits GSK3β signalling. We have shown that FLT3-ITD is an upstream regulator of NOX4D-generated pro-survival H_2O_2. Activation of AKT and STAT5 signalling by FLT3-ITD results in the activation and production of NOX4D-generated H_2O_2 at the nuclear membrane where it may be contributing to DNA damage and disease progression (Figure 5.21.).

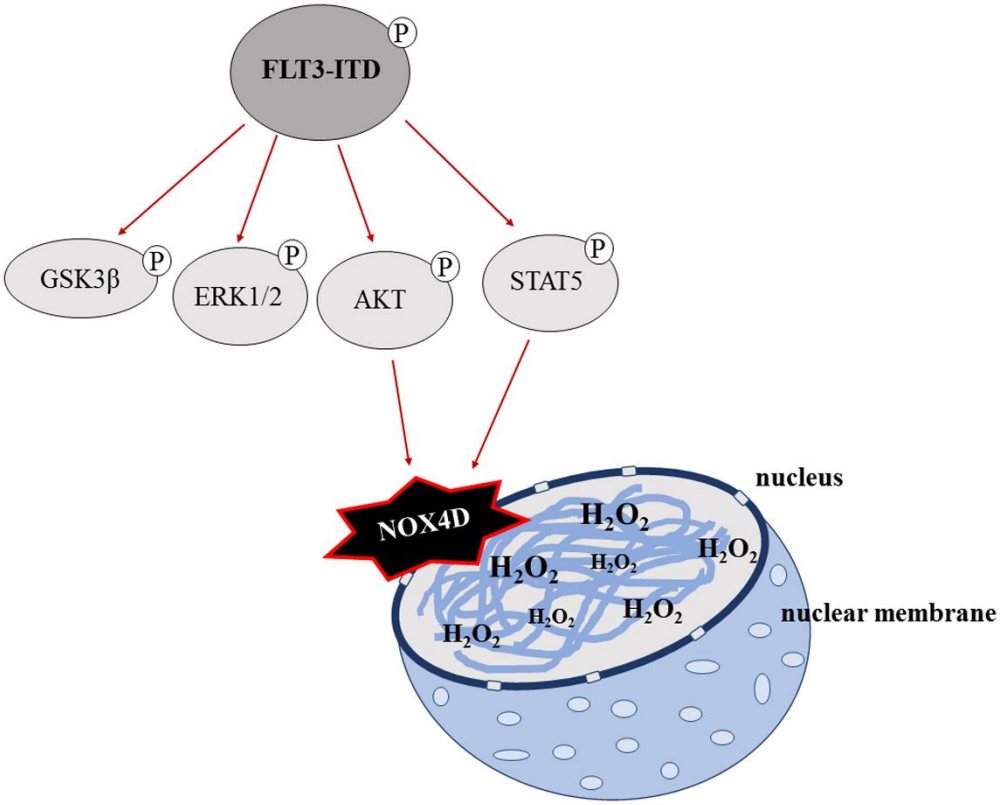

Figure 5.21. A schematic of the proposed mechanism of FLT3-ITD-driven NOX4D-generated H_2O_2 in AML. GSK3β, ERK1/2, PI3K/AKT and STAT5 pro-survival pathways are located downstream of FLT3-ITD. Phosphorylation and activation of AKT and STAT5 signalling by the FLT3-ITD oncogene results in the activation and production of DNA damaging NOX4D-generated H_2O_2 at the nuclear membrane.

5.3.15. BCR-ABL expressing CML K562 cells express the NOX4 splice variant NOX4D 28 kDa primarily in the cytoplasm

The BCR-ABL mutation in CML is involved in a cycle of genomic instability similar to that of the FLT3-ITD mutation. BCR-ABL is known to activate downstream pro-survival pathways, for example, PI3K/AKT, JAK/STAT, and Raf/MEK/ERK, resulting in resistance to apoptosis and proliferation. BCR-ABL-expressing cells have been reported to generate increased levels of ROS compared to untransformed cells (Jayavelu et al., 2016b). Naughton et al., reported that NOX4-generated ROS contribute significantly to total endogenous ROS on BCR-ABL induction (Naughton et al., 2009). The oncogenic effects of BCR-ABL cause increased levels of ROS production, leading to enhanced DNA damage and compromised DNA repair. Not only are levels of DNA damage much higher in BCR-ABL-transformed cells compared with non-transformed cells, the rate of DNA repair is also much higher because of unfaithful end joining systems (Nowicki et al., 2004). Importantly, the resulting accumulation of DNA damage and genetic abnormalities contributes to resistance against drugs that are commonly used in the treatment of CML including imatinib (Koptyra et al., 2006).

Moreover, we investigated if BCR-ABL expressing CML cells express NOX4D. We show that BCR-ABL expressing CML K562 cells express the NOX4D 28 kDa splice variant primarily in the cytoplasmic fraction. NOX4D is also expressed in the membrane and soluble nuclear fractions of K562 cells (Figure 5.22.).

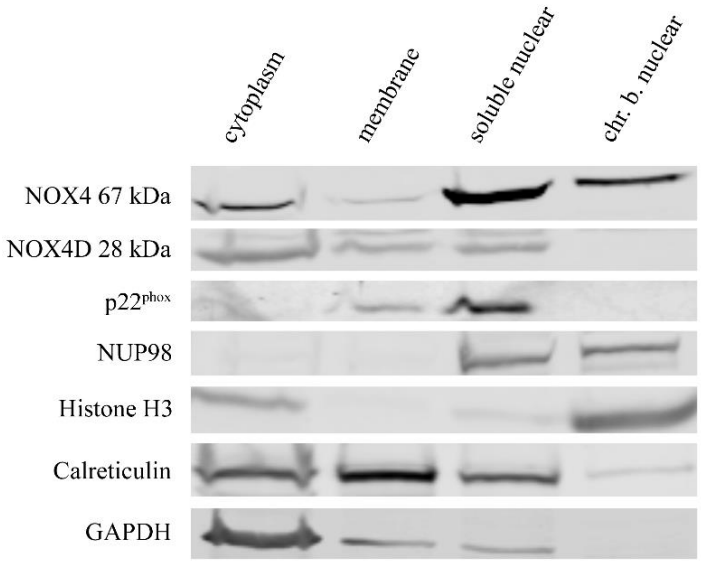

Figure 5.22. BCR-ABL expressing CML K562 cells express the NOX4D 28 kDa isoform. Subcellular fractionation was carried out in BCR-ABL expressing CML cell line, K562, using a subcellular fractionation kit. Expression of NOX4 67 kDa, NOX4D 28 kDa and $p22^{phox}$ was assessed by means of western blot analysis. Equal loading of samples and verification of the subcellular fractions were demonstrated by probing for nuclear-localised NUP98 and Histone H3, membrane-localised calreticulin and cytosolic-localised GAPDH. Western blots are representative of three independent experiments.

5.4. Discussion

FLT3-ITD is the most prevalent mutation in AML accounting for 15-35% of patient cases (Gilliland and Griffin, 2002, Network, 2013, Jayavelu et al., 2016b) and has been associated with an aggressive phenotype (Small, 2008, Konig and Levis, 2015). NOX-derived ROS have been shown to have numerous roles in leukaemia including cell survival, cell proliferation and a differentiation block (Naughton et al., 2009, Reddy et al., 2011). Leukaemic oncogenes have been widely documented in the regulation of NOX proteins and their partner protein $p22^{phox}$ (Jayavelu et al., 2016b, Landry et al., 2013, Moloney et al., 2017b). Our group has shown that 32D cells transfected with FLT3-ITD possess higher NOX4 and $p22^{phox}$ levels than their wild-type counterpart contributing to genomic instability in FLT3-ITD expressing AML. Furthermore, 32D/FLT3-ITD cells exhibit higher levels of total endogenous and nuclear H_2O_2 and DNA damage than 32D/FLT3-WT cells (Stanicka et al., 2015).

Unlike other NOX family members, NOX4 is constitutively activated (Martyn et al., 2006). Subcellular localisation of NOX4 is key to its role in ROS production and genetic instability. NOX4 has been reported to be expressed in the nucleus (Spencer et al., 2011, Gordillo et al., 2010, Weyemi and Dupuy, 2012, Weyemi et al., 2012, Guida et al., 2013, Guida et al., 2014, Maraldi et al., 2015, Weyemi et al., 2015) amongst other previously identified locations including the cytoskeleton (Hilenski et al., 2004), ER (Ambasta et al., 2004, Chen et al., 2008b, Helmcke et al., 2008, Zhang et al., 2011), mitochondria (Block et al., 2009, Case et al., 2013) and plasma membrane (Zhang et al., 2011, Lee et al., 2006). Our laboratory has previously shown that NOX4 and $p22^{phox}$ colocalise to the nuclear membrane (Stanicka et al., 2015) and that $p22^{phox}$ also colocalises to the ER (Woolley et al., 2012) of FLT3-ITD expressing

MV4-11 cells. Previous studies have identified the presence of NOX4 isoforms or splice variants (Goyal et al., 2005). NOX4D 28 kDa is of particular interest, as it is found in the nucleus and nucleolus of multiple cell types including human aortic smooth muscle cells, HUVECs, H9C2 rat cardiomyocyte cells, HEK cells, mouse primary cardiac fibroblasts and rat neonatal cardiomyocytes, where it contributes to ROS production and DNA damage (Anilkumar et al., 2013).

To investigate if FLT3-ITD expressing AML cells express NOX4D and in order to identify the localisation of NOX4D we utilised subcellular fractionation. Following optimisation of the subcellular fractionation technique, it proved very difficult to detect the membrane-localised markers, calreticulin and KDEL, in the membrane fraction only. The membrane-localised markers were detected in the soluble nuclear fractions of MV4-11, 32D/FLT3-ITD and 32D/FLT3-WT cells (Figure 5.3. - Figure 5.6., Figure 5.12. b, Figure 5.16. - Figure 5.20.). The MV4-11, 32D/FLT3-ITD and 32D/FLT3-WT cell structures did not facilitate in the generation of clean fractions. Leukaemia cells have very little cytoplasm, a large nucleus and distinct nucleoli (Lowenberg et al., 1999). We have shown this in MV4-11 cells stained with haematoxylin (Figure 3.1.). Previous studies in our laboratory have shown MV4-11 cells to have a large endoplasmic reticulum using an ER marker and have also shown that the ER is in close proximity with the nuclear membrane (Woolley et al., 2012). In support of previous work, we confirmed the ER as being a large organelle in the MV4-11 cell structure (Figure 3.2. and Figure 3.4.). Further studies in our laboratory have identified MV4-11 cells as having a large nucleus using the nuclear marker, Hoechst, and that Hoechst strongly correlates with the nuclear H_2O_2 specific probe, Nuclear Peroxy Emerald 1 (NucPE1) (Stanicka et al., 2015). The ER marker strongly correlated with PO1 (Woolley et al., 2012). PO1 and NucPE1 are in very

close proximity (Stanicka et al., 2015), the nuclear membrane is contiguous with the lumen of the ER. These findings confirm that the MV4-11 cell structure does not facilitate in the collection of clean fractions, particularly soluble nuclear fractions. This might account for the detection of membrane-localised calreticulin marker in the soluble nuclear fractions of MV4-11 cells. The membrane-localised marker, calreticulin, has previously been detected in the cytosol of HeLa and MDA-MB-435 cells and the perinuclear region of MDA-MB-435 cells (Shaiken and Opekun, 2014). The ER permeates much of the cytoplasm and this might be an explanation for the detection of calreticulin in the cytoplasmic fraction of MV4-11 cells (Burke, 2015).

In this study, we investigated the expression, localisation and regulation of NOX4D-generated pro-survival ROS in FLT3-ITD expressing AML. We found that FLT3-ITD expressing AML patients and cells possess the NOX4D splice variant (Figure 5.1., Figure 5.3. - Figure 5.6.). FLT3-ITD expressing AML cells express NOX4D in the membrane and soluble nuclear fractions. NOX4D was not detected in the FLT3-WT expressing patient samples and cells (Figure 5.1., Figure 5.5. and Figure 5.6.), suggesting a role for nuclear membrane-localised NOX4D 28 kDa in the generation of pro-survival ROS in FLT3-ITD expressing AML. In line with previous work, we detected NOX4 67 kDa in the soluble nuclear fraction and its partner protein $p22^{phox}$ in the membrane and soluble nuclear fractions of MV4-11 and 32D/FLT3-ITD cells (Figure 5.3. - Figure 5.6.). Although the soluble nuclear fraction contains membrane-localised protein, calreticulin, NOX4 67 kDa was detected in the soluble nuclear fraction and not in the membrane fraction, justifying its localisation to the nuclear membrane of MV4-11 cells. 32D cells stably transfected with FLT3-ITD express NOX4D 28 kDa and possess elevated levels of total endogenous H_2O_2 compared to their wild-type counterpart (Figure 5.8.). Importantly, to our knowledge,

this is the first study to identify the role of nuclear membrane-localised NOX4D 28 kDa in pro-survival ROS production and genomic instability in FLT3-ITD expressing AML cells.

$p22^{phox}$ is a partner protein of NOX1-4 and is required for NOX4 activation (Ambasta et al., 2004). We found that $p22^{phox}$ knockdown had no significant effect on NOX4 67 kDa and NOX4D 28 kDa protein levels (Figure 5.9.). Interestingly, previous studies have shown that NOX4 knockdown resulted in depletion of $p22^{phox}$ protein levels in HUVECs with no change in $p22^{phox}$ mRNA expression (Kuroda et al., 2005). This suggests that the formation of NOX4 and $p22^{phox}$ complex in the nucleus of HUVECs is responsible for the stabilisation of $p22^{phox}$ at the protein level.

Recent studies in our laboratory have revealed that NOX4 67 kDa is glycosylated in FLT3-ITD expressing MV4-11 cells (Figure 3.25.) (Moloney et al., 2017b). We show that NOX4D 28 kDa is also glycosylated in MV4-11 cells, by using a glycosylation inhibitor, tunicamycin, and a receptor trafficking inhibitor, brefeldin A. By inhibiting glycosylation, NOX4D 28 kDa was observed at a lower molecular weight (Figure 5.10.). Indeed, NOX4D 28 kDa is glycosylated in A549 cells (Goyal et al., 2005). We have shown that deglycosylation of NOX4 67 kDa and now NOX4D 28 kDa coincides with significant decreases in total endogenous H_2O_2 (Figure 3.11.) (Moloney et al., 2017b). This suggests that the glycosylation of NOX4 67 kDa and NOX4D 28 kDa may be important for their role in the production of pro-survival ROS and DNA damage in AML. Tunicamycin and brefeldin A have recently been shown to inhibit receptor trafficking of the FLT3-ITD receptor to the plasma membrane which caused inactivation of both the AKT and ERK1/2 pathways (Choudhary et al., 2009, Moloney et al., 2017b). Although tunicamycin and brefeldin A inhibit many glycosylated proteins, mild inhibition of glycosylation using tunicamycin in

combination with FLT3 kinase inhibitors has shown therapeutic potential for the treatment of FLT3-ITD expressing AML (Tsitsipatis et al., 2017).

It has been previously demonstrated that FLT3-ITD is involved in the up-regulation of NOX4 both at mRNA and protein levels (Stanicka et al., 2015, Jayavelu et al., 2016a). Inhibition of FLT3-ITD activity using several FLT3 receptor inhibitors including AC220, tyrphostin (AG1295) and PKC412 caused a decrease in NOX4 mRNA and protein levels (Jayavelu et al., 2016a, Moloney et al., 2017b) presenting a role for FLT3-ITD in NOX4-generated ROS production in AML. Here, we have shown that FLT3-ITD patient samples and FLT3-ITD expressing MV4-11 and 32D cells express the NOX4D 28 kDa splice variant alongside a dramatic increase in total endogenous H_2O_2 compared to their wild-type counterpart that do not express NOX4D (Figure 5.8.). Inhibition of the FLT3 receptor using PKC412 caused a decrease in total endogenous H_2O_2 in 32D/FLT3-ITD cells compared to 32D/FLT3-WT cells (Figure 5.11.). FLT3-ITD inhibition in MV4-11 cells treated with PKC412 resulted in down-regulation of NOX4 67 kDa, NOX4D 28 kDa and $p22^{phox}$ protein levels alongside a decrease in H_2O_2 levels (Figure 5.12. and Figure 5.13.). Treatment of MV4-11 and 32D/FLT3-ITD cells with FLT3 receptor inhibitor AC220 also led to decreased levels of NOX4D 28 kDa (Figure 5.14.). Inhibition of the FLT3 receptor in MOLM13 cells treated with AC220 also resulted in decreased NOX4D 28 kDa protein levels (Figure 5.15.). PKC412 (midostaurin) has recently been approved by the FDA and AC220 is currently being tested in clinical trials for the treatment of AML (Smith et al., 2012, Stone et al., 2012, AML, 2017). Previous studies have shown that FLT3-ITD inhibition using PKC412 and NOX inhibition via diphenyleneiodonium (DPI) in 32D/FLT3-ITD cells resulted in approximately 25-40% decrease in γH2AX levels, a marker of dsbs (Stanicka et al., 2015). Together these findings suggest that the FLT3-

ITD oncogene is responsible for the regulation and production of nuclear membrane-localised NOX4D-generated H_2O_2 in AML contributing to genetic instability and an aggressive phenotype.

Three major pro-survival pathways are activated downstream of FLT3-ITD in AML: PI3K/AKT, ERK1/2 and STAT5 pathways (Figure 4.10.) (Choudhary et al., 2009). We have shown that the PI3K/AKT pathway needs to be activated in order for NOX4 to generate its oncogenic effects in AML (Figure 4.5.) (Moloney et al., 2017b). Inhibition of the PI3K/AKT pathway revealed that the PI3K/AKT pathway is responsible for the generation of NOX4-, NOX4D- and $p22^{phox}$-generated H_2O_2 (Figure 5.16.). Although the ERK1/2 pathway is located downstream of FLT3-ITD, inhibition of ERK1/2 signalling was found to have no noticeable effect on NOX4- and NOX4D-protein levels. However, inactivation of ERK1/2 signalling revealed that ERK1/2 activation is involved in the stimulation and production of $p22^{phox}$-mediated H_2O_2 production in AML (Figure 5.17.). $p22^{phox}$ is a partner protein of NOX1, NOX2 and NOX3 as well as NOX4, all of which have a role in ROS production. We have previously demonstrated that NOX2 is also involved in ROS production and DNA damage contributing to genetic instability in FLT3-ITD expressing AML. This same study confirmed that NOX1 does not contribute significantly to ROS production or dsbs (Stanicka et al., 2015). Patient derived FLT3-expressing myeloid cells have been shown to express NOX2, NOX4 and NOX5. However, their murine counterpart have been shown to express NOX1, NOX2 and NOX4. These cells did not express NOX3 (Reddy et al., 2011). Therefore it is likely that ERK1/2 activation is involved in the production of NOX2-generated H_2O_2 in FLT3-ITD expressing AML. Recent findings have identified STAT5 signalling downstream of FLT3-ITD and its requirement for the up-regulation of NOX4-generated H_2O_2, alongside the inactivation of DEP-1 PTP

a negative regulator of FLT3 signalling activity (Jayavelu et al., 2016a). Inhibition of STAT5 signalling revealed that activated STAT5 is required for the production of NOX4-, NOX4D- and $p22^{phox}$-generated ROS (Figure 5.18.). This suggests that NOX4D may also have a role in the partial inactivation of DEP-1 PTP resulting in cellular transformation in FLT3-ITD expressing AML.

GSK3β is another pathway known to be located downstream of FLT3-ITD. Inhibition of the PI3K/AKT pathway in MV4-11 cells resulted in increased levels of pGSK3β (Ser9) suggesting that the GSK3β pathway is not located downstream of the PI3K/AKT pathway (Figure 4.5. and Figure 4.12.) (Moloney et al., 2017b). Phosphorylation of GSK3β at Serine 9 decreased following ERK1/2 inhibition suggesting that the GSK3β pathway is located downstream of ERK1/2 (Figure 4.13.). Inhibition of FLT3-ITD signalling caused a decrease in phosphorylation of GSK3β (Ser9), resulting in increased GSK3β activation (Figure 4.8. and Figure 4.10.) which has been shown previously to play a crucial role in the post-translational regulation of $p22^{phox}$ (Woolley et al., 2012, Moloney et al., 2017b). SB216763 is described as an inhibitor of GSK3β, and GSK3β is inhibited when it is phosphorylated. In disagreement with this, SB216763 was found to decrease levels of pGSK3β in MV4-11 cells (Figure 5.19.), suggesting that it is acting as an activator of GSK3β. It is possible that SB216763 could have different effects in other cell types. However, based on our findings, we advise careful consideration and assessment of pGSK3β levels when using this drug. Activation of GSK3β was found to have no noticeable effect on NOX4-, NOX4D- and $p22^{phox}$ protein levels, however an increase in H_2O_2 levels was observed (Figure 5.19.). The activation of GSK3β signalling has been found to be pro-apoptotic in several systems and can provoke mitochondrial injury and this may be responsible for the increase in H_2O_2 levels (Bijur et al., 2000, Macanas-Pirard

et al., 2005, Maurer et al., 2006). Lithium chloride, also described as an inhibitor of GSK3β, resulted in the expected increase in pGSK3β in MV4-11 cells, indicating inhibition (Figure 5.20.). Inhibition of GSK3β signalling using LiCl revealed an increase in NOX4D protein levels, however, $p22^{phox}$ protein levels decreased. Moreover, inhibition of GSK3β signalling had little or no effect on total endogenous H_2O_2 (Figure 5.20.).

The BCR-ABL mutation in CML is involved in a cycle of genomic instability similar to that of the FLT3-ITD mutation in AML. BCR-ABL mutation is known to activate several pro-survival signalling pathways, for example, PI3K/AKT, STAT and ERK resulting in elevated ROS production compared to their wild-type counterpart, particularly NOX4-generated ROS, leading to enhanced DNA damage and compromised DNA repair (Jayavelu et al., 2016b, Naughton et al., 2009, Nowicki et al., 2004). We investigated the expression and localisation of NOX4D 28 kDa in K562 cells. We found that BCR-ABL expressing CML cells possess the NOX4D splice variant in the cytoplasmic, membrane and soluble nuclear fractions (Figure 5.22.). NOX4D is primarily located in the cytoplasm of BCR-ABL expressing K562 cells, however, NOX4D is localised to the nuclear membrane of FLT3-ITD expressing MV4-11 cells, suggesting that nuclear membrane-localised NOX4D-generated H_2O_2 in FLT3-ITD expressing AML is associated with rapid disease progression due to close proximity with DNA in the nucleus resulting in an inferior outcome.

In conclusion, we suggest that the FLT3-ITD oncogene is responsible for the activation and generation of NOX4D-generated pro-survival H_2O_2 at the nuclear membrane contributing to DNA damage and genetic instability in AML. Glycosylation of NOX4 and NOX4D is essential for the production of pro-survival ROS. Activation of PI3K/AKT and STAT5 signalling is required in order for NOX4D

to generate its oncogenic effects. These findings are summarised in Figure 5.21. This study emphasises the potential of NOX4 and NOX4D as an effective therapeutic target in FLT3-ITD expressing AML, as inhibition and deglycosylation of NOX4 and NOX4D can decrease the levels of H_2O_2 and DNA damage that would otherwise contribute to genetic instability.

Chapter 6. General Discussion

Until recently the strategy of AML treatment had not changed substantially in over 30 years. The worldwide standard of care for AML patients who are not participating in clinical trials, receive an induction of chemotherapy consisting of cytarabine and idarubicin/daunorubicin, followed by either one to four cycles of consolidation therapy and autologous or allogeneic stem cell transplantation (Roboz, 2012). This standard treatment with chemotherapy maximally results in 70-80% patients less than 65 years achieving complete remission, most will eventually relapse and an overall survival rate of only 40-50% at 5 years (Emadi and Karp, 2014, Büchner et al., 2012). Several factors have been associated with more severe outcomes at relapse including unfavourable cytogenetics at diagnosis, old age and also prior history of haematopoietic stem cell transplantation (Breems et al., 2005). This demonstrates the importance and need for the development of new drugs for the treatment of AML. Furthermore, the high percentage of relapse in AML highlights the requirement for investigations into the molecular sources and mechanisms which are involved and contribute to drug resistance and relapse.

Imatinib mesylate was the first small-molecule tyrosine kinase inhibitor (TKI) used as a standard cancer therapy targeting the BCR-ABL oncoprotein in CML. Treatment of CML patients in clinic with imatinib has increased the 5 year survival rate from 50% to 90%, demonstrating the effectiveness of molecular targeted chemotherapy in cancer (Druker, 2009). Following the proven effectiveness of imatinib, there has been great interest in the development of more specific and effective chemotherapeutics against other cancer-driving oncoproteins.

Genetic alterations in AML have been classified into two classes collectively known as the ‘two-hit’ model. Class I mutations are mutations that result in the activation of signal transduction pathways that lead to increased cell survival and

proliferation, for example, FLT3, BCR-ABL, RAS and JAK2 (Conway O'Brien et al., 2014). Class II mutations are mutations that affect differentiation preventing maturation of cells and also affect self-renewal, for instance, CEBPA, MLL and NPM1. In order for AML to develop, a class I mutation must be accompanied by a class II mutation (Shih et al., 2012, Naoe and Kiyoi, 2013).

FLT3 is a type III RTK expressed in approximately 90% of AML cases and is involved in the early stages of haematopoiesis (Stirewalt and Radich, 2003, Gilliland and Griffin, 2002). Mutations in FLT3 are present in 25-45% of AML patients, making it the most prevalent genetic aberration in AML (Stirewalt and Radich, 2003) and an attractive therapeutic target. There are two types of FLT3 mutations implicated in AML; the FLT3 internal tandem duplication (FLT3-ITD) mutation and mutations of the activation loop of the tyrosine kinase domain of FLT3 (FLT3-TKD). The FLT3-ITD mutation is the most common mutation expressed in 15-35% of AML cases, 1-3% of ALL cases and 5-10% of patients with myelodysplastic syndromes (MDS) (Stirewalt and Radich, 2003). In recent months, advances have been made in AML treatments. Midostaurin (Rydapt), a tyrosine kinase inhibitor has been approved by the FDA for the treatment of FLT3-positive AML (AML, 2017). This is a major improvement for the treatment of AML. More specific tyrosine kinase inhibitors including quizartinib are currently in clinical trials and are showing promising effects.

Our laboratory and other laboratories have demonstrated that patient AML blasts generate increased levels of ROS (Stanicka et al., 2015, Hole et al., 2013), which are known to be involved in DNA damage and genetic instability. However, it is well established that ROS also act as cell signalling molecules in a wide array of processes regulating cell survival and differentiation, proliferation and growth (Clerkin et al., 2008, Gough and Cotter, 2011, Schieber and Chandel, 2014). ROS have been long

associated with cancer where different types of tumour cells have been shown to produce elevated levels of ROS compared to their wild-type counterpart (Panieri and Santoro, 2016). Enhanced ROS production, particularly from NOXs, are thought to be oncogenic resulting in enhanced cell survival and proliferation, DNA damage and genetic instability, adaptation, cellular injury and cell death, autophagy and resistance to drugs (Moloney and Cotter, 2017). Regulation of ROS in tumour cells must be tightly regulated to prevent tumour cell death. An overproduction of ROS results in increased antioxidant levels. However, the antioxidant capacity cannot cope with the high concentrations of ROS and is involved in the maintenance of pro-tumourigenic signalling allowing disease progression and for the tumour cells to develop resistance against apoptosis (Gorrini et al., 2013). From a clinical point of view, adaptation of tumour cells to enhanced ROS production may result in tumour cells being less responsive to cytotoxic chemotherapy, which operates through severe oxidative stress (Schumacker, 2006, Pelicano et al., 2004, Trachootham et al., 2009). Therefore, delineation of the sources and mechanism of regulation and production could identify novel protein targets in cancer, which in combination with standard chemotherapy, would effectively increase and prolong the response of cancer to chemotherapy.

A number of studies have investigated the function of ROS, specifically NOX4-generated ROS in AML. Our group has identified NOX4 and $p22^{phox}$, a small membrane subunit of the NOX complex, as major sources of ROS in AML (Woolley et al., 2012, Stanicka et al., 2015). FLT3-ITD expressing cells have been shown to express increased levels of NOX4 and $p22^{phox}$ proteins as well as elevated ROS compared to FLT3-WT expressing cells (Stanicka et al., 2015). Furthermore, FLT3-ITD expressing cells exhibit higher levels of total endogenous and nuclear H_2O_2 and DNA damage than FLT3-WT (Stanicka et al., 2015). The mechanism in which FLT3-

ITD regulates and generates NOX4- and $p22^{phox}$-generated ROS is not clear. The overall aim of this thesis was to delineate the mechanisms in which FLT3-ITD-generated pro-survival ROS contribute to DNA damage and genetic instability in AML.

The FLT3-ITD mutation results in ligand-independent constitutive activation of the receptor at the plasma membrane and impaired trafficking of the receptor in compartments of its biosynthetic route, such as the ER (Choudhary et al., 2009, Moloney et al., 2017b). FLT3-ITD expressing cells produced elevated levels of H_2O_2 compared to FLT3-WT expressing cells (Stanicka et al., 2015). The molecular mechanism describing how mislocalised activation of FLT3-ITD stimulates the aberrant signalling of downstream pathways resulting in the production of pro-survival ROS is not known. Previous studies investigated the role of mislocalised activation of FLT3-ITD in AML using a mutant of FLT3-ITD, containing a deletion in the extracellular ligand-binding domain of FLT3-ITD, eliminating many sites of glycosylation, resulting in glycosylation independent trafficking of the FLT3-ITD receptor. In the same study, they used two receptor trafficking inhibitors, tunicamycin and brefeldin A, as an alternative method to study the effects of mislocalised activation of FLT3-ITD on aberrant signalling cascades (Choudhary et al., 2009). The findings in this study endorsed the use of receptor trafficking inhibitors, such as tunicamycin and brefeldin A, as a method for us to investigate the effect of subcellular localisation of FLT3-ITD on the generation of ROS in this study. In this study, we have shown that FLT3-ITD at the plasma membrane is responsible for the activation and expression of NOX4- and $p22^{phox}$-generated pro-survival ROS in FLT3-ITD expressing AML cells. $p22^{phox}$ is an essential component of NOX1-4 and is required for NOX activity and is essential for the maintenance of pro-survival ROS signalling

in AML. For FLT3-ITD to generate its oncogenic effects it has to be located at the plasma membrane. Plasma membrane FLT3-ITD induced activation of PI3K/AKT signalling is responsible for the activation of NOX4- and $p22^{phox}$- generated ROS in AML. ER retention of FLT3-ITD resulted in NOX4 deglycosylation, decreased $p22^{phox}$ mRNA levels and proteasomal degradation of $p22^{phox}$ protein. This work is published in *Leukemia Research* (Moloney et al., 2017b) and presents FLT3-ITD at the plasma membrane as a potential therapeutic target, in preventing downstream ROS-driven oncogenic effects (Chapter 3&4).

Increased production of NOX4-generated ROS has been documented to have a role in cell survival, cell proliferation and a differentiation block in AML (Moloney and Cotter, 2017, Jayavelu et al., 2016b). In Chapter 4, we also studied which pro-survival pathways were activated downstream of the FLT3-ITD receptor and examined the effects of FLT3-ITD subcellular localisation on the regulation and activation of aberrant signalling cascades. Activation of the FLT3-ITD receptor in AML stimulates downstream pro-survival signalling pathways including AKT, GSK3β, ERK1/2 and STAT5. In this study, we have demonstrated that the AKT and ERK1/2 signalling pathways are activated and the GSK3β signalling pathway is inhibited downstream of FLT3-ITD at the plasma membrane. The STAT5 signalling pathway is activated downstream of FLT3-ITD at the ER. These findings support previous studies investigating the effects of mislocalised activation of FLT3-ITD on the initiation of aberrant signalling cascades in 32D cells expressing the FLT3-ITD mutation (Choudhary et al., 2009). Previous studies have identified the PI3K/AKT pathway to be responsible for the regulation of GSK3β signalling through the phosphorylation of GSK3β on serine 9 resulting in the inhibition of GSK3β signalling (Kurosu et al., 2013). However, we have shown for the first time that GSK3β is

inhibited downstream of ERK1/2 activation in FLT3-ITD expressing AML. Chapters 3 and 4 nicely tie together the mechanism in which mislocalised activation of FLT3-ITD at the plasma membrane results in the activation of AKT and ERK1/2 and inhibition of GSK3β signalling and FLT3-ITD at the ER activates STAT5 pro-survival signalling. The PI3K/AKT pathway is responsible for the activation and generation of NOX4- and $p22^{phox}$-generated pro-survival ROS in AML. Together these findings delineate the mechanism involved in the activation and regulation of NOX4- and $p22^{phox}$- generated H_2O_2 in AML, identifying FLT3-ITD at the plasma membrane as a potential therapeutic target.

Our laboratory has identified NOX4 as a major source of ROS in FLT3-ITD expressing AML (Stanicka et al., 2015). Among the NOX family members, NOX4 is unique. It is constitutively activated, generating H_2O_2, unlike its family members NOX1 and NOX2, which require an agonist for activation (Martyn et al., 2006, Serrander et al., 2007, Takac et al., 2011). NOX4 subcellular localisation plays an important role given its constitutive activity. NOX4 and $p22^{phox}$ have been shown to colocalise to the nuclear membrane of FLT3-ITD expressing AML MV4-11 cell line contributing to DNA oxidation and dsbs, possibly driving genetic instability (Stanicka et al., 2015). Previous studies have identified NOX4 isoforms at varying levels in the presence of the prototype in the human lung cancer cell line, A549 (Goyal et al., 2005). NOX4 splice variant D (NOX4D 28 kDa) is of particular interest and has been shown to localise to the nucleus and nucleolus of VSMC, A7R5 cells as well as many other cell lines where it is contributing to elevated ROS production and DNA damage (Anilkumar et al., 2013, Goyal et al., 2005). In this study, we identified the expression of NOX4D in FLT3-ITD expressing patient samples and cells for the first time. NOX4D expression was absent from FLT3-WT expressing patient samples and cells.

We show that the FLT3-ITD oncogene is responsible for the activation and generation of NOX4D-generated pro-survival H_2O_2 at the nuclear membrane where it may be contributing to DNA damage and genetic instability in AML. Glycosylation of NOX4 and NOX4D is essential for the production of pro-survival H_2O_2. Activation of PI3K/AKT and STAT5 signalling is required in order for NOX4D to generate its oncogenic effects. This study emphasises NOX4 and NOX4D as effective and attractive therapeutic targets in FLT3-ITD expressing AML (Chapter 5) as the inhibition and deglycosylation of NOX4 and NOX4D can decrease the levels of H_2O_2 that would otherwise contribute to genetic instability. This work is published in *Oncotarget* (Moloney et al., 2017a).

Together our findings from Chapter 3, 4 and 5 have identified FLT3-ITD at the plasma membrane, PI3K/AKT, STAT5, NOX4 and NOX4D as attractive therapeutic targets for the treatment of FLT3-ITD expressing AML. Further studies have supported our findings. Inhibition of N-glycosylation of RTKs such as FLT3-ITD and c-KIT has been shown to have anti-leukaemic activity in AML. For example, loss of surface expression of FLT3-ITD and c-KIT results in induction of apoptotic cell death, mitigation of resistance to TKIs including the most potent FLT3 inhibitor currently in clinical trials, quizartinib, and also restores sensitivity to the chemotherapy drug cytarabine (Williams et al., 2012). More recently, our collaborators have demonstrated the synergistic killing of FLT3-ITD expressing AML MV4-11 cell line and primary cells through combined inhibition of FLT3-ITD tyrosine kinase activity and N-glycosylation using low doses of tunicamycin (Tsitsipatis et al., 2017). Taken together these studies confirm FLT3-ITD surface expression and NOX4 and NOX4D expression as promising therapeutic targets in AML.

In conclusion, this thesis has delineated the mechanism in which activation of the FLT3-ITD receptor at the plasma membrane and ER results in the activation of PI3K/AKT and STAT5 pro-survival signalling cascades, which are responsible for the activation and generation of NOX4-, NOX4D- and $p22^{phox}$-generated pro-survival H_2O_2 in AML. Furthermore, it has been demonstrated that NOX4 and NOX4D are important producers of ROS. This confirms the importance of NOX proteins in pro-tumourigenic signalling in leukaemia and highlights the importance of research in the area of ROS signalling in cancer and leukaemia. Together the data presented in this thesis identifies receptor trafficking inhibitors/glycosylation inhibitors and NOX inhibitors as potential therapies for the treatment of AML, which when treated in combination with standard chemotherapy may improve the effectiveness of the treatment.

Bibliography

ACHKAR, W. A., WAFA, A., ALI, B. Y., MANVELYAN, M. & LIEHR, T. 2010. A rare chronic myeloid leukemia case with Philadelphia chromosome, BCR-ABL e13a3 transcript and complex translocation involving four different chromosomes. *Oncology Letters,* 1**,** 797-800.

AGO, T., KITAZONO, T., KURODA, J., KUMAI, Y., KAMOUCHI, M., OOBOSHI, H., WAKISAKA, M., KAWAHARA, T., ROKUTAN, K., IBAYASHI, S. & IIDA, M. 2005. NAD(P)H Oxidases in Rat Basilar Arterial Endothelial Cells. *Stroke,* 36**,** 1040-1046.

AHMAD, I. M., ABDALLA, M. Y., AYKIN-BURNS, N., SIMONS, A. L., OBERLEY, L. W., DOMANN, F. E. & SPITZ, D. R. 2008. 2-Deoxyglucose combined with wild type p53 over expression enhances cytotoxicity in human prostate cancer cells via oxidative stress. *Free radical biology & medicine,* 44**,** 826-834.

AHMED, K. M., CAO, N. & LI, J. J. 2006. HER-2 and NF-κB as the Targets for Therapy-resistant Breast Cancer. *Anticancer research,* 26**,** 4235-4243.

AHN, J.-S., KIM, H.-J., KIM, Y.-K., JUNG, S.-H., YANG, D.-H., LEE, J.-J., LEE, I.-K., KIM, N. Y., MINDEN, M. D., JUNG, C. W., JANG, J.-H., KIM, H. J., MOON, J. H., SOHN, S. K., WON, J.-H., KIM, S.-H., KIM, N., YOSHIDA, K., OGAWA, S. & KIM, D. D. H. 2015. Adverse prognostic effect of homozygous TET2 mutation on the relapse risk of acute myeloid leukemia in patients of normal karyotype. *Haematologica,* 100**,** e351-e353.

AITA, V. M., LIANG, X. H., MURTY, V. V. V. S., PINCUS, D. L., YU, W., CAYANIS, E., KALACHIKOV, S., GILLIAM, T. C. & LEVINE, B. 1999. Cloning and Genomic Organization of Beclin 1, a Candidate Tumor Suppressor Gene on Chromosome 17q21. *Genomics,* 59**,** 59-65.

ALEEM, E. & ARCECI, R. J. 2015. Targeting cell cycle regulators in hematologic malignancies. *Frontiers in Cell and Developmental Biology,* 3**,** 16.

ALONSO, A. & PULIDO, R. 2016. The extended human PTPome: a growing tyrosine phosphatase family. *FEBS Journal,* 283**,** 1404-1429.

ALTENHÖFER, S., RADERMACHER, K. A., KLEIKERS, P. W. M., WINGLER, K. & SCHMIDT, H. H. H. W. 2015. Evolution of NADPH Oxidase Inhibitors: Selectivity and Mechanisms for Target Engagement. *Antioxidants & Redox Signaling,* 23**,** 406-427.

AMBASTA, R. K., KUMAR, P., GRIENDLING, K. K., SCHMIDT, H. H. H. W., BUSSE, R. & BRANDES, R. P. 2004. Direct Interaction of the Novel Nox Proteins with $p22^{phox}$ Is Required for the Formation of a Functionally Active NADPH Oxidase. *Journal of Biological Chemistry,* 279**,** 45935-45941.

AMES, B. N., SHIGENAGA, M. K. & HAGEN, T. M. 1993. Oxidants, antioxidants, and the degenerative diseases of aging. *Proceedings of the National Academy of Sciences,* 90**,** 7915-7922.

AML, M. G. F. N. F. 2017. Midostaurin Gets FDA Nod for AML. *Cancer Discovery,* 7**,** OF5-OF5.

AN, H. J., FROEHLICH, J. W. & LEBRILLA, C. B. 2009. Determination of Glycosylation Sites and Site-specific Heterogeneity in Glycoproteins. *Current opinion in chemical biology,* 13**,** 421-426.

ANILKUMAR, N., JOSE, G. S., SAWYER, I., SANTOS, C. X. C., SAND, C., BREWER, A. C., WARREN, D. & SHAH, A. M. 2013. A 28-kDa Splice Variant of NADPH Oxidase-4 Is Nuclear-Localized and Involved in Redox Signaling in Vascular Cells. *Arteriosclerosis, Thrombosis, and Vascular Biology,* 33**,** e104-e112.

ANILKUMAR, N., WEBER, R., ZHANG, M., BREWER, A. & SHAH, A. M. 2008. Nox4 and Nox2 NADPH Oxidases Mediate Distinct Cellular Redox Signaling Responses to Agonist Stimulation. *Arteriosclerosis, Thrombosis, and Vascular Biology,* 28**,** 1347-1354.

ARNOLD, R. S., HE, J., REMO, A., RITSICK, D., YIN-GOEN, Q., LAMBETH, J. D., DATTA, M. W., YOUNG, A. N. & PETROS, J. A. 2007. Nox1 Expression Determines Cellular Reactive Oxygen and Modulates c-fos-Induced Growth Factor, Interleukin-8, and Cav-1. *The American Journal of Pathology,* 171**,** 2021-2032.

ARORA, D., KÖTHE, S., VAN DEN EIJNDEN, M., VAN HUIJSDUIJNEN, R. H., HEIDEL, F., FISCHER, T., SCHOLL, S., TÖLLE, B., BÖHMER, S.-A., LENNARTSSON, J., ISKEN, F., MÜLLER-TIDOW, C. & BÖHMER, F.-D. 2012. Expression of protein-tyrosine phosphatases in Acute Myeloid Leukemia cells: FLT3 ITD sustains high levels of DUSP6 expression. *Cell Communication and Signaling : CCS,* 10**,** 19-19.

ARORA, D., STOPP, S., BÖHMER, S.-A., SCHONS, J., GODFREY, R., MASSON, K., RAZUMOVSKAYA, E., RÖNNSTRAND, L., TÄNZER, S., BAUER, R., BÖHMER, F.-D. & MÜLLER, J. P. 2011. Protein-tyrosine Phosphatase DEP-1 Controls Receptor Tyrosine Kinase FLT3 Signaling. *The Journal of Biological Chemistry,* 286**,** 10918-10929.

AYDIN, E., JOHANSSON, J., NAZIR, F. H., HELLSTRAND, K. & MARTNER, A. 2017. Role of NOX2-derived reactive oxygen species in NK cell-mediated control of murine melanoma metastasis. *Cancer Immunology Research,* 5**,** 804-811.

AYKIN-BURNS, N., AHMAD, I. M., ZHU, Y., OBERLEY, L. W. & SPITZ, D. R. 2009. Increased Levels Of Superoxide And Hydrogen Peroxide Mediate The Differential Susceptibility Of Cancer Cells VS. Normal Cells To Glucose Deprivation. *The Biochemical journal,* 418**,** 29-37.

AZOITEI, N., KLEGER, A., SCHOO, N., THAL, D. R., BRUNNER, C., PUSAPATI, G. V., FILATOVA, A., GENZE, F., MÖLLER, P., ACKER, T., KUEFER, R., VAN LINT, J., BAUST, H., ADLER, G. & SEUFFERLEIN, T. 2011. Protein kinase D2 is a novel regulator of glioblastoma growth and tumor formation. *Neuro-Oncology,* 13**,** 710-724.

BACHUR, N. R., GORDON, S. L. & GEE, M. V. 1977. Anthracycline Antibiotic Augmentation of Microsomal Electron Transport and Free Radical Formation. *Molecular Pharmacology,* 13**,** 901-910.

BACHUR, N. R., GORDON, S. L. & GEE, M. V. 1978. A General Mechanism for Microsomal Activation of Quinone Anticancer Agents to Free Radicals. *Cancer Research,* 38**,** 1745-1750.

BÁNFI, B., MALGRANGE, B., KNISZ, J., STEGER, K., DUBOIS-DAUPHIN, M. & KRAUSE, K.-H. 2004a. NOX3, a Superoxide-generating NADPH Oxidase of the Inner Ear. *Journal of Biological Chemistry,* 279**,** 46065-46072.

BÁNFI, B., MATURANA, A., JACONI, S., ARNAUDEAU, S., LAFORGE, T., SINHA, B., LIGETI, E., DEMAUREX, N. & KRAUSE, K.-H. 2000. A Mammalian H^+ Channel Generated Through Alternative Splicing of the NADPH Oxidase Homolog *NOH-1*. *Science,* 287**,** 138-142.

BÁNFI, B., TIRONE, F., DURUSSEL, I., KNISZ, J., MOSKWA, P., MOLNÁR, G. Z., KRAUSE, K.-H. & COX, J. A. 2004b. Mechanism of Ca^{2+} Activation of

the NADPH Oxidase 5 (NOX5). *Journal of Biological Chemistry,* 279**,** 18583-18591.
BASSIK, M. C. & KAMPMANN, M. 2011. Knocking out the door to tunicamycin entry. *Proceedings of the National Academy of Sciences,* 108**,** 11731-11732.
BATES, D. A. & WINTERBOURN, C. C. 1982. Deoxyribose breakdown by the adriamycin semiquinone and H_2O_2: evidence for hydroxyl radical participation. *FEBS Letters,* 145**,** 137-142.
BAUER, K. M., HUMMON, A. B. & BUECHLER, S. 2012. Right-side and left-side colon cancer follow different pathways to relapse. *Molecular carcinogenesis,* 51**,** 411-421.
BAYLIN, S. B. 2005. DNA methylation and gene silencing in cancer. *Nature Clinical Practice Oncology,* 2**,** S4-S11.
BEDARD, K., JAQUET, V. & KRAUSE, K.-H. 2012. NOX5: from basic biology to signaling and disease. *Free Radical Biology and Medicine,* 52**,** 725-734.
BEDARD, K. & KRAUSE, K.-H. 2007. The NOX Family of ROS-Generating NADPH Oxidases: Physiology and Pathophysiology. *Physiological Reviews,* 87**,** 245-313.
BEHREND, L., HENDERSON, G. & ZWACKA, R. M. 2003. Reactive oxygen species in oncogenic transformation. *Biochemical Society Transactions,* 31**,** 1441-1444.
BENCHEKROUN, M. N., SINHA, B. K. & ROBERT, J. 1993. Doxorubicin-induced oxygen free radical formation in sensitive and doxorubicin-resistant variants of rat glioblastoma cell lines. *FEBS letters,* 322**,** 295-298.
BERENSTEIN, R. 2015. Class III Receptor Tyrosine Kinases in Acute Leukemia – Biological Functions and Modern Laboratory Analysis. *Biomarker Insights,* 10**,** 1-14.
BHAYAT, F., DAS-GUPTA, E., SMITH, C., MCKEEVER, T. & HUBBARD, R. 2009. The incidence of and mortality from leukaemias in the UK: a general population-based study. *BMC Cancer,* 9**,** 252-252.
BIEBERICH, E. 2014. Synthesis, processing, and function of N-glycans in N-glycoproteins. *Advances in neurobiology,* 9**,** 47-70.
BIENERT, G. P. & CHAUMONT, F. 2014. Aquaporin-facilitated transmembrane diffusion of hydrogen peroxide. *Biochimica et Biophysica Acta (BBA) - General Subjects,* 1840**,** 1596-1604.
BIENERT, G. P., MØLLER, A. L. B., KRISTIANSEN, K. A., SCHULZ, A., MØLLER, I. M., SCHJOERRING, J. K. & JAHN, T. P. 2007. Specific Aquaporins Facilitate the Diffusion of Hydrogen Peroxide across Membranes. *Journal of Biological Chemistry,* 282**,** 1183-1192.
BIJUR, G. N., DE SARNO, P. & JOPE, R. S. 2000. Glycogen Synthase Kinase-3β Facilitates Staurosporine- and Heat Shock-induced Apoptosis: Protection By Lithium. *Journal of Biological Chemistry,* 275**,** 7583-7590.
BLOCK, K. & GORIN, Y. 2012. Aiding and abetting roles of NOX oxidases in cellular transformation. *Nat Rev Cancer,* 12**,** 627-637.
BLOCK, K., GORIN, Y. & ABBOUD, H. E. 2009. Subcellular localization of Nox4 and regulation in diabetes. *Proceedings of the National Academy of Sciences of the United States of America,* 106**,** 14385-14390.
BLOCK, K., GORIN, Y., HOOVER, P., WILLIAMS, P., CHELMICKI, T., CLARK, R. A., YONEDA, T. & ABBOUD, H. E. 2007. NAD(P)H Oxidases Regulate HIF-2α Protein Expression. *Journal of Biological Chemistry,* 282**,** 8019-8026.

BLOCK, K., GORIN, Y., NEW, D. D., EID, A., CHELMICKI, T., REED, A., CHOUDHURY, G. G., PAREKH, D. J. & ABBOUD, H. E. 2010. The NADPH Oxidase Subunit $p22^{phox}$ Inhibits the Function of the Tumor Suppressor Protein Tuberin. *The American Journal of Pathology,* 176**,** 2447-2455.

BLUME-JENSEN, P. & HUNTER, T. 2001. Oncogenic kinase signalling. *Nature,* 411**,** 355-365.

BÖHMER, S.-A., WEIBRECHT, I., SÖDERBERG, O. & BÖHMER, F.-D. 2013. Association of the Protein-Tyrosine Phosphatase DEP-1 with Its Substrate FLT3 Visualized by In Situ Proximity Ligation Assay. *PLOS ONE,* 8**,** e62871.

BONNET, D. & DICK, J. E. 1997. Human acute myeloid leukemia is organized as a hierarchy that originates from a primitive hematopoietic cell. *Nat Med,* 3**,** 730-737.

BRADFORD, G. B., WILLIAMS, B., ROSSI, R. & BERTONCELLO, I. 1997. Quiescence, cycling, and turnover in the primitive hematopoietic stem cell compartment. *Experimental hematology,* 25**,** 445-453.

BRANDES, R. P., WEISSMANN, N. & SCHRÖDER, K. 2014. Nox family NADPH oxidases: Molecular mechanisms of activation. *Free Radical Biology and Medicine,* 76**,** 208-226.

BRANDTS, C. H., SARGIN, B., RODE, M., BIERMANN, C., LINDTNER, B., SCHWÄBLE, J., BUERGER, H., MÜLLER-TIDOW, C., CHOUDHARY, C., MCMAHON, M., BERDEL, W. E. & SERVE, H. 2005. Constitutive Activation of Akt by Flt3 Internal Tandem Duplications Is Necessary for Increased Survival, Proliferation, and Myeloid Transformation. *Cancer Research,* 65**,** 9643-9650.

BRAR, S. S., CORBIN, Z., KENNEDY, T. P., HEMENDINGER, R., THORNTON, L., BOMMARIUS, B., ARNOLD, R. S., WHORTON, A. R., STURROCK, A. B., HUECKSTEADT, T. P., QUINN, M. T., KRENITSKY, K., ARDIE, K. G., LAMBETH, J. D. & HOIDAL, J. R. 2003. NOX5 NAD(P)H oxidase regulates growth and apoptosis in DU 145 prostate cancer cells. *American Journal of Physiology - Cell Physiology,* 285**,** C353-C369.

BRAR, S. S., KENNEDY, T. P., STURROCK, A. B., HUECKSTEADT, T. P., QUINN, M. T., WHORTON, A. R. & HOIDAL, J. R. 2002. An NAD(P)H oxidase regulates growth and transcription in melanoma cells. *American Journal of Physiology - Cell Physiology,* 282**,** C1212-C1224.

BREEMS, D. A., VAN PUTTEN, W. L. J., HUIJGENS, P. C., OSSENKOPPELE, G. J., VERHOEF, G. E. G., VERDONCK, L. F., VELLENGA, E., DE GREEF, G. E., JACKY, E., VAN DER LELIE, J., BOOGAERTS, M. A. & LÖWENBERG, B. 2005. Prognostic Index for Adult Patients With Acute Myeloid Leukemia in First Relapse. *Journal of Clinical Oncology,* 23**,** 1969-1978.

BREWER, T. F., GARCIA, F. J., ONAK, C. S., CARROLL, K. S. & CHANG, C. J. 2015. Chemical approaches to discovery and study of sources and targets of hydrogen peroxide redox signaling through NADPH oxidase proteins. *Annual review of biochemistry,* 84**,** 765-790.

BROWN, D. I. & GRIENDLING, K. K. 2009. Nox proteins in signal transduction. *Free Radical Biology and Medicine,* 47**,** 1239-1253.

BRUNET, A., BONNI, A., ZIGMOND, M. J., LIN, M. Z., JUO, P., HU, L. S., ANDERSON, M. J., ARDEN, K. C., BLENIS, J. & GREENBERG, M. E.

1999. Akt Promotes Cell Survival by Phosphorylating and Inhibiting a Forkhead Transcription Factor. *Cell,* 96**,** 857-868.

BÜCHNER, T., SCHLENK, R. F., SCHAICH, M., DÖHNER, K., KRAHL, R., KRAUTER, J., HEIL, G., KRUG, U., SAUERLAND, M. C., HEINECKE, A., SPÄTH, D., KRAMER, M., SCHOLL, S., BERDEL, W. E., HIDDEMANN, W., HOELZER, D., HEHLMANN, R., HASFORD, J., HOFFMANN, V. S., DÖHNER, H., EHNINGER, G., GANSER, A., NIEDERWIESER, D. W. & PFIRRMANN, M. 2012. Acute Myeloid Leukemia (AML): Different Treatment Strategies Versus a Common Standard Arm—Combined Prospective Analysis by the German AML Intergroup. *Journal of Clinical Oncology,* 30**,** 3604-3610.

BUETTNER, G. R., NG, C. F., WANG, M., RODGERS, V. G. J. & SCHAFER, F. Q. 2006. A New Paradigm: Manganese Superoxide Dismutase Influences the Production of H_2O_2 in Cells and Thereby Their Biological State. *Free radical biology & medicine,* 41**,** 1338-1350.

BURDICK, A. D., DAVIS, J. W., LIU, K. J., HUDSON, L. G., SHI, H., MONSKE, M. L. & BURCHIEL, S. W. 2003. Benzo(***a***)pyrene Quinones Increase Cell Proliferation, Generate Reactive Oxygen Species, and Transactivate the Epidermal Growth Factor Receptor in Breast Epithelial Cells. *Cancer Research,* 63**,** 7825-7833.

BURKE, B. 2015. Nuclear dilemma resolved. *Nature,* 522**,** 159.

BUSTAMANTE, J., GALLEANO, M., MEDRANO, E. E. & BOVERIS, A. 1990. Adriamycin effects on hydroperoxide metabolism and growth of human breast tumor cells. *Breast Cancer Research and Treatment,* 17**,** 145-153.

BUZDAR, A. U., MARCUS, C., BLUMENSCHEIN, G. R. & SMITH, T. L. 1985. Early and delayed clinical cardiotoxicity of doxorubicin. *Cancer,* 55**,** 2761-2765.

CARMODY, R. J. & COTTER, T. G. 2001. Signalling apoptosis: a radical approach. *Redox Report,* 6**,** 77-90.

CASE, A. J., LI, S., BASU, U., TIAN, J. & ZIMMERMAN, M. C. 2013. Mitochondrial-localized NADPH oxidase 4 is a source of superoxide in angiotensin II-stimulated neurons. *American Journal of Physiology - Heart and Circulatory Physiology,* 305**,** H19-H28.

CAZZOLA, M. 2016. Introduction to a review series: the 2016 revision of the WHO classification of tumors of hematopoietic and lymphoid tissues. *Blood,* 127**,** 2361-2364.

CHALLEN, G. A., SUN, D., JEONG, M., LUO, M., JELINEK, J., BERG, J. S., BOCK, C., VASANTHAKUMAR, A., GU, H., XI, Y., LIANG, S., LU, Y., DARLINGTON, G. J., MEISSNER, A., ISSA, J.-P. J., GODLEY, L. A., LI, W. & GOODELL, M. A. 2011. Dnmt3a is essential for hematopoietic stem cell differentiation. *Nature genetics,* 44**,** 23-31.

CHAN, D. W., LIU, V. W. S., TSAO, G. S. W., YAO, K.-M., FURUKAWA, T., CHAN, K. K. L. & NGAN, H. Y. S. 2008. Loss of MKP3 mediated by oxidative stress enhances tumorigenicity and chemoresistance of ovarian cancer cells. *Carcinogenesis,* 29**,** 1742-1750.

CHEN, J., DENG, F., SINGH, S. V. & WANG, Q. J. 2008a. Protein Kinase D3 (PKD3) Contributes to Prostate Cancer Cell Growth and Survival Through a PKCε/PKD3 Pathway Downstream of Akt and ERK 1/2. *Cancer Research,* 68**,** 3844-3853.

CHEN, K., KIRBER, M. T., XIAO, H., YANG, Y. & KEANEY, J. F. 2008b. Regulation of ROS signal transduction by NADPH oxidase 4 localization. *The Journal of Cell Biology,* 181**,** 1129-1139.

CHENG, G., CAO, Z., XU, X., MEIR, E. G. V. & LAMBETH, J. D. 2001. Homologs of gp91^{phox}: cloning and tissue expression of Nox3, Nox4, and Nox5. *Gene,* 269**,** 131-140.

CHENG, G., DIEBOLD, B. A., HUGHES, Y. & LAMBETH, J. D. 2006. Nox1-dependent Reactive Oxygen Generation Is Regulated by Rac1. *Journal of Biological Chemistry,* 281**,** 17718-17726.

CHENG, G. & LANZA-JACOBY, S. 2015. Metformin decreases growth of pancreatic cancer cells by decreasing reactive oxygen species: Role of NOX4. *Biochemical and Biophysical Research Communications,* 465**,** 41-46.

CHOI, A. M. K., RYTER, S. W. & LEVINE, B. 2013. Autophagy in Human Health and Disease. *New England Journal of Medicine,* 368**,** 651-662.

CHOI, J.-A., LEE, J.-W., KIM, H., KIM, E.-Y., SEO, J.-M., KO, J. & KIM, J.-H. 2010. Pro-survival of estrogen receptor-negative breast cancer cells is regulated by a BLT2–reactive oxygen species-linked signaling pathway. *Carcinogenesis,* 31**,** 543-551.

CHOUDHARY, C., BRANDTS, C., SCHWABLE, J., TICKENBROCK, L., SARGIN, B., UEKER, A., BÖHMER, F.-D., BERDEL, W. E., MÜLLER-TIDOW, C. & SERVE, H. 2007. Activation mechanisms of STAT5 by oncogenic Flt3-ITD. *Blood,* 110**,** 370-374.

CHOUDHARY, C., MÜLLER-TIDOW, C., BERDEL, W. E. & SERVE, H. 2005a. Signal Transduction of Oncogenic Flt3. *International Journal of Hematology,* 82**,** 93-99.

CHOUDHARY, C., OLSEN, J. V., BRANDTS, C., COX, J., REDDY, P. N. G., BÖHMER, F. D., GERKE, V., SCHMIDT-ARRAS, D.-E., BERDEL, W. E., MÜLLER-TIDOW, C., MANN, M. & SERVE, H. 2009. Mislocalized Activation of Oncogenic RTKs Switches Downstream Signaling Outcomes. *Molecular Cell,* 36**,** 326-339.

CHOUDHARY, C., SCHWÄBLE, J., BRANDTS, C., TICKENBROCK, L., SARGIN, B., KINDLER, T., FISCHER, T., BERDEL, W. E., MÜLLER-TIDOW, C. & SERVE, H. 2005b. AML-associated Flt3 kinase domain mutations show signal transduction differences compared with Flt3 ITD mutations. *Blood,* 106**,** 265-273.

CHRISTIANSEN, M. N., CHIK, J., LEE, L., ANUGRAHAM, M., ABRAHAMS, J. L. & PACKER, N. H. 2014. Cell surface protein glycosylation in cancer. *PROTEOMICS,* 14**,** 525-546.

CLERKIN, J. S., NAUGHTON, R., QUINEY, C. & COTTER, T. G. 2008. Mechanisms of ROS modulated cell survival during carcinogenesis. *Cancer Letters,* 266**,** 30-36.

COHEN, P. & GOEDERT, M. 2004. GSK3 inhibitors: development and therapeutic potential. *Nat Rev Drug Discov,* 3**,** 479-487.

COLEMAN, M. C., ASBURY, C. R., DANIELS, D., DU, J., AYKIN-BURNS, N., SMITH, B. J., LI, L., SPITZ, D. R. & CULLEN, J. J. 2008. 2-Deoxy-d-glucose causes cytotoxicity, oxidative stress, and radiosensitization in pancreatic cancer. *Free Radical Biology and Medicine,* 44**,** 322-331.

CONRAD, M., SANDIN, Å., FÖRSTER, H., SEILER, A., FRIJHOFF, J., DAGNELL, M., BORNKAMM, G. W., RÅDMARK, O., VAN HUIJSDUIJNEN, R. H., ASPENSTRÖM, P., BÖHMER, F. & ÖSTMAN, A.

2010. 12/15-lipoxygenase–derived lipid peroxides control receptor tyrosine kinase signaling through oxidation of protein tyrosine phosphatases. *Proceedings of the National Academy of Sciences,* 107**,** 15774-15779.
CONTESSA, J. N., BHOJANI, M. S., FREEZE, H. H., ROSS, B. D., REHEMTULLA, A. & LAWRENCE, T. S. 2010. Molecular Imaging of N-linked Glycosylation Suggests Glycan Biosynthesis is a Novel Target for Cancer Therapy. *Clinical cancer research : an official journal of the American Association for Cancer Research,* 16**,** 3205-3214.
CONWAY O'BRIEN, E., PRIDEAUX, S. & CHEVASSUT, T. 2014. The Epigenetic Landscape of Acute Myeloid Leukemia. *Advances in Hematology,* 2014**,** 15.
COOKE, M. S., EVANS, M. D., DIZDAROGLU, M. & LUNEC, J. 2003. Oxidative DNA damage: mechanisms, mutation, and disease. *The FASEB Journal,* 17**,** 1195-1214.
COX, ANDREW G., WINTERBOURN, CHRISTINE C. & HAMPTON, MARK B. 2010. Mitochondrial peroxiredoxin involvement in antioxidant defence and redox signalling. *Biochemical Journal,* 425**,** 313-325.
DANG, C. V. 2012. Links between metabolism and cancer. *Genes & Development,* 26**,** 877-890.
DANG, C. V. & SEMENZA, G. L. 1999. Oncogenic alterations of metabolism. *Trends in Biochemical Sciences,* 24**,** 68-72.
DASH, P. K., JOHNSON, D., CLARK, J., ORSI, S. A., ZHANG, M., ZHAO, J., GRILL, R. J., MOORE, A. N. & PATI, S. 2011. Involvement of the Glycogen Synthase Kinase-3 Signaling Pathway in TBI Pathology and Neurocognitive Outcome. *PLOS ONE,* 6**,** e24648.
DAVIES, M. J. 2005. The oxidative environment and protein damage. *Biochimica et Biophysica Acta (BBA) - Proteins and Proteomics,* 1703**,** 93-109.
DE KOUCHKOVSKY, I. & ABDUL-HAY, M. 2016. 'Acute myeloid leukemia: a comprehensive review and 2016 update'. *Blood Cancer Journal,* 6**,** e441.
DEBNATH, J. 2011. The Multifaceted Roles of Autophagy In Tumors--Implications For Breast Cancer. *Journal of mammary gland biology and neoplasia,* 16**,** 173-187.
DESOUKI, M. M., KULAWIEC, M., BANSAL, S., DAS, G. C. & SINGH, K. K. 2005. Cross talk between mitochondria and superoxide generating NADPH oxidase in breast and ovarian tumors. *Cancer biology & therapy,* 4**,** 1367-1373.
DHANASEKARAN, D. N. & REDDY, E. P. 2008. JNK Signaling in Apoptosis. *Oncogene,* 27**,** 6245-6251.
DIATCHUK, V., LOTAN, O., KOSHKIN, V., WIKSTROEM, P. & PICK, E. 1997. Inhibition of NADPH Oxidase Activation by 4-(2-Aminoethyl)-benzenesulfonyl Fluoride and Related Compounds. *Journal of Biological Chemistry,* 272**,** 13292-13301.
DICKINSON, B. C. & CHANG, C. J. 2011. Chemistry and biology of reactive oxygen species in signaling or stress responses. *Nat Chem Biol,* 7**,** 504-511.
DÖHNER, K. & DÖHNER, H. 2008. Molecular characterization of acute myeloid leukemia. *Haematologica,* 93**,** 976-982.
DONKÓ, Á., PÉTERFI, Z., SUM, A., LETO, T. & GEISZT, M. 2005. Dual oxidases. *Philosophical Transactions of the Royal Society B: Biological Sciences,* 360**,** 2301-2308.

DRUKER, B. J. 2009. Perspectives on the development of imatinib and the future of cancer research. *Nat Med,* 15**,** 1149-1152.
DRUMMOND, G. R., SELEMIDIS, S., GRIENDLING, K. K. & SOBEY, C. G. 2011. Combating oxidative stress in vascular disease: NADPH oxidases as therapeutic targets. *Nat Rev Drug Discov,* 10**,** 453-471.
DUFFEY, D., CROWL-BANCROFT, C., CHEN, Z., ONDREY, F., NEJAD-SATTARI, M., DONG, G. & VAN WAES, C. 2000. Inhibition of transcription factor nuclear factor-κB by a mutant inhibitor-κBα attenuates resistance of human head and neck squamous cell carcinoma to TNF-α caspase-mediated cell death. *British journal of cancer,* 83**,** 1367-1374.
EDDERKAOUI, M., NITSCHE, C., ZHENG, L., PANDOL, S. J., GUKOVSKY, I. & GUKOVSKAYA, A. S. 2011. NADPH Oxidase Activation in Pancreatic Cancer Cells Is Mediated through Akt-dependent Up-regulation of $p22^{phox}$. *Journal of Biological Chemistry,* 286**,** 7779-7787.
EHRLICH, M. 2009. DNA hypomethylation in cancer cells. *Epigenomics,* 1**,** 239-259.
EL-MIR, M.-Y., NOGUEIRA, V., FONTAINE, E., AVÉRET, N., RIGOULET, M. & LEVERVE, X. 2000. Dimethylbiguanide Inhibits Cell Respiration via an Indirect Effect Targeted on the Respiratory Chain Complex I. *Journal of Biological Chemistry,* 275**,** 223-228.
EMADI, A. & KARP, J. E. 2014. The state of the union on treatment of acute myeloid leukemia. *Leukemia & Lymphoma,* 55**,** 2423-2425.
ESTEY, E. & DÖHNER, H. 2006. Acute myeloid leukaemia. *The Lancet,* 368**,** 1894-1907.
FAN, J., LI, L., SMALL, D. & RASSOOL, F. 2010. Cells expressing FLT3/ITD mutations exhibit elevated repair errors generated through alternative NHEJ pathways: implications for genomic instability and therapy. *Blood,* 116**,** 5298-5305.
FATHI, A. & LEVIS, M. 2011. FLT3 inhibitors: A Story of the Old and the New. *Current opinion in hematology,* 18**,** 71-76.
FENSKI, R., FLESCH, K., SERVE, S., MIZUKI, M., OELMANN, E., KRATZ, A. K., KIENAST, J., LEO, R., SCHWARTZ, S., BERDEL, W. E. & SERVE, H. 2000. Constitutive activation of FLT3 in acute myeloid leukaemia and its consequences for growth of 32D cells. *British Journal of Haematology,* 108**,** 322-330.
FERLAY, J., SOERJOMATARAM, I., DIKSHIT, R., ESER, S., MATHERS, C., REBELO, M., PARKIN, D. M., FORMAN, D. & BRAY, F. 2015. Cancer incidence and mortality worldwide: Sources, methods and major patterns in GLOBOCAN 2012. *International Journal of Cancer,* 136**,** E359-E386.
FERREIRA, H. J., HEYN, H., VIZOSO, M., MOUTINHO, C., VIDAL, E., GOMEZ, A., MARTÍNEZ-CARDÚS, A., SIMÓ-RIUDALBAS, L., MORAN, S., JOST, E. & ESTELLER, M. 2015. DNMT3A mutations mediate the epigenetic reactivation of the leukemogenic factor MEIS1 in acute myeloid leukemia. *Oncogene,* 35**,** 3079-3082.
FIGUEROA, M. E., ABDEL-WAHAB, O., LU, C., WARD, P. S., PATEL, J., SHIH, A., LI, Y., BHAGWAT, N., VASANTHAKUMAR, A., FERNANDEZ, H. F., TALLMAN, M. S., SUN, Z., WOLNIAK, K., PEETERS, J. K., LIU, W., CHOE, S. E., FANTIN, V. R., PAIETTA, E., LÖWENBERG, B., LICHT, J. D., GODLEY, L. A., DELWEL, R., VALK, P. J. M., THOMPSON, C. B., LEVINE, R. L. & MELNICK, A. 2010.

Leukemic IDH1 and IDH2 Mutations Result in a Hypermethylation Phenotype, Disrupt TET2 Function, and Impair Hematopoietic Differentiation. *Cancer Cell,* 18**,** 553-567.
FINKEL, T. 2011. Signal transduction by reactive oxygen species. *The Journal of Cell Biology,* 194**,** 7-15.
FREEZE, H. H. & NG, B. G. 2011. Golgi Glycosylation and Human Inherited Diseases. *Cold Spring Harbor Perspectives in Biology,* 3**,** a005371.
FU, X., BEER, D. G., BEHAR, J., WANDS, J., LAMBETH, D. & CAO, W. 2006. cAMP-response Element-binding Protein Mediates Acid-induced NADPH Oxidase NOX5-S Expression in Barrett Esophageal Adenocarcinoma Cells. *Journal of Biological Chemistry,* 281**,** 20368-20382.
FUJIWARA, T., ODA, K., YOKOTA, S., TAKATSUKI, A. & IKEHARA, Y. 1988. Brefeldin A causes disassembly of the Golgi complex and accumulation of secretory proteins in the endoplasmic reticulum. *Journal of Biological Chemistry,* 263**,** 18545-52.
FUKAI, T. & USHIO-FUKAI, M. 2011. Superoxide Dismutases: Role in Redox Signaling, Vascular Function, and Diseases. *Antioxidants & Redox Signaling,* 15**,** 1583-1606.
FUKUYAMA, M., ROKUTAN, K., SANO, T., MIYAKE, H., SHIMADA, M. & TASHIRO, S. 2005. Overexpression of a novel superoxide-producing enzyme, NADPH oxidase 1, in adenoma and well differentiated adenocarcinoma of the human colon. *Cancer Letters,* 221**,** 97-104.
GAO, H.-M., ZHOU, H. & HONG, J.-S. 2012. NADPH oxidases: novel therapeutic targets for neurodegenerative diseases. *Trends in Pharmacological Sciences,* 33**,** 295-303.
GILLILAND, D. G. & GRIFFIN, J. D. 2002. The roles of FLT3 in hematopoiesis and leukemia. *Blood,* 100**,** 1532-1542.
GIORGIO, M., TRINEI, M., MIGLIACCIO, E. & PELICCI, P. G. 2007. Hydrogen peroxide: a metabolic by-product or a common mediator of ageing signals? *Nat Rev Mol Cell Biol,* 8**,** 722-728.
GODFREY, R., ARORA, D., BAUER, R., STOPP, S., MÜLLER, J. P., HEINRICH, T., BÖHMER, S.-A., DAGNELL, M., SCHNETZKE, U., SCHOLL, S., ÖSTMAN, A. & BÖHMER, F.-D. 2012. Cell transformation by FLT3 ITD in acute myeloid leukemia involves oxidative inactivation of the tumor suppressor protein-tyrosine phosphatase DEP-1/ PTPRJ. *Blood,* 119**,** 4499-4511.
GONCALVES, R. L. S., QUINLAN, C. L., PEREVOSHCHIKOVA, I. V., HEY-MOGENSEN, M. & BRAND, M. D. 2015. Sites of Superoxide and Hydrogen Peroxide Production by Muscle Mitochondria Assessed *ex Vivo* under Conditions Mimicking Rest and Exercise. *Journal of Biological Chemistry,* 290**,** 209-227.
GONZALEZ DE PEREDO, A., KLEIN, D., MACEK, B., HESS, D., PETER-KATALINIC, J. & HOFSTEENGE, J. 2002. C-Mannosylation and O-Fucosylation of Thrombospondin Type 1 Repeats. *Molecular & Cellular Proteomics,* 1**,** 11-18.
GOODMAN, J. & HOCHSTEIN, P. 1977. Generation of free radicals and lipid peroxidation by redox cycling of adriamycin and daunomycin. *Biochemical and Biophysical Research Communications,* 77**,** 797-803.
GORDILLO, G., FANG, H., PARK, H. & ROY, S. 2010. Nox-4–Dependent Nuclear H_2O_2 Drives DNA Oxidation Resulting in 8-OHdG as Urinary

Biomarker and Hemangioendothelioma Formation. *Antioxidants & Redox Signaling,* 12**,** 933-943.
GORIN, Y. & BLOCK, K. 2013. Nox as a target for diabetic complications. *Clinical Science,* 125**,** 361-382.
GORRINI, C., HARRIS, I. S. & MAK, T. W. 2013. Modulation of oxidative stress as an anticancer strategy. *Nat Rev Drug Discov,* 12**,** 931-947.
GOUAZÉ, V., MIRAULT, M.-E., CARPENTIER, S., SALVAYRE, R., LEVADE, T. & ANDRIEU-ABADIE, N. 2001. Glutathione Peroxidase-1 Overexpression Prevents Ceramide Production and Partially Inhibits Apoptosis in Doxorubicin-Treated Human Breast Carcinoma Cells. *Molecular Pharmacology,* 60**,** 488-496.
GOUGH, D. R. & COTTER, T. G. 2011. Hydrogen peroxide: a Jekyll and Hyde signalling molecule. *Cell Death and Dis,* 2**,** e213.
GOYAL, P., WEISSMANN, N., ROSE, F., GRIMMINGER, F., SCHÄFERS, H. J., SEEGER, W. & HÄNZE, J. 2005. Identification of novel Nox4 splice variants with impact on ROS levels in A549 cells. *Biochemical and Biophysical Research Communications,* 329**,** 32-39.
GRAFONE, T., PALMISANO, M., NICCI, C. & STORTI, S. 2012. An overview on the role of FLT3-tyrosine kinase receptor in acute myeloid leukemia: biology and treatment. *Oncology Reviews,* 6**,** e8.
GRAHAM, K. A., KULAWIEC, M., OWENS, K. M., LI, X., DESOUKI, M. M., CHANDRA, D. & SINGH, K. K. 2010. NADPH oxidase 4 is an oncoprotein localized to mitochondria. *Cancer Biology & Therapy,* 10**,** 223-231.
GROEGER, G., QUINEY, C. & COTTER, T. G. 2009. Hydrogen Peroxide as a Cell-Survival Signaling Molecule. *Antioxidants & Redox Signaling,* 11**,** 2655-2671.
GROEMPING, Y., LAPOUGE, K., SMERDON, S. J. & RITTINGER, K. 2003. Molecular Basis of Phosphorylation-Induced Activation of the NADPH Oxidase. *Cell,* 113**,** 343-355.
GROEMPING, Y. & RITTINGER, K. 2005. Activation and assembly of the NADPH oxidase: a structural perspective. *Biochemical Journal,* 386**,** 401-416.
GRUNDLER, R., MIETHING, C., THIEDE, C., PESCHEL, C. & DUYSTER, J. 2005. FLT3-ITD and tyrosine kinase domain mutants induce 2 distinct phenotypes in a murine bone marrow transplantation model. *Blood,* 105**,** 4792-4799.
GUAN, Y., RALPH, S. & HOGGE, D. E. 2002. Polyclonal normal hematopoietic progenitors in patients with acute myeloid leukemia. *Experimental Hematology,* 30**,** 721-728.
GUIDA, M., MARALDI, T., BERETTI, F., FOLLO, M. Y., MANZOLI, L. & DE POL, A. 2014. Nuclear Nox4-Derived Reactive Oxygen Species in Myelodysplastic Syndromes. *BioMed Research International,* 2014**,** 11.
GUIDA, M., MARALDI, T., RESCA, E., BERETTI, F., ZAVATTI, M., BERTONI, L., LA SALA, G. B. & DE POL, A. 2013. Inhibition of Nuclear Nox4 Activity by Plumbagin: Effect on Proliferative Capacity in Human Amniotic Stem Cells. *Oxidative Medicine and Cellular Longevity,* 2013**,** 12.
HÁJKOVÁ, H., MARKOVÁ, J., HAŠKOVEC, C., ŠÁROVÁ, I., FUCHS, O., KOSTEČKA, A., CETKOVSKÝ, P., MICHALOVÁ, K. & SCHWARZ, J. 2012. Decreased DNA methylation in acute myeloid leukemia patients with

DNMT3A mutations and prognostic implications of DNA methylation. *Leukemia Research,* 36**,** 1128-1133.
HAN, M., ZHANG, T., YANG, L., WANG, Z., RUAN, J. & CHANG, X. 2016. Association between NADPH oxidase (NOX) and lung cancer: a systematic review and meta-analysis. *Journal of Thoracic Disease,* 8**,** 1704-1711.
HANDY, D. E. & LOSCALZO, J. 2012. Redox Regulation of Mitochondrial Function. *Antioxidants & Redox Signaling,* 16**,** 1323-1367.
HAO, Q., MCKENZIE, R., GAN, H. & TANG, H. 2013. Protein Kinases D2 and D3 Are Novel Growth Regulators in HCC1806 Triple-negative Breast Cancer Cells. *Anticancer Research,* 33**,** 393-399.
HARRIS, A. L. 2002. Hypoxia — a key regulatory factor in tumour growth. *Nat Rev Cancer,* 2**,** 38-47.
HART, P. C., MAO, M., DE ABREU, A. L. P., ANSENBERGER-FRICANO, K., EKOUE, D. N., GANINI, D., KAJDACSY-BALLA, A., DIAMOND, A. M., MINSHALL, R. D., CONSOLARO, M. E. L., SANTOS, J. H. & BONINI, M. G. 2015. MnSOD upregulation sustains the Warburg effect via mitochondrial ROS and AMPK-dependent signalling in cancer. *Nature Communications,* 6**,** 6053.
HAWKES, W. C. & ALKAN, Z. 2010. Regulation of Redox Signaling by Selenoproteins. *Biological Trace Element Research,* 134**,** 235-251.
HAYAKAWA, F., TOWATARI, M., KIYOI, H., TANIMOTO, M., KITAMURA, T., SAITO, H. & NAOE, T. 2000. Tandem-duplicated Flt3 constitutively activates STAT5 and MAP kinase and introduces autonomous cell growth in IL-3-dependent cell lines. *Oncogene,* 19**,** 624-631.
HAYNES, P. A. 1998. Phosphoglycosylation: A new structural class of glycosylation? *Glycobiology,* 8**,** 1-5.
HELENIUS, A. & AEBI, M. 2004. Roles of N-linked glycans in the endoplasmic reticulum. *Annual review of biochemistry,* 73**,** 1019-1049.
HELMCKE, I., HEUMÜLLER, S., TIKKANEN, R., SCHRÖDER, K. & BRANDES, R. P. 2008. Identification of Structural Elements in Nox1 and Nox4 Controlling Localization and Activity. *Antioxidants & Redox Signaling,* 11**,** 1279-1287.
HERTOG, J. D., ÖSTMAN, A. & BÖHMER, F. D. 2008. Protein tyrosine phosphatases: regulatory mechanisms. *FEBS journal,* 275**,** 831-847.
HILENSKI, L. L., CLEMPUS, R. E., QUINN, M. T., LAMBETH, J. D. & GRIENDLING, K. K. 2004. Distinct Subcellular Localizations of Nox1 and Nox4 in Vascular Smooth Muscle Cells. *Arteriosclerosis, Thrombosis, and Vascular Biology,* 24**,** 677-683.
HOLE, P. S., DARLEY, R. L. & TONKS, A. 2011. Do reactive oxygen species play a role in myeloid leukemias? *Blood,* 117**,** 5816-5826.
HOLE, P. S., ZABKIEWICZ, J., MUNJE, C., NEWTON, Z., PEARN, L., WHITE, P., MARQUEZ, N., HILLS, R. K., BURNETT, A. K., TONKS, A. & DARLEY, R. L. 2013. Overproduction of NOX-derived ROS in AML promotes proliferation and is associated with defective oxidative stress signaling. *Blood,* 122**,** 3322-3330.
HOLMSTROM, K. M. & FINKEL, T. 2014. Cellular mechanisms and physiological consequences of redox-dependent signalling. *Nat Rev Mol Cell Biol,* 15**,** 411-421.
HOLZ-SCHIETINGER, C., MATJE, D. M. & REICH, N. O. 2012. Mutations in DNA Methyltransferase (DNMT3A) Observed in Acute Myeloid Leukemia

Patients Disrupt Processive Methylation. *The Journal of Biological Chemistry,* 287**,** 30941-30951.
HOSHI, T. & HEINEMANN, S. H. 2001. Regulation of cell function by methionine oxidation and reduction. *The Journal of Physiology,* 531**,** 1-11.
HOUNSELL, E. F., DAVIES, M. J. & RENOUF, D. V. 1996. O-linked protein glycosylation structure and function. *Glycoconjugate Journal,* 13**,** 19-26.
HUANG, W.-C., LI, X., LIU, J., LIN, J. & CHUNG, L. W. K. 2012. Activation of Androgen Receptor, Lipogenesis, and Oxidative Stress Converged by SREBP-1 Is Responsible for Regulating Growth and Progression of Prostate Cancer Cells. *Molecular Cancer Research,* 10**,** 133-142.
HURTADO-NEDELEC, M., CSILLAG-GRANGE, M.-J., BOUSSETTA, T., BELAMBRI, S. A., FAY, M., CASSINAT, B., GOUGEROT-POCIDALO, M.-A., DANG, P. M.-C. & EL-BENNA, J. 2013. Increased reactive oxygen species production and $p47^{phox}$ phosphorylation in neutrophils from myeloproliferative disorders patients with *JAK2* (V617F) mutation. *Haematologica,* 98**,** 1517-1524.
IRANI, K., XIA, Y., ZWEIER, J. L., SOLLOTT, S. J., DER, C. J., FEARON, E. R., SUNDARESAN, M., FINKEL, T. & GOLDSCHMIDT-CLERMONT, P. J. 1997. Mitogenic Signaling Mediated by Oxidants in Ras-Transformed Fibroblasts. *Science,* 275**,** 1649-1652.
ISLAM, M., MOHAMED, Z. & ASSENOV, Y. 2017. Differential Analysis of Genetic, Epigenetic, and Cytogenetic Abnormalities in AML. *International Journal of Genomics,* 2017**,** 13.
JACKSON, S. H., DEVADAS, S., KWON, J., PINTO, L. A. & WILLIAMS, M. S. 2004. T cells express a phagocyte-type NADPH oxidase that is activated after T cell receptor stimulation. *Nat Immunol,* 5**,** 818-827.
JANSSEN, A., BOSMAN, C., KRUIDENIER, L., GRIFFIOEN, G., LAMERS, C., VAN KRIEKEN, J., VAN DE VELDE, C. & VERSPAGET, H. 1999. Superoxide dismutases in the human colorectal cancer sequence. *Journal of cancer research and clinical oncology,* 125**,** 327-335.
JAYAVELU, A., MÜLLER, J., BAUER, R., BÖHMER, S., LÄSSIG, J., CERNY-REITERER, S., SPERR, W., VALENT, P., MAURER, B. & MORIGGL, R. 2016a. NOX4-driven ROS formation mediates PTP inactivation and cell transformation in FLT3ITD-positive AML cells. *Leukemia,* 30**,** 473-483.
JAYAVELU, A. K., MOLONEY, J. N., BÖHMER, F.-D. & COTTER, T. G. 2016b. NOX-driven ROS formation in cell transformation of FLT3-ITD-positive AML. *Experimental Hematology,* 44**,** 1113-1122.
JEFFERIS, R. 2007. 4.20 - Human IgG Glycosylation in Inflammation and Inflammatory Disease A2 - Kamerling, Hans. *Comprehensive Glycoscience.* Oxford: Elsevier.
JITSCHIN, R., HOFMANN, A. D., BRUNS, H., GIEßL, A., BRICKS, J., BERGER, J., SAUL, D., ECKART, M. J., MACKENSEN, A. & MOUGIAKAKOS, D. 2014. Mitochondrial metabolism contributes to oxidative stress and reveals therapeutic targets in chronic lymphocytic leukemia. *Blood,* 123**,** 2663-2672.
JUHASZ, A., GE, Y. U. N., MARKEL, S., CHIU, A., MATSUMOTO, L., VAN BALGOOY, J., ROY, K. & DOROSHOW, J. H. 2009. Expression of NADPH oxidase homologues and accessory genes in human cancer cell lines, tumours and adjacent normal tissues. *Free radical research,* 43**,** 523-532.

KAMIGUTI, A. S., SERRANDER, L., LIN, K., HARRIS, R. J., CAWLEY, J. C., ALLSUP, D. J., SLUPSKY, J. R., KRAUSE, K.-H. & ZUZEL, M. 2005. Expression and Activity of NOX5 in the Circulating Malignant B Cells of Hairy Cell Leukemia. *The Journal of Immunology,* 175**,** 8424-8430.

KAWAHARA, T., KOHJIMA, M., KUWANO, Y., MINO, H., TESHIMA-KONDO, S., TAKEYA, R., TSUNAWAKI, S., WADA, A., SUMIMOTO, H. & ROKUTAN, K. 2005a. *Helicobacter pylori* lipopolysaccharide activates Rac1 and transcription of NADPH oxidase Nox1 and its organizer NOXO1 in guinea pig gastric mucosal cells. *American Journal of Physiology - Cell Physiology,* 288**,** C450-C457.

KAWAHARA, T., RITSICK, D., CHENG, G. & LAMBETH, J. D. 2005b. Point Mutations in the Proline-rich Region of $p22^{phox}$ Are Dominant Inhibitors of Nox1- and Nox2-dependent Reactive Oxygen Generation. *Journal of Biological Chemistry,* 280**,** 31859-31869.

KAWAMURA, N., KUGIMIYA, F., OSHIMA, Y., OHBA, S., IKEDA, T., SAITO, T., SHINODA, Y., KAWASAKI, Y., OGATA, N., HOSHI, K., AKIYAMA, T., CHEN, W. S., HAY, N., TOBE, K., KADOWAKI, T., AZUMA, Y., TANAKA, S., NAKAMURA, K., CHUNG, U.-I. & KAWAGUCHI, H. 2007. Akt1 in Osteoblasts and Osteoclasts Controls Bone Remodeling. *PLOS ONE,* 2**,** e1058.

KAYSER, S., SCHLENK, R. F., LONDONO, M. C., BREITENBUECHER, F., WITTKE, K., DU, J., GRONER, S., SPÄTH, D., KRAUTER, J., GANSER, A., DÖHNER, H., FISCHER, T. & DÖHNER, K. 2009. Insertion of *FLT3* internal tandem duplication in the tyrosine kinase domain-1 is associated with resistance to chemotherapy and inferior outcome. *Blood,* 114**,** 2386-2392.

KENNEDY, N. J. & DAVIS, R. J. 2003. Role of JNK in tumor development. *Cell cycle (Georgetown, Tex.),* 2**,** 199-201.

KHAVARI, T. A. & RINN, J. L. 2007. Ras/Erk MAPK signaling in epidermal homeostasis and neoplasia. *Cell Cycle,* 6**,** 2928-2931.

KIM, J. H., CHU, S. C., GRAMLICH, J. L., PRIDE, Y. B., BABENDREIER, E., CHAUHAN, D., SALGIA, R., PODAR, K., GRIFFIN, J. D. & SATTLER, M. 2005. Activation of the PI3K/mTOR pathway by BCR-ABL contributes to increased production of reactive oxygen species. *Blood,* 105**,** 1717-1723.

KLEIN, E. A., THOMPSON, I. M., TANGEN, C. M., CROWLEY, J. J., LUCIA, M. S., GOODMAN, P. J., MINASIAN, L., FORD, L. G., PARNES, H. L., GAZIANO, J. M., KARP, D. D., LIEBER, M. M., WALTHER, P. J., KLOTZ, L., PARSONS, J. K., CHIN, J. L., DARKE, A. K., LIPPMAN, S. M., GOODMAN, G. E., MEYSKENS, F. L. & BAKER, L. H. 2011. Vitamin E and the Risk of Prostate Cancer: Updated Results of The Selenium and Vitamin E Cancer Prevention Trial (SELECT). *JAMA,* 306**,** 1549-1556.

KOBAYASHI, S., NOJIMA, Y., SHIBUYA, M. & MARU, Y. 2004. Nox1 regulates apoptosis and potentially stimulates branching morphogenesis in sinusoidal endothelial cells. *Experimental Cell Research,* 300**,** 455-462.

KOCH, S., JACOBI, A., RYSER, M., EHNINGER, G. & THIEDE, C. 2008. Abnormal Localization and Accumulation of FLT3-ITD, a Mutant Receptor Tyrosine Kinase Involved in Leukemogenesis. *Cells Tissues Organs,* 188**,** 225-235.

KOMATSU, M., KUROKAWA, H., WAGURI, S., TAGUCHI, K., KOBAYASHI, A., ICHIMURA, Y., SOU, Y.-S., UENO, I., SAKAMOTO, A., TONG, K. I.,

KIM, M., NISHITO, Y., IEMURA, S.-I., NATSUME, T., UENO, T., KOMINAMI, E., MOTOHASHI, H., TANAKA, K. & YAMAMOTO, M. 2010. The selective autophagy substrate p62 activates the stress responsive transcription factor Nrf2 through inactivation of Keap1. *Nat Cell Biol,* 12**,** 213-223.

KONIG, H. & LEVIS, M. 2015. Targeting FLT3 to treat leukemia. *Expert opinion on therapeutic targets,* 19**,** 37-54.

KOPTYRA, M., FALINSKI, R., NOWICKI, M. O., STOKLOSA, T., MAJSTEREK, I., NIEBOROWSKA-SKORSKA, M., BLASIAK, J. & SKORSKI, T. 2006. BCR/ABL kinase induces self-mutagenesis via reactive oxygen species to encode imatinib resistance. *Blood,* 108**,** 319-327.

KÖTHE, S., MÜLLER, J. P., BÖHMER, S.-A., TSCHONGOV, T., FRICKE, M., KOCH, S., THIEDE, C., REQUARDT, R. P., RUBIO, I. & BÖHMER, F. D. 2013. Features of Ras activation by a mislocalized oncogenic tyrosine kinase: FLT3 ITD signals through K-Ras at the plasma membrane of acute myeloid leukemia cells. *Journal of Cell Science,* 126**,** 4746-4755.

KRÖLLER-SCHÖN, S., STEVEN, S., KOSSMANN, S., SCHOLZ, A., DAUB, S., OELZE, M., XIA, N., HAUSDING, M., MIKHED, Y., ZINßIUS, E., MADER, M., STAMM, P., TREIBER, N., SCHARFFETTER-KOCHANEK, K., LI, H., SCHULZ, E., WENZEL, P., MÜNZEL, T. & DAIBER, A. 2014. Molecular Mechanisms of the Crosstalk Between Mitochondria and NADPH Oxidase Through Reactive Oxygen Species—Studies in White Blood Cells and in Animal Models. *Antioxidants & Redox Signaling,* 20**,** 247-266.

KRUISWIJK, F., LABUSCHAGNE, C. F. & VOUSDEN, K. H. 2015. p53 in survival, death and metabolic health: a lifeguard with a licence to kill. *Nat Rev Mol Cell Biol,* 16**,** 393-405.

KUMAR, B., KOUL, S., KHANDRIKA, L., MEACHAM, R. B. & KOUL, H. K. 2008. Oxidative Stress Is Inherent in Prostate Cancer Cells and Is Required for Aggressive Phenotype. *Cancer Research,* 68**,** 1777-1785.

KUMAR, C. C. 2011. Genetic Abnormalities and Challenges in the Treatment of Acute Myeloid Leukemia. *Genes & Cancer,* 2**,** 95-107.

KUO, L. J. & YANG, L.-X. 2008. γ-H2AX - A Novel Biomarker for DNA Double-strand Breaks. *In Vivo,* 22**,** 305-309.

KURODA, J., NAKAGAWA, K., YAMASAKI, T., NAKAMURA, K.-I., TAKEYA, R., KURIBAYASHI, F., IMAJOH-OHMI, S., IGARASHI, K., SHIBATA, Y., SUEISHI, K. & SUMIMOTO, H. 2005. The superoxide-producing NAD(P)H oxidase Nox4 in the nucleus of human vascular endothelial cells. *Genes to Cells,* 10**,** 1139-1151.

KUROSU, T., NAGAO, T., WU, N., OSHIKAWA, G. & MIURA, O. 2013. Inhibition of the PI3K/Akt/GSK3 Pathway Downstream of BCR/ABL, Jak2-V617F, or FLT3-ITD Downregulates DNA Damage-Induced Chk1 Activation as Well as G2/M Arrest and Prominently Enhances Induction of Apoptosis. *PLOS ONE,* 8**,** e79478.

LADDHA, S. V., GANESAN, S., CHAN, C. S. & WHITE, E. 2014. Mutational Landscape of the Essential Autophagy Gene BECN1 in Human Cancers. *Molecular cancer research : MCR,* 12**,** 485-490.

LAL, R., LIND, K., HEITZER, E., ULZ, P., AUBELL, K., KASHOFER, K., MIDDEKE, J. M., THIEDE, C., SCHULZ, E., ROSENBERGER, A., HOFER, S., FEILHAUER, B., RINNER, B., SVENDOVA, V., SCHIMEK, M. G., RÜCKER, F. G., HOEFLER, G., DÖHNER, K., ZEBISCH, A.,

WÖLFLER, A. & SILL, H. 2017. Somatic *TP53* mutations characterize preleukemic stem cells in acute myeloid leukemia. *Blood,* 129**,** 2587-2591.
LANDRY, W. D., WOOLLEY, J. F. & COTTER, T. G. 2013. Imatinib and Nilotinib inhibit Bcr–Abl-induced ROS through targeted degradation of the NADPH oxidase subunit $p22^{phox}$. *Leukemia Research,* 37**,** 183-189.
LANE, S. W. & GILLILAND, D. G. 2010. Leukemia stem cells. *Seminars in Cancer Biology,* 20**,** 71-76.
LANE, S. W., SCADDEN, D. T. & GILLILAND, D. G. 2009. The leukemic stem cell niche: current concepts and therapeutic opportunities. *Blood,* 114**,** 1150-1157.
LEE, J.-W. & HELMANN, J. D. 2006. The PerR transcription factor senses H_2O_2 by metal-catalysed histidine oxidation. *Nature,* 440**,** 363-367.
LEE, J. K., EDDERKAOUI, M., TRUONG, P., OHNO, I., JANG, K. T., BERTI, A., PANDOL, S. J. & GUKOVSKAYA, A. S. 2007. NADPH Oxidase Promotes Pancreatic Cancer Cell Survival via Inhibiting JAK2 Dephosphorylation by Tyrosine Phosphatases. *Gastroenterology,* 133**,** 1637-1648.
LEE, S.-R., YANG, K.-S., KWON, J., LEE, C., JEONG, W. & RHEE, S. G. 2002. Reversible Inactivation of the Tumor Suppressor PTEN by H_2O_2. *Journal of Biological Chemistry,* 277**,** 20336-20342.
LEE, W. C., CHOI, C. H., CHA, S. H., OH, H. L. & KIM, Y. K. 2005. Role of ERK in hydrogen peroxide-induced cell death of human glioma cells. *Neurochemical research,* 30**,** 263-270.
LEE, Y.-M., KIM, B.-J., CHUN, Y.-S., SO, I., CHOI, H., KIM, M.-S. & PARK, J.-W. 2006. NOX4 as an oxygen sensor to regulate TASK-1 activity. *Cellular Signalling,* 18**,** 499-507.
LESLIE, N. R., BENNETT, D., LINDSAY, Y. E., STEWART, H., GRAY, A. & DOWNES, C. P. 2003. Redox regulation of PI 3-kinase signalling via inactivation of PTEN. *The EMBO Journal,* 22**,** 5501-5510.
LEVINE, A. J. & OREN, M. 2009. The first 30 years of p53: growing ever more complex. *Nat Rev Cancer,* 9**,** 749-758.
LEVINE, E. G. & BLOOMFIELD, C. D. 1992. Leukemias and myelodysplastic syndromes secondary to drug, radiation, and environmental exposure. *Seminars in oncology,* 19**,** 47-84.
LEVIS, M. 2011. FLT3/ITD AML and the law of unintended consequences. *Blood,* 117**,** 6987-6990.
LEVIS, M. 2013. FLT3 mutations in acute myeloid leukemia: what is the best approach in 2013? *Hematology / the Education Program of the American Society of Hematology. American Society of Hematology. Education Program,* 2013**,** 220-226.
LEVIS, M., RAVANDI, F., WANG, E. S., BAER, M. R., PERL, A., COUTRE, S., ERBA, H., STUART, R. K., BACCARANI, M., CRIPE, L. D., TALLMAN, M. S., MELONI, G., GODLEY, L. A., LANGSTON, A. A., AMADORI, S., LEWIS, I. D., NAGLER, A., STONE, R., YEE, K., ADVANI, A., DOUER, D., WIKTOR-JEDRZEJCZAK, W., JULIUSSON, G., LITZOW, M. R., PETERSDORF, S., SANZ, M., KANTARJIAN, H. M., SATO, T., TREMMEL, L., BENSEN-KENNEDY, D. M., SMALL, D. & SMITH, B. D. 2011. Results from a randomized trial of salvage chemotherapy followed by lestaurtinib for patients with FLT3 mutant AML in first relapse. *Blood,* 117**,** 3294-3301.

LEVIS, M. & SMALL, D. 2003. FLT3: ITDoes matter in leukemia. *Leukemia,* 17**,** 1738-1752.

LEY, T. J., DING, L., WALTER, M. J., MCLELLAN, M. D., LAMPRECHT, T., LARSON, D. E., KANDOTH, C., PAYTON, J. E., BATY, J., WELCH, J., HARRIS, C. C., LICHTI, C. F., TOWNSEND, R. R., FULTON, R. S., DOOLING, D. J., KOBOLDT, D. C., SCHMIDT, H., ZHANG, Q., OSBORNE, J. R., LIN, L., O'LAUGHLIN, M., MCMICHAEL, J. F., DELEHAUNTY, K. D., MCGRATH, S. D., FULTON, L. A., MAGRINI, V. J., VICKERY, T. L., HUNDAL, J., COOK, L. L., CONYERS, J. J., SWIFT, G. W., REED, J. P., ALLDREDGE, P. A., WYLIE, T., WALKER, J., KALICKI, J., WATSON, M. A., HEATH, S., SHANNON, W. D., VARGHESE, N., NAGARAJAN, R., WESTERVELT, P., TOMASSON, M. H., LINK, D. C., GRAUBERT, T. A., DIPERSIO, J. F., MARDIS, E. R. & WILSON, R. K. 2010. DNMT3A Mutations in Acute Myeloid Leukemia. *The New England journal of medicine,* 363**,** 2424-2433.

LI, L., ISHDORJ, G. & GIBSON, S. B. 2012. Reactive oxygen species regulation of autophagy in cancer: Implications for cancer treatment. *Free Radical Biology and Medicine,* 53**,** 1399-1410.

LIANG, X. H., JACKSON, S., SEAMAN, M., BROWN, K., KEMPKES, B., HIBSHOOSH, H. & LEVINE, B. 1999. Induction of autophagy and inhibition of tumorigenesis by beclin 1. *Nature,* 402**,** 672-676.

LIM, S. D., SUN, C., LAMBETH, J. D., MARSHALL, F., AMIN, M., CHUNG, L., PETROS, J. A. & ARNOLD, R. S. 2005. Increased Nox1 and hydrogen peroxide in prostate cancer. *The Prostate,* 62**,** 200-207.

LIMAYE, V., LI, X., HAHN, C., XIA, P., BERNDT, M. C., VADAS, M. A. & GAMBLE, J. R. 2005. Sphingosine kinase-1 enhances endothelial cell survival through a PECAM-1–dependent activation of PI-3K/Akt and regulation of Bcl-2 family members. *Blood,* 105**,** 3169-3177.

LIN, T. L. & LEVY, M. Y. 2012. Acute Myeloid Leukemia: Focus on Novel Therapeutic Strategies. *Clinical Medicine Insights. Oncology,* 6**,** 205-217.

LIOU, G.-Y., DÖPPLER, H., DELGIORNO, KATHLEEN E., ZHANG, L., LEITGES, M., CRAWFORD, HOWARD C., MURPHY, MICHAEL P. & STORZ, P. 2016. Mutant KRas-Induced Mitochondrial Oxidative Stress in Acinar Cells Upregulates EGFR Signaling to Drive Formation of Pancreatic Precancerous Lesions. *Cell Reports,* 14**,** 2325-2336.

LIOU, G.-Y. & STORZ, P. 2010. Reactive oxygen species in cancer. *Free radical research,* 44**,** 479-496.

LIS, H. & SHARON, N. 1993. Protein glycosylation. *European Journal of Biochemistry,* 218**,** 1-27.

LIU, L.-Z., HU, X.-W., XIA, C., HE, J., ZHOU, Q., SHI, X., FANG, J. & JIANG, B.-H. 2006. Reactive oxygen species regulate epidermal growth factor-induced vascular endothelial growth factor and hypoxia-inducible factor-1α expression through activation of AKT and P70S6K1 in human ovarian cancer cells. *Free Radical Biology and Medicine,* 41**,** 1521-1533.

LIU, R.-M., CHOI, J., WU, J.-H., GASTON PRAVIA, K. A., LEWIS, K. M., BRAND, J. D., MOCHEL, N. S. R., KRZYWANSKI, D. M., LAMBETH, J. D., HAGOOD, J. S., FORMAN, H. J., THANNICKAL, V. J. & POSTLETHWAIT, E. M. 2010. Oxidative Modification of Nuclear Mitogen-activated Protein Kinase Phosphatase 1 Is Involved in Transforming Growth

Factor β1-induced Expression of Plasminogen Activator Inhibitor 1 in Fibroblasts. *Journal of Biological Chemistry,* 285**,** 16239-16247.
LIVAK, K. J. & SCHMITTGEN, T. D. 2001. Analysis of Relative Gene Expression Data Using Real-Time Quantitative PCR and the 2−ΔΔCT Method. *Methods,* 25**,** 402-408.
LLS. 2011. *The Leukemia and Lymphoma Society, Leukemia facts and statistics* [Online]. [Accessed].
LOEB, L. A., LOEB, K. R. & ANDERSON, J. P. 2003. Multiple mutations and cancer. *Proceedings of the National Academy of Sciences,* 100**,** 776-781.
LOTEM, J., PELED-KAMAR, M., GRONER, Y. & SACHS, L. 1996. Cellular oxidative stress and the control of apoptosis by wild-type p53, cytotoxic compounds, and cytokines. *Proceedings of the National Academy of Sciences of the United States of America,* 93**,** 9166-9171.
LOWENBERG, B., DOWNING, J. R. & BURNETT, A. 1999. Acute myeloid leukemia. *New England Journal of Medicine,* 341**,** 1051-1062.
LUXEN, S., BELINSKY, S. A. & KNAUS, U. G. 2008. Silencing of *DUOX* NADPH Oxidases by Promoter Hypermethylation in Lung Cancer. *Cancer Research,* 68**,** 1037-1045.
MACANAS-PIRARD, P., YAACOB, N.-S., LEE, P. C., HOLDER, J. C., HINTON, R. H. & KASS, G. E. N. 2005. Glycogen Synthase Kinase-3 Mediates Acetaminophen-Induced Apoptosis in Human Hepatoma Cells. *Journal of Pharmacology and Experimental Therapeutics,* 313**,** 780-789.
MALONEY, E., SWEET, I. R., HOCKENBERY, D. M., PHAM, M., RIZZO, N. O., TATEYA, S., HANDA, P., SCHWARTZ, M. W. & KIM, F. 2009. Activation of NF-κB by Palmitate in Endothelial Cells. *A Key Role for NADPH Oxidase-Derived Superoxide in Response to TLR4 Activation,* 29**,** 1370-1375.
MANDAL, CHANDI C., GANAPATHY, S., GORIN, Y., MAHADEV, K., BLOCK, K., ABBOUD, HANNA E., HARRIS, STEPHEN E., GHOSH-CHOUDHURY, G. & GHOSH-CHOUDHURY, N. 2011. Reactive oxygen species derived from Nox4 mediate *BMP2* gene transcription and osteoblast differentiation. *Biochemical Journal,* 433**,** 393-402.
MARALDI, T., GUIDA, M., ZAVATTI, M., RESCA, E., BERTONI, L., LA SALA, G. B. & DE POL, A. 2015. Nuclear Nox4 Role in Stemness Power of Human Amniotic Fluid Stem Cells. *Oxidative Medicine and Cellular Longevity,* 2015**,** 11.
MARCHETTI, M., RESNICK, L., GAMLIEL, E., KESARAJU, S., WEISSBACH, H. & BINNINGER, D. 2009. Sulindac Enhances the Killing of Cancer Cells Exposed to Oxidative Stress. *PLOS ONE,* 4**,** e5804.
MARTYN, K. D., FREDERICK, L. M., VON LOEHNEYSEN, K., DINAUER, M. C. & KNAUS, U. G. 2006. Functional analysis of Nox4 reveals unique characteristics compared to other NADPH oxidases. *Cellular Signalling,* 18**,** 69-82.
MAS, V. M.-D., BEZOMBES, C., QUILLET-MARY, A., BETTAÏEB, A., D'ORGEIX, A. D. T., LAURENT, G. & JAFFRÉZOU, J.-P. 1999. Implication of Radical Oxygen Species in Ceramide Generation, c-Jun N-Terminal Kinase Activation and Apoptosis Induced by Daunorubicin. *Molecular Pharmacology,* 56**,** 867-874.

MASSON, K. & RÖNNSTRAND, L. 2009. Oncogenic signaling from the hematopoietic growth factor receptors c-Kit and Flt3. *Cellular Signalling,* 21**,** 1717-1726.
MATSUSHIMA, S., KURODA, J., AGO, T., ZHAI, P., PARK, J. Y., XIE, L.-H., TIAN, B. & SADOSHIMA, J. 2013. Increased Oxidative Stress in the Nucleus Caused by Nox4 Mediates Oxidation of HDAC4 and Cardiac Hypertrophy. *Circulation research,* 112**,** 651-663.
MAURER, U., CHARVET, C., WAGMAN, A. S., DEJARDIN, E. & GREEN, D. R. 2006. Glycogen Synthase Kinase-3 Regulates Mitochondrial Outer Membrane Permeabilization and Apoptosis by Destabilization of MCL-1. *Molecular Cell,* 21**,** 749-760.
MCCUBREY, J. A., STEELMAN, L. S., CHAPPELL, W. H., ABRAMS, S. L., WONG, E. W. T., CHANG, F., LEHMANN, B., TERRIAN, D. M., MILELLA, M., TAFURI, A., STIVALA, F., LIBRA, M., BASECKE, J., EVANGELISTI, C., MARTELLI, A. M. & FRANKLIN, R. A. 2007. Roles of the Raf/MEK/ERK pathway in cell growth, malignant transformation and drug resistance. *Biochimica et Biophysica Acta (BBA) - Molecular Cell Research,* 1773**,** 1263-1284.
MEHDIPOUR, P., SANTORO, F. & MINUCCI, S. 2015. Epigenetic alterations in acute myeloid leukemias. *FEBS Journal,* 282**,** 1786-1800.
MESHINCHI, S. & ARCECI, R. J. 2007. Prognostic Factors and Risk-Based Therapy in Pediatric Acute Myeloid Leukemia. *The Oncologist,* 12**,** 341-355.
METZELER, K. H., MAHARRY, K., RADMACHER, M. D., MRÓZEK, K., MARGESON, D., BECKER, H., CURFMAN, J., HOLLAND, K. B., SCHWIND, S., WHITMAN, S. P., WU, Y.-Z., BLUM, W., POWELL, B. L., CARTER, T. H., WETZLER, M., MOORE, J. O., KOLITZ, J. E., BAER, M. R., CARROLL, A. J., LARSON, R. A., CALIGIURI, M. A., MARCUCCI, G. & BLOOMFIELD, C. D. 2011. TET2 Mutations Improve the New European LeukemiaNet Risk Classification of Acute Myeloid Leukemia: A Cancer and Leukemia Group B Study. *Journal of Clinical Oncology,* 29**,** 1373-1381.
MIKI, H. & FUNATO, Y. 2012. Regulation of intracellular signalling through cysteine oxidation by reactive oxygen species. *The Journal of Biochemistry,* 151**,** 255-261.
MIRANDA, A., JANSSEN, L., BOSMAN, C. B., VAN DUIJN, W., OOSTENDORP-VAN DE RUIT, M. M., KUBBEN, F. J. G. M., GRIFFIOEN, G., LAMERS, C. B. H. W., HAN, J., VAN KRIEKEN, J. M., VAN DE VELDE, C. J. H. & VERSPAGET, H. W. 2000. Superoxide Dismutases in Gastric and Esophageal Cancer and the Prognostic Impact in Gastric Cancer. *Clinical Cancer Research,* 6**,** 3183-3192.
MIZUKI, M., FENSKI, R., HALFTER, H., MATSUMURA, I., SCHMIDT, R., MÜLLER, C., GRÜNING, W., KRATZ-ALBERS, K., SERVE, S., STEUR, C., BÜCHNER, T., KIENAST, J., KANAKURA, Y., BERDEL, W. E. & SERVE, H. 2000. Flt3 mutations from patients with acute myeloid leukemia induce transformation of 32D cells mediated by the Ras and STAT5 pathways. *Blood,* 96**,** 3907-3914.
MOCHIZUKI, T., FURUTA, S., MITSUSHITA, J., SHANG, W. H., ITO, M., YOKOO, Y., YAMAURA, M., ISHIZONE, S., NAKAYAMA, J., KONAGAI, A., HIROSE, K., KIYOSAWA, K. & KAMATA, T. 2006. Inhibition of NADPH oxidase 4 activates apoptosis via the AKT//apoptosis

signal-regulating kinase 1 pathway in pancreatic cancer PANC-1 cells. *Oncogene,* 25**,** 3699-3707.
MOLONEY, J. N. & COTTER, T. G. 2017. ROS signalling in the biology of cancer. *Seminars in Cell & Developmental Biology*.
MOLONEY, J. N., JAYAVELU, A. K., STANICKA, J., ROCHE, S. L., O'BRIEN, R. L., SCHOLL, S., BÖHMER, F.-D. & COTTER, T. G. 2017a. Nuclear membrane-localised NOX4D generates pro-survival ROS in FLT3-ITD-expressing AML. *Oncotarget,* 8**,** 105440-105457.
MOLONEY, J. N., STANICKA, J. & COTTER, T. G. 2017b. Subcellular localization of the FLT3-ITD oncogene plays a significant role in the production of NOX- and $p22^{phox}$-derived reactive oxygen species in acute myeloid leukemia. *Leukemia Research,* 52**,** 34-42.
MOON, D.-O., KIM, M.-O., CHOI, Y. H., HYUN, J. W., CHANG, W. Y. & KIM, G.-Y. 2010. Butein induces G2/M phase arrest and apoptosis in human hepatoma cancer cells through ROS generation. *Cancer Letters,* 288**,** 204-213.
MOREMEN, K. W., TIEMEYER, M. & NAIRN, A. V. 2012. Vertebrate protein glycosylation: diversity, synthesis and function. *Nature reviews. Molecular cell biology,* 13**,** 448-462.
MORSELLI, E., GALLUZZI, L., KEPP, O., VICENCIO, J.-M., CRIOLLO, A., MAIURI, M. C. & KROEMER, G. 2009. Anti- and pro-tumor functions of autophagy. *Biochimica et Biophysica Acta (BBA) - Molecular Cell Research,* 1793**,** 1524-1532.
MRÓZEK, K., MARCUCCI, G., NICOLET, D., MAHARRY, K. S., BECKER, H., WHITMAN, S. P., METZELER, K. H., SCHWIND, S., WU, Y.-Z., KOHLSCHMIDT, J., PETTENATI, M. J., HEEREMA, N. A., BLOCK, A. W., PATIL, S. R., BAER, M. R., KOLITZ, J. E., MOORE, J. O., CARROLL, A. J., STONE, R. M., LARSON, R. A. & BLOOMFIELD, C. D. 2012. Prognostic Significance of the European LeukemiaNet Standardized System for Reporting Cytogenetic and Molecular Alterations in Adults With Acute Myeloid Leukemia. *Journal of Clinical Oncology,* 30**,** 4515-4523.
MULLER, F. L., LIU, Y. & VAN REMMEN, H. 2004. Complex III Releases Superoxide to Both Sides of the Inner Mitochondrial Membrane. *Journal of Biological Chemistry,* 279**,** 49064-49073.
MULLER, J. P., SCHONHERR, C., MARKOVA, B., BAUER, R., STOCKING, C. & BOHMER, F. D. 2008. Role of SHP2 for FLT3-dependent proliferation and transformation in 32D cells. *Leukemia,* 22**,** 1945-1948.
MURPHY, MICHAEL P. 2009. How mitochondria produce reactive oxygen species. *Biochemical Journal,* 417**,** 1-13.
NABINGER, S. C., LI, X., RAMDAS, B., HE, Y., ZHANG, X., ZENG, L., RICHINE, B., BOWLING, J. D., FUKUDA, S., GOENKA, S., LIU, Z., FENG, G.-S., YU, M., SANDUSKY, G. E., BOSWELL, H. S., ZHANG, Z.-Y., KAPUR, R. & CHAN, R. J. 2013. The Protein Tyrosine Phosphatase, Shp2, Positively Contributes to FLT3-ITD-Induced Hematopoietic Progenitor Hyperproliferation and Malignant Disease *In Vivo*. *Leukemia,* 27**,** 398-408.
NAOE, T. & KIYOI, H. 2013. Gene mutations of acute myeloid leukemia in the genome era. *International Journal of Hematology,* 97**,** 165-174.

NAUGHTON, R., QUINEY, C., TURNER, S. D. & COTTER, T. G. 2009. Bcr-Abl-mediated redox regulation of the PI3K/AKT pathway. *Leukemia,* 23**,** 1432-1440.

NETWORK, T. C. G. A. R. 2013. Genomic and Epigenomic Landscapes of Adult De Novo Acute Myeloid Leukemia. *New England Journal of Medicine,* 368**,** 2059-2074.

NISIMOTO, Y., JACKSON, H. M., OGAWA, H., KAWAHARA, T. & LAMBETH, J. D. 2010. Constitutive NADPH-Dependent Electron Transferase Activity of the Nox4 Dehydrogenase Domain. *Biochemistry,* 49**,** 2433-2442.

NO, J. H., KIM, Y.-B. & SONG, Y. S. 2014. Targeting Nrf2 Signaling to Combat Chemoresistance. *Journal of Cancer Prevention,* 19**,** 111-117.

NOLTE, F. & HOFMANN, W. K. 2010. Molecular mechanisms involved in the progression of myelodysplastic syndrome. *Future Oncology,* 6**,** 445-455.

NOTO, H., GOTO, A., TSUJIMOTO, T. & NODA, M. 2012. Cancer Risk in Diabetic Patients Treated with Metformin: A Systematic Review and Meta-analysis. *PLoS ONE,* 7**,** e33411.

NOWICKI, M. O., FALINSKI, R., KOPTYRA, M., SLUPIANEK, A., STOKLOSA, T., GLOC, E., NIEBOROWSKA-SKORSKA, M., BLASIAK, J. & SKORSKI, T. 2004. BCR/ABL oncogenic kinase promotes unfaithful repair of the reactive oxygen species–dependent DNA double-strand breaks. *Blood,* 104**,** 3746-3753.

OMENN , G. S., GOODMAN , G. E., THORNQUIST , M. D., BALMES , J., CULLEN , M. R., GLASS , A., KEOGH , J. P., MEYSKENS , F. L. J., VALANIS , B., WILLIAMS , J. H. J., BARNHART , S. & HAMMAR , S. 1996. Effects of a Combination of Beta Carotene and Vitamin A on Lung Cancer and Cardiovascular Disease. *New England Journal of Medicine,* 334**,** 1150-1155.

ÖSTMAN, A., FRIJHOFF, J., SANDIN, Å. & BÖHMER, F.-D. 2011. Regulation of protein tyrosine phosphatases by reversible oxidation. *The Journal of Biochemistry,* 150**,** 345-356.

OWEN, M. R., DORAN, E. & HALESTRAP, A. P. 2000. Evidence that metformin exerts its anti-diabetic effects through inhibition of complex 1 of the mitochondrial respiratory chain. *Biochemical Journal,* 348**,** 607-614.

PADMANABHAN, B., TONG, K. I., OHTA, T., NAKAMURA, Y., SCHARLOCK, M., OHTSUJI, M., KANG, M.-I., KOBAYASHI, A., YOKOYAMA, S. & YAMAMOTO, M. 2006. Structural Basis for Defects of Keap1 Activity Provoked by Its Point Mutations in Lung Cancer. *Molecular Cell,* 21**,** 689-700.

PAN, S.-S., PEDERSEN, L. & BACHUR, N. R. 1981. Comparative Flavoprotein Catalysis of Anthracycline Antibiotic. *Reductive Cleavage and Oxygen Consumption,* 19**,** 184-186.

PANIERI, E. & SANTORO, M. M. 2016. ROS homeostasis and metabolism: a dangerous liason in cancer cells. *Cell Death Dis,* 7**,** e2253.

PARK, J. E., YUEN, H. F., ZHOU, J. B., AL-AIDAROOS, A. Q. O., GUO, K., VALK, P. J., ZHANG, S. D., CHNG, W. J., HONG, C. W., MILLS, K. & ZENG, Q. 2013. Oncogenic roles of PRL-3 in FLT3-ITD induced acute myeloid leukaemia. *EMBO Molecular Medicine,* 5**,** 1351-1366.

PARK, S.-A., NA, H.-K., KIM, E.-H., CHA, Y.-N. & SURH, Y.-J. 2009. 4-Hydroxyestradiol Induces Anchorage-Independent Growth of Human

Mammary Epithelial Cells via Activation of IκB Kinase: Potential Role of Reactive Oxygen Species. *Cancer Research,* 69**,** 2416-2424.
PASCHKA, P., SCHLENK, R. F., GAIDZIK, V. I., HABDANK, M., KRÖNKE, J., BULLINGER, L., SPÄTH, D., KAYSER, S., ZUCKNICK, M., GÖTZE, K., HORST, H.-A., GERMING, U., DÖHNER, H. & DÖHNER, K. 2010. IDH1 and IDH2 Mutations Are Frequent Genetic Alterations in Acute Myeloid Leukemia and Confer Adverse Prognosis in Cytogenetically Normal Acute Myeloid Leukemia With NPM1 Mutation Without FLT3 Internal Tandem Duplication. *Journal of Clinical Oncology,* 28**,** 3636-3643.
PASTORINO, J. G., TAFANI, M. & FARBER, J. L. 1999. Tumor Necrosis Factor Induces Phosphorylation and Translocation of BAD through a Phosphatidylinositide-3-OH Kinase-dependent Pathway. *Journal of Biological Chemistry,* 274**,** 19411-19416.
PATEL , J. P., GÖNEN , M., FIGUEROA , M. E., FERNANDEZ , H., SUN , Z., RACEVSKIS , J., VAN VLIERBERGHE , P., DOLGALEV , I., THOMAS , S., AMINOVA , O., HUBERMAN , K., CHENG , J., VIALE , A., SOCCI , N. D., HEGUY , A., CHERRY , A., VANCE , G., HIGGINS , R. R., KETTERLING , R. P., GALLAGHER , R. E., LITZOW , M., VAN DEN BRINK , M. R. M., LAZARUS , H. M., ROWE , J. M., LUGER , S., FERRANDO , A., PAIETTA , E., TALLMAN , M. S., MELNICK , A., ABDEL-WAHAB , O. & LEVINE , R. L. 2012. Prognostic Relevance of Integrated Genetic Profiling in Acute Myeloid Leukemia. *New England Journal of Medicine,* 366**,** 1079-1089.
PELICANO, H., CARNEY, D. & HUANG, P. 2004. ROS stress in cancer cells and therapeutic implications. *Drug Resistance Updates,* 7**,** 97-110.
PELICANO, H., FENG, L., ZHOU, Y., CAREW, J. S., HILEMAN, E. O., PLUNKETT, W., KEATING, M. J. & HUANG, P. 2003. Inhibition of Mitochondrial Respiration: A Novel Strategy To Enhance Drug-Induced Apoptosis In Human Leukemia Cells By A Reactive Oxygen Species-Mediated Mechanism. *Journal of Biological Chemistry,* 278**,** 37832-37839.
PETTIGREW, C. A., CLERKIN, J. S. & COTTER, T. G. 2012. DUOX Enzyme Activity Promotes AKT Signalling in Prostate Cancer Cells. *Anticancer Research,* 32**,** 5175-5181.
PIERLEONI, A., MARTELLI, P. L. & CASADIO, R. 2008. PredGPI: a GPI-anchor predictor. *BMC Bioinformatics,* 9**,** 392.
PIETRAS, E. M. 2017. Inflammation: a key regulator of hematopoietic stem cell fate in health and disease. *Blood,* 130**,** 1693-1698.
PLASS, C., OAKES, C., BLUM, W. & MARCUCCI, G. 2008. Epigenetics in Acute Myeloid Leukemia. *Seminars in oncology,* 35**,** 378-387.
POILLET-PEREZ, L., DESPOUY, G., DELAGE-MOURROUX, R. & BOYER-GUITTAUT, M. 2015. Interplay between ROS and autophagy in cancer cells, from tumor initiation to cancer therapy. *Redox Biology,* 4**,** 184-192.
PRATA, C., MARALDI, T., FIORENTINI, D., ZAMBONIN, L., HAKIM, G. & LANDI, L. 2008. Nox-generated ROS modulate glucose uptake in a leukaemic cell line. *Free Radical Research,* 42**,** 405-414.
PREISLER, H. D. & LYMAN, G. H. 1977. Acute myelogenous leukemia subsequent to therapy for a different neoplasm: Clinical features and response to therapy. *American Journal of Hematology,* 3**,** 209-218.

QI, X.-J., WILDEY, G. M. & HOWE, P. H. 2006. Evidence That Ser87 of BimEL Is Phosphorylated by Akt and Regulates BimEL Apoptotic Function. *Journal of Biological Chemistry,* 281**,** 813-823.
QUAN, W., LIM, Y.-M. & LEE, M.-S. 2012. Role of autophagy in diabetes and endoplasmic reticulum stress of pancreatic β-cells. *Experimental & Molecular Medicine,* 44**,** 81-88.
RAKHEJA, D., KONOPLEV, S., MEDEIROS, L. J. & CHEN, W. 2012. IDH mutations in acute myeloid leukemia. *Human Pathology,* 43**,** 1541-1551.
RAMSAY, R. G. & GONDA, T. J. 2008. MYB function in normal and cancer cells. *Nat Rev Cancer,* 8**,** 523-534.
RASSOOL, F. V., GAYMES, T. J., OMIDVAR, N., BRADY, N., BEURLET, S., PLA, M., REBOUL, M., LEA, N., CHOMIENNE, C., THOMAS, N. S. B., MUFTI, G. J. & PADUA, R. A. 2007. Reactive Oxygen Species, DNA Damage, and Error-Prone Repair: A Model for Genomic Instability with Progression in Myeloid Leukemia? *Cancer Research,* 67**,** 8762-8771.
RAVANDI, F., KANTARJIAN, H., FADERL, S., GARCIA-MANERO, G., O'BRIEN, S., KOLLER, C., PIERCE, S., BRANDT, M., KENNEDY, D., CORTES, J. & BERAN, M. 2010. Outcome Of Patients With FLT3 Mutated Acute Myeloid Leukemia In First Relapse. *Leukemia research,* 34**,** 752-756.
RECZEK, C. R. & CHANDEL, N. S. 2015. ROS-dependent signal transduction. *Current Opinion in Cell Biology,* 33**,** 8-13.
REDDY, K. B. & GLAROS, S. 2007. Inhibition of the MAP kinase activity suppresses estrogen-induced breast tumor growth both *in vitro* and *in vivo*. *International journal of oncology,* 30**,** 971-976.
REDDY, M. M., FERNANDES, M. S., SALGIA, R., LEVINE, R. L., GRIFFIN, J. D. & SATTLER, M. 2011. NADPH oxidases regulate cell growth and migration in myeloid cells transformed by oncogenic tyrosine kinases. *Leukemia,* 25**,** 281-289.
REGAD, T. 2015. Targeting RTK Signaling Pathways in Cancer. *Cancers,* 7**,** 1758-1784.
RHEE, S. G. 2006. H_2O_2, a Necessary Evil for Cell Signaling. *Science,* 312**,** 1882-1883.
RICHARDS, S. M. & CLARK, E. A. 2009. BCR-induced superoxide negatively regulates B-cell proliferation and T-cell-independent type 2 Ab responses. *European Journal of Immunology,* 39**,** 3395-3403.
ROBERTS, P. J. & DER, C. J. 2007. Targeting the Raf-MEK-ERK mitogen-activated protein kinase cascade for the treatment of cancer. *Oncogene,* 26**,** 3291-3310.
ROBOZ, G. J. 2012. Current treatment of acute myeloid leukemia. *Current opinion in oncology,* 24**,** 711-719.
ROSNET, O., BÜHRING, H. J., MARCHETTO, S., RAPPOLD, I., LAVAGNA, C., SAINTY, D., ARNOULET, C., CHABANNON, C., KANZ, L., HANNUM, C. & BIRNBAUM, D. 1996. Human FLT3/FLK2 receptor tyrosine kinase is expressed at the surface of normal and malignant hematopoietic cells. *Leukemia,* 10**,** 238-248.
ROSZKOWSKI, K., JOZWICKI, W., BLASZCZYK, P., MUCHA-MALECKA, A. & SIOMEK, A. 2011. Oxidative damage DNA: 8-oxoGua and 8-oxodG as molecular markers of cancer. *Medical Science Monitor : International Medical Journal of Experimental and Clinical Research,* 17**,** CR329-CR333.

ROWLEY, J. D. 1973. A New Consistent Chromosomal Abnormality in Chronic Myelogenous Leukaemia identified by Quinacrine Fluorescence and Giemsa Staining. *Nature,* 243**,** 290-293.
ROY, K., WU, Y., MEITZLER, JENNIFER L., JUHASZ, A., LIU, H., JIANG, G., LU, J., ANTONY, S. & DOROSHOW, JAMES H. 2015. NADPH oxidases and cancer. *Clinical Science,* 128**,** 863-875.
RUSSELL, E. G., GUO, J., O'SULLIVAN, E. C., O'DRISCOLL, C. M., MCCARTHY, F. O. & COTTER, T. G. 2016. 7-formyl-10-methylisoellipticine, a novel ellipticine derivative, induces mitochondrial reactive oxygen species (ROS) and shows anti-leukaemic activity in mice. *Investigational New Drugs,* 34**,** 15-23.
RUSSELL, E. G., O'SULLIVAN, E. C., MILLER, C. M., STANICKA, J., MCCARTHY, F. O. & COTTER, T. G. 2014. Ellipticine derivative induces potent cytostatic effect in acute myeloid leukaemia cells. *Investigational New Drugs,* 32**,** 1113-1122.
RYDAPT 2017. [prescribing information] East Hanover, NJ: Novartis Pharmaceuticals Corp.
RYGIEL, T. P., MERTENS, A. E., STRUMANE, K., VAN DER KAMMEN, R. & COLLARD, J. G. 2008. The Rac activator Tiam1 prevents keratinocyte apoptosis by controlling ROS-mediated ERK phosphorylation. *Journal of Cell Science,* 121**,** 1183-1192.
SABHARWAL, S. S. & SCHUMACKER, P. T. 2014. Mitochondrial ROS in cancer: initiators, amplifiers or an Achilles' heel? *Nat Rev Cancer,* 14**,** 709-721.
SALLMYR, A., FAN, J., DATTA, K., KIM, K.-T., GROSU, D., SHAPIRO, P., SMALL, D. & RASSOOL, F. 2008a. Internal tandem duplication of FLT3 (FLT3/ITD) induces increased ROS production, DNA damage, and misrepair: implications for poor prognosis in AML. *Blood,* 111**,** 3173-3182.
SALLMYR, A., FAN, J. & RASSOOL, F. V. 2008b. Genomic instability in myeloid malignancies: Increased reactive oxygen species (ROS), DNA double strand breaks (DSBs) and error-prone repair. *Cancer Letters,* 270**,** 1-9.
SALMEEN, A., ANDERSEN, J. N., MYERS, M. P., MENG, T.-C., HINKS, J. A., TONKS, N. K. & BARFORD, D. 2003. Redox regulation of protein tyrosine phosphatase 1B involves a sulphenyl-amide intermediate. *Nature,* 423**,** 769-773.
SATTLER, M., VERMA, S., SHRIKHANDE, G., BYRNE, C. H., PRIDE, Y. B., WINKLER, T., GREENFIELD, E. A., SALGIA, R. & GRIFFIN, J. D. 2000. The BCR/ABL Tyrosine Kinase Induces Production of Reactive Oxygen Species in Hematopoietic Cells. *Journal of Biological Chemistry,* 275**,** 24273-24278.
SCHIEBER, M. & CHANDEL, NAVDEEP S. 2014. ROS Function in Redox Signaling and Oxidative Stress. *Current Biology,* 24**,** R453-R462.
SCHILLER, G. J. 2013. High-risk acute myelogenous leukemia: treatment today … and tomorrow. *ASH Education Program Book,* 2013**,** 201-208.
SCHMIDT-ARRAS, D.-E., BÖHMER, A., MARKOVA, B., CHOUDHARY, C., SERVE, H. & BÖHMER, F.-D. 2005. Tyrosine Phosphorylation Regulates Maturation of Receptor Tyrosine Kinases. *Molecular and Cellular Biology,* 25**,** 3690-3703.
SCHMIDT-ARRAS, D., BÖHMER, S.-A., KOCH, S., MÜLLER, J. P., BLEI, L., CORNILS, H., BAUER, R., KORASIKHA, S., THIEDE, C. & BÖHMER,

F.-D. 2009. Anchoring of FLT3 in the endoplasmic reticulum alters signaling quality. *Blood,* 113**,** 3568-3576.
SCHMITTGEN, T. D. & LIVAK, K. J. 2008. Analyzing real-time PCR data by the comparative CT method. *Nat. Protocols,* 3**,** 1101-1108.
SCHUMACKER, P. T. 2006. Reactive oxygen species in cancer cells: Live by the sword, die by the sword. *Cancer Cell,* 10**,** 175-176.
SEEDHOUSE, C. H., HUNTER, H. M., LLOYD-LEWIS, B., MASSIP, A. M., PALLIS, M., CARTER, G. I., GRUNDY, M., SHANG, S. & RUSSELL, N. H. 2006. DNA repair contributes to the drug-resistant phenotype of primary acute myeloid leukaemia cells with FLT3 internal tandem duplications and is reversed by the FLT3 inhibitor PKC412. *Leukemia,* 20**,** 2130-2136.
SENA, LAURA A. & CHANDEL, NAVDEEP S. 2012. Physiological Roles of Mitochondrial Reactive Oxygen Species. *Molecular Cell,* 48**,** 158-167.
SERRANDER, L., CARTIER, L., BEDARD, K., BANFI, B., LARDY, B., PLASTRE, O., SIENKIEWICZ, A., FÓRRÓ, L., SCHLEGEL, W. & KRAUSE, K.-H. 2007. NOX4 activity is determined by mRNA levels and reveals a unique pattern of ROS generation. *The Biochemical Journal,* 406**,** 105-114.
SHAH, A. M. 2015. Parsing the Role of Nox Enzymes and ROS in Heart Failure. *Circulation*.
SHAIKEN, T. E. & OPEKUN, A. R. 2014. Dissecting the cell to nucleus, perinucleus and cytosol. *Scientific Reports,* 4**,** 4923.
SHIH, A. H., ABDEL-WAHAB, O., PATEL, J. P. & LEVINE, R. L. 2012. The role of mutations in epigenetic regulators in myeloid malignancies. *Nat Rev Cancer,* 12**,** 599-612.
SHIMADA, K., FUJII, T., ANAI, S., FUJIMOTO, K. & KONISHI, N. 2011. ROS generation via NOX4 and its utility in the cytological diagnosis of urothelial carcinoma of the urinary bladder. *BMC Urology,* 11**,** 22.
SHIMADA, K., NAKAMURA, M. & ANAI, S. 2009. A novel human AlkB homologue, ALKBH8, contributes to human bladder cancer progression. *Cancer research,* 69**,** 3157-3164.
SHTIVELMAN, E., LIFSHITZ, B., GALE, R. P. & CANAANI, E. 1985. Fused transcript of abl and bcr genes in chronic myelogenous leukaemia. *Nature,* 315**,** 550-554.
SIEBER, O. M., HEINIMANN, K. & TOMLINSON, I. P. M. 2003. Genomic instability — the engine of tumorigenesis? *Nat Rev Cancer,* 3**,** 701-708.
SINGAL , P. K. & ILISKOVIC , N. 1998. Doxorubicin-Induced Cardiomyopathy. *New England Journal of Medicine,* 339**,** 900-905.
SINGH, R. & CZAJA, M. J. 2007. Regulation of hepatocyte apoptosis by oxidative stress. *Journal of Gastroenterology and Hepatology,* 22**,** S45-S48.
SKORSKI, T. 2002. BCR/ABL regulates response to DNA damage: the role in resistance to genotoxic treatment and in genomic instability. *Oncogene,* 21**,** 8591-8604.
SKORSKI, T. 2007. Genomic instability: The cause and effect of BCR/ABL tyrosine kinase. *Current Hematologic Malignancy Reports,* 2**,** 69-74.
SMALL, D. 2008. Targeting FLT3 for treatment of leukemia. *Seminars in hematology,* 45**,** S17-S21.
SMITH, C. C., WANG, Q., CHIN, C.-S., SALERNO, S., DAMON, L. E., LEVIS, M. J., PERL, A. E., TRAVERS, K. J., WANG, S., HUNT, J. P., ZARRINKAR, P. P., SCHADT, E. E., KASARSKIS, A., KURIYAN, J. &

SHAH, N. P. 2012. Validation of ITD mutations in FLT3 as a therapeutic target in human acute myeloid leukaemia. *Nature,* 485**,** 260-263.
SONG, L., JIANG, W., LIU, W., JI, J.-H., SHI, T.-F., ZHANG, J. & XIA, C.-Q. 2016. Protein tyrosine phosphatases receptor type D is a potential tumour suppressor gene inactivated by deoxyribonucleic acid methylation in paediatric acute myeloid leukaemia. *Acta Paediatrica,* 105**,** e132-e141.
SONGYANG, Z., BALTIMORE, D., CANTLEY, L. C., KAPLAN, D. R. & FRANKE, T. F. 1997. Interleukin 3-dependent survival by the Akt protein kinase. *Proceedings of the National Academy of Sciences of the United States of America,* 94**,** 11345-11350.
SPENCER, N. Y., YAN, Z., BOUDREAU, R. L., ZHANG, Y., LUO, M., LI, Q., TIAN, X., SHAH, A. M., DAVISSON, R. L., DAVIDSON, B., BANFI, B. & ENGELHARDT, J. F. 2011. Control of Hepatic Nuclear Superoxide Production by Glucose 6-Phosphate Dehydrogenase and NADPH Oxidase-4. *Journal of Biological Chemistry,* 286**,** 8977-8987.
SPIRO, R. G. 2002. Protein glycosylation: nature, distribution, enzymatic formation, and disease implications of glycopeptide bonds. *Glycobiology,* 12**,** 43R-56R.
STANICKA, J., RUSSELL, E. G., WOOLLEY, J. F. & COTTER, T. G. 2015. NADPH Oxidase-generated Hydrogen Peroxide Induces DNA Damage in Mutant FLT3-expressing Leukemia Cells. *Journal of Biological Chemistry,* 290**,** 9348-9361.
STANLEY, P. 2011. Golgi Glycosylation. *Cold Spring Harbor Perspectives in Biology,* 3**,** a005199.
STEELMAN, L. S., ABRAMS, S. L., WHELAN, J., BERTRAND, F. E., LUDWIG, D. E., BASECKE, J., LIBRA, M., STIVALA, F., MILELLA, M., TAFURI, A., LUNGHI, P., BONATI, A., MARTELLI, A. M. & MCCUBREY, J. A. 2008. Contributions of the Raf//MEK//ERK, PI3K//PTEN//Akt//mTOR and Jak//STAT pathways to leukemia. *Leukemia,* 22**,** 686-707.
STEELMAN, L. S., POHNERT, S. C., SHELTON, J. G., FRANKLIN, R. A., BERTRAND, F. E. & MCCUBREY, J. A. 2004. JAK//STAT, Raf//MEK//ERK, PI3K//Akt and BCR-ABL in cell cycle progression and leukemogenesis. *Leukemia,* 18**,** 189-218.
STIREWALT, D. L. & RADICH, J. P. 2003. The role of FLT3 in haematopoietic malignancies. *Nat Rev Cancer,* 3**,** 650-665.
STONE, R. M., FISCHER, T., PAQUETTE, R., SCHILLER, G., SCHIFFER, C. A., EHNINGER, G., CORTES, J., KANTARJIAN, H. M., DEANGELO, D. J., HUNTSMAN-LABED, A., DUTREIX, C., DEL CORRAL, A. & GILES, F. 2012. Phase IB study of the FLT3 kinase inhibitor midostaurin with chemotherapy in younger newly diagnosed adult patients with acute myeloid leukemia. *Leukemia,* 26**,** 2061-2068.
STONE, R. M., MANDREKAR, S. J., SANFORD, B. L., LAUMANN, K., GEYER, S., BLOOMFIELD, C. D., THIEDE, C., PRIOR, T. W., DÖHNER, K., MARCUCCI, G., LO-COCO, F., KLISOVIC, R. B., WEI, A., SIERRA, J., SANZ, M. A., BRANDWEIN, J. M., DE WITTE, T., NIEDERWIESER, D., APPELBAUM, F. R., MEDEIROS, B. C., TALLMAN, M. S., KRAUTER, J., SCHLENK, R. F., GANSER, A., SERVE, H., EHNINGER, G., AMADORI, S., LARSON, R. A. & DÖHNER, H. 2017. Midostaurin plus Chemotherapy for Acute Myeloid Leukemia with a FLT3 Mutation. *New England Journal of Medicine,* 377**,** 454-464.

STORZ, P. & TOKER, A. 2003. NF-κB Signaling: An ALternate Pathway for Oxidate Stress Responses. *Cell Cycle,* 2**,** 9-10.

SUMIMOTO, H., HATA, K., MIZUKI, K., ITO, T., KAGE, Y., SAKAKI, Y., FUKUMAKI, Y., NAKAMURA, M. & TAKESHIGE, K. 1996. Assembly and Activation of the Phagocyte NADPH Oxidase: Specific Interaction Of The N-Terminal Src Homology 3 Domain Of $p47^{phox}$ With $p22^{phox}$ Is Required For Activation Of The NADPH Oxidase. *Journal of Biological Chemistry,* 271**,** 22152-22158.

SUNDARESAN, M., YU, Z.-X., FERRANS, V. J., IRANI, K. & FINKEL, T. 1995. Requirement for Generation of H_2O_2 for Platelet-Derived Growth Factor Signal Transduction. *Science,* 270**,** 296-299.

SZATROWSKI, T. P. & NATHAN, C. F. 1991. Production of Large Amounts of Hydrogen Peroxide by Human Tumor Cells. *Cancer Research,* 51**,** 794-798.

TAKAC, I., SCHRÖDER, K., ZHANG, L., LARDY, B., ANILKUMAR, N., LAMBETH, J. D., SHAH, A. M., MOREL, F. & BRANDES, R. P. 2011. The E-loop Is Involved in Hydrogen Peroxide Formation by the NADPH Oxidase Nox4. *The Journal of Biological Chemistry,* 286**,** 13304-13313.

TAL, M. C., SASAI, M., LEE, H. K., YORDY, B., SHADEL, G. S. & IWASAKI, A. 2009. Absence of autophagy results in reactive oxygen species-dependent amplification of RLR signaling. *Proceedings of the National Academy of Sciences of the United States of America,* 106**,** 2770-2775.

TAO, L., FAN, F., LIU, Y., LI, W., ZHANG, L., RUAN, J., SHEN, C., SHENG, X., ZHU, Z., WANG, A., CHEN, W., HUANG, S. & LU, Y. 2013. Concerted Suppression of STAT3 and GSK3β Is Involved in Growth Inhibition of Non-Small Cell Lung Cancer by Xanthatin. *PLOS ONE,* 8**,** e81945.

TARTAGLIA, M., NIEMEYER, C. M., FRAGALE, A., SONG, X., BUECHNER, J., JUNG, A., HAHLEN, K., HASLE, H., LICHT, J. D. & GELB, B. D. 2003. Somatic mutations in PTPN11 in juvenile myelomonocytic leukemia, myelodysplastic syndromes and acute myeloid leukemia. *Nat Genet,* 34**,** 148-150.

TEOH-FITZGERALD, M. L., FITZGERALD, M. P., ZHONG, W., ASKELAND, R. W. & DOMANN, F. E. 2014. Epigenetic reprogramming governs EcSOD expression during human mammary epithelial cell differentiation, tumorigenesis and metastasis. *Oncogene,* 33**,** 358-368.

THIEDE, C., STEUDEL, C., MOHR, B., SCHAICH, M., SCHÄKEL, U., PLATZBECKER, U., WERMKE, M., BORNHÄUSER, M., RITTER, M., NEUBAUER, A., EHNINGER, G. & ILLMER, T. 2002. Analysis of FLT3-activating mutations in 979 patients with acute myelogenous leukemia: association with FAB subtypes and identification of subgroups with poor prognosis. *Presented in part at the 42nd Annual Meeting of the American Society of Hematology, December 1-5, 2000, San Francisco, CA (abstract 2334).* 99**,** 4326-4335.

TOLEDANO, M. B., PLANSON, A.-G. & DELAUNAY-MOISAN, A. 2010. Reining in H_2O_2 for Safe Signaling. *Cell,* 140**,** 454-456.

TOMINAGA, K., KAWAHARA, T., SANO, T., TOIDA, K., KUWANO, Y., SASAKI, H., KAWAI, T., TESHIMA-KONDO, S. & ROKUTAN, K. 2007. Evidence for cancer-associated expression of NADPH oxidase 1 (Nox1)-based oxidase system in the human stomach. *Free Radical Biology and Medicine,* 43**,** 1627-1638.

TONKS, N. K. 2013. Protein tyrosine phosphatases – from housekeeping enzymes to master regulators of signal transduction. *FEBS Journal,* 280**,** 346-378.
TRACHOOTHAM, D., ALEXANDRE, J. & HUANG, P. 2009. Targeting cancer cells by ROS-mediated mechanisms: a radical therapeutic approach? *Nat Rev Drug Discov,* 8**,** 579-591.
TSITSIPATIS, D., JAYAVELU, A. K., MÜLLER, J. P., BAUER, R., SCHMIDT-ARRAS, D., MAHBOOBI, S., SCHNÖDER, T. M., HEIDEL, F. & BÖHMER, F.-D. 2017. Synergistic killing of FLT3ITD-positive AML cells by combined inhibition of tyrosine-kinase activity and N-glycosylation. *Oncotarget,* 8**,** 26613-26624.
TURNER, A., LIN, N., ISSARACHAI, S., LYMAN, S. & BROUDY, V. 1996. FLT3 receptor expression on the surface of normal and malignant human hematopoietic cells. *Blood,* 88**,** 3383-3390.
UENO, N., TAKEYA, R., MIYANO, K., KIKUCHI, H. & SUMIMOTO, H. 2005. The NADPH Oxidase Nox3 Constitutively Produces Superoxide in a $p22^{phox}$-dependent Manner: Its Regulation By Oxidase Organizers And Activators. *Journal of Biological Chemistry,* 280**,** 23328-23339.
UNGAR, D. 2009. Golgi linked protein glycosylation and associated diseases. *Seminars in Cell & Developmental Biology,* 20**,** 762-769.
USUI, S., OVESON, B. C., LEE, S. Y., JO, Y.-J., YOSHIDA, T., MIKI, A., MIKI, K., IWASE, T., LU, L. & CAMPOCHIARO, P. A. 2009. NADPH oxidase plays a central role in cone cell death in retinitis pigmentosa. *Journal of Neurochemistry,* 110**,** 1028-1037.
VAN DER VLIET, A. 2011. Nox enzymes in allergic airway inflammation. *Biochimica et Biophysica Acta (BBA) - General Subjects,* 1810**,** 1035-1044.
VANDER HEIDEN, M. G., CANTLEY, L. C. & THOMPSON, C. B. 2009. Understanding the Warburg Effect: The Metabolic Requirements of Cell Proliferation. *Science,* 324**,** 1029-1033.
VAQUERO, E. C., EDDERKAOUI, M., PANDOL, S. J., GUKOVSKY, I. & GUKOVSKAYA, A. S. 2004. Reactive Oxygen Species Produced by NAD(P)H Oxidase Inhibit Apoptosis in Pancreatic Cancer Cells. *Journal of Biological Chemistry,* 279**,** 34643-34654.
VAUGHN, A. E. & DESHMUKH, M. 2008. Glucose Metabolism Inhibits Apoptosis in Neurons and Cancer Cells by Redox Inactivation of Cytochrome c. *Nature cell biology,* 10**,** 1477-1483.
VEAL, E. A., DAY, A. M. & MORGAN, B. A. 2007. Hydrogen Peroxide Sensing and Signaling. *Molecular Cell,* 26**,** 1-14.
WAJED, S. A., LAIRD, P. W. & DEMEESTER, T. R. 2001. DNA Methylation: An Alternative Pathway to Cancer. *Annals of Surgery,* 234**,** 10-20.
WANG, S., KONOREV, E. A., KOTAMRAJU, S., JOSEPH, J., KALIVENDI, S. & KALYANARAMAN, B. 2004a. Doxorubicin Induces Apoptosis in Normal and Tumor Cells via Distinctly Different Mechanisms: Intermediacy Of H_2O_2- And p53-Dependent Pathways. *Journal of Biological Chemistry,* 279**,** 25535-25543.
WANG, Y., HUANG, X., CANG, H., GAO, F., YAMAMOTO, T., OSAKI, T. & YI, J. 2007. The endogenous reactive oxygen species promote NF-κB activation by targeting on activation of NF-κB-inducing kinase in oral squamous carcinoma cells. *Free Radic Res,* 41**,** 963-71.
WANG, Y., SCHATTENBERG, J. M., RIGOLI, R. M., STORZ, P. & CZAJA, M. J. 2004b. Hepatocyte Resistance to Oxidative Stress Is Dependent on Protein

Kinase C-mediated Down-regulation of c-Jun/AP-1. *Journal of Biological Chemistry,* 279**,** 31089-31097.
WEISS, A. & SCHLESSINGER, J. 1998. Switching Signals On or Off by Receptor Dimerization. *Cell,* 94**,** 277-280.
WEYEMI, U., CAILLOU, B., TALBOT, M., AMEZIANE-EL-HASSANI, R., LACROIX, L., LAGENT-CHEVALLIER, O., AL GHUZLAN, A., ROOS, D., BIDART, J.-M., VIRION, A., SCHLUMBERGER, M. & DUPUY, C. 2010. Intracellular expression of reactive oxygen species-generating NADPH oxidase NOX4 in normal and cancer thyroid tissues. *Endocrine-Related Cancer,* 17**,** 27-37.
WEYEMI, U. & DUPUY, C. 2012. The emerging role of ROS-generating NADPH oxidase NOX4 in DNA-damage responses. *Mutation Research/Reviews in Mutation Research,* 751**,** 77-81.
WEYEMI, U., LAGENTE-CHEVALLIER, O., BOUFRAQECH, M., PRENOIS, F., COURTIN, F., CAILLOU, B., TALBOT, M., DARDALHON, M., AL GHUZLAN, A., BIDART, J. M., SCHLUMBERGER, M. & DUPUY, C. 2012. ROS-generating NADPH oxidase NOX4 is a critical mediator in oncogenic H-Ras-induced DNA damage and subsequent senescence. *Oncogene,* 31**,** 1117-1129.
WEYEMI, U., REDON, C. E., AZIZ, T., CHOUDHURI, R., MAEDA, D., PAREKH, P. R., BONNER, M. Y., ARBISER, J. L. & BONNER, W. M. 2015. NADPH oxidase 4 is a critical mediator in Ataxia telangiectasia disease. *Proceedings of the National Academy of Sciences of the United States of America,* 112**,** 2121-2126.
WHEATON, W. W., WEINBERG, S. E., HAMANAKA, R. B., SOBERANES, S., SULLIVAN, L. B., ANSO, E., GLASAUER, A., DUFOUR, E., MUTLU, G. M., BUDIGNER, G. R. S. & CHANDEL, N. S. 2014. Metformin inhibits mitochondrial complex I of cancer cells to reduce tumorigenesis. *eLife,* 3**,** e02242.
WILLIAMS, A. B., LI, L., NGUYEN, B., BROWN, P., LEVIS, M. & SMALL, D. 2012. Fluvastatin inhibits FLT3 glycosylation in human and murine cells and prolongs survival of mice with FLT3/ITD leukemia. *Blood,* 120**,** 3069-3079.
WINTERBOURN, C. C. & HAMPTON, M. B. 2008. Thiol chemistry and specificity in redox signaling. *Free Radical Biology and Medicine,* 45**,** 549-561.
WOOD, Z. A., SCHRÖDER, E., ROBIN HARRIS, J. & POOLE, L. B. 2003. Structure, mechanism and regulation of peroxiredoxins. *Trends in Biochemical Sciences,* 28**,** 32-40.
WOOLLEY, J. F., NAUGHTON, R., STANICKA, J., GOUGH, D. R., BHATT, L., DICKINSON, B. C., CHANG, C. J. & COTTER, T. G. 2012. H_2O_2 Production Downstream of FLT3 Is Mediated by $p22^{phox}$ in the Endoplasmic Reticulum and Is Required for STAT5 Signalling. *PLOS ONE,* 7**,** e34050.
WOUTERS, B. J. & DELWEL, R. 2016. Epigenetics and approaches to targeted epigenetic therapy in acute myeloid leukemia. *Blood,* 127**,** 42-52.
WU, H., GOEL, V. & HALUSKA, F. G. 2003. PTEN signaling pathways in melanoma. *Oncogene,* 22**,** 3113-3122.
XIA, C., MENG, Q., LIU, L.-Z., ROJANASAKUL, Y., WANG, X.-R. & JIANG, B.-H. 2007. Reactive Oxygen Species Regulate Angiogenesis and Tumor Growth through Vascular Endothelial Growth Factor. *Cancer Research,* 67**,** 10823-10830.

XIN, M. & DENG, X. 2005. Nicotine Inactivation of the Proapoptotic Function of Bax through Phosphorylation. *Journal of Biological Chemistry,* 280**,** 10781-10789.

YAMAMOTO, J. F. & GOODMAN, M. T. 2008. Patterns of leukemia incidence in the United States by subtype and demographic characteristics, 1997–2002. *Cancer Causes & Control,* 19**,** 379-390.

YAMAMOTO, Y., KIYOI, H., NAKANO, Y., SUZUKI, R., KODERA, Y., MIYAWAKI, S., ASOU, N., KURIYAMA, K., YAGASAKI, F., SHIMAZAKI, C., AKIYAMA, H., SAITO, K., NISHIMURA, M., MOTOJI, T., SHINAGAWA, K., TAKESHITA, A., SAITO, H., UEDA, R., OHNO, R. & NAOE, T. 2001. Activating mutation of D835 within the activation loop of FLT3 in human hematologic malignancies. *Blood,* 97**,** 2434-2439.

YOO, N. J., KIM, H. R., KIM, Y. R., AN, C. H. & LEE, S. H. 2012. Somatic mutations of the KEAP1 gene in common solid cancers. *Histopathology,* 60**,** 943-952.

YOSHIMI, A., TOYA, T., KAWAZU, M., UENO, T., TSUKAMOTO, A., IIZUKA, H., NAKAGAWA, M., NANNYA, Y., ARAI, S., HARADA, H., USUKI, K., HAYASHI, Y., ITO, E., KIRITO, K., NAKAJIMA, H., ICHIKAWA, M., MANO, H. & KUROKAWA, M. 2014. Recurrent CDC25C mutations drive malignant transformation in FPD/AML. *Nature Communications,* 5**,** 4770.

ZARRINKAR, P. P., GUNAWARDANE, R. N., CRAMER, M. D., GARDNER, M. F., BRIGHAM, D., BELLI, B., KARAMAN, M. W., PRATZ, K. W., PALLARES, G., CHAO, Q., SPRANKLE, K. G., PATEL, H. K., LEVIS, M., ARMSTRONG, R. C., JAMES, J. & BHAGWAT, S. S. 2009. AC220 is a uniquely potent and selective inhibitor of FLT3 for the treatment of acute myeloid leukemia (AML). *Blood,* 114**,** 2984-2992.

ZHANG, J., VAKHRUSHEVA, O., BANDI, SRINIVASA R., DEMIREL, Ö., KAZI, JULHASH U., FERNANDES, RAMONA G., JAKOBI, K., EICHLER, A., RÖNNSTRAND, L., RIEGER, MICHAEL A., CARPINO, N., SERVE, H. & BRANDTS, CHRISTIAN H. 2015. The Phosphatases STS1 and STS2 Regulate Hematopoietic Stem and Progenitor Cell Fitness. *Stem Cell Reports,* 5**,** 633-646.

ZHANG, L., NGUYEN, M. V. C., LARDY, B., JESAITIS, A. J., GRICHINE, A., ROUSSET, F., TALBOT, M., PACLET, M.-H., QIAN, G. & MOREL, F. 2011. New insight into the Nox4 subcellular localization in HEK293 cells: First monoclonal antibodies against Nox4. *Biochimie,* 93**,** 457-468.

ZHANG, X. & WANG, Y. 2016. Glycosylation quality control by the Golgi structure. *Journal of molecular biology,* 428**,** 3183-3193.

ZHOU, J., BI, C., CHNG, W.-J., CHEONG, L.-L., LIU, S.-C., MAHARA, S., TAY, K.-G., ZENG, Q., LI, J., GUO, K., TAN, C. P. B., YU, H., ALBERT, D. H. & CHEN, C.-S. 2011. PRL-3, a Metastasis Associated Tyrosine Phosphatase, Is Involved in FLT3-ITD Signaling and Implicated in Anti-AML Therapy. *PLOS ONE,* 6**,** e19798.

ZOROV, D. B., JUHASZOVA, M. & SOLLOTT, S. J. 2014. Mitochondrial Reactive Oxygen Species (ROS) and ROS-Induced ROS Release. *Physiological Reviews,* 94**,** 909-950.